University of East Anglia

Initial studies on the development of a solid phase synthesis of vancomycin and analogues

By

Muayyad Safar Tahir Al-Shinayyin

University of East Anglia-School of Pharmacy

Ph.D.

February 2018

Acknowledgements

Foremost, I would like to express my sincere gratitude to my supervisor, Prof. Mark Searcey, for the continued assistance, support, encouragement and patient guidance that he has provided during my study over four years as a PhD student. He is, indeed, that sort of person who is so easy to deal with, and never imposes a pressure nevertheless he is so enthusiastic and keen to have everything you do in the best possible way. I have been so fortunate to have him as a supervisor in spirt of a mentor and friend.

My thanks are extending to the postdocs, Dr. Marco Cominetti and Dr. Andrew Beckman, for their kind assistance and help during my work in the lab. Their presence was as important as I could overcome number of obstacles, at more than one occasion. I have been very grateful to the University of East Anglia for granting me such a great opportunity to complete my PhD. Everything has been provided in a fantastic manner to have your work and study facilitated and supported in a right way.

I would also like to thank my sponsor, the Higher committee for Education Development in Iraq (HCEDI), for granting me such a great honour to be nominated to the study in the UK. Special thanks to my lab and officemates, Oliver, Issa, Dom and Emma, for their cooperation and the time we have spent with fun and lough. I cannot imagine it would be easy to spend the hard hours of work over the four years without such nice company. I would also like to thank Dr Lesley Howell for her close assistance throughout the first year of my study.

I would express my deep thankfulness to my amazing wife, Ban, for her support during my study and taking most of the role, looking after our children. She was indeed, the unknown soldier that has done her best to provide me with the convenient atmosphere to let me focus in my work. I never forget to thank my children; my lovely daughter, Jana, and the most adorable baby, Zayd. They have been the driving power that is still pushing me forward to do what it is the best. I never want to forget thanking my parents for their continuous encouragement. I am sure that their prayers for me were the light that illuminates my path so I recognise every good. Finally, and before all, I thank my god and my creator for giving me everything I own and for his continued blessings. Praise to Allah, Lord of the Worlds.

Abstract.

Vancomycin is a member of an important antibiotic group known as the glycopeptide antibiotics, which mainly act as bactericidal agents against Gram positive bacteria. Vancomycin acts by destroying the integrity of the bacterial cell wall and thereby exerts its detrimental effect on the most virulent gram-positive bacteria such as MRSA. Emergence of resistant strains against vancomycin has drawn scientists' curiosity to find new analogues to restore its powerful activity or to avoid loss of its efficiency against infectious bacteria. One of the routes that has been followed to find a novel vancomycin analogue is via chemical modification to its structure relying on its well-known mechanism of action. Our approach was to synthesise the constituent amino acids of the backbone of vancomycin in Fmoc-protected form to be suitable for conjugation using solid phase peptide chemistry (SPPS). The SPPS procedure potentially ensures rapid synthesis and modification of a peptide through concise and less demanding chemistry.

The central amino acid of vancomycin was synthesised in Fmoc-protected form at the α-amine terminal with a free carboxylic acid group. The synthesis proceeded through chemistry modification of the route developed by Nicoloau and co-workers and involved a series of reactions such as Sharpless AD reaction, Mitsunobu reaction and a TEMPO oxidation reaction. The Fmoc protected amino acid was successfully obtained and was potentially suitable for the conjugation with other amino acids using Fmoc chemistry and SPPS. Several trials were performed for the conjugation of the central unit on SPPS. Although different coupling reagents and solid supports were used, the results were unsuccessful. To confirm that peptide coupling with this amino acid was possible, it was demonstrated that solution phase coupling led to the successful generation of a tripeptide containing this unit. The suggestion here is that the triazene unit on the central amino acid is too unstable for incorporation into the SPPS protocol.

Finally, the successful synthesis of the Fmoc-protected ethyl ester analogues of the two tyrosine isomers, amino acid 2 and amino acid 6, in the vancomycin structure was completed. Several trials were attempted to hydrolyse the ethyl ester to release the carboxylic acid but were unsuccessful. Due to the time constrains, further efforts for hydrolysis reaction attempts were halted. ^{1}H NMR, ^{13}C NMR, IR, and mass-spectrometry were used throughout for assignments and characterisation of all the products and intermediates of the chemical reactions.

Table of Contents

List of figures

9

List of tables.

List of schemes.

Abreviations.

Alloc	Allyloxycarbonyl
D-Ala	Dextro-alanine
AMR	Antimicrobial resistance
Asn	Asparagine
BnBr	Benzyl bromide
Boc	*tert*-Butyloxycarbonyl
Boc₂O	Di-*tert*-butyl dicarbonate
B(OMe)₃	Trimethylborate
BOP	Benzotriazol-1-yloxy) tris(dimethylamino)phosphonium hexafluorophosphate
Bu	Butyl
***n*-BuLi**	*n*-Butyllithium
Bz	Benzoyl
C	Carbon
Cbz	Carboxybenzyl
COMU	1-[(1-(Cyano-2-ethoxy-2-oxoethylideneaminooxy) dimethylaminomorpholino)] uronium hexafluorophosphate
Cr	Chromium
4-CBP	4-Chlorobiphenyl
COSY	Correlation spectroscopy
DIBAL-H	Diisobutylaluminium hydride
DBU	1, 8-Diazabicyclo [5.4.0] undec-7-ene
DCM	Dichloromethane
D-Lac	dextro-Lactic acid

DIC	Diisopropylcarbodiimide
DCC	*N, N'*-Dicyclohexylcarbodiimide
(DHQ)₂	Dihydroquinine
(DHQD)₂	Dihydroquinidine
DEAD	Diethyl azodicarboxylate
DIAD	Diisopropyl azodicarboxylate
DIPEA	*N, N*-Diisopropylethylamine
DMAP	4-Dimethylaminopyridine
DNA	Deoxyribonucleic acid
DMF	*N, N*-dimethylformamide
DMSO	Dimethylsulfoxide
DPPA	Diphenylphosphoryl azide
D-Ser	dextro-Serine
EDCI	1-Ethyl-3-(3-dimethylaminopropyl) carbodiimide
Et₃N	Triethylamine
ee	Enantiomeric excess
equiv	Equivalents
Et	Ethyl
Fmoc	Fluorenylmethyloxycarbonyl
Fmoc-Cl	Fluorenylmethyloxycarbonyl chloride
g	Gram
GlcNAc	*N*-Acetylglucosamine
Gln	Glycine
HATU	1-[Bis(dimethylamino)methylene]-1H-1,2,3-triazolo[4,5-b] pyridinium 3-oxid hexafluorophosphate

HBTU	*O*-(Benzotriazol-1-yl)-*N, N, N′, N′*-tetramethyluronium hexafluorophosphate
HCl	Hydrochloric acid
HF	Hydrogenfluoride
Hpg	Hydroxyphenylglycine
HOAt	1-Hydroxy-7-azabenzotriazole
HOBt	1-Hydroxybenzotriazole
HPLC	High performance liquid chromatography
K	Potassium
KI	Potassium iodide
LiAlH$_4$	Lithium aluminium hydride
LC-MS	Liquid chromatography–mass spectrometry
Lys	Lysine
M	Molar
Me	Methyl
MeSO$_2$NH$_2$	Methanesulfonamide
MeOH	Methanol
min	Minute
MTS	3-(4,5-Dimethylthiazol-2-yl)-5-(3-carboxymethoxyphenyl)-2-(4-sulfophenyl)-2H-tetrazolium
Ms	Mesylate
MIC	Minimum inhibitory concentration
MRSA	Methicillin resistant *S. aureus*
Mtt	*N*-Methyltrityl
MurNAc	*N*-Acetylmuramic acid
MDR	Multiple drug resistance

NaH	Sodium hydride
NBP	*N*-Bromophthalimide
NMR	nuclear magnetic resonance spectroscopy
ºC	Degrees Celsius
PBP	Penicillin binding protein
PEG	Polyethylene glycol
Pd(PPh₃)₄	Palladium-tetrakis(triphenylphosphine)
Ph₃P	Triphenylphosphine
Ph	Phenyl
pH	Log hydrogen cation concentration
PHAL	Phthalazine
PhSiH₃	Phenylsilane
PyBop	(Benzotriazol-1-yloxy) tripyrrolidinophosphonium Hexafluorophosphate
PCC	Pyridinium chlorochromate
RNA	Ribonucleic acid
rt	Room temperature
SAD	Sharpless asymmetric dihydroxylation
SAR	Structure activity relationship
SCF	Supercritical fluid
Ser	Serine
SO₂Cl₂	Thionyl chloride
Sₙ	Nucleophilic substitution
SₙAr	Nucleophilic aromatic substitution
SM	Starting material
SnCl₂	Tin (II) chloride

SPPS	Solid phase peptide synthesis
TFAA	Trifluoroacetic anhydride
TMS	Trimethylsilane
TBAF	*tetra*-Butylammonium fluoride solution
TBS	*tert*-Butyldimethylsilane
TBSOTf	*tert*-Butyldimethylsilyl Trifluoromethanesulfonate
t-BuOH	*tert*-Butanol
t-butyl	*tert*-butyl
TEMPO	(2,2,6,6-Tetramethylpiperidin-1-yl) oxyl or (2,2,6,6-tetramethylpiperidin-1-yl) oxidanyl
TFA	Trifluoroacetic acid
Tfa	Trifluoroacetamide
THF	*tetra*-hydrofuran
TIPS	Triisopropylsilane
TLC	Thin-layer chromatography
Tyr	Tyrosine
UV	Ultraviolet
VOF$_3$	Vanadium(V)oxytrifluoride
VRE	Vancomycin resistant *Enterococci*
VSSA	Vancomycin sensitive resistance *S. aureus*

Chapter 1. Introduction

1.1. Antibiotics.

The discovery of penicillin in 1928 represented the starting point for the discovery and development of other active antimicrobials via the study of the interactions between the drug and its targets and/or manipulating the chemical structures of existing effective medicines.[1, 2] Antibiotics are defined as chemical entities produced by living organisms, whether they are microorganisms such as fungi and bacteria or animals or plants. They are used for the treatment and prevention of infectious diseases and exert their mode of activity suppressing bacterial growth and/or survival.[3] In general, the classification of antibiotics is divided into two main categories depending on the cellular target site they affect; 1) bactericidal, which cause microbial cell death, 2) bacteriostatic, which causes cell growth inhibition.[3, 4] The main cellular targets of bactericidal antibiotics are the cell wall, DNA, RNA, or proteins (Figure 1.1).[5] β-lactam antibiotics such as penicillin, and cephalosporins, are bactericidal antibiotics that inhibit cell wall synthesis by binding to penicillin binding proteins (PBP) destroying the mechanical supporting layer, peptidoglycan, of the cell wall,[6] so rendering bacteria susceptible to the surrounding changes in osmotic pressure causing their lysis and death.[7]

Other examples of bactericidal antibiotics include vancomycin and teicoplanin, which are glycopeptidic antibiotics that act on the integrity of the Gram positive bacterial cell wall via prevention of cross-linking of the peptidoglycan layer components to each other.[8] The quinolone antibiotics such as ciprofloxacin and levofloxacin, inhibit DNA synthesis via interference with the action of the enzymes, topoisomerase II and topoisomerase IV, that act to rejoin DNA strands during the chromosomal supercoiling process.[5] There are other three classes of bactericidal antibiotics that act by inhibiting ribosomal protein synthesis; macrolides such as erythromycin, tetracyclines such as doxycycline, and aminoglycomycins such as streptomycin.[9] Rifampicin is one of the most important antibiotics used for serious infections such as tuberculosis, and acts via inhibition of protein synthesis in bacteria.[10]
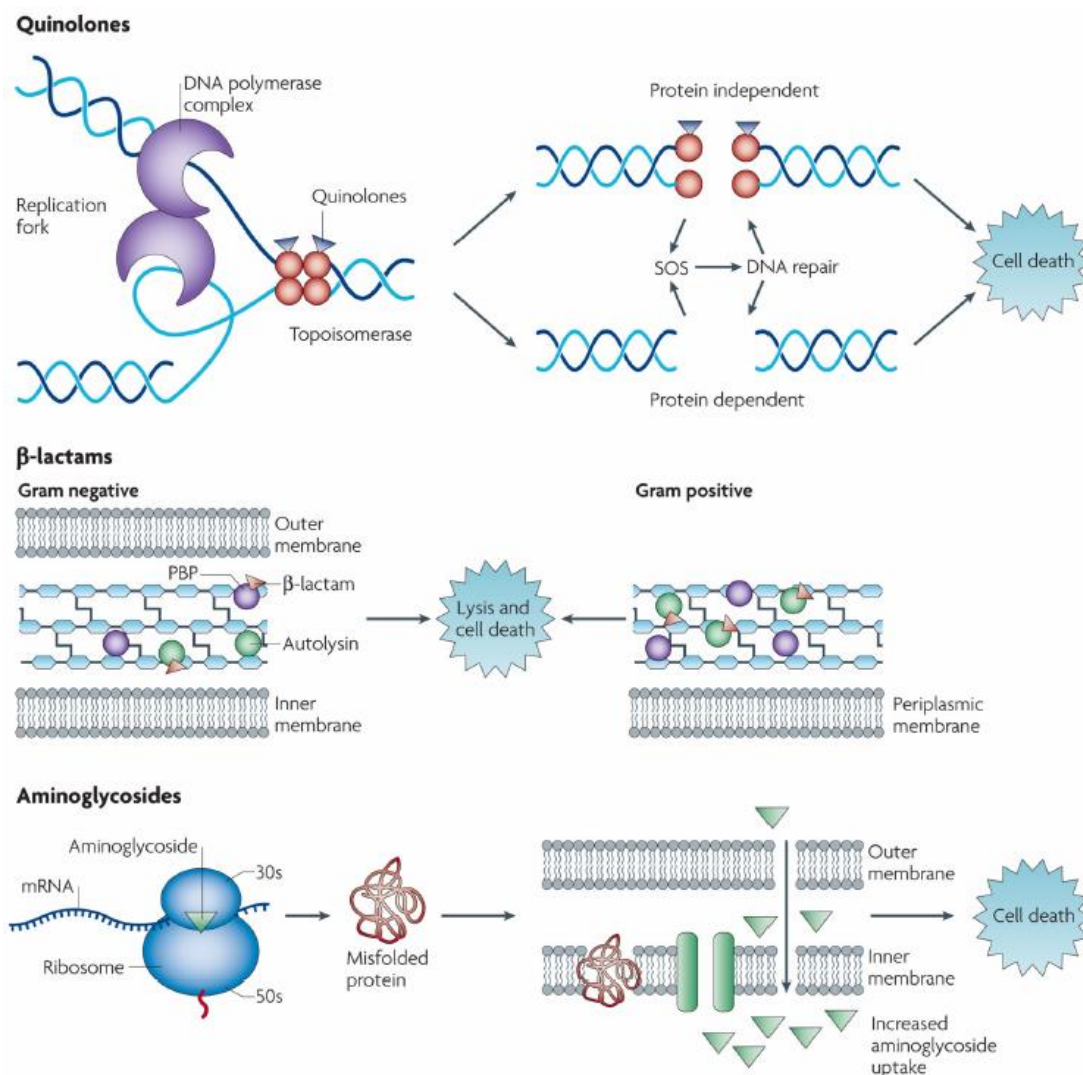
Figure 1.1: Mechanism of action of commonly used bactericidal antibiotics. a) Quinolone antibiotics cause a defect in DNA supercoiling via binding to topoisomerase. b) β-lactams inhibit integration process of the peptidoglycan strands by binding to PBPs. c) Aminoglycosides bind to the ribosomal units and inhibit elongation process of peptides. (Taken from reference[5]).

1.1.2. Antibiotic resistance.

Antibiotic resistance is defined as an adaptive ability of bacteria to resist and survive the use of antibiotics reducing their susceptibility of treatment and leading to aggravation of the infective diseases.[11] Evolutionary changes, called mutations, are behind the development of such bacterial ability, and are responsible for generating resistance genes. Mutations can be transferred horizontally, between species, or vertically, to the new offspring.[8] The ability of bacteria to pick up and pass on information between each other is the main route to the development of resistance

against the activity of many antibiotics.[12] The transferable information is disseminated by circular DNA structures called plasmids, which enable bacteria to encode drug resistance and spread it over different bacterial species.[13] Antibiotic resistance has had a great impact on human and animal health and as a consequence has influenced the economic sector.[14] Gene transfer is not restricted to virulent species. Antibiotic resistance can be gained by normal living microflora in the human body as well.[15] The prevalence of antibiotic resistance is related to several factors including geographic locations and poor hygiene. Overuse and misuse of antibiotics is the most important factor relevant to the emergence of antibiotic resistance.[16] Emergence of multiple-drug resistant bacteria represents the most detrimental consequence of misuse of antibiotics.[8]

1.1.3. Causes of antibiotic resistance.

As was noted above, the irrational use and increase in the amount of prescribed antibiotics has been the main contributor to the spread of multidrug resistance (MDR) and emergence of virulent resistant bacteria.[17] Overprescribed and/or inappropriately-prescribed antibiotics, especially broad-spectrum ones for even unindicated infections as viral infections, has been a main contributor in the dispertion of antibiotic resistance.[18] Increase in medical admissions to hospitals, and morbidity and mortality of patients as a consequence of inappropriate antibiotic prescription, leads to a proportional increase in medical cost and economic impact.[19] The appearance of Methicillin Resistant *S. aureus* (MRSA) is one of the consequences of misuse of antibiotics and is a main cause of many serious infections particularly for immune compromised people, such as those with HIV infection.[20] Norway has introduced restrictions to prevent dissemination of MRSA, which involve intensive screening of the patient before admission, during the stay, and after discharge from hospitals.[21] Other factors that have a direct and/or indirect role in antibiotic resistance can be listed as follows: 1) poor hand hygiene of medical staff and hospital equipment has been recognised as an important factor in distribution of MRSA in medical sectors; 2) contaminated food with resistant antibiotics and their role in increased human infections may have an important contribution in a rising antibiotic resistance level;[22] 3) human migration has increased the concerns of distribution of antibiotic resistance over a large area of the world.[23] Recent investigations of refugees that are coming from countries at war such as Syria, Afghanistan, and Iraq, display they are carrying dfferent kinds of MDR;[24] 4) excretion of incomplete metabolised antibiotics from humans and animals to sewage increases the possibility of resistant genes being transferred between bacterial cells and leads to elevation in the toxicity

to the environment and public health;[25, 26] 5) Use of antibiotics as a means for promotion of animal growth in their food and as a preventive and therapeutic procedure for infections, has led to rising levels of antibiotic resistance and adaptive ability of microorganisms.[27],[28] In addition, formation of bacterial biofilms is considered a very important mechanism of resistance by which even susceptible strains of bacteria can survive.[29] When bacteria attach to a surface such as an inflamed tissue or implanted organ or medical device, they can aggregate and encapsulate themselves in a sheet of polysaccharides and proteins.[30, 31] Bacteria in biofilms obtain an obvious resistance as the antibiotic penetration is greatly retarded.[29, 30] Therefore, bacterial biofilms are a cause of several chronic infections such as periodontitis and lung infections.[29, 32]

1.1.4. Measurements to tackle antibiotic resistance.

The increasing number of resistant pathogens has been a challenging problem to scientific research and the pharmaceutical industry as the number of novel antibiotics has declined.[33, 34] The main reason for the diminishing amount of innovative antibiotics is that their production or discovery is costly and time consuming.[35, 36] Most of the novel synthetic antimicrobials are structurally simple, so the bacteria easily develop resistance against them. This differs from previously discovered natural product antibiotics, which consist of complex structures, often acting by more than one mechanism so the possibility of resistance is diminished.[36] The structure simplicity of recent antibiotics is important for oral active antibiotic according to the Lipinski rule. Lipiniski and co-workers in 1997,[37] had set four properties of a candidate compound to be orally active. These properties are; the molecular weight, no more than 500 daltons, the octanol-water partion coeffiecient (log$P$), no more than 5, number of hydrogen bond donors, no more than 5, and number of hydrogen bond acceptors, no more than 10.[38] It is crucial to know the applicable measures by which antimicrobial resistance (AMR) could be controlled. There are several steps for controlling the dissemination and progression of antibiotic resistance: 1) Appropriate use of antibiotics and restricting their use to evidence-based infections and illnesses caused by bacteria, is the key effective procedure to tackle the AMR problem. Therefore, keeping antibiotics for only bacterial-caused infection and mostly for treatment protocol other than preventive procedures, and improving the diagnostic procedures to avoid prescribing antibiotics for viral infections, can lead to a reduction in the serious consequence of infections.[39] Moreover, optimisation of antibiotic prescriptions, which relates to using the most efficient antibiotic in a certain bacterial infection with optimised dose and concentration, can contribute to a large extent in

AMR control.[40] 2) Minimisation of antibiotic use in animal food could lead to a considerable decline in the growth of AMR.[28]

3) Establish an efficient protocol to keep sewage bacteria isolated and avoid their contact with other microorganisms and hence the genes that responsible on antibiotic resistance can be prevented from conveying the AMR to new bacteria.[25] 4) Another approach to avoid progression of AMR is the synthesis of new and efficient antibiotics and/or chemical modifications to the existing drugs. That is, to find new antimicrobial drugs working with unfamiliar mechanisms to the resistant bacteria, which should not be liable to cross-resistance with other antimicrobial agents.[41] An example of antimicrobial agent that has been produced via chemical modification is the second and third generation of β-lactam containing antibiotics, penicillin and cephalosporin. Example of the semi-synthesised antimicrobial agents is the second generation of erythromycins such as azithromycin.[9]

1.1.5. Mechanisms of antibiotic resistance in bacteria.

Generally, there are two types of mechanisms by which bacteria exhibit their resistance against antibiotics; intrinsic resistance, which is a natural capability of bacteria to avoid antibiotic effects, and acquired resistance, which is described as the ability of bacteria to develop mutations responsible for their resistance property or acquire genetic information from other species.(8) Bacteria can obtain antibiotic resistance via four basic types of mechanisms (Figure 1.2).[42]

1) Enzymatic inactivation or modification. Antibiotic modification, is a characteristic of bacteria to keep their sensitive targets unmodified as those of antibiotic sensitive species but block the access of drugs to them. Some bacteria produce enzymes that destroy the chemical structure of some antibiotics.[12] For example, many Gram-positive and Gram-negative bacteria produce a β-lactamase enzyme that hydrolyses the structural β-lactam ring of some antibiotics, such as first generation penicillin rendering them ineffective (Scheme 1.1).[8, 43, 44] The main difference between Gram negative and Gram positive bacteria relys on the cell wall components. The lipid content of the cell wall of Gram negative is much higher than that of Gram positive. Therefore, the resistance of Gram negative bacteria to various chemicals is attributed to their cell wall lipid content.[45] The Gram terminology is reffered to Hans Christian Gram who developed a staining technique in 1884 by which the two types of bacteria can be differentiated.[46]
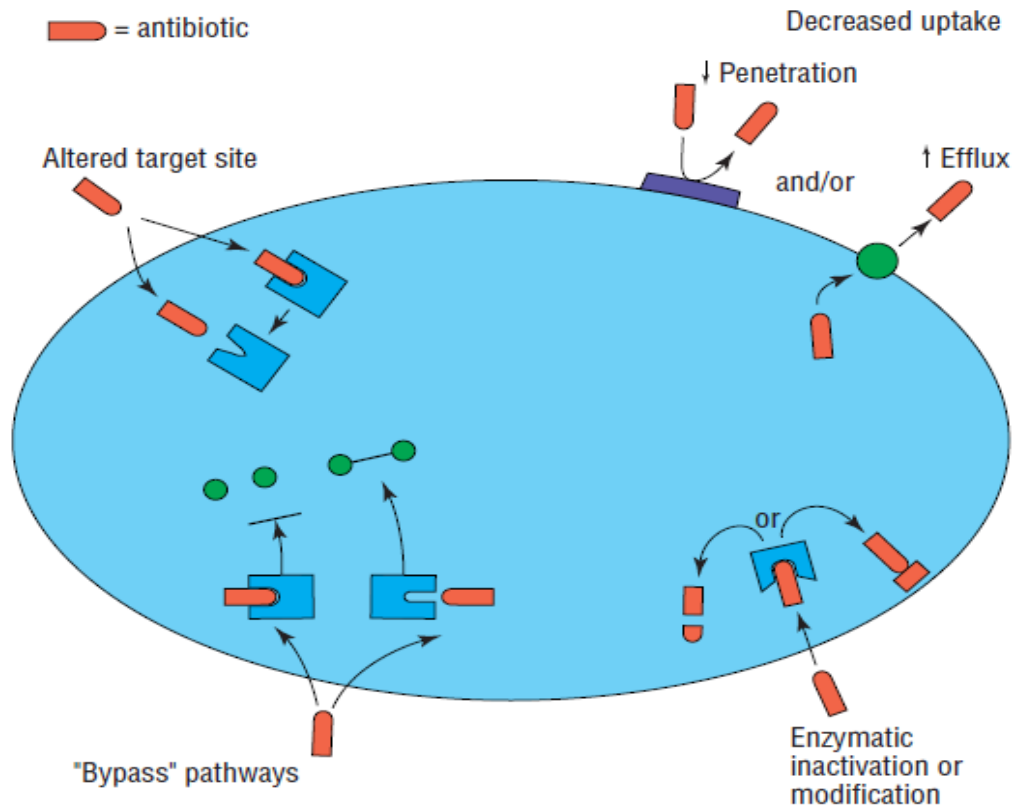
Figure 1.2: Four main resistance mechanisms of antibiotics. 1) Enzymatic inactivation or modification. 2) Decreased uptake or reduced antibiotic intake into the bacterial cell. 3) Alteration or inactivation of enzymes. 4) Bypass pathways. (Taken from reference[44]).

A single base change in the gene for a β-lactamase can change the substrate specificity of the enzyme.
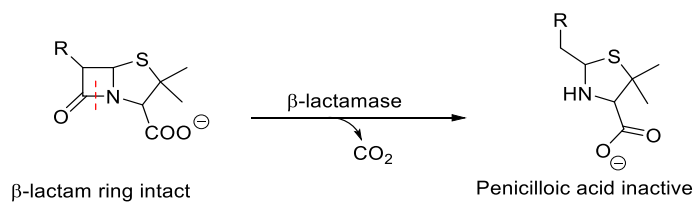
Scheme 1.1: Chemical alteration to the β-lactam ring by β-lactamase developed by resistance bacteria. (Taken from reference(9)).

2) Decreased uptake: drug efflux mechanisms which involve prevention of the antibiotic from entering the bacterial cell or removing them at a rate faster than it is entering. It is an active transport process, energy-dependent mechanism, mediated by proteins located in the cytoplasmic membrane.[47]

For example, imipenem gains its access to the sensitive bacteria through the cell membrane via a transporting protein called porin. In *Pseudomonas aeruginosa* bacteria, which is imipenem resistant, the lack of porin protein gives it resistance as imipenem cannot enter the bacterial cell (Scheme 1.2).[44] This mechanism is also found to a lesser extent in resistance to fluoroquinolones and aminoglycosides. Pumping of tetracyclines out by a positive transport method in *Enterobacteriaceae*, which is encoded by a specific gene called tet (A), is considered an efficient strategy of resistance for this type of bacteria.[48]
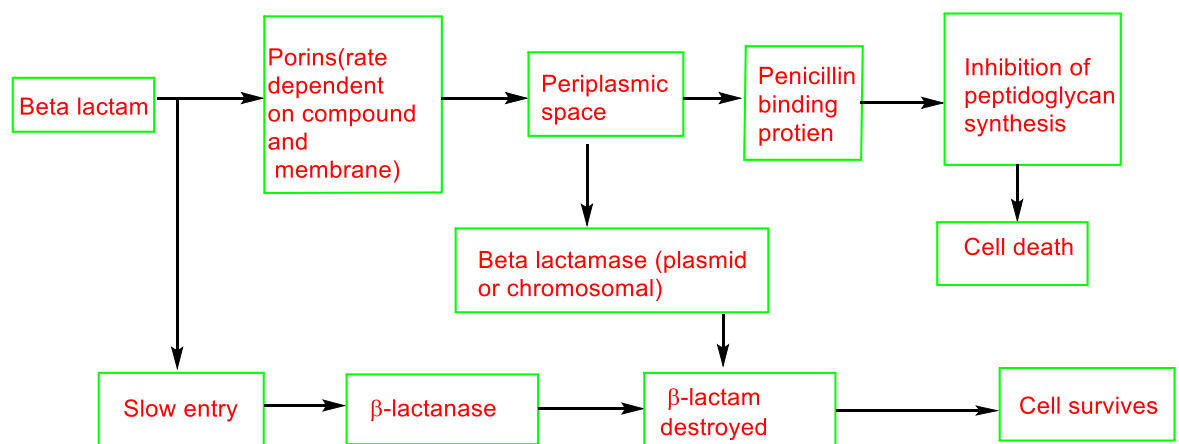
Scheme 1. 2: Diagram shows the natural resistance of Gram negative bacteria, *Pseudomonas aeruginosa*, to β-lactam antibiotics. (Taken from reference [44]).

3) Altered target site: in which the antibiotic may reach its target inside the bacterial cell but because of structural changes it would not affect any of the cellular components function. Cephalosporins, broad-spectrum antibiotics, introduce their bactericidal effect by the inhibition of cell wall synthesis. Binding to the penicillin binding proteins, responsible for the formation of integrating structures in the cell wall, peptidoglycan, leads to bacterial lysis and death. *Enterococci* bacteria exhibit resistance against cephalosporins by producing lower affinity proteins to cephalosporin than that of sensitive strains and therefore the formation of the peptidoglycan layer is not suppressed.[49, 50] The modified enzymes still function properly although they have a different structure.[51]

4) Bypass pathways: Production of an alternative target alongside the original one is considered one of the important mechanisms by which bacteria avoid antibiotic action. Methicillin resistant *Staphylococcus aureus* (MRSA) produce an alternative penicillin binding protein (PBP2a) that differs in structure to the normal one and thereby MRSA develops its resistance against penicillin-based antibiotics.[52]

1.1.6. Bacterial cell wall biosynthesis.

The biosynthesis process of the bacterial cell wall is a target of action of the most efficient antimicrobials.[53] The cell wall is defined as the peripheral layer that protects the bacterial cell from harmful environmental influences and changes in osmotic pressure, maintaining its integrity, shape and functionality.[54] The main function of the cell wall is mechanical support, therefore it is composed of supportive components, sugars and peptides, which are integrated together forming what is called peptidoglycan.[55] The sugar part is a thread of polysaccharides consisting of two alternating sugars, *N*-acetylglucosamine (GlcNAc) and *N*-acetylmuramic acid (MurNAc) units.[56] Both the latter units are cross-linked via covalent bonds to segments of peptide forming a stable polymer structure.[56] The core structure of the cell wall is synthesized inside the cytoplasm. The synthesis process starts with formation of what is called lipid II, which is transported to the outer surface (Scheme 1.3). At the outer surface, two type of enzymes exert their action on lipid II, transglycosylase and transpeptidase.[57] The former polymerises lipid II and the later enzyme connects peptide segments to each other via peptide linkages.[58] There are five amino acid units constituting the peptide part in the peptidoglycan layer, L-Ala, D-Glu, L-Lys, D-Ala and D-Ala, which are attached to the sugar units in a sequential manner.[58, 59]

1.1.7. Glycopeptide antibiotic resistance.

Two important examples of glycopeptide antibiotics are vancomycin and teicoplanin. They are bactericidal antibiotics that prevent cell wall synthesis. They are used for the treatment of Gram positive infections, such as skin infections and septicaemia.[60] They act specifically on the prevention of formation of the peptidoglycan through forming complexes with their precursors preventing their transfer to the cell wall. Hence, their integration into the cell wall would be prevented. Glycopeptides form a complex with the enzyme substrates rather than the enzymes themselves.[61],[60] Consequently, the substrate specificity of glycopeptide antibiotics is considered as a detriment to their activity rather than their enzyme affinity.[61, 62]
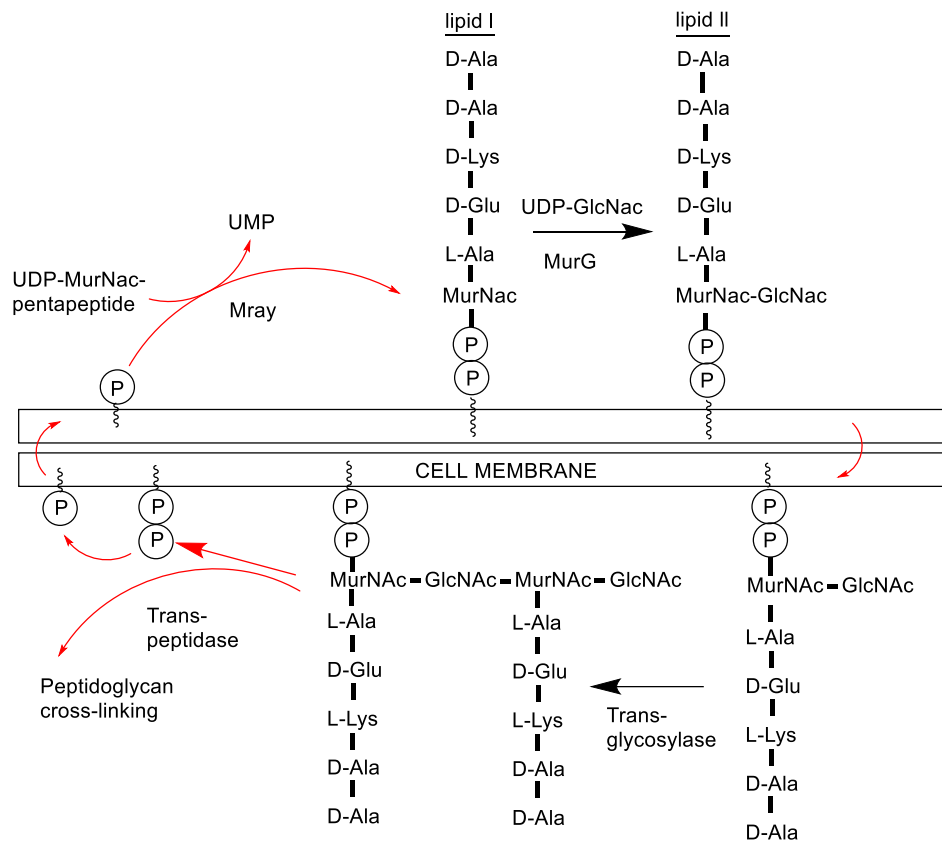
Scheme 1.3: The basic processes for cell wall biosynthesis in vivo. UMP=uridine-5'
monophosphate. (Taken from reference[63]).

Glycopeptide antibiotics complex with the peptidic part in the cell wall via hydrogen
bonding with the carboxylic acid terminal of the D-Ala residue. This complexation
occurs at the outer surface and no penetration of these antibiotics happens into the
cytoplasm.[61] This leads to accumulation of the complexes out of the cytoplasm rather
than their incorporation to the growing cell wall.[64] The resistant strain produces lower
affinity substrates than those produced by the sensitive bacteria to the glycopeptide
antibiotics. The genetic factors that are responsible for such changes are obtained
from external sources.[61]
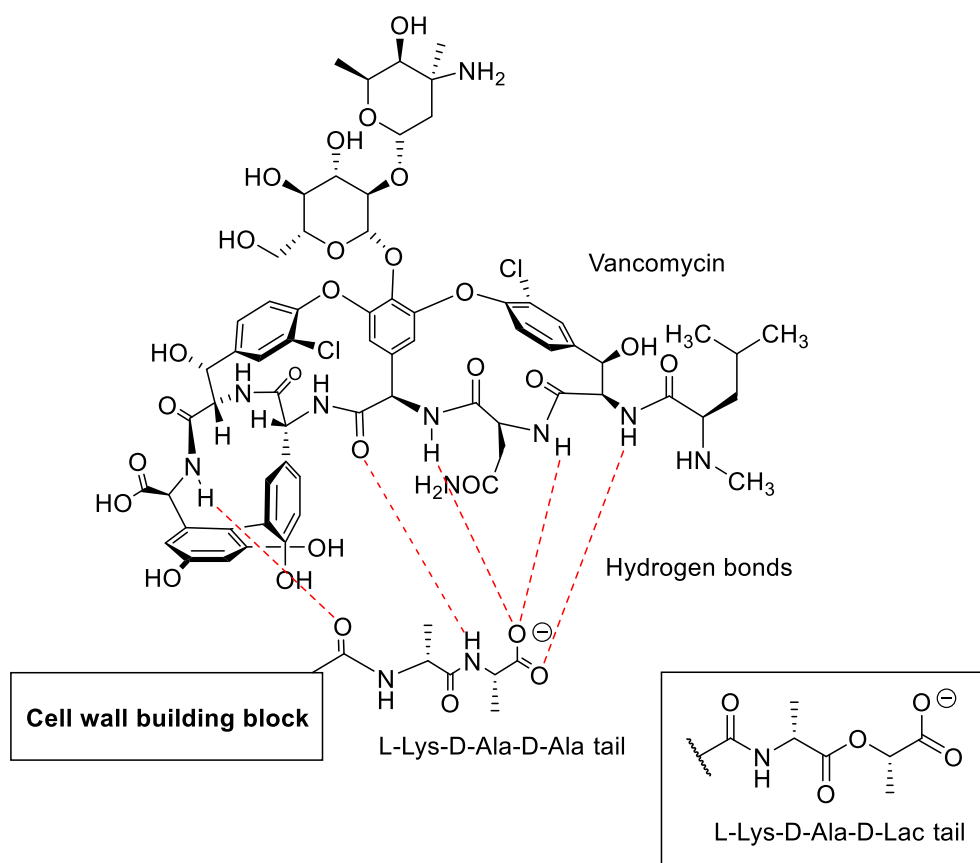
Figure 1. 3: Chemical interpretation of vancomycin inhibition to the peptidoglycan precursors via forming of five hydrogen bonds between vancomycin and carboxy-terminal D-alanine (D-Ala) residues of peptidoglycan precursors.

1.1.8. Vancomycin resistance.

Vancomycin is one of the most important members of the family of glycopeptide antibiotics. It acts mainly on Gram positive bacteria including MRSA. Its importance is derived from the fact that it is clinically the last antibiotic of resort acting against Gram positive including MRSA bacteria.[65] Recognition of a resistant strain of *Enterococci* to vancomycin in 1987 has increased concern that this resistance could be transferred to *S. aureus* bacteria.[60] Vancomycin exerts its action via binding to the terminal D-Ala-D-Ala residue in the peptide strand through five hydrogen bonds (Figure 1.3). Moreover, its bulky size and high molecular weight blocks further cross-linking between peptide segments that are necessary for the integrity of the peptidoglycan layer.[66] *Enterococci* acquired its resistance via acquisition of two types of genes, VanA and VanB. These genes have given the bacterial chromosomal system the ability to replace the terminal D-Ala residue with D-Lac. Thus, vancomycin would complex to the terminal peptide residue, D-Ala-D-Lac in resistant bacteria via

four hydrogen bonds instead of five to D-Ala-D-Ala in the susceptible strains. This change reduces vancomycin's affinity to its substrate by 1000-fold, which in turn results in a sharp decline in its efficiency.[67] The more the substrates carry the modified unit, the greater degree of resistance the bacteria gain.[65]

It is noteworthy that another genetic modification can also occur and contribute to antibiotic resistance: This involves changing the terminal dipeptide D-Ala-D-Ala to D-Ala-D-Ser. This change leads to a 7-fold reduction in the affinity of vancomycin to its substrates.[66]

1.2. The chemical structure of vancomycin.

The structure of vancomycin (Figure 1.4) consists of a sugar part and a peptide part. The peptide part involves seven amino acids, a heptapeptide backbone, and the sugar part consists of two sugar moieties glucose and vancosamine.[68] There are three macrocyles formed as a result of connections of the side chains of the heptapeptide backbone to each other. Two are 16-membered rings, C-O-D and D-O-E, formed as a result of linking the aromatic side chain of the amino acid-6 and amino acid-4, and between amino acid-2 and amino acid-4 respectively. Both are connected through biaryl ether bonds.[68] The third macrocycle is a 12-membered ring formed through a lactam linkage between the side chains of amino acid-6 and amino acid-7.[69] The disaccharide, is connected to the phenolic part of the central amino acid 4 through a β-glycoside linkage.[70],[71]

In addition, there are two chlorine atoms attached to the *ortho* positions of each of the aromatic ring side chains of amino acid-2 and amino acid-6.[72] These chlorine atoms are situated in opposite positions, one of them is affixed to the front of the compound, and the other is situated to the back.[68] It is noticeable that the glycopeptide antibiotics are structurally complex and affect their action on bacteria by more than one mechanism. Therefore, the study of the structure of this type of drug and the basic reasons behind its bacterial resistance is an attractive subject in the medicinal chemistry field.[73]

One approach to establishing a structure activity relationship (SAR) for vancomycin is through synthesis. This requires a relatively easy synthesis that can rapidly generate analogues. In the following section, the approaches to the synthesis of vancomycin and of analogues that have been disclosed to date, will be discussed.
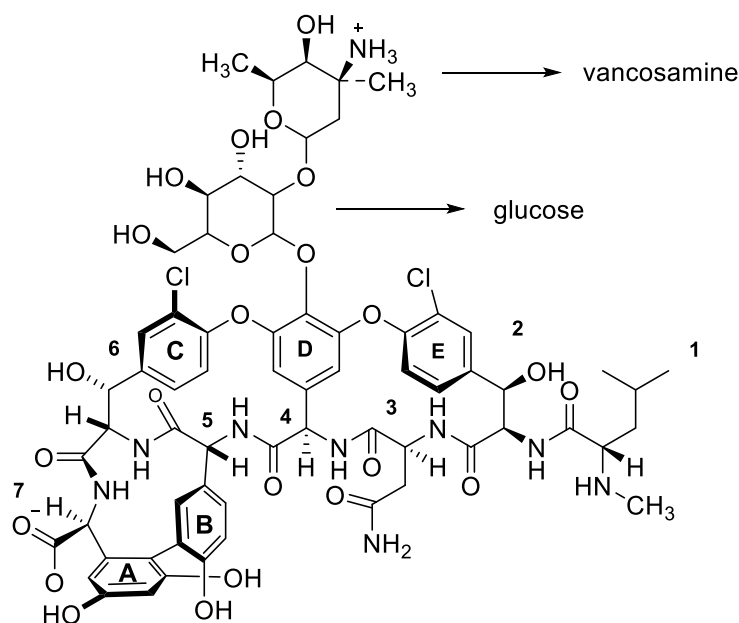
Figure 1. 4: The chemical structure of vancomycin.

1.3. Review of the chemical synthesis of vancomycin;

1.3.1. Solution phase synthesis of vancomycin.

The earliest reports of the total synthesis of vancomycin aglycon **1** (Figure 1.5) were made by David A. Evans,[74] and K. C. Nicolaou,[75, 76] in 1998 which both culminated in successful approaches. Although Nicolaou's approach was carried out in a liquid phase synthesis, it forms the basis for our approach to synthesise vancomycin on the solid phase.

In the Evans approach, the derivatives of the amino acid-4, amino acid-5, and amino acid-7 (Figure 1.6) were synthesised in a previous work.[74] The amino acid-6 was formed from reaction of (isothiocyanoacetyl)-oxazolidinone **2** with 3-chloro-4-flouro-5-nitrobenzaldehyde **3** (scheme 1.4) in an aldol reaction utilising stannous fluoride. This generated **4** in a stereoselective manner. Following *N*-Boc protection, the chiral auxiliary (Xp) was removed to give **5**.[77],[74]
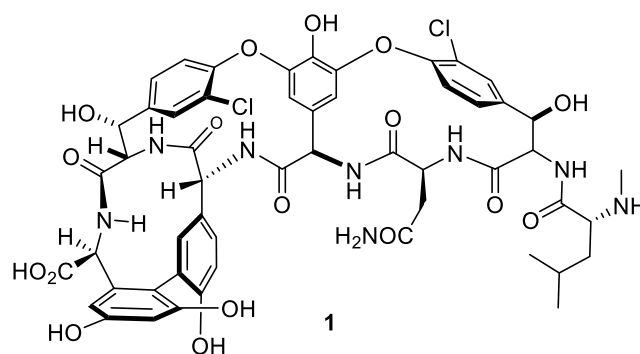
Figure 1. 5: The chemical structure of the vancomycin aglycon **1**.[74]

The latter was attached to amino acid-7 through peptide coupling, using the EDCl.HCl/HOBt system, affording dipeptide **6**. Cleavage of the endocyclic oxazolidinone of **6** could be performed using Li_2CO_3 in methanol to provide **7**. After removal of the Boc group, tripeptide **8** was obtained via coupling dipeptide **7** to the amino acid 5. The Boc group on amino acid 5 was exchanged with a trifluoroacetamide protecting group to give **9**.[74] The cyclic tripeptide (5-7) **10** was obtained via an oxidative reaction using VOF_3. After removal of the trifluoroacetamide protecting group using $NaHCO_3$ in $MeOH/H_2O$ generating amine compound **11**, incorporation of amino acid-4 to the latter was achieved via peptide coupling affording the tetrapeptide **12**.[74] Silyl de-protection of the phenol group of the ring 4 was affected under fluoride (HF· pyridine) to give **13**.

amino acid-4   amino acid-5   amino acid-7
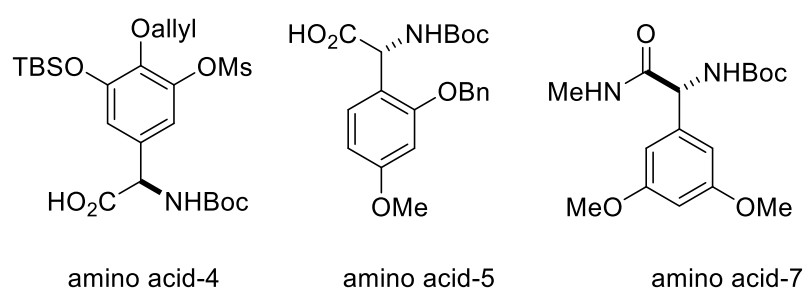
Figure 1. 6: Derivatives of amino acids 4, 5, and 7 in vancomycin.
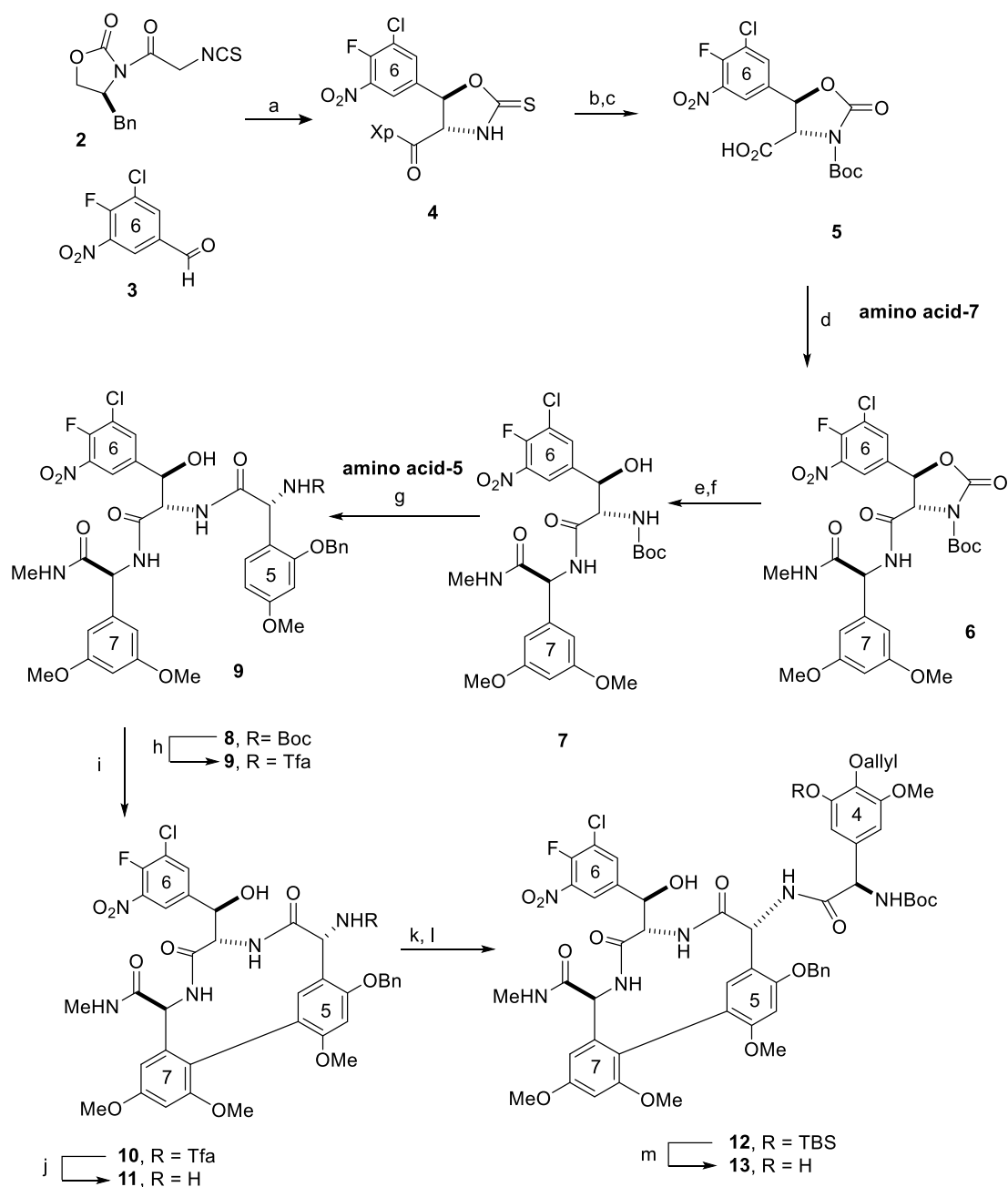
Scheme 1. 4: Synthesis of the cyclic tetrapeptide (5-7). a) Sn(OTf)$_2$, *N*-ethylpiperidine, THF, -78 °C, then **3**; b) Boc$_2$O, DMAP, CH$_2$Cl$_2$, then 1:1 HCO$_2$H/30% H$_2$O$_2$; c) 3.1 equiv LiOOH, -5 °C, 1.2 equiv LiOOH, -10 °C; d) amino acid 7, TFA, DMS, CH$_2$Cl$_2$, 0 °C, then **5**, EDCl.HCl, HOBt, CH$_2$Cl$_2$/DMF, 0 °C; e) Li$_2$CO$_3$, MeOH, rt; f) LiOH, MeOH/H$_2$O; g) TFA, DMS, CH$_2$Cl$_2$, 0 °C, then amino acid-5, EDCl.HCl, HOBt, THF, 0 °C; h) TFA, DMS, CH$_2$Cl$_2$, 0 °C, then TFAA, 2,6-lutidine, CH$_2$Cl$_2$, rt; i) VOF$_3$, BF$_3$.Et$_2$O, AgBF$_4$, TFA/CH$_2$Cl$_2$, 0 °C, then NaHB(78)$_3$; j) NaHCO$_3$, MeOH, H$_2$O, rt, 6 d; k) amino acid-4, HATU, HOAt, collidine, CH$_2$Cl$_2$/DMF, -20 °C, 16 h; l) Isobutyl chloroformate, *N*-methylmorpholine, EtOAc, -10 ⟶ -5 °C, 30 min, then amino acid-4 in EtOAc/DMF, -20 °C ⟶ rt, 2 h; m) HF. pyridine, THF, rt, 1 h.

Cyclisation of the 6-4 ring was carried out using Na_2CO_3, (DMSO, rt) to give the bicyclic peptide **14** in a relatively rapid reaction (1.5 h) (Scheme 1.5). The authors argued that the presence of the chloride substituent enhances the electrophilicity to get such fast cyclisation. Also, the dissolution of compound **13** in the aprotic solvent, DMSO, has an impact on the rate of the reaction without added base (Scheme 1.5).[74] Submission of the bicyclic **14** to a palladium catalysed reduction deprotected both the aryl triflate and the phenolic allyl group on ring-5 and on ring-4 respectively giving phenol **15**. Bicyclic peptide **16** was obtained after replacement of the Boc group with Tfa and protection of the phenol group of ring-4 with pivaloyl chloride. The bicyclic peptide **17** with required *S* configuration (95:5) was given via deprotection of the methyl ether groups on rings 5 and 7 followed by 5-7 ring atropisomerisation (MeOH, 55 °C, 24 h). To prepare the bicyclic tetrapeptide **17** for the final peptide coupling in Evan's approach, hydroxyl groups on rings 7 and 5 were benzylated. Protection of the phenolic hydroxyl group of the amino acid-4 with allyl protecting group and removal of mesylate and trifluoroacetamide afforded the free amine bicyclic tetrapeptide **18**.[74]

Coupling of **18** (EDCI.HCl, HOAt, THF, 0 °C) with the prepared tripeptide **19,** previously described by Evans[79] (Scheme 1.6), afforded heptapeptide **20** without apparent epimerisation. The tricyclic core of vancomycin **21** was obtained via intramolecular S_NAr cyclisation with excess of desired R configuration of 2-4 ring by 5:1. By reduction and purification of the nitro atropisomers mixture, followed by Sandmeyer transformation, a single atropisomer of the protected vancomycin aglycon **22** was obtained. Compound **23** with the free carboxylic terminal group was afforded by selective removal of the *N*-methyl amide function through nitrosation and treatment with lithium hydrogen peroxide. Finally, vancomycin aglycon **1** was obtained through deprotection of **23**.[74]
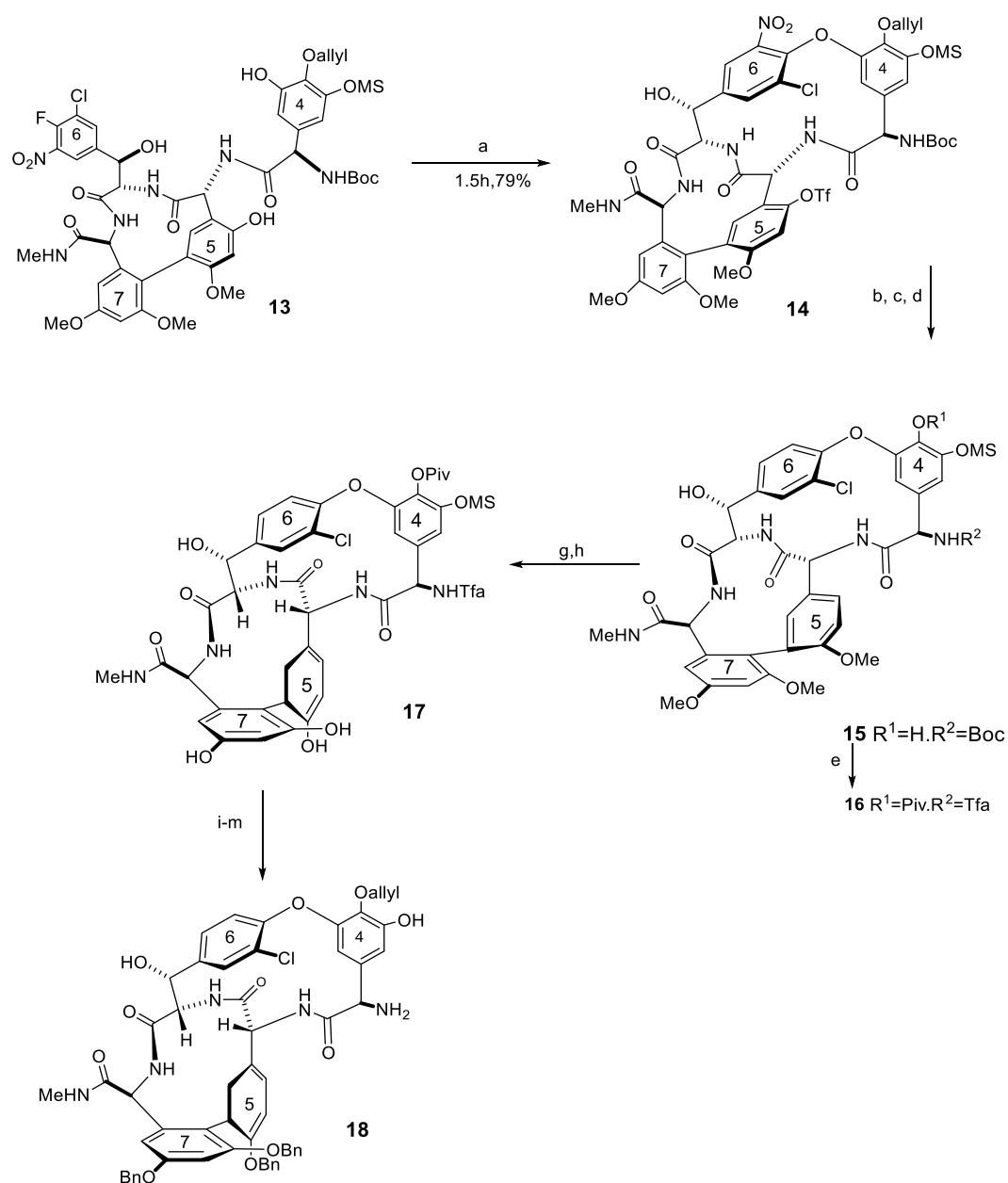
Scheme 1. 5: Synthesis of the bicyclic tetrapeptide. Synthesis of the M (4-6) (5-7) bicyclic tetrapeptide. a) Na$_2$CO$_3$, DMSO, rt, 1.5 h, then Tf$_2$NPh, 1 h; b) Zn^0, HOAc, EtOH, 40 °C; c) NaNO$_2$, H$_3$PO$_2$, cat. Cu$_2$O, THF/H$_2$O, 0 °C, 1 h; d) [Pd(dppf)Cl$_2$] ´CH$_2$Cl$_2$, Et$_3$N, HCO$_2$H, DMF, 75 °C; e) PivCl, Et$_3$N, THF, rt; f) TFA, DMS, CH$_2$Cl$_2$, 0 °C, then TFAA, 2,6-lutidine, CH$_2$Cl$_2$, 0 °C to rt; g) AlBr$_3$, then EtSH, 0 °C; h) MeOH, 55 °C; i) BnBr, Cs$_2$CO$_3$, Bu$_4$NI, DMF, 0 °C; j) LiSEt, THF, 0 °C; k) allyl-Br, Cs$_2$CO$_3$, DMF, 0 °C; l) LDA, THF, -78 °C; m) LiOH, THF/H$_2$O/MeOH, 0 °C.
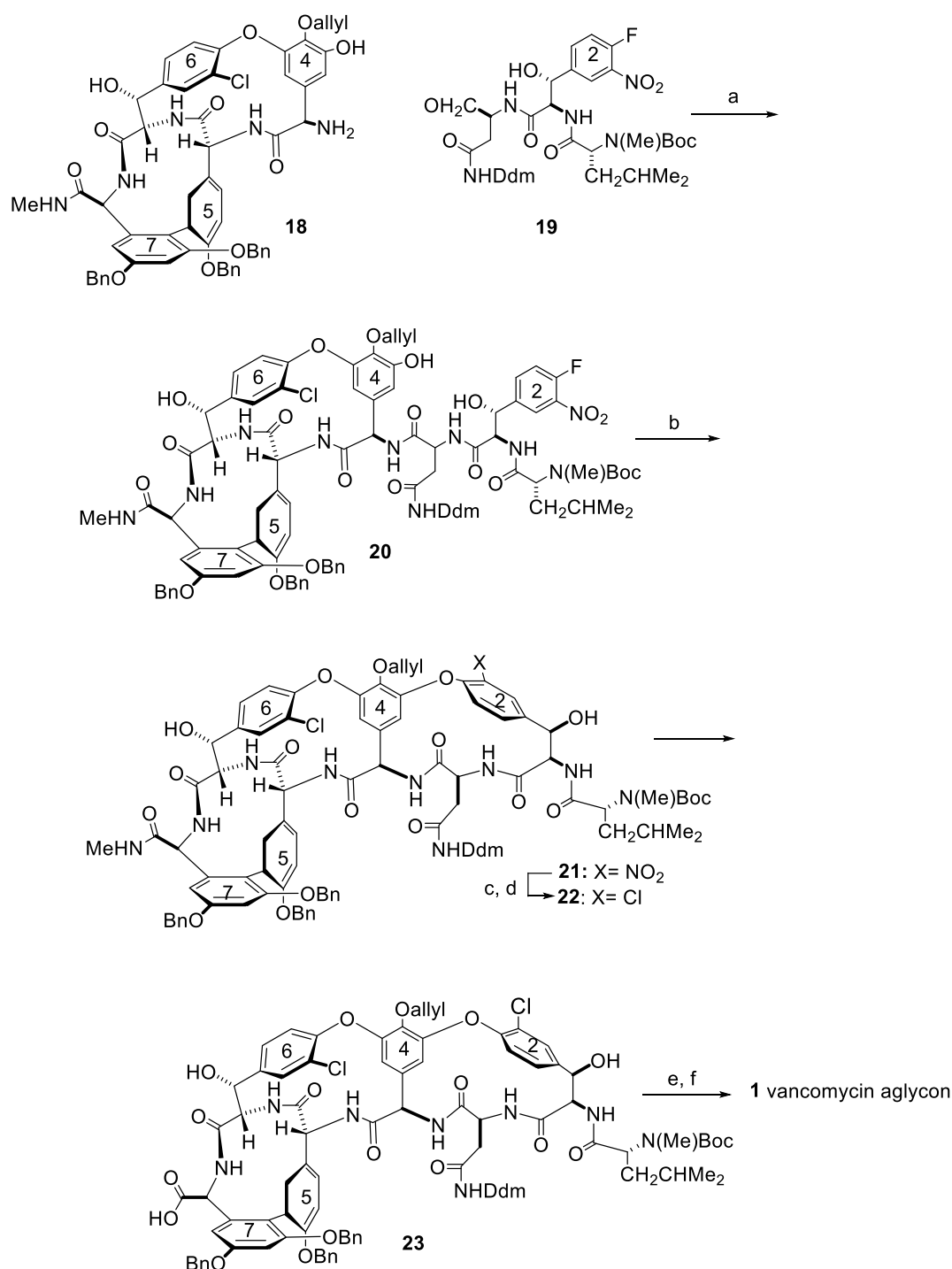
Scheme 1. 6: Assemblage of the vancomycin aglycon **1**. a) EDCI, HOAt, THF, 0 °C; b) CsF, DMSO, rt; c) Zn^0, HOAc, EtOH, 40 °C; d) HBF$_4$, t-BuONO, MeCN, then CuCl, CuCl$_2$, H$_2$O; e) N$_2$O$_4$, NaOAc, CH$_2$Cl$_2$/CH$_3$CN, 0 °C; f) H$_2$O$_2$, LiOH, THF/H$_2$O.

In the same year, Nicolaou and co-workers synthesised the vancomycin aglycon adopting a triazene-driven method for cyclisation of the C-O-D and D-O-E rings.[75] As it has been argued in the literature, its facile formation and removal, and its lability to chemical manipulation were the reasons behind choosing the triazene moiety. The

possibility of triazene conversion to the required aromatic phenol to be the acceptor for the sugar part of the vancomycin addressed one of the targeted steps in the synthesis. Herein, all the synthesis strategies of the seven vancomycin amino acids that were conducted by Nicolaou et al, will be discussed. As noted earlier, Nicolaou's approach for the synthesis of vancomycin building units in solution phase represents the starting point for the current work towards the solid phase synthesis of vancomycin.

The synthesis of the amino acid-6, started with commercially available 4-hydroxy benzaldehyde **24**, which was benzylated to afford **25** (Scheme 1.7). Using a Horner-Wadsworth-Emmons reaction with $(EtO)_2P(O)CH_2COOEt$, styrene **26** was obtained.[75] The latter was subjected to the Sharpless asymmetric aminohydroxylation reaction that afforded directly the required Cbz-protected amino alcohol **27** in 87% ee. The hydroxyl group in **27** was then protected using TBSOTf, and the resulting compound **28** was subjected to hydrogenolysis, which caused cleavage of both the benzyl and Cbz groups, affording phenol **29**. Finally, chlorination of **29** at the *ortho* position was carried out with SO_2Cl_2, resulting in the production of the desired building unit **30**.[75]
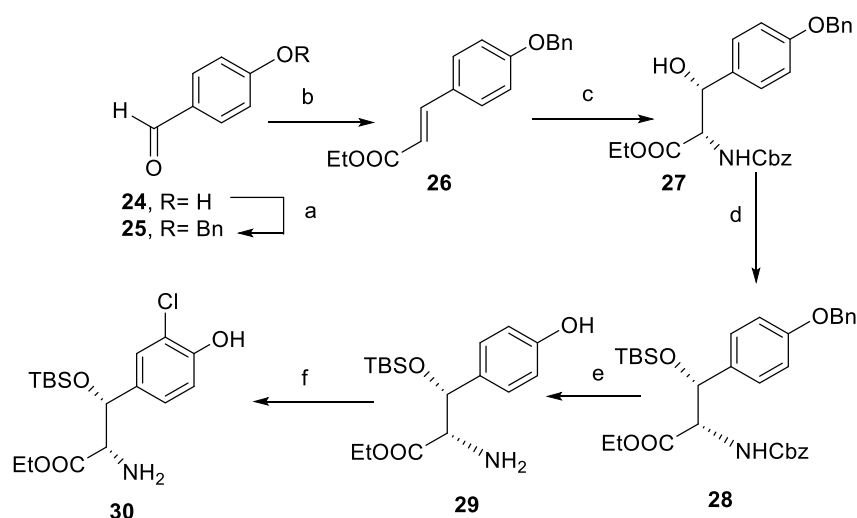
Scheme 1. 7: Synthetic route of the compound **30**. Reagents and conditions: a) K_2CO_3 (1.5 equiv), BnBr (1.0 equiv), KI (0.1 equiv), DMF, 25 °C, 12 h, 98%; b) $(EtO)_2(O)PCH_2$-COOEt (1.1 equiv), KOH (1.5 equiv), THF, 25 °C, 12 h, 95%; c) NaOH (3.0 equiv), $BnOCONH_2$ (3.1 equiv), *t*-BuOCl (3.0 equiv), $(DHQD)_2AQN$ (0.05 equiv), $K_2[OsO_2(OH)_4]$ (0.04 equiv), *n*-PrOH:H_2O (1:1), 25 °C, 12 h, 45% (87% ee); d) TBSOTf (1.1 equiv), 2,6-lutidine (1.5 equiv), CH_2Cl_2, 0 °C, 0.5 h, 98%; e) H_2, $Pd(OH)_2/C$ (0.01 equiv), MeOH, 0.5 h, 95%; f) SO_2Cl_2 (1.0 equiv), Et_2O (3.0 equiv), CH_2Cl_2, 0 °C, 1 h, 80%.

For the synthesis of the central amino acid-4, 4-aminobenzoic acid **31** was used as the SM (Scheme 1.8). Thus, after methylation and bromination, dibromide **33** was formed through methyl ester **32**. Reduction of the methyl ester using LiAlH$_4$ afforded alcohol **34.** Triazene compound **35** was synthesised via a two step-reaction. The first step is the diazotization of the amino group by NaNO$_2$ furnishing the diazonium salt, which was then treated with pyrrolidine to give triazene **35**. Using PCC, oxidation of the alcohol to the aldehyde **36** was carried out. The latter was converted to a terminal olefin **37** by Wittig olefination. Asymmetric dihydroxylation using AD-mix-α, was performed affording diol **38** in 95% *ee*. Reaction of the primary alcohol in **38** with TBSCl afforded TBS-protected **39**. Conversion of the alcohol **39** to the azide compound **40** was conducted with DPPA via a Mitsunobu reaction. The azide compound was then reduced to the desired amine **41** using Ph$_3$P. After Boc protection of the amino group to give **42**, desilylation of the primary alcohol with TBAF afforded **43.** The latter was oxidised with TEMPO to give the required building unit **44**.[75]

The synthesis of amino acid-5, which is equivalent to compound **49** was accomplished using 4-hydroxyphenyl glycine **45** as SM (Scheme 1.9). Methylation of **45** in methanol and TMSCl gave the methyl ester **46**, followed by Boc protection to the amino group affording **47**. Methylation of the phenol group with MeI gave the fully protected compound **48**.
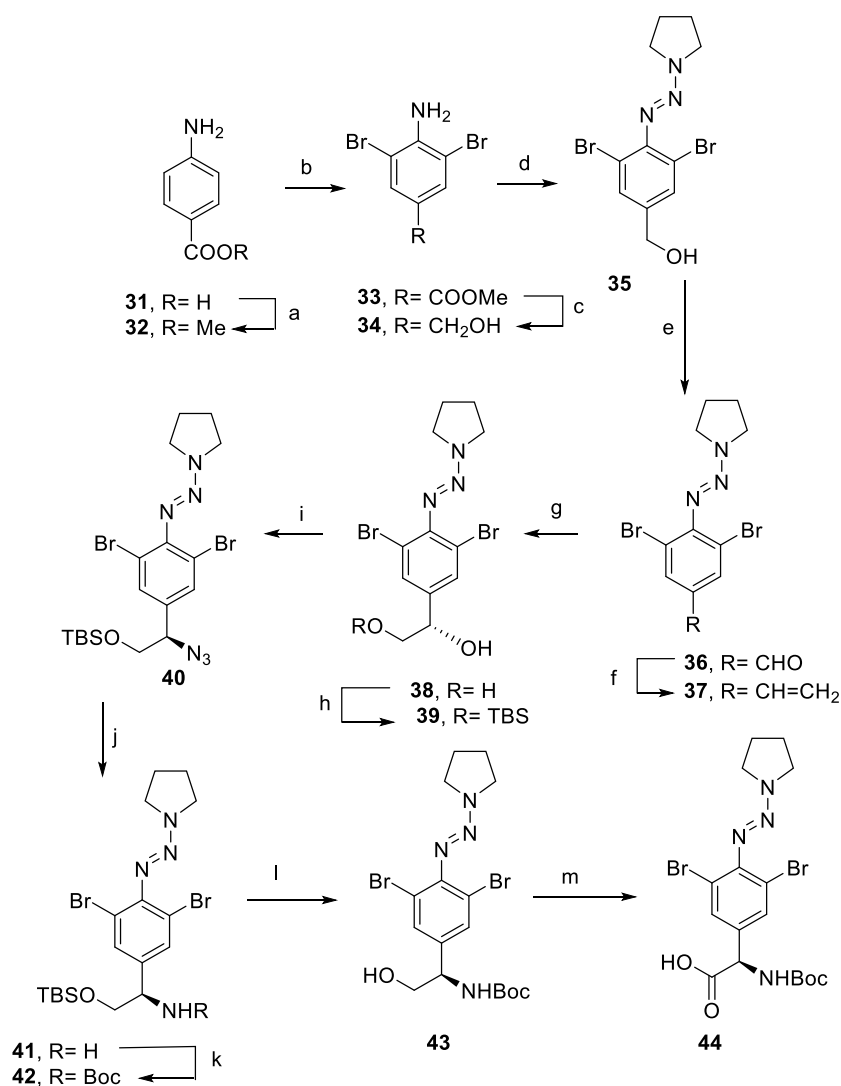
Scheme 1. 8: Synthesis of the central amino acid-4 derivative. Reagents and conditions: a) $SOCl_2$ (1.0 equiv), MeOH, reflux, 2 h, 100%; b) Br_2 (2.0 equiv), AcOH, 25 °C, 0.5 h, 98%; c) $LiAlH_4$ (1.5 equiv), THF, 0 °C, 2 h, 95%; d) 6 M HCl (5.0 equiv), $NaNO_2$ (1.2 equiv), AcOH:H_2O (1:2), 0 °C, 0.5 h, then KOH (8.0 equiv), pyrrolidine (1.5 equiv), 0 °C, 0.5 h, 75%; e) PCC (1.5 equiv), CH_2Cl_2 , 25 °C, 2 h, 88%; f) n-BuLi (1.4 equiv), CH_3PPh_3Br (1.5 equiv), THF, -20 °C, 2 h, 92%; g) AD-Mix-α (1.4 gmmol^{-1}), t-BuOH/H_2O (1:1), 6 h, 95%, (95% ee); h) TBSCl (1.1 equiv), imidazole (1.5 equiv), DMF, 0 °C, 5 h, 88%; i) Ph_3P (2.5 equiv), DEAD (2.5 equiv), DPPA (2.5 equiv), THF, 0 °C, 2 h, 79%; j) Ph_3P (3.0 equiv), H_2O (10.0 equiv), THF, 60 °C, 3 h, 78%; k) $(80)_2O$, Et_3N,CH_2Cl_2 , 25 °C , 4 h, 95%; l) TBAF (1.2 equiv), THF, 0 °C, 2 h, 93%; m) TEMPO (1.0 equiv), 5% aq. NaOCl (3.0 equiv), 5% $NaHCO_3$, KBr (0.05 equiv), Me_2CO, 0 °C, 1 h, 75%.

The final step involved a regioselective iodination using I_2 and trifluoroacetate, which produced the desired amino acid 5 (**49**).[75]

The boronic acid derivative **54,** which is equivalent to amino acid-7 was synthesised from 3,5-dimethoxy benzaldehyde **50** (Scheme 1.9). Thus, Wittig olefination was

performed to give styrene compound **51**. Via Sharpless asymmetric dihydroxylation, the diol **52** was afforded. Selective monobenzylation to the terminal hydroxyl group was carried out giving **53**. Finally, the desired building block **54** was obtained by lithiation with *n*-BuLi followed by quenching with $B(OMe)_3$.

45, R= H ⌐ a
46, R= Me ◄─┘

47, R= H ⌐ c   **49**
48, R= Me ◄─┘

50, R= CHO ──┐ e
51, R= CH=CH2 ◄┘

52, R= H ──┐ g
53, R= Bn ◄─┘

54
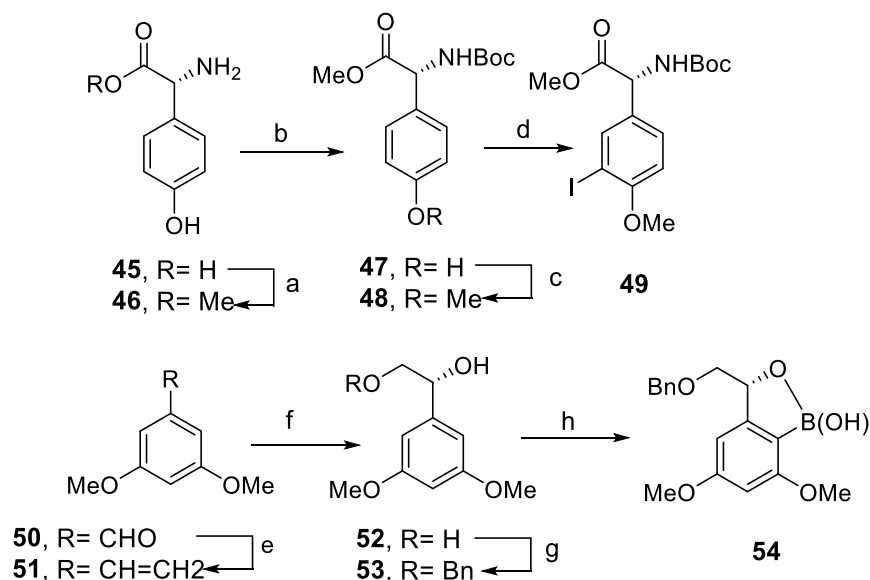
Scheme 1. 9: Synthetic route of the amino acid-5 and amino acid-7. Reagents and conditions: a) TMSCl (2.1 equiv), MeOH, 25 °C,15 h, 98%; b) (8O)$_2$O (1.1 equiv), K_2CO_3 (4.0 equiv), dioxane: H_2O (1:1), 25 °C, 4 h, 95%; c) MeI (2.0 equiv), K_2CO_3 (4.0 equiv), DMF, 25 °C, 6 h,93%; d) I_2 (1.2 equiv), CF_3COOAg (2.2 equiv), $CHCl_3$, 25 °C, 12 h, 90%; e) *n*-BuLi (1.3 equiv), $CH_3PPh3Br$ (1.5 equiv), THF, -20 °C, 10 h, 91%; f) AD-β (1.4 gmmol^{-1}), *t*-BuOH/H$_2$O (1:1), 25 °C, 8 h, 92% (96% ee); g) *n*-Bu$_2$SnO (1.0 equiv), toluene, reflux, 1 h, then BnBr (1.5 equiv), *n*-Bu$_4$NI (0.5 equiv), 70 °C, 2 h, 89%; h) *n*-BuLi (2.2 equiv), benzene, 0 ⟶ 25 °C, 2 h, then $B(OMe)_3$, THF, -78 °C ⟶ 25 °C, 6 h, dilute HCl, 55%.

The amino acid-5 and amino acid-7, compounds **49** and **54** respectively, were coupled to each other using a Suzuki coupling reaction (Pd(Ph$_3$P)$_4$, Na$_2$CO$_3$, 90 °C) giving the desired atropisomer **55** in an excess ratio (2:1) (Scheme 1.10). After chromatographic separation, the latter was converted to azide **56** using a Mitsunobu reaction. To prepare this biaryl compound **56** for the peptide coupling with amino acid-6, it was hydrolysed with LiOH to its carboxylic acid form **57** (Scheme 1.10).[75]
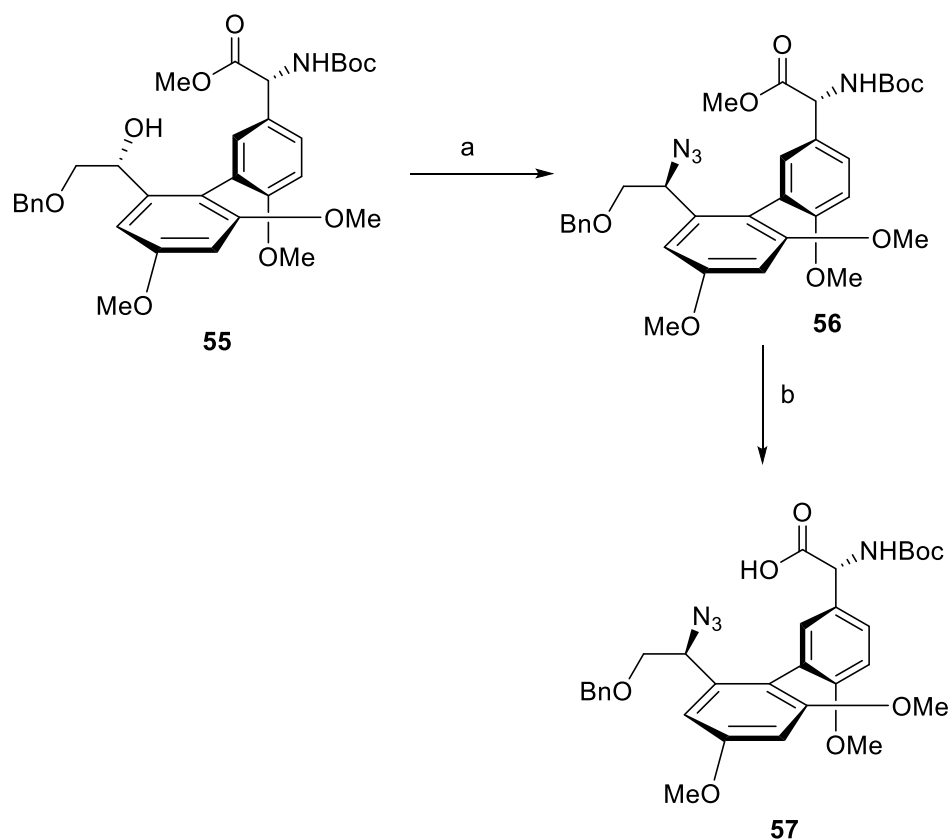
Scheme 1. 10: Synthesis of the compound **57**, carboxylic acid form. Reagents and conditions. a) DPPA (2.5 equiv), DEAD (2.5 equiv), Ph$_3$P (2.5 equiv), THF, -20 °C, 2 h, 95%, b) LiOH (1.5 equiv), THF/H$_2$O (1:1), 0 °C, 0.5 h, 99%.(75)

The coupling of biaryl compound **57** to compound **30** was accomplished using (EDC/HOAt) and afforded tripeptide **58** (Scheme 1.11).[81] The Boc group was deprotected using excess of TMSOTf to prepare the amine tripeptide **59** for the subsequent coupling reaction to compound **44** (amino acid-4). Thus, the amine tripeptide was coupled to compound **44** using EDC/HOAt affording tetrapeptide **60** (Scheme 1.11). Then, C-O-D ring closure of **60** was accomplished using CuBr· SMe$_2$, K$_2$CO$_3$, and pyridine in CH$_3$CN with reflux and resulted in equal ratios (1:1) of the two atropisomers **61a** and **61b**.

Both atropisomers were taken through three steps of reactions; TBS deprotection affording **62a** and **62b**, reduction of azide giving **63a** and **63b**, and hydrolysis of the ethyl ester furnishing **64a** and **64b**. For the AB ring closure, the latter two atropisomers were exposed to macrolactamisation reaction using FDPP and iPr$_2$NEt in DMF giving the two atropisomers **65a** and **65b** of AB/COD ring system (Scheme 1.12).[75, 81]
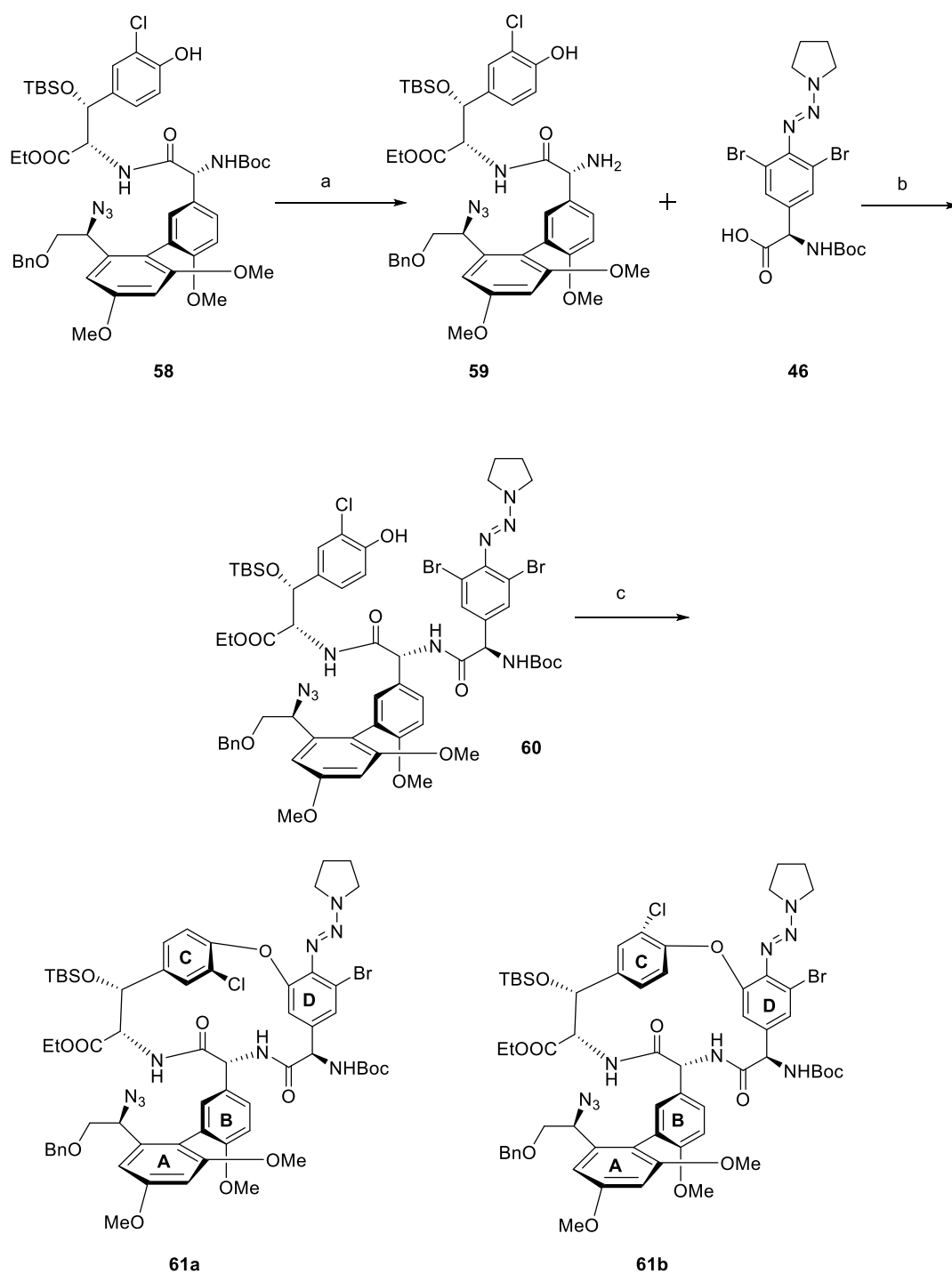
Scheme 1. 11: Synthetic route of compound **60** and closure of C-O-D ring. Reagents and conditions. a) 3.3 equiv of TMSOTf, 3.0 equiv of 2,6-lutidine, CH_2Cl_2 , 0 °C, 3 h, 90%; b) EDC (3.0 equiv), HOAt (3.3 equiv), THF, -5 °C, 12 h, 76%; c) CuBr .SMe$_2$ (3.0 equiv), K_2CO_3 (3.0 equiv), pyridine (3.0 equiv), MeCN, reflux, 20 min, ca. 1:1 ratio of atropisomers, 60% combined yield.[75]
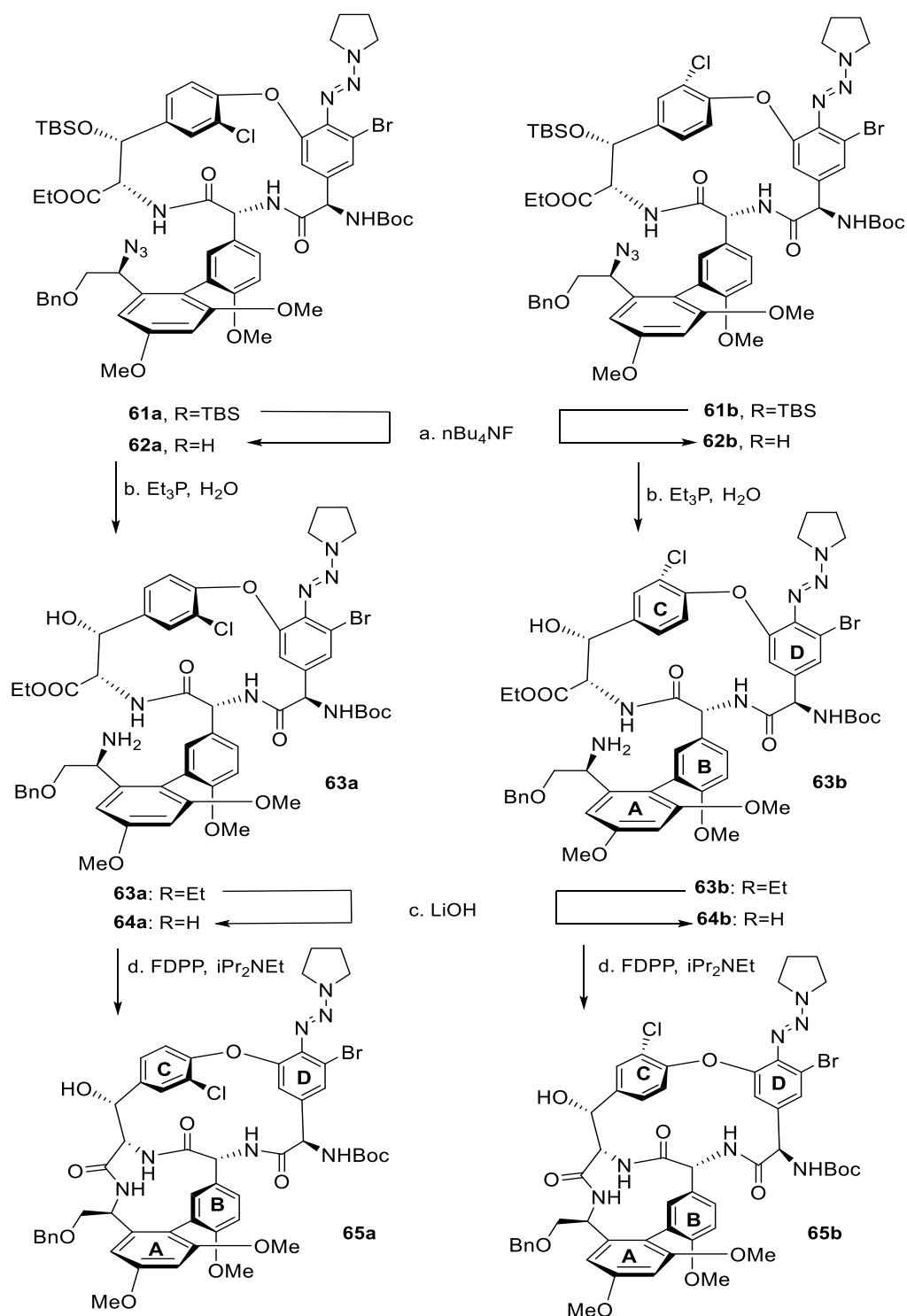
Scheme 1. 12: Construction of AB/C-O-D bicyclic systems **65a** and **65b** from natural biaryl system. a) 1.1 equiv of *n*-Bu4NF, THF, -25 → -15 °C, 3 h, 95% of **62a**, 98% of **62b**; b) 2.0 equiv of Et₃P, MeCN/H₂O (4:1), 25 °C, 20 h, 78% of **63a**, 79% of **63b**; c) 5.0 equiv of LiOH, THF/H₂O (1:1), -5 → 0 °C, 10 min, 92% of **64a**, 90% of **64b**, crude yields; d) 3.0 equiv of FDPP, 5.0 equiv of iPr₂NEt, DMF, 0 → 25 °C, 12 h, 86% of **65a**, 60% of **65b**.[81]

In order to complete the synthesis of the whole AB-COD-DOE complex, Nicolaou and co-workers needed to synthesise the rest of the molecule, amino acids-1, amino acid-2 and amino acid-3.[76] Thus, the derivative of the amino acid-2 was prepared using the previously synthesised intermediate, ethyl cinnamate **26** (Scheme 1.13)**,** via the following four-step sequence: 1) Sharpless asymmetric dihydroxylation of the double bond to give **66**, 2) protection of the hydroxyl group with nosyl protecting group afforded **67**, 3) production of azide **68** using NaN$_3$, 4) finally, reduction of the azide with SnCl$_2$ furnished the desired amino acid-2 derivative, compound **69**.[76]

For the synthesis of the amino acid-3 derivative, compound **72,** asparagine was used as the SM (Scheme 1.14). After protection of both nitrogen with Cbz, and Ddm to afford compound **70**, the carboxylic acid group was methylated using MeI giving compound **71**. Then, the Cbz was removed via hydrogenolysis to afford the required asparagine derivative **72.** For the amino acid-1 unit, the commercially available *N*-methyl leucine Boc derivative **73** was used (Figure 1.7).
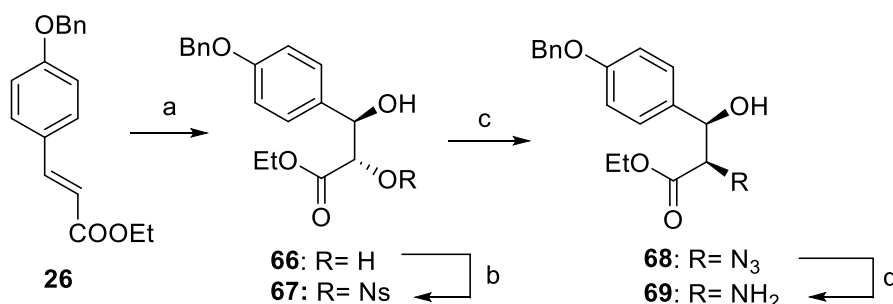
Scheme 1. 13: Synthesis pathway of amino acid-2 derivative, compound **69**. Reagents and conditions: a) AD-β, (1.4 gmmol^{-1}), MeSO$_2$NH$_2$ (1.0 equiv), *t*-BuOH/H$_2$O (1:1), 25 °C, 12 h, 79% (92% ee); b) NsCl (1.0 equiv), Et$_3$N (2.0 equiv), DMF, 0 °C, 5 h, 60%; c) NaN$_3$ (1.5 equiv), DMF, 55 °C, 12 h, 90%; d) SnCl$_2$.H$_2$O (2.0 equiv), MeOH, 25 °C, 2 h, 90%.
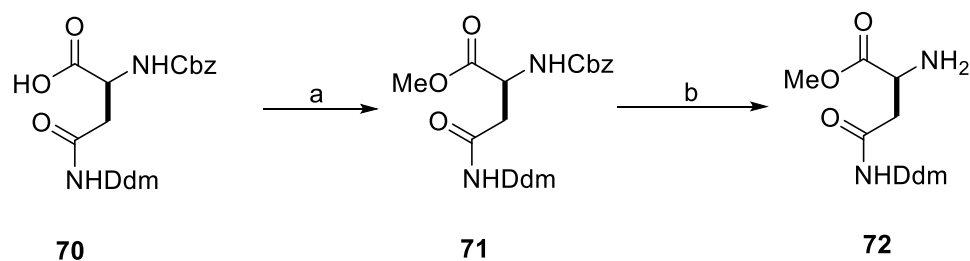
Scheme 1. 14: Synthestic route of the amino acid-3 derivative. Reagents and conditions: a) MeI (2.0 equiv), K_2CO_3 (2.0 equiv), DMF, 25 °C, 12 h, 70%; b) H_2, 20 wt% $Pd(OH)_2$/C, MeOH, 25 °C, 1 h, 99%.[76]
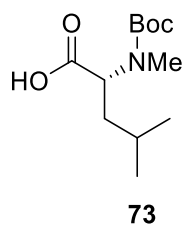
Figure 1. 7: *N*-methyl leucine Boc derivative.

These three amino acids, -1, -2 and -3, were assembled to form the desired tripeptide **80** of the vancomycin heptapeptide backbone (Scheme 1.15). Thus, by coupling **69** to **73** using EDC/HOBt the dipeptide **74** was formed. To have it ready for the subsequent coupling to **72**, amino acid-3, the dipeptide ethyl ester was hydrolysed to its carboxylic form **75** using LiOH. The third amino acid was attached using EDC/HOAt leading to formation of the tripeptide **76**. Protection of the hydroxy group of the latter with TBSOTf giving **77**, cleavage of the benzyl group by hydrogenolysis to give **78,** chlorination at *ortho* position using SO_2Cl_2 to furnish **78,** and hydrolysis of the methyl ester using LiOH, in consequent reactions afforded the requisite tripeptide **80**.[82]
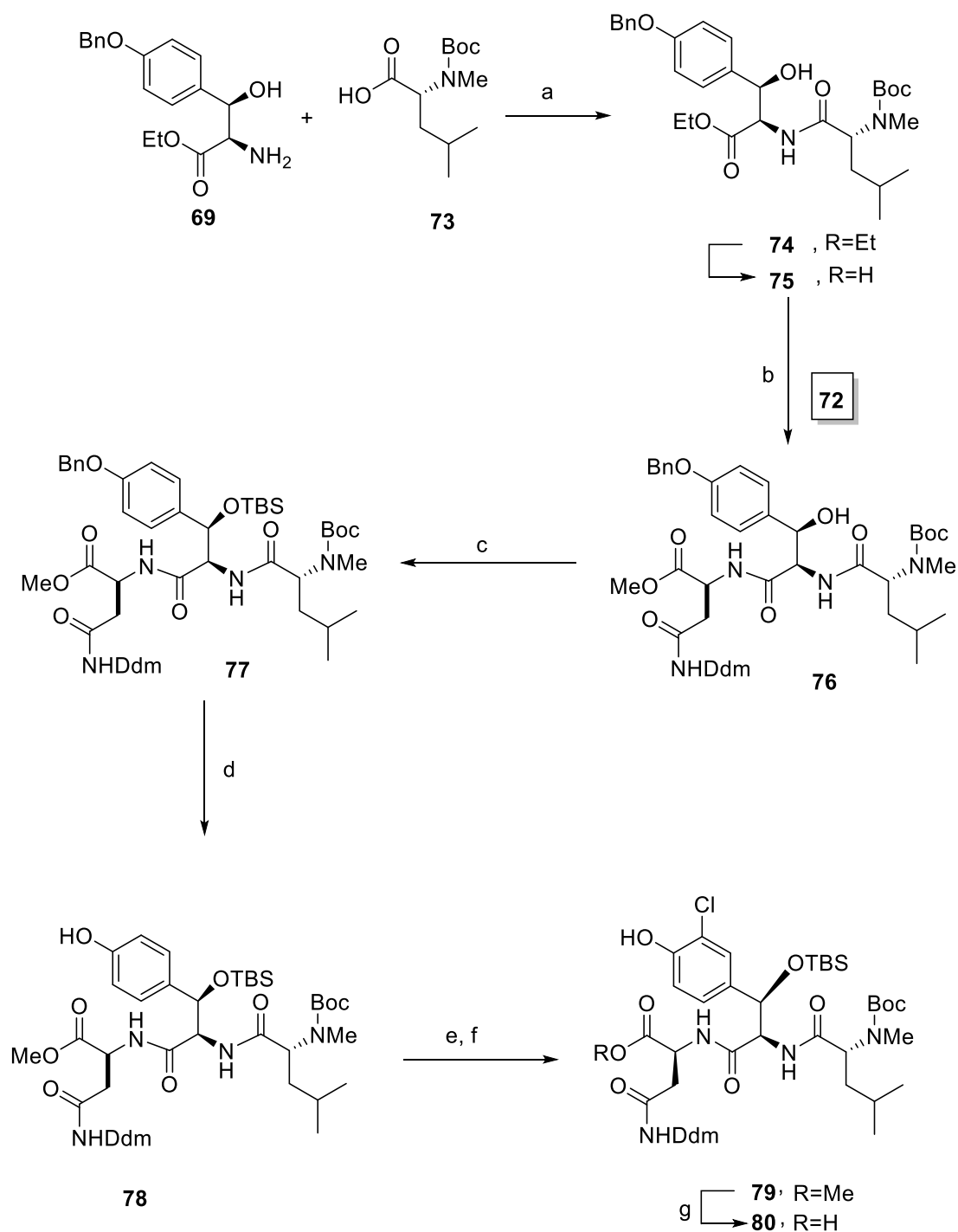
Scheme 1. 15: Synthesis of tripeptide **80**.(82) a) 3.0 equiv of EDC, 3.3 equiv of HOBt, THF, 0 °C, 12 h, 93%; b) 2.0 equiv of LiOH, THF/H$_2$O (1:1), 0 °C, 1 h, 99%; c) 3.0 equiv of EDC, 3.3 equiv of HOAt, THF, 0 °C, 12 h, 82%; d) 1.3 equiv of TBSOTf, 2.2 equiv of 2,6-lutidine, CH$_2$Cl$_2$, 0 °C, 2 h, 81%; e) H$_2$, 20% Pd(OH)$_2$/C, MeOH, 25 °C, 1 h, 99%; f) 1.1 equiv of SO$_2$Cl$_2$, Et$_2$O, 0 °C, 75%; g) 4.0 equiv of LiOH, t-BuOH/H$_2$O (2:1), 0 °C, 0.5 h, 95%.

Before the coupling process between the two synthesised parts of vancomycin, the tetrapeptide and the tripeptide, the natural atropisomer of the tetrapeptide **65a** was Boc-deprotected using an excess of TMSOTf. The resulting natural amino form of the tetrapeptide **81a** was taken through the coupling process with the tripeptide part **80**.[81] The coupling was performed using the EDC/HOAt system furnishing the uncyclised-D-O-E ring heptapeptide **82**. The cyclisation process to the D-O-E ring was carried out using (CuBr·Me$_2$S, K$_2$CO$_3$, pyr·CH$_3$CN Δ), furnishing the targeted polycyclic intermediate in a good yield as a mixture of the two atropisomers **83a** and **83b** (Scheme 1.16).[81] Nicolaou and co-workers then converted the triazene into the required phenol group for the glycosidation reaction and universally deprotected the polycyclic intermediate in preparation for the synthesis of vancomycin itself. In the following work,[83] he was able to end up with the synthesis of the whole vancomycin structure after attachment of the two sugar moieties.
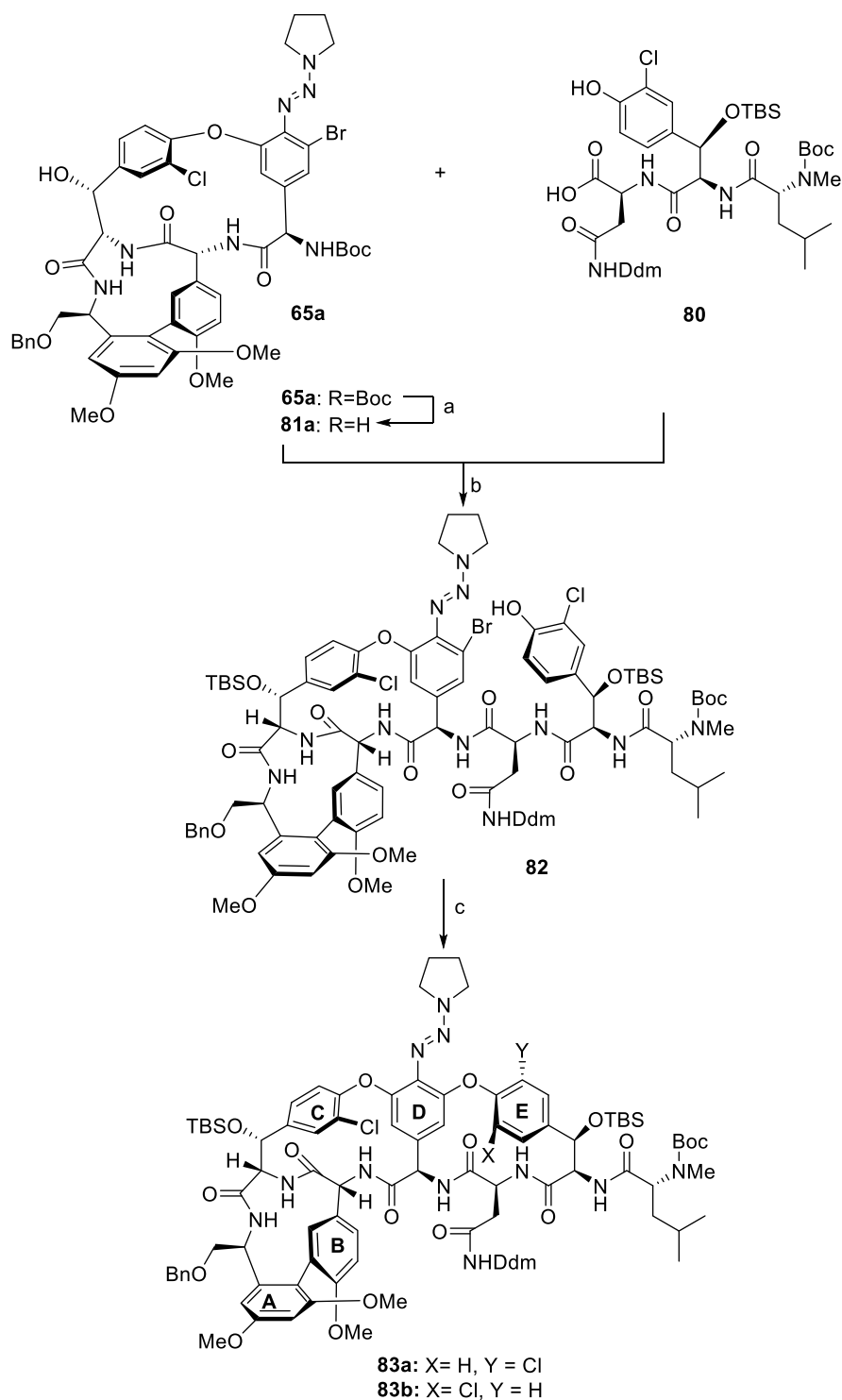
Scheme 1. 16: Construction of AB/C-O-D/D-O-E tricyclic systems **83a** and **83b**. a) 2.0 equiv of TMSOTf, 3.0 equiv of 2,6-lutidine, CH$_2$Cl$_2$, -10 °C, 0.5 h, 96%; b) 2.0 equiv of EDC, 10.0 equiv of HOAt, THF, -15 → 0 °C, 12 h, 86%; c) 5.0 equiv of CuBr ´Me$_2$S, 5.0 equiv of K$_2$CO$_3$, 5.0 equiv of pyr., MeCN, reflux, 2 h, **83a**: **83b** ca. 1:3 ratio of atroipisomers, 74% combined yield.[81]

1.3.1.1. Summary.

Both the Evans and Nicolaou syntheses gave the vancomycin aglycon, and ultimately vancomycin, through an extended solution phase synthesis, with protection of intermediates at each step. Solid phase synthesis offers, potentially, a more rapid approach to develop vancomycin analogues. In addition, the purification process to obtain the required peptide in SPPS involves mainly filteration, which makes the synthesis process rapid and facile. In contrary, with the solution phase, the purification process requires for crude after each reaction step, which is time consuming and costly. The following section will focus on some literatures that considered the solid phase synthesis of vancomycin.

1.3.2. The solid phase synthesis of vancomycin.

Given the key goal of the research in this thesis is the synthesis of vancomycin on solid phase, the literature that has dealt with such chemistry is reviewed here. In 1999 Ernst Freund and John A. Robinson synthesised a heptapeptide using solid phase methods relying on Alloc protecting group chemistry for the *N*-terminal elongation,[84] (Scheme 1.17). 2-Chlorotrityl chloride resin was used as a solid support and the benzyl ether protecting group for aromatic side chain protection.[84] (S)-Alloc-Dhpg(OBn)$_2$-OH was first attached to 2-chlorotrityl chloride resin using DCM as a solvent to give **84**. The elongation of the peptide chain was accomplished using HATU/HOAt (4 equiv). DMF was used as a solvent for the required amino acids alongside the coupling agents. Alloc removal after each coupling process was carried out with Pd(PPh$_3$)$_4$ and PhSiH$_3$.

Upon completion of the synthesis of the protected form of heptapeptide **85** on the solid phase, deprotection of the side chains was carried out universally and the heptapeptide was cleaved from the resin giving the desired linear heptapeptide **86**. Noteworthy, the final attached amino acid was protected with Boc at the N-terminus, therefore it was removed in a separate step.[84] The researchers argued that the use of Alloc protecting groups for chain elongation was to avoid epimerisation of several amino acids through the use of Fmoc/Boc system in solid phase. Alloc deprotection proceeded under neutral conditions rather than basic or acidic conditions with Fmoc and Boc respectively.[84] The desired linear heptapeptide **86** was produced in 16% yield. As it is noticeable, this protocol proceeded with non-chlorinated tyrosine derivatives.
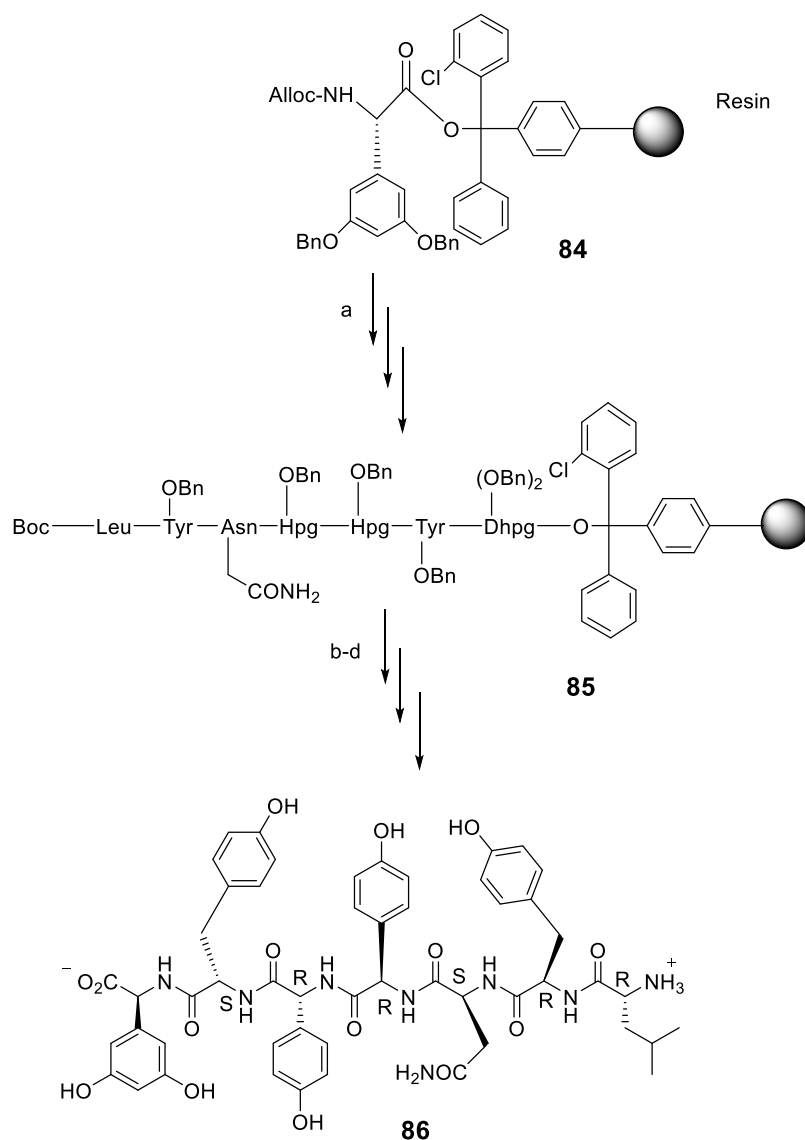
Scheme 1. 17: Synthesis of the linear heptapeptide **86** by Ernst Freund and John A. Robinson. Reagents and conditions: a) for coupling (R)-Alloc-Hpg(OBn)-OH, (R)- and (S)-Alloc-Tyr(OBn)-OH, L-Alloc-Asn(Mtt)-OH, or D-Boc-Leu-OH (4 equiv), HATU and HOAt (each 4 equiv.), NMM, DMF, and for Alloc deprotection Pd(PPh$_3$)$_4$ (0.5 equiv) and PhSiH$_3$ (30 equiv.) in CH$_2$Cl$_2$; b) CF$_3$CH$_2$OH–AcOH–CH$_2$Cl$_2$ (1:1:3); c) TFA–CH$_2$Cl$_2$ (1:1) + 5% Pri$_3$SiH, 0 °C, 2 h; d) TFA, thioanisole (3:1), 20 °C, 3 h.[84]

One year later, Robinson and co-workers described the synthesis of the linear heptapeptide intermediate with *m*-chlorinated tyrosine derivatives **87** using the Alloc strategy (Figure 1.9).[85] The required amino acid residues **88**-**94** were synthesised in solution phase using detailed literature methods (Figure 1.8). All of them were protected with the Alloc protecting group at the *N*-terminus. The amino acid **95** was commercially available.[85]
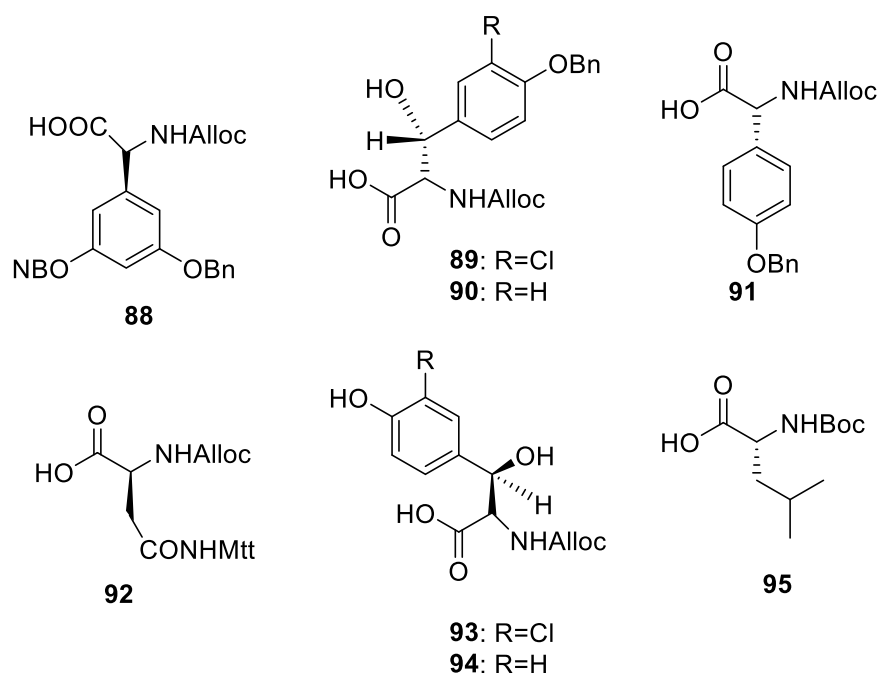
Figure 1. 8: The chemical structure of the amino acid-building blocks required for synthesis of the chlorinated variant of linear heptapeptide.[85]

The solid-phase synthesis was carried out using the same protocol that was used in the previous work regarding the type of the solid support and peptide elongation process. The monitoring of the coupling process was performed using reversed-phase HPLC. After coupling of the hydroxyphenyl glycine residue (Hpg) **91**, two compounds were obtained in a 4:1 ratio. This was due to epimerization, which persisted to the end of the synthesis.[85] Upon completion of the sequence, the heptapeptide was cleaved from the resin in its side-chain protected form, using a mixture of $CH_2Cl_2/CF_3CH_2OH/AcOH$. The deprotection of all side chain protecting groups was carried out with CF_3COOH/thioanisole (i-Pr)$_3$ SiH, and the purification of the product by reversed-phase HPLC.[85] The overall yield of the product was 13%.
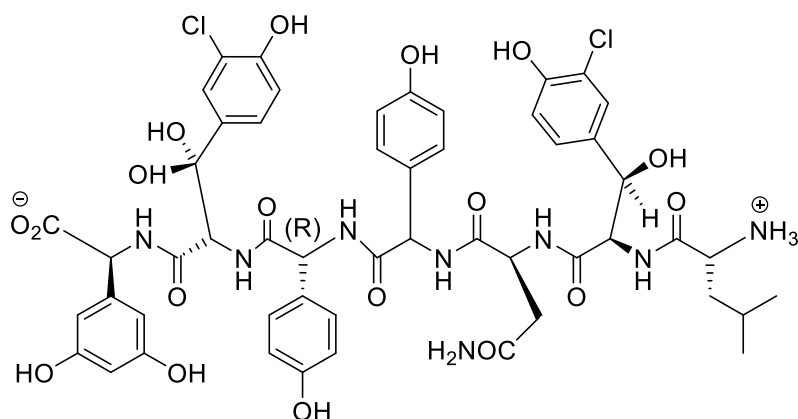
87

Figure 1. 9: The chlorinated form of the linear heptapeptide made by Robinson.[85]

In 2001 K. C. Nicolaou et al,[71] showed the solid phase semisynthesis of vancomycin based on their previous work on the total synthesis of vancomycin.[75, 76] They chose vancomycin to be attached at its C-terminus and protected at its functional moieties with silicon protecting groups. Therefore, choosing a convenient linker that would be stable under acidic and basic conditions and suitable with protecting groups was of significant importance in this work. Already prepared and protected vancomycin was set to be loaded on a solid support.[71]

Initially, two photocleavable resins linkers, **96** and **97**, (Figure 1.10) were employed because of their compatibility with the above requirements.[71, 86] The vancomycin loading on resin linker **96** proceeded smoothly but the removal from the resin could not be performed. On the other hand, vancomycin loading on resin linker **97** gave low yields, attributed to the steric hindrance.[71]
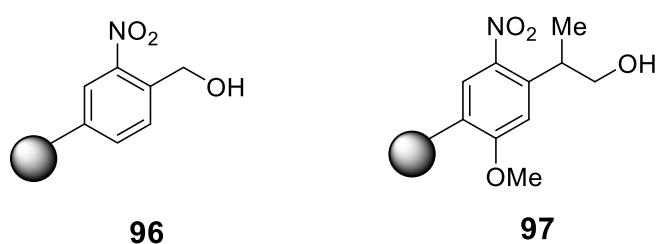
96   **97**

Figure 1. 10: The chemical structures of the unsuccessful photolabile linkers.[71]

After that, three allyl linkers, **98-100**, were trialled (Figure 1.11). The loading and cleavage of vancomycin and its analogue proceeded with ease with these linkers. The glycosidation step to install the sugar part of vancomycin, required Lewis acidic conditions. The resin-loaded vancomycin variants, **101** and **102**, which correspond to

the resins **98** and **99** respectively, underwent a diminished cleavage process, a fact that was attributed to a [3,3]-sigmatropic rearrangement.[71] Using an acrylate linker-loaded vancomycin **103**, led to a noticeable improvement in the cleavage process due to lack of the problematic [3,3]-sigmatropic rearrangement, but the analogues suffered from premature cleavage. This was attributed to the acrylate resin linkers susceptibility to nucleophilic attack (Scheme 1.18).[71]
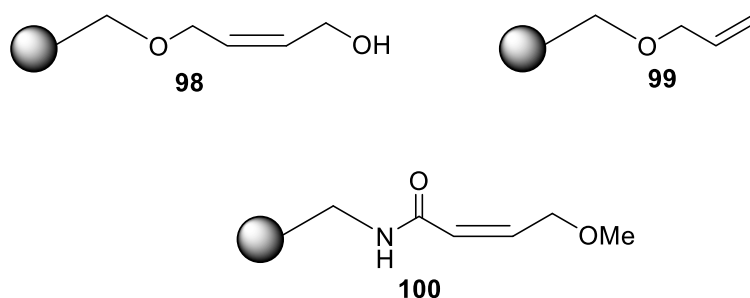
Figure 1. 11: The allyl linkers that were not appropriate for the solid-phase semisynthesis of vancomycin.[71]
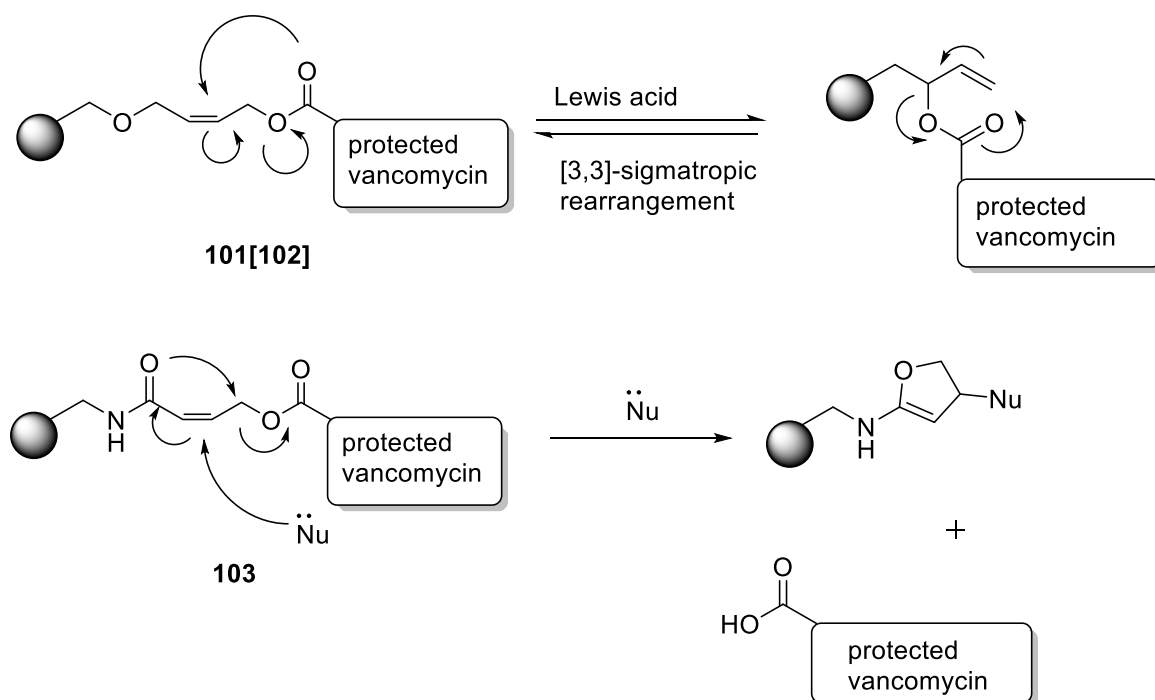
Scheme 1.18: Presumed side reactions of allyl linkers 101, 102, and 103.[71]

Nicolaou et al[71] used pro-allyl and pro-alloc selenium resins in which the allyl group is masked, **104** and **105** (Figure 1.12).[71, 87] The pro-allyl safety catch linker would have the advantage of the C-terminus protection and the stability for the conditions involved in the synthesis of vancomycin.[71] With this successful linking strategy,

Nicolaou and co-workers were able to proceed with the solid phase semisynthesis of vancomycin as the loading and cleavage processes proceeded in a facile manner.[71]
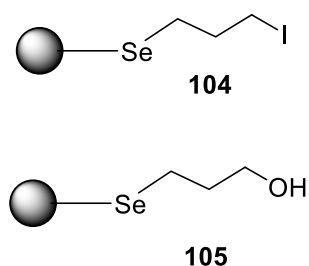
Figure 1. 12: The pro-allyl selenium resins.[71]

Accordingly, several modifications of the two amino groups, the leucine amino acid, and deglycosidation/reglycosidation were performed, and all the derivatives were biologically examined and evaluated.[71]

In 2014 Clara Brieke and Max J. Cryle, used an optimised Fmoc protocol for the solid phase synthesis of a vancomycin-type hexapeptide **106** (Figure 1.13). They argued that the Fmoc chemistry still has advantages over other solid phase methods. The main advantage is the facile synthesis of building blocks and therefore, there are a wide range of such available starting materials. In addition, the monitoring process is easy and simple. In contrast, the Alloc chemistry is characterised by a tedious synthesis of the building blocks and use of palladium-mediated procedure for the peptide cleavage.[88] Therefore, they explored different conditions to optimise the Fmoc protocol. That is, to reduce the epimerization associated with the *N*-Fmoc deprotection with piperidine, especially in arylglycine derivatives, to the minimum. For the deprotection of the *N*-Fmoc group, a 1% solution of DBU in DMF gave the best outcome, which allows for deprotection of phenylglycine residues in as short a time as 30 s with a very small ratio of racemisation.[88] For an effective coupling reaction, COMU and Et$_3$N reagents were used in four equiv each and did not produce racemisation. A TFA/TIPS/H$_2$O mixture was used for the final cleavage of the peptide from the resin. Noteworthy, using any type of base whether for scavenging the side products as diphenylfulvene or as an activator in the coupling step leads to increased racemisation. Moreover, using 4-hydroxyphenylglycine (4-HPg) has less influence in increasing racemisation than HPg. Consequently, one major product was obtained without occurrence of racemisation as was revealed by analytical HPLC-MS analysis.[88]

106
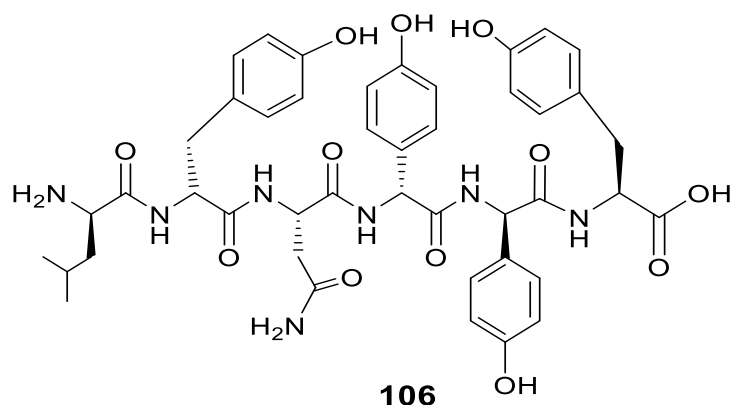
Figure 1. 13: The hexapeptide of vancomycin synthesised on SPPS by Clara Brieke and Max J. Cryle.[88]

1.3.3. The modification of vancomycin.

Several attempts have been carried out on the modification of vancomycin as endeavours to find new analogues to function effectively against vancomycin resistant species. The loss of vancomycin binding affinity, and subsequently its antimicrobial activity, is largely attributed to the repulsion between the lone pairs of the carbonyl oxygen of the central amino acid in vancomycin and the oxygen of the D-Ala-D-Lac terminus of the peptidoglycan precursor in the resistant bacteria (Figure 1.14).[89] Based on this idea, Boger and co-workers replaced the carbonyl functional group of the central residue-4 with a methylene group producing the analogue of the vancomycin aglycon **107** (Figure 1.15).[90]
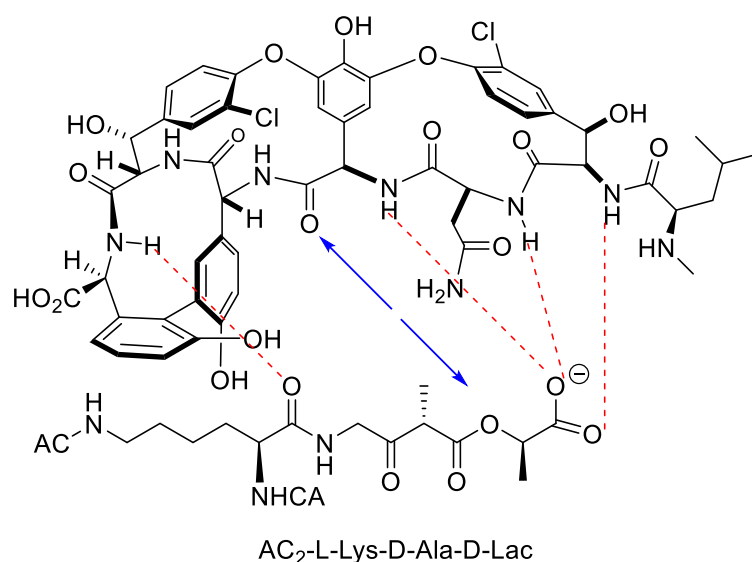
Figure 1. 14: Illustration of the repulsive lone pair interaction between the vancomycin central residue carbonyl and the D-Ala-D-Lac oxygen.
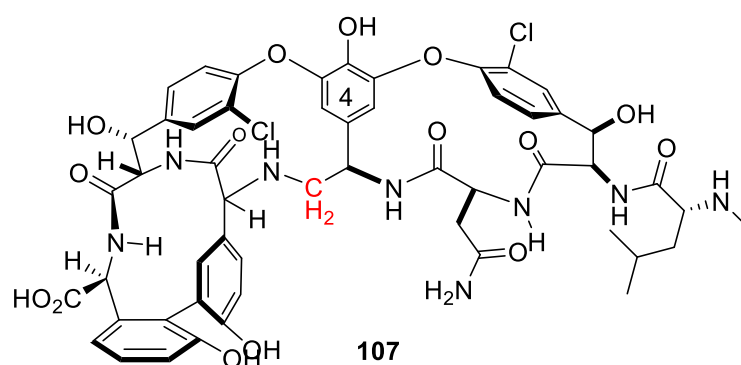
Figure 1. 15: Replacement of carbonyl oxygen by a methylene group in vancomycin aglycon **107**.

This modification exhibited a 40-fold increase in affinity for the ligand D-Ala-D-Lac, and showed a reduction in binding to the ligand D-Ala-D-Ala by 35-fold. Amidine and thioamide derivatives of the central residue were anticipated to have a significant activity against resistant bacteria with a D-Ala-D-Lac peptidoglycan cell wall precursor (e.g., VanD, which is one of the non-transferable genes responsible for the vancomycin resistance of *E. faecium* strains[67]). On the other hand, amidine and thioamide derivatives were inactive against sensitive and inducible resistant bacteria (VanA and VanB) that maintain or at least start with a D-Ala-D-Ala peptidoglycan cell wall precursor.[90]

Restoration of H bonding between vancomycin and peptidoglycan in the bacterial cell wall was one of the targeting approaches that Boger and his team attempted. In 2009, Boger and co-workers introduced unnatural amino acids to the *N*-terminus of

vancomycin aglycon creating different analogues (Figure 1.16). The amino acids contain functional groups exhibiting H-bonding to the carbonyl group of two ligand models, **108** and **109**, mimicking the peptidoglycan layers present in susceptible and resistant bacterial species (Figure 1.17).[91]

The analogues containing N-terminal D-serine (**110**), *O-tert*-butyl-D-serine (**111**), D-threonine (**112**), mono- or bi-dentate analogues of 3-amino-D-phenylalanine (**113-115**), 3-aminomethyl-D-phenylalanine (**116**) and their corresponding hydrazine counterparts **117-119** were examined. Analogue **119** was the only compound that showed a noticeable antimicrobial activity against the VanA strain, although the reason for this was unclear.[91]
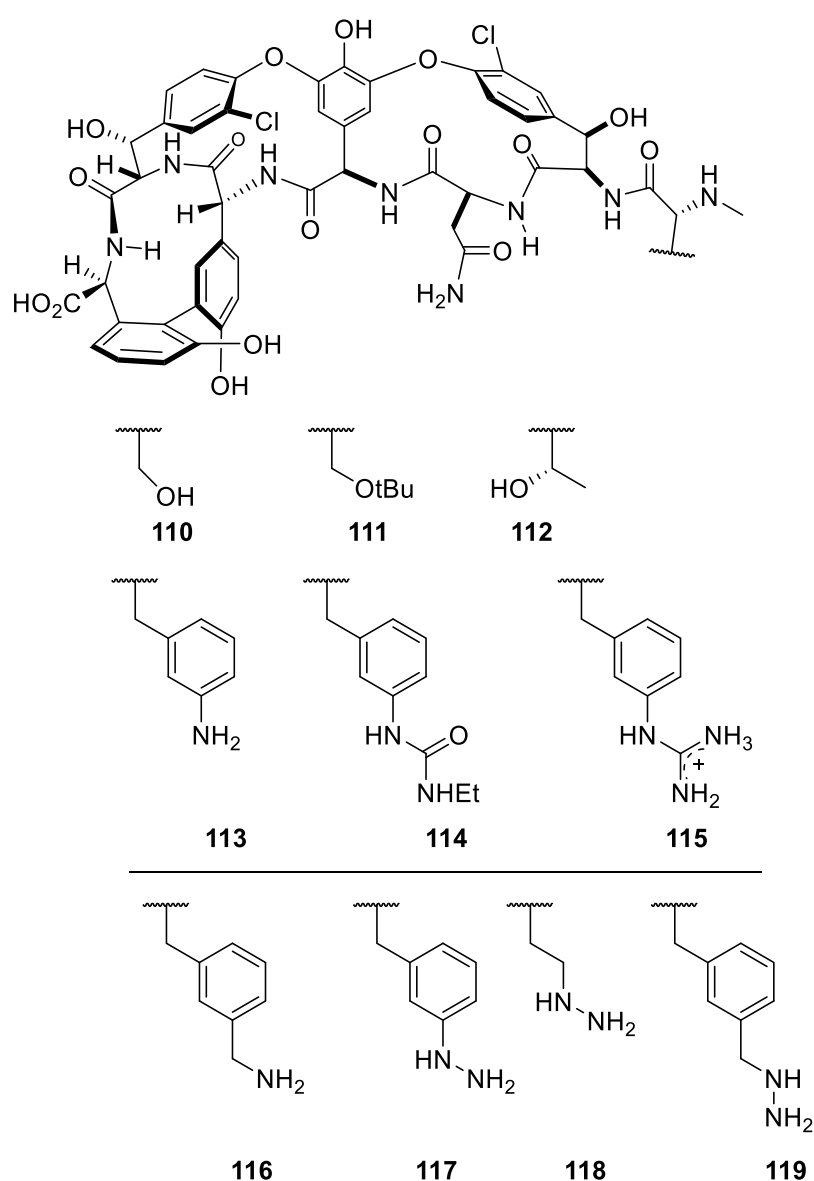
Figure 1. 16: The vancomycin analogues with a modified N-terminus.
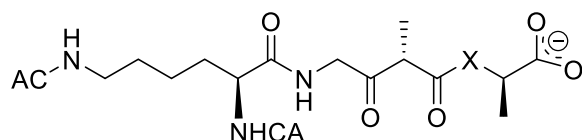
N,N'-Ac$_2$-L-Lys-D-Ala-D-Ala, X=NH   Ligand **108**
N,N'-Ac$_2$-L-Lys-D-Ala-D-Lac, X=O   Ligand **109**

Figure 1. 17: The model ligands mimic the bacterial cell wall binding to vancomycin.

In 2010, Boger and co-workers introduced new derivatives of the vancomycin aglycon via protection of each of the four phenols with methyl groups.[92] Six analogues of vancomycin aglycon **1** were made (Figure 1.18). Analogues **120** and **121** showed considerable antimicrobial activity against sensitive and resistant bacteria (VanB), with an increased activity against VanA, without a significant change in the binding affinity to the model ligands. The antimicrobial activity was attributed to the hydrophobicity of permethylated analogues of the vancomycin aglycon, which have the ability to penetrate into the bacterial cell membrane sufficiently to avoid induction of the route where switching between D-Ala-D-Ala, and D-Ala-D-Lac would happen.[92]
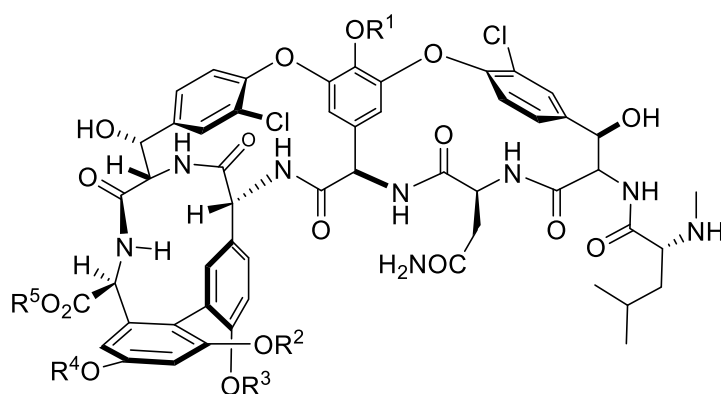
Compound	R^1	R^2	R^3	R^4	R^5
1	H	H	H	H	H
120	Me	Me	Me	Me	H
121	Me	Me	Me	Me	Me
122	H	Me	H	Me	H
123	H	H	Me	Me	H
124	H	Me	Me	Me	H
125	Me	H	H	H	H

Figure 1. 18: Analogues of vancomycin aglycon.

Boger and co-workers also made a change in the vancomycin aglycon **1** structure, that was able to exhibit a dual activity against both resistant and susceptible strains.[93]

They replaced the amide of the central residue with an amidine and investigated its antimicrobial activity (Figure 1.19). Compound **126** exhibited activity 1000-fold more potent than vancomycin and vancomycin aglycon against VanA resistant bacteria, and approximately the same activity against sensitive bacteria. They proposed that the significantly enhanced activity of the amidine derivative against the most virulent VanA species is due to the stabilising electrostatic interactions and the H-bonding donor property of the protonated form of amidine (Figure 1.20a). Accordingly, that leads to a significant reduction in the destabilising lone pair repulsion of the ester oxygen of the model ligand D-Ala-D-Lac **109**.[93]
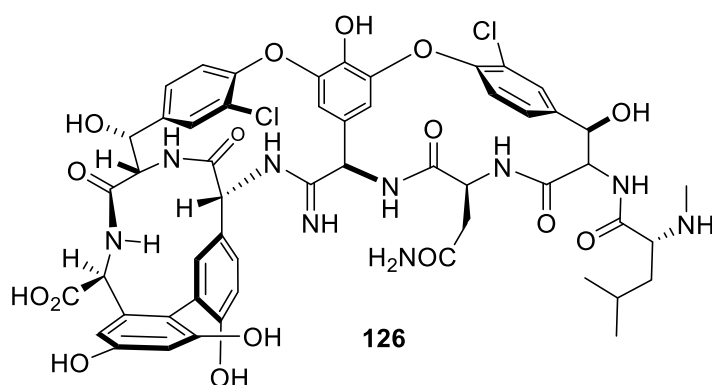
Figure 1. 19: The potential dual binding behaviour of the amidine derivative.
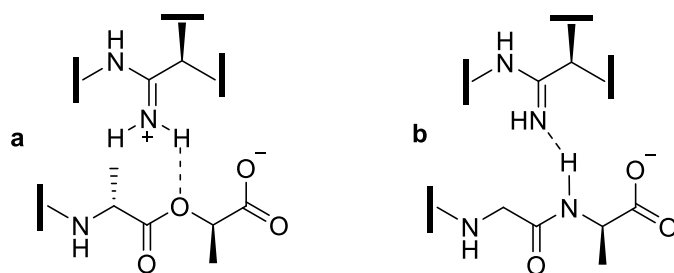
Figure 1. 20: Illustration of the electronic interaction between amidine and protonated amidine derivatives and ester oxygen.

On the other hand, the susceptibility of the sensitive bacteria was attributed to the re-establishment of the stabilising H-bonding between the amidine nitrogen and the amide group in the model ligand **108,** and thereby showed an equal antimicrobial activity as vancomycin (Figure 1.20b). Regarding the binding affinity, the central residue amidine derivative showed a significant binding for both models, D-Ala-D-Ala and D-Ala-D-Lac, within a level of 2-3-fold of that displayed by vancomycin for D-Ala-D-Ala.

In the same work, Boger and co-workers prepared vancomycin derivatives in which the amide of the central residue was replaced by a methylene and thioamide groups, compounds **127** and **128** respectively (Figure 1.21).[93]
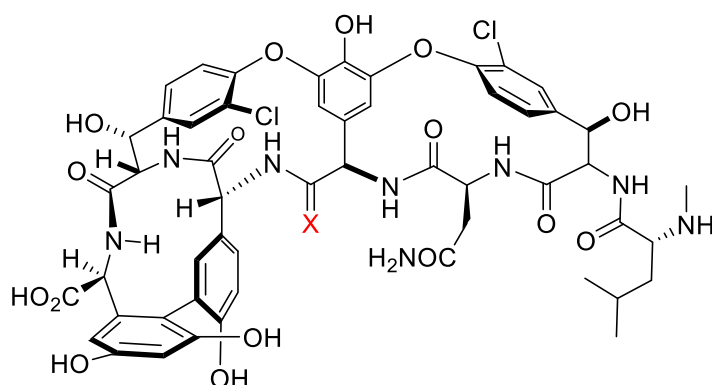
1, X= O, vancomycin aglycon.
127, X=S, thioamide derivative of vancomycin aglycon.
128, X=CH$_2$, methylene drivative of vancomycin aglycon.

Figure 1.21: The methylene and thioamide derivatives of vancomycin aglycon.

Vancomycin aglycon with residue-4 methylene derivatives displayed a slightly improved antimicrobial activity against resistant bacteria as it exhibited a 40-fold higher affinity to D-Ala-D-Lac than vancomycin aglycon. On the other hand, its affinity for D-Ala-D-Ala was reduced by 35-fold. Thioamide derivatives displayed neither significant antimicrobial activity nor binding affinity to either of the models, ligand **108** and **109**. They attributed the failure of thioamide derivatives to the weak ability of the thioamide thiocarbonyl to form H-bonds, the long bond of the thiocarbonyl and the large van der Waals radii of sulfur.[93]

In the same year, Miller and Pathk,[94] reported different bromination approaches for vancomycin based on the fact that is the activity of bioactive compounds can be further modified and tuned, especially in the case of aromatic compounds, to produce different products via introduction of bromine. By a reaction of unprotected vancomycin with *N*-bromophthalimide (NBP) in H$_2$O, mixtures of brominated isomers in addition to the unreacted vancomycin were produced (Figure 1.22).[94]
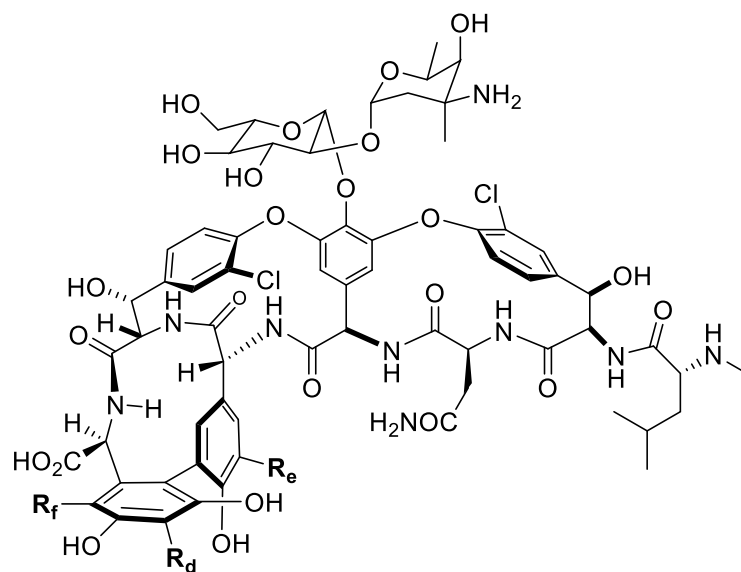
1, Rf, Rd, Re=H, vancomycin
129, Rf=**Br**, Rd, Re=H
130, Rf=H, Rd=**Br**, Re=H
131, Rf=H, Rd=H, Re=**Br**
132, Rf=**Br,** Rd=**Br,** Re=H
133, Rf=**Br**, Rd=**Br**, Re=**Br**

Figure 1. 22: Illustration of the three presumed sites (in red) for site-selective bromination of vancomycin.

Focussing on the fact that it is important to explore other analogues of vancomycin to retain its essential and potent activity against resistant bacteria, in 2012 Miller made these different variants of brominated vancomycin (Figure 1.22), through a selective method using peptide based ligands.[94] These ligands (Figure 1.23), were designed based on the mechanism of the vancomycin activity and its binding affinity to its target, D-Ala-D-Ala, of the bacterial cell wall. *N*-bromophthalimide (NBP) was used as a source of bromination of vancomycin and H_2O as a solvent.

Monobrominated compound **130** was produced predominately when ligand **134**, Asn (Me_2)-D-AlaD-Ala, was used. Dibromide compound **132** was the predominant product when ligand **135,** $Gln(Me_2)$ residue instead of $Asn(Me_2)$, was added. Lowering and increasing in the concentration of the ligand **134** significantly affected the monobrominated isomers ratio (**129,130**). Moreover, changing the position of the $Asn(Me_2)$ group within the tripeptide had diminished both activity and selectivity of the ligand. On the other hand, using a limited quantity of NBP (0.5 equiv) preserved the selectivity to the monobromide compound **130** and reduced the yield of dibromide isomer **132**.[94]

Ligand **134**   Ligand **135**
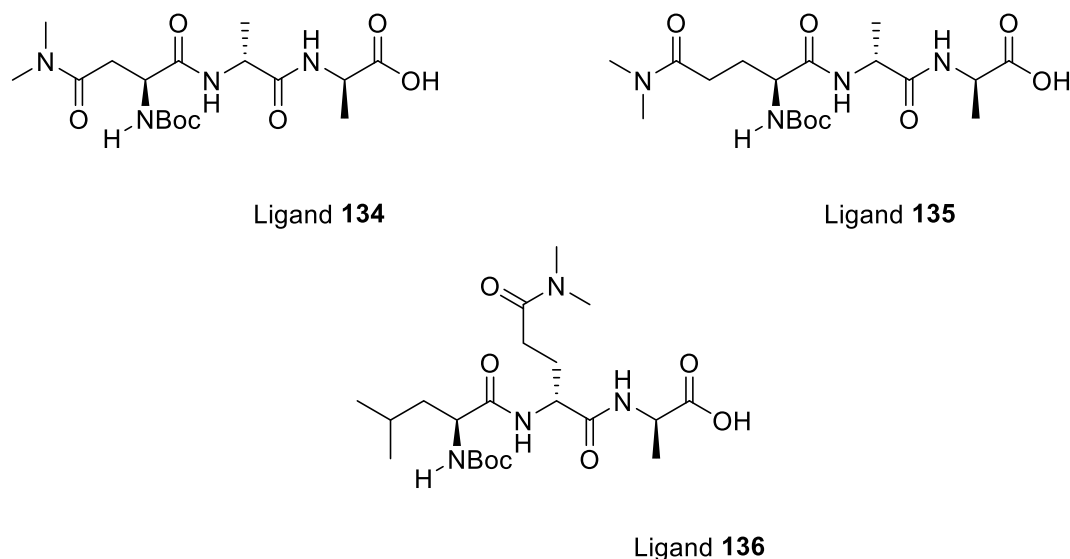
Ligand **136**

Figure 1. 23: The ligands used for bromination of vancomycin.

Production of dibromide compound **132** in excellent yield was achieved by use of NBP with an excess quantity (3 equiv) with 100 mol% of ligand **134.** The tribromide isomer **133** was produced in a significant yield with use of peptide ligand **136**. After production of **130**, **132**, and **133** preferentially, they sought a way to improve the reaction selectivity for monobromide isomer **129**. They found that the use of guanidine as an additive to the reaction condition that had provided the isomer **129** with good selectivity. The efficiency of guanidine came from its ability to bind the proximal acid of vancomycin and direct the bromide ion to the specific site (Figure 1.22).[94]

Building on the earlier achievements by Boger in 2012,[93] in 2015, he and co-workers examined the effect of the introduction of a 4-chlorobiphenyl (4-CBP) substitution to the different three vancomycin analogues (amidine, methylene, and thioamide) (Figure 1.24).[95] Thus, with the different aglycon analogues in hand from the previous work,[93] enzymatic glycosylations of the carbohydrate moieties had been carried out using GtfE and GtfD for the introduction of glucose and vancosamine respectively. After the introduction of the 4-CBP was performed, the investigation of the antimicrobial activity of the different analogues was explored. Attachment of the 4-CBP to vancomycin **137**, resulted in an improvement of the antimicrobial activity against VanA and VanB by 100-fold (MIC=2.5 μg/ml) and against VSSA and MRSA by 20-fold (MIC= 0.03 µg/ml).[95]
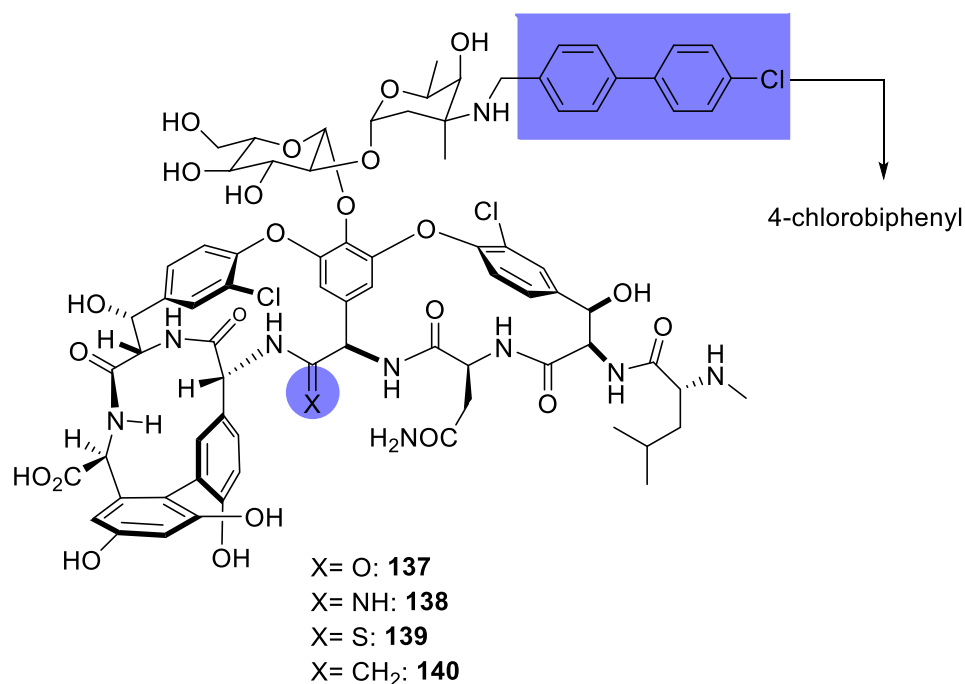
Figure 1. 24: The vancomycin analogues with 4-CBP substitution.

The most striking outcome of this work was after the introduction of 4-CBP substitution to the amidine analogue **138,** where the antimicrobial activity increased by 500 and 50000-fold against most virulent and resistant bacteria, in comparison to the amidine analogue of vancomycin and to vancomycin itself, respectively. Regarding the methylene analogue, introduction of 4-CBP **140** showed equal activity as for the amidine analogue against both sensitive and resistant strains, though the amidine analogue was still more active than the methylene analogue by 15-fold.[95] Although, the thioamide analogue **139** showed no activity against both sensitive and resistant bacteria, introduction of 4-CBP resulted in a great improvement in its antimicrobial activity against both resistant and sensitive strains (MIC= 2-4 µg/ml).

Accordingly, it was suggested that such impressive activity may belong to another mechanism alongside the assigned mechanisms via which vancomycin produces its antibacterial effect. This mechanism may involve enhancing antibiotic dimerisation for cell membrane anchoring, and disruption of the integrity of bacterial cell membrane. In addition, the direct suppression of the enzymatic system, transglycosylase and transpeptidase, that maintains bacterial cell wall integrity was presumed as another potential mechanism.[95]

1.3.4. Summary.

In summary, while the total synthesis of vancomycin has been achieved, it is a multi-step process that is not readily amenable to the generation of analogues. However, the value in generating new methods based on the vancomycin scaffold has been made clear by the approach taken by Boger and co-workers. This has generated new compounds with potential against resistant bacteria through small and simple variation. This suggested to us that a solid phase synthesis of the vancomycin aglycon could have the potential to generate new analogues in a relatively rapid way, providing molecules could be developed to synthesise suitably protected monomers for Fmoc-chemistry and suitablely derivatised to aid the on-resin formation of the macrocyclic rings. This thesis describes the initial studies towards the goal of generating suitably protected monomers and initial studies of their application to the solid phase.

Chapter 2.

Synthesis of an analogue of the vancomycin central amino acid suitably protected for Fmoc solid phase synthesis

2.1. The design of the central unit.

This chapter focuses on the synthesis of the central amino acid (Figure 2.1) of the vancomycin structure as a first step towards the introduction of a solid phase synthesis method. The central amino acid is part of two important macrocycles, therefore, access to both of these structures can be gained. It also contributes directly to the mechanism by which vancomycin inhibits the synthesis of the bacterial cell wall via hydrogen bonding.
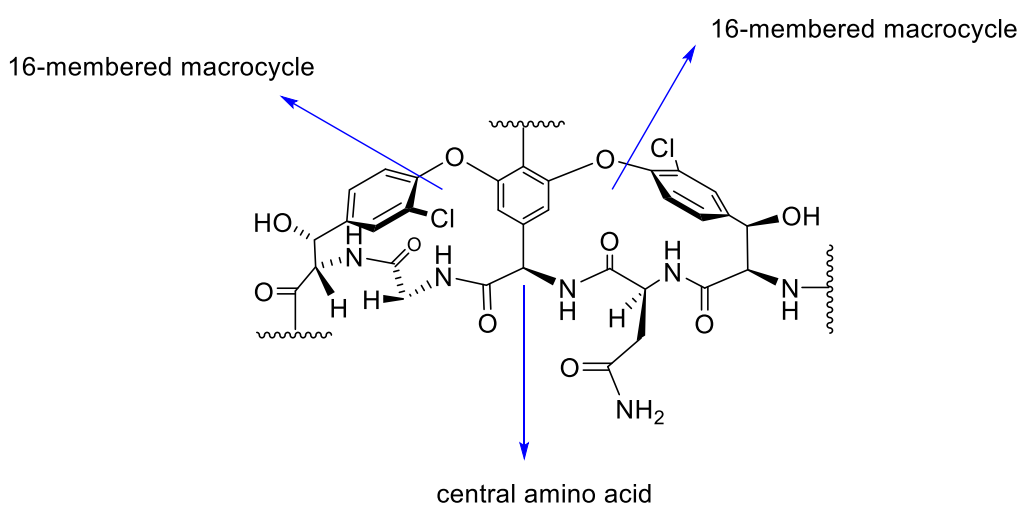
Figure 2. 1: Heptapeptide part of vancomycin. Illustration of the position of the central amino acid as a connecting bridge between two macrocycles in the vancomycin structure.

The central unit is the only residue that has five linkages within the structure of vancomycin (Figure 2.2), two amide linkages and two ether bridges to the neighbouring amino acids, and one glycosidic linkage. With all these observations in mind, the route for the synthesis of the central unit for solid phase synthesis had to be designed. There were some considerations before commencing with the synthesis of the central unit:

1) Protection of the amine group with Fmoc to be consistent with the standard strategy followed in SPPS.

 2) At the end of the synthesis, the carboxylic acid group must be unprotected so that it can be used for amide bond formation via a coupling step, (Figure 2.3).
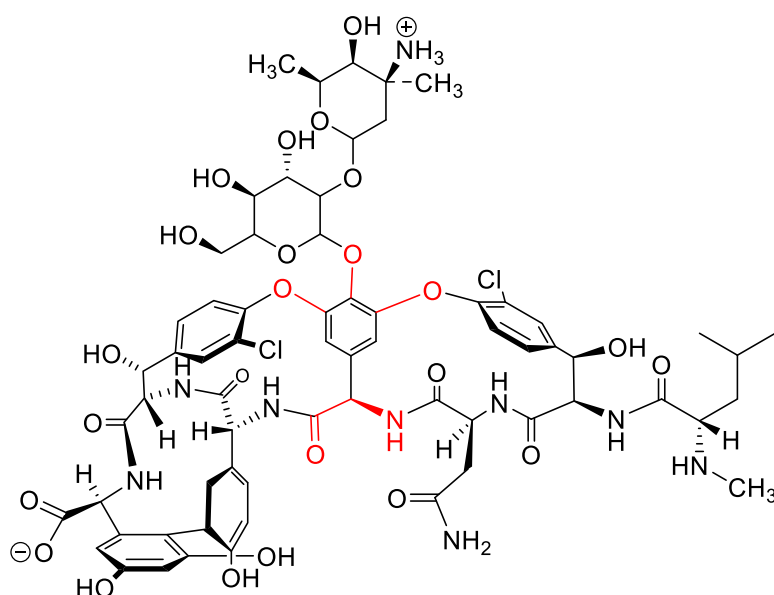
Figure 2. 2: Illustrating of the five connections of the central amino acid to other parts of vancomycin.

3) A suitable aromatic substitution was required on the *ortho* positions to allow the macrocyclisation on both sides of the aromatic ring to be facile and smooth. Dibromide substitution on the *ortho* positions of the central unit was found to have an important role in Ullman coupling and could be applied for cyclisation.[70, 96]

4) A suitable capping procedure for a phenolic hydroxyl group was required. The triazene moiety is relatively stable to the basic conditions used in Fmoc-SPPS but is labile to acid under relatively mild conditions (50% TFA/ DCM).[97]

The triazene group can be easily formed and modified,[70] so potentially can be converted to phenol, which is a good acceptor for the vancomycin sugar moiety.[82] In addition, it has an ability to protect a reactive diazonium salt through several reactions.[98] For these important reasons, the triazene was chosen as a protecting group throughout the synthesis process. Moreover, its ability to activate the *ortho* bromide for a facile macrocyclisation, triazene-driven cyclisation, added another factor for its importance.[70, 96]
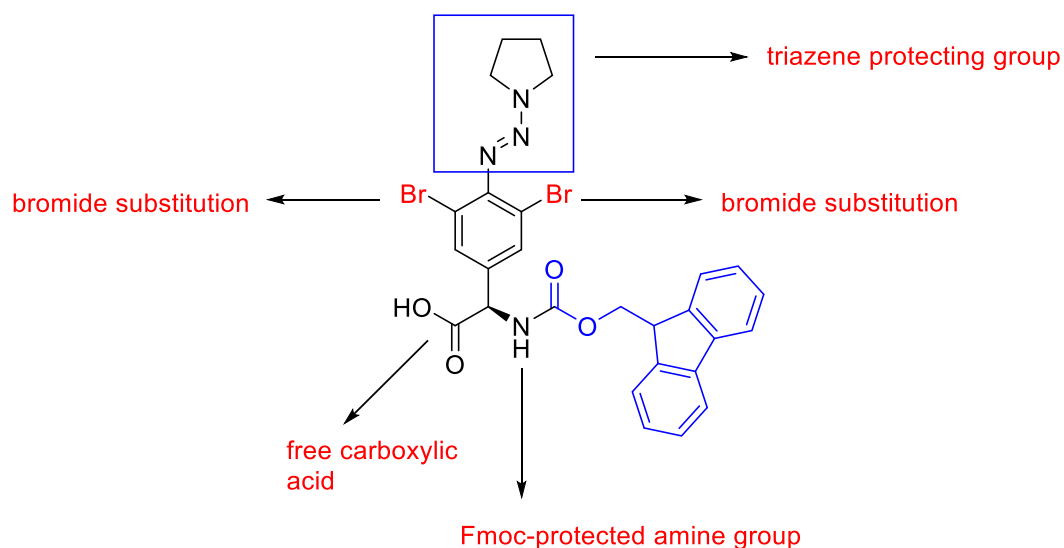
Figure 2. 3: The design of the central unit **C2** for solid phase synthesis compatibility.

2.2. The synthesis of the central unit.

The proposed route to synthesis of the target compound is shown in scheme 2.1. Although the route parallels Nicolaou's approach,[99] several modifications had to be made to achieve the final Fmoc-protected target **C14**. The steps of the synthetic route will be discussed in detail in below.

2.2.1. Synthesis of the methyl ester C2.

The formation of the acid chloride intermediate is a key step in the reaction (Scheme 2.2). Acid chlorides are more reactive than carboxylic acids when used in the generation of carboxylic acid derivatives. Due to their high reactivity they can react even with weak nucleophilic species.[100],[101] Thionyl chloride is regularly utilised in the preparation of acid chloride intermediates.[102]

The esterification of the carboxylic acid **C1** was performed by dissolving the starting material in methanol and adding thionyl chloride followed by heating of the reaction mixture at reflux and 4-aminomethyl benzoate **C2** was obtained in 97% yield without purification.
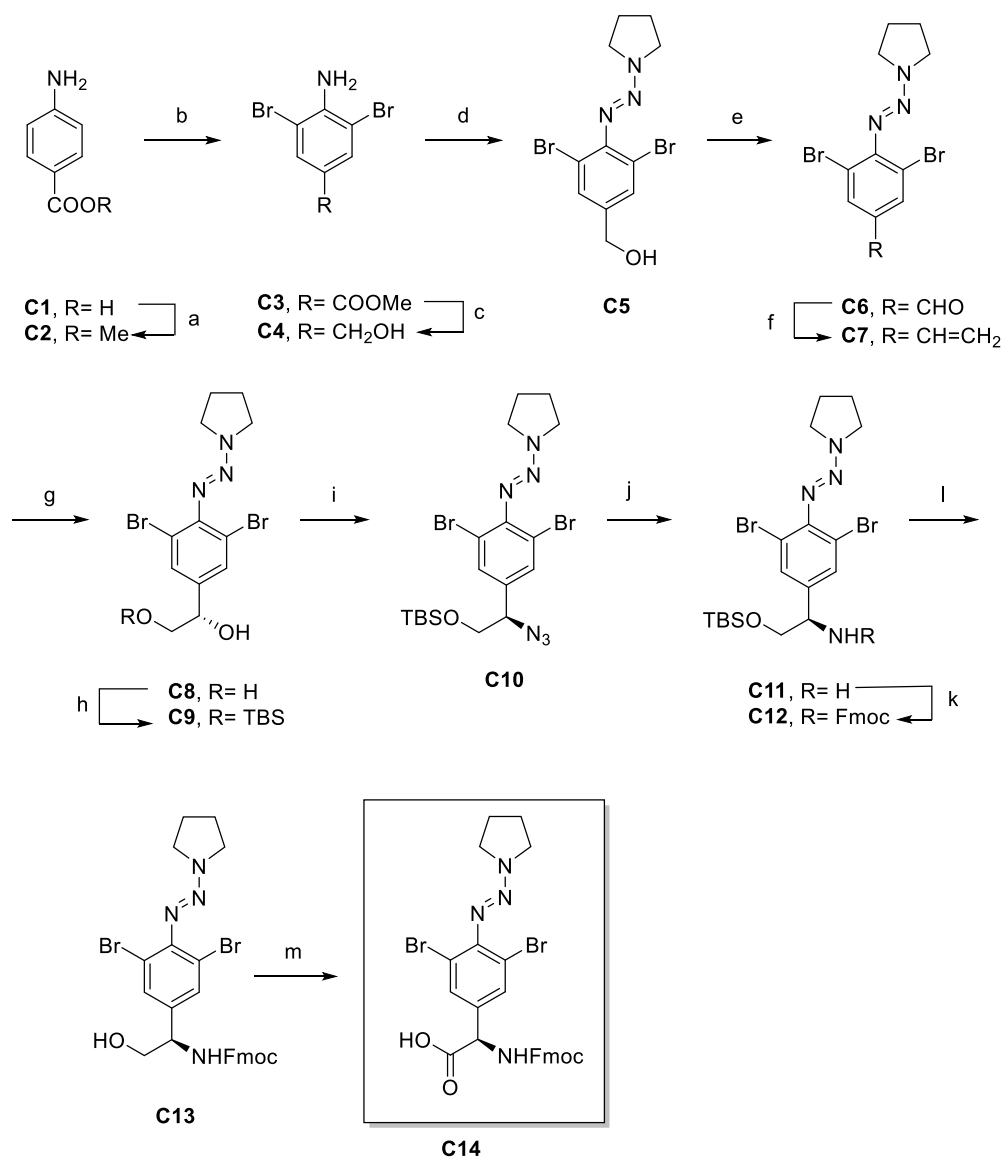
Scheme 2. 1: The route to synthesis of the central amino acid in vancomycin: Reagents and conditions: a) $SOCl_2$ (1.0 equiv.), MeOH, reflux, 2 h; b) Br_2 (2.0 equiv), AcOH, 25 °C, 1 h; c) $LiAlH_4$ (2 equiv), anhydrous THF, 0 °C, 2 h; d) 6 M HCl (5.0 equiv), $NaNO_2$ (1.2 equiv), $AcOH:H_2O$ (1:1), 0 °C, 1 h, then KOH (30 equiv), pyrrolidine (1.5 equiv), 0 °C, 0.5; e) PCC (1.5 equiv), CH_2Cl_2, 25 °C, 2 h; f) n-BuLi (1.4 equiv), $CH_3Ph_3P^+Br^-$ (1.5 equiv), anhydrous THF, under N_2, -20 °C, 4 h; g) AD-Mix-α (1.4 g $mmol^{-1}$), t-BuOH/H_2O (1:1), 24 h; h) TBSCl (1.1 equiv), DMAP (0.1 equiv), Et_3N (1.5 equiv), DCM, 0 °C, 2 h; i) Ph_3P (2.5 equiv), DIAD (2.5 equiv), DPPA (2.5 equiv), anhydrous THF, 0 °C, 2 h; j) Ph_3P (3.0 equiv), H_2O (10.0 equiv), THF, 60 °C, 2 h; k) Fmoc-Cl (1.1 equiv), $NaHCO_3$ (2 equiv), THF, H_2O, 0 °C, 3 h; l) TBAF (1.2 equiv), AcOH (3 equiv), THF, 0 °C, 6 h; m) TEMPO (1.0 equiv), 5% aq. NaOCl (3.0 equiv), 5% $NaHCO_3$, KBr (0.1 equiv), Me_2CO, 0 °C, 2 h.
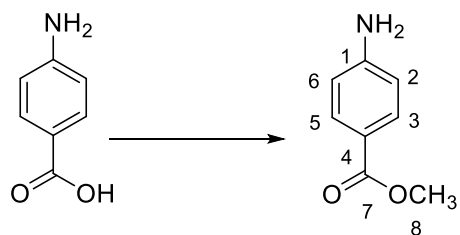
Scheme 2. 2: The atom numbering of the 4-aminomethyl benzoate **C2**.

The reaction product was confirmed using ^{1}H NMR spectroscopy (see scheme 2.4 for atom numbering). A singlet peak at 3.85 ppm corresponded to the newly formed ester methyl group. The position is downfield because the two oxygen atoms of the ester are so electronegative that electron density around the methyl protons decreases. The two protons of C-3 and C-5 give rise to a doublet at 7.85 ppm, with coupling constant of 8.8 Hz, characteristic of coupling to neighbouring C-2 and C-6. The reason for a downfield shift compared with unsubstituted benzene proton (usually at 7.2 ppm) is due to the proximity to the ester moiety, which is electron-withdrawing to the relative *ortho* and *para* positions through a conjugation effect (Scheme 2.5).
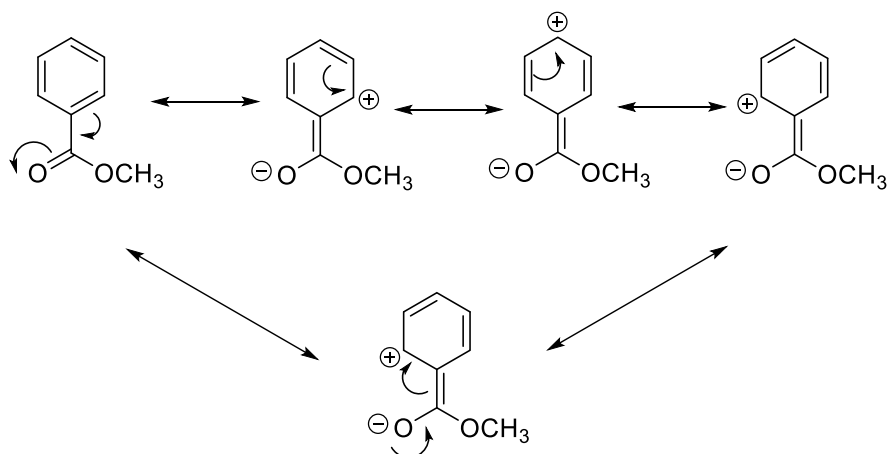
Scheme 2. 3: Effect of the ester moiety on the ortho and para proton position through the conjugation influence.

A second doublet can be seen at 6.64 ppm with 8.8 Hz coupling constant. This is due to the protons at positions C-2 and C-6 which are shielded from the field due to the electron-donating amino group.

2.2.2. Synthesis of the dibrominated compound C3.
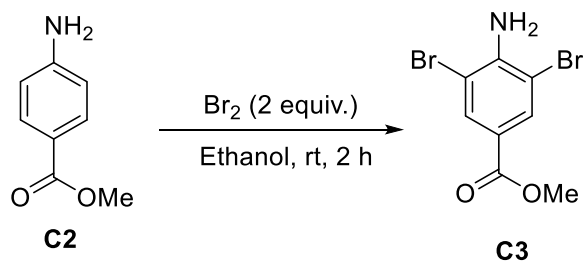
Scheme 2. 4: The synthesis reaction of the dibrominated compound **C3** using bromine.

Bromination of compound **C2** was affected via dissolving it in ethanol and adding bromine dropwise at room temperature (Scheme 2.6). Within 30 minutes a yellow precipitate was formed and filtered by suction filtration affording the di-brominated **C3** compound in 97% without purification.

This reaction is an electrophilic aromatic substitution reaction (Scheme 2.7).[103], [104] The two substituents of **C2**, amino and methyl ester groups, have a great impact in directing the bromide ions. The amine is an electron-donating group that significantly increases the activity of the aromatic ring at both *ortho* and *para* positions. The methyl ester substituent is electron-withdrawing, which in turn directs other substituents to the meta position of the aromatic ring. As a consequence, it can be envisioned that this reaction would be fast and drive the substitution to be on the C-2 and C-6 positions and to be deactivating for the C-3 and C-5 positions (see scheme 2.7 for carbon atom positions). Noteworthy, the second introduction of bromide ion would likely be rather slower than the first one. That is because the bromide is an activating substituent, so it would deactivate the second substitution on the *meta* position. However, the impact would be minor due to presence of the other substituents. Electrons of the aromatic π system would attack one of the bromine atoms resulting in addition of a bromine atom, positively polarised, to the *ortho* position.
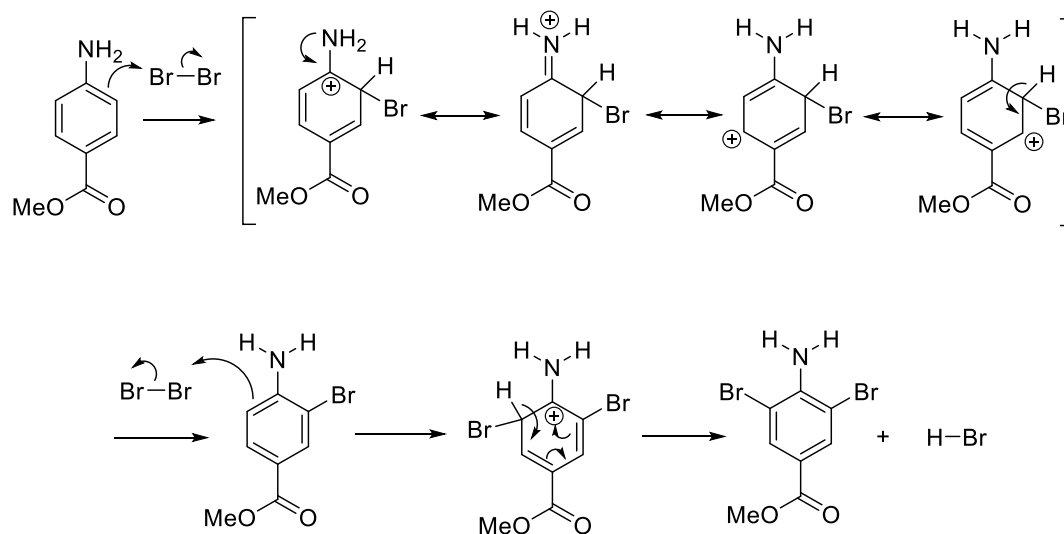
Scheme 2. 5: Mechanism of the synthesis of the dibrominated compound **C3**.

Accordingly, the aromaticity of the ring would be restored when the other negatively charged bromine atom abstracts a proton. With another equivalent of bromine, the same mechanism would proceed for the second bromination.
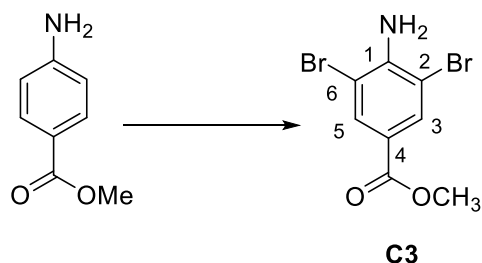
Scheme 2. 6: Atom numbering of the dibrominated compound **C3**.

The dibrominated product was confirmed using ^{1}H NMR spectroscopy (see scheme 2.8 for atom numbering). It was noticeable that both doublets had disappeared as evidence that the proton substitution at aromatic C-2 and C-6 with bromine atoms was successful. The singlet at 8.07 ppm corresponds to the protons of C-3 and C-5. It was transformed from a doublet in **C2** to a singlet in **C3** due to the regioselective substitution of the protons at C-2 and C-6 with bromine atoms that removed the effect of the coupling between the two pairs of proton. The singlet position moved to a higher position characteristic of the added electron-withdrawing effect of bromide substituents that pull electrons away from the protons of C-3 and C-5 leaving them in more de-shielded situation. The chemical shift of the methyl group almost remained the same (3.87 ppm) due to its position distant from the changes to the compound. A

broad singlet peak can be recognised at 4.99 ppm corresponding to the two protons of the aniline group.

During the scale up of this reaction, the product was washed with sodium thiosulfate to remove any bromine left. Consequently, a yellow precipitate of sulfur was formed, which was dissolved upon addition of 1M NaOH. This reaction was purified with flash chromatography giving an 82% yield of the product.

2.2.3 Reduction of methyl ester to alcohol C4.

In an attempt to shorten the pathway toward the required product, an alternative method was trialled to reduce the two subsequent steps, via reduction of the methyl ester **C3** to an alcohol then re-oxidation of the alcohol to an aldehyde, to one step using DIBAL-H reagent to go directly to the aldehyde (Scheme 2.9). The ability of the latter to reduce an ester to an aldehyde has been reported.[105] Thus, the ester was dissolved in toluene and added to a solution DIBAL-H at -70 °C. After 8 h, there was no apparent reaction. Due to the lack of the product this approach was not continued.
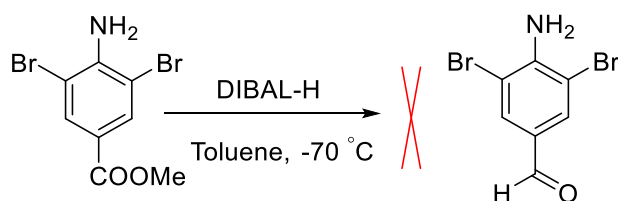
Scheme 2. 7: The unsuccessful reduction of the methyl ester to the correspondent aldehyde using DIBAL-H.
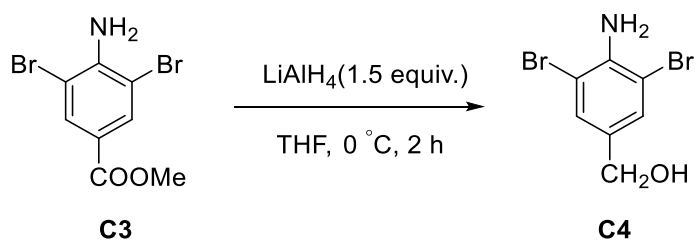
Scheme 2. 8: The reduction reaction of the methyl ester compound to alcohol **C4** using LiAlH$_4$.

Following Nicolaou's approach, reduction of the ester compound with LiAlH$_4$ in THF was carried out and afforded the alcohol compound **C4** in a good yield of 90% (Scheme 2.10). The reaction required an excess of LiAlH$_4$ to drive it to completion. Mechanistically, the reaction proceeds via a nucleophilic addition of two equivalents of hydride ion in two stages (Scheme 2.11). A hydride ion from LiAlH$_4$ attacks the carbonyl of the methyl ester **C3** of the substrate and the Li$^+$ ion coordinates to the carbonyl oxygen forming a tetrahedral intermediate. This intermediate, rapidly

collapses and loses methoxide resulting in formation of an aldehyde intermediate. In the second stage of the reduction, another hydride ion attacks the aldehyde carbonyl while Li$^+$ ion is coordinating to the oxygen. Then, upon work-up, aqueous ammonium chloride is added to protonate the alkoxide oxygen affording primary alcohol **C4**.
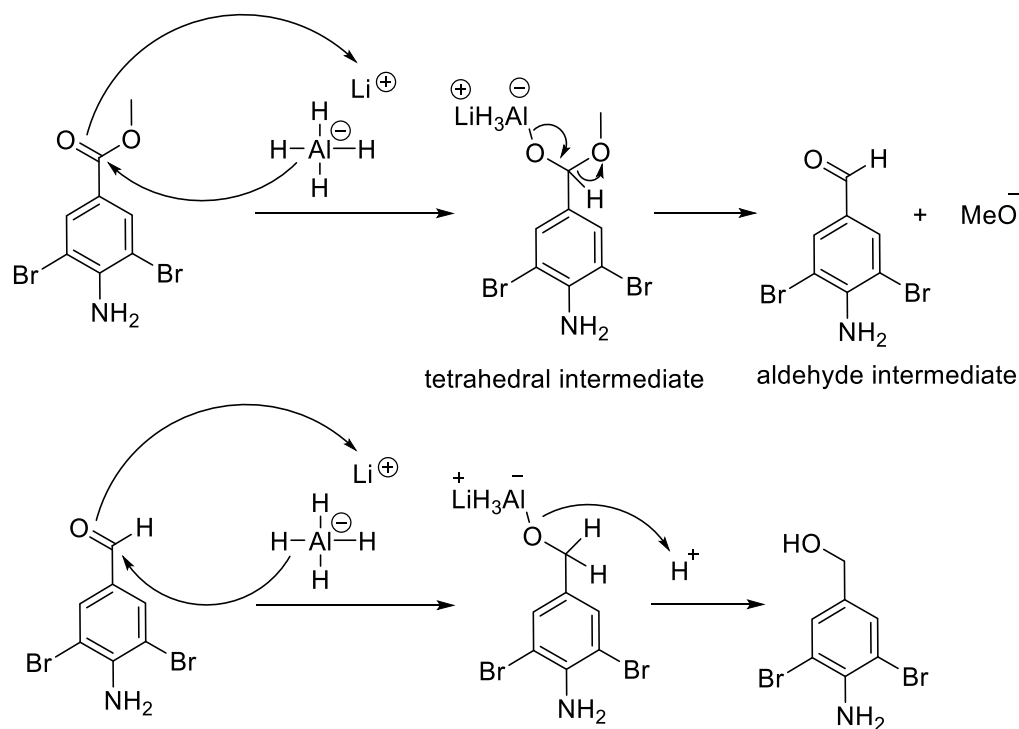
Scheme 2. 9: Mechanism of the reduction reaction of the methyl ester **C3** to the alcohol compound **C4** using LiAH$_4$.
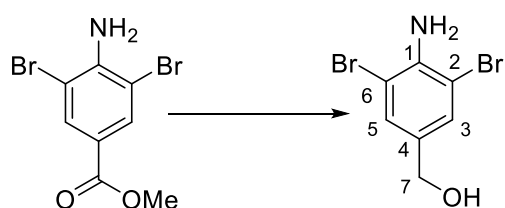
Scheme 2. 10: Atom numbering of the alcohol compound **C4.**

The reduction reaction was confirmed using ^{1}H NMR spectroscopy (see scheme 2.12 for atom numbering). The singlet corresponding to the methyl group at 3.87 ppm in **C3** has disappeared and a singlet of the two protons of the methylene C-7 appeared at 4.54 ppm. Moreover, the singlet of the aromatic protons at C-3 and C-5 moved to a lower position (from 8.07 to 7.40 ppm) due to loss of the de-shielding effect of the

ester carbonyl. The integration of the peak at 4.54 ppm was equivalent to 4, due to overlapping of the aniline-NH_2 protons and methylene protons.

In the larger scale synthesis, it was found that two equivalents of $LiAlH_4$ were required to drive the reaction to the completion and maintain the optimum yield of 86%.

2.2.4 Synthesis of the triazene derivative C5.
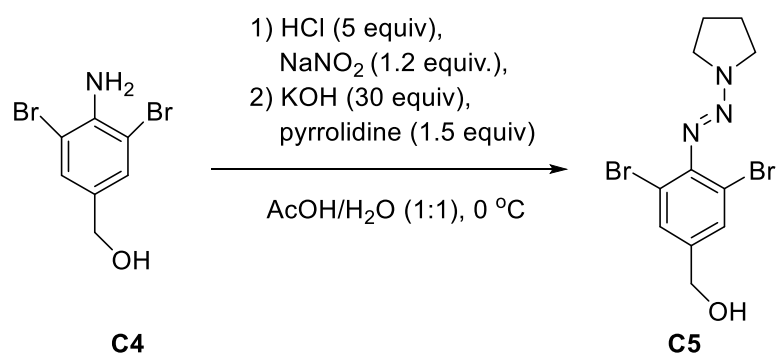
Scheme 2. 11: Synthesis of the triazene-protected aniline **C5** using $NaNO_2$ and pyrrolidine.

The triazene product **C5** was afforded in a good yield of 93% after purification. Its synthesis consisted of two stages: 1) diazonium salt formation, by treatment with HCl and $NaNO_2$, 2) triazene formation, by treatment of the diazonium salt with pyrrolidine and KOH (Scheme 2.13). Formation of the diazonium salt is called diazotisation and involves reaction of aniline with nitrous acid.

The reaction starts when nitrous acid is formed by the reaction of $NaNO_2$ with aqueous acid (Scheme 2.14). Following protonation and elimination of water, aqueous nitrous chloride is formed. The latter reacts with the amine through nucleophilic attack of the amine at the nitrogen. Following protonation, tautomerisation and elimination of water, the diazo salt is formed. Treatment of this salt, without isolation, with an excess of pyrrolidine and strong base then generates the product through direct nucleophilic attack of the pyrrolidine on the diazo compound followed by deprotonation by base.
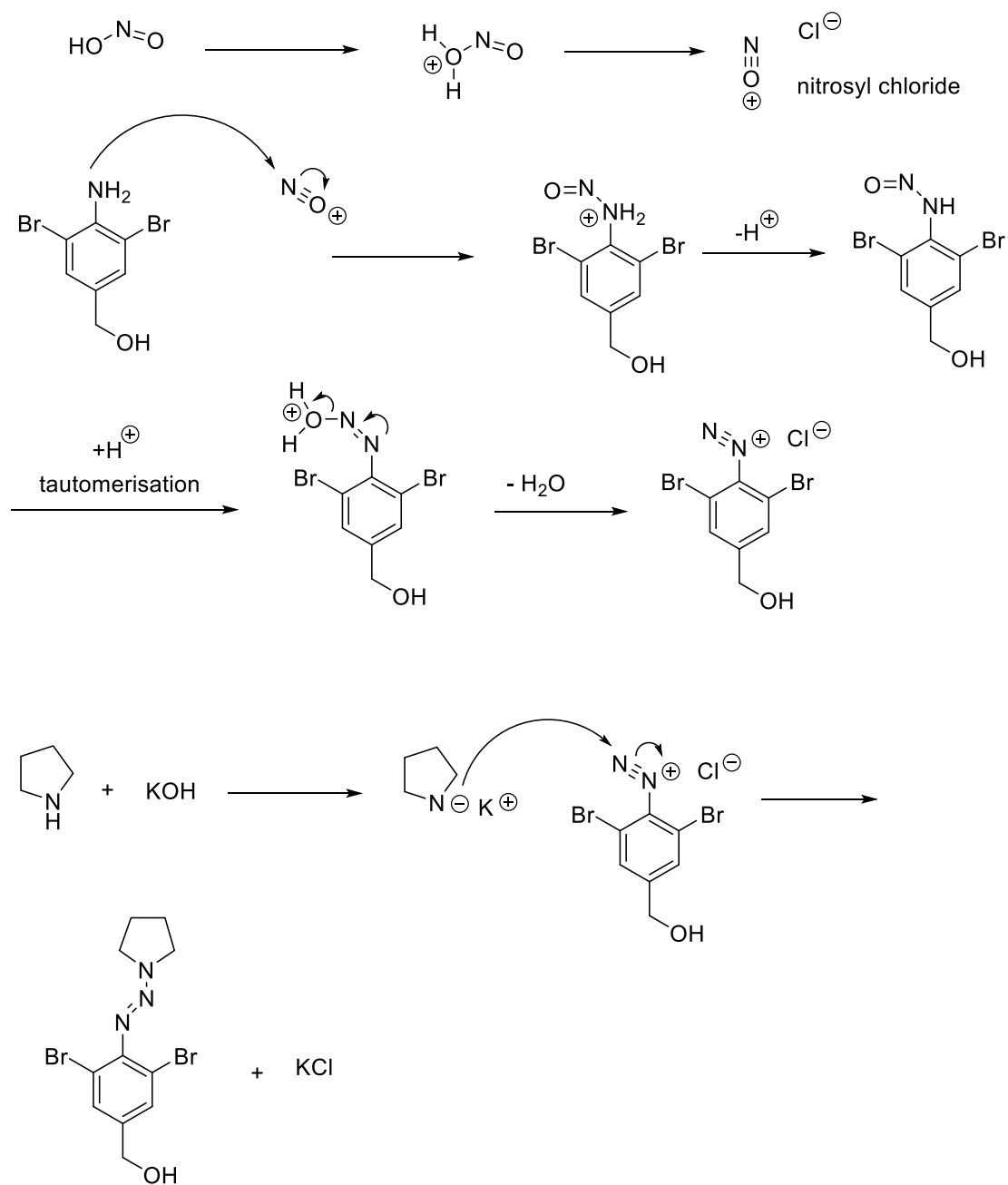
Scheme 2. 12: Mechanism of the triazene derivative **C5** formation using $NaNO_2$ and pyrrolidine reagents.
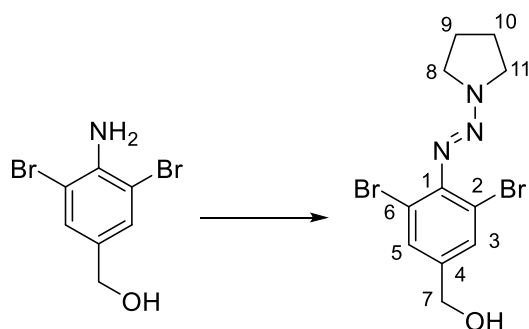
Scheme 2. 13: Atom numbering of the triazene protected-aniline compound **C5**.

^{1}H NMR spectroscopy was used for characterization of the triazene product (Scheme 2.15 for numbering). The two single broad peaks at 3.95 ppm and 3.73 ppm corresponded to the four protons of methylene C-8 and C-11 of the pyrrolidine; each of them integrates to two protons. The single broad peak at 2.08 ppm was assigned to the four protons of C-9 and C-10 of the pyrrolidine. The electron-withdrawing effect of the recently attached triazene group caused the singlets corresponding to the aromatic protons of C-5 and C-3 and methylene protons of C-7 to be moved to a more downfield position.

2.2.5. Synthesis of the aldehyde compound C6.
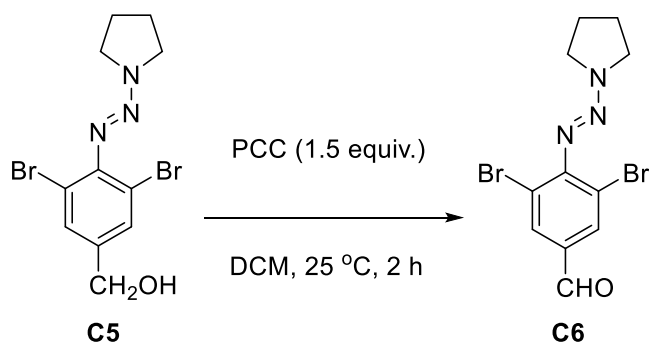
Scheme 2. 14: Oxidation reaction of the primary alcohol compound to the aldehyde **C6** using PCC reagent.

The aldehyde **C6** was obtained via reaction of the primary alcohol with pyridinium chlorochromate (PCC) at room temperature for 2 h (Scheme 2.16). PCC is known for its toxic chromate by-product, which can make work up difficult giving rise to a lower yield (53%). This problem was solved by introducing silica into the reaction flask so that the chromate by-product adhered to the silica making the separation process easier. Florisil® (100-400 mesh) was used for the product filtration, which added another technique that improved the reaction yield up to 90%.

In terms of the mechanism of reaction, it is an oxidation reaction, in which the alcohol is oxidized to aldehyde and chromium(VI) is reduced to chromium(IV) (Scheme 2.17). A lone pair of the nucleophilic alcohol oxygen attacks chromium (VI), so a Cr-O bond forms. After the proton transfers from the positively charged OH to one of the two negatively charged chromium-oxygens, the other negatively charged chromium oxygen regenerates the Cr=O with expulsion of chloride ion. Intramolecular proton transfer occurs from the methylene group by the oxygen atom of Cr=O leading to aldehyde formation and removing the reduced chromium (IV) as a leaving group.
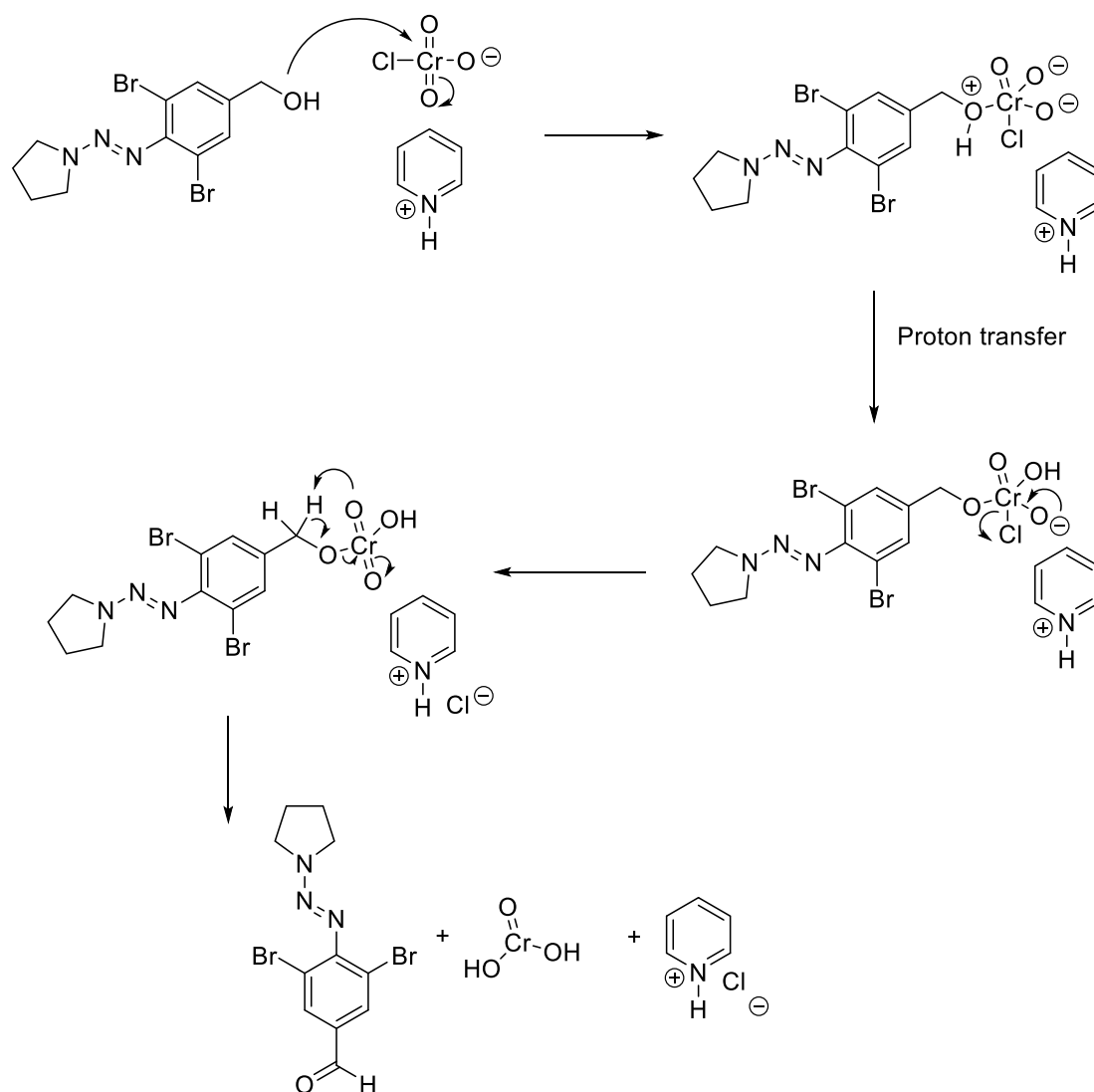
Scheme 2. 15: Mechanism of oxidation reaction of the alcohol **C5** to aldehyde **C6** using PCC reagent.
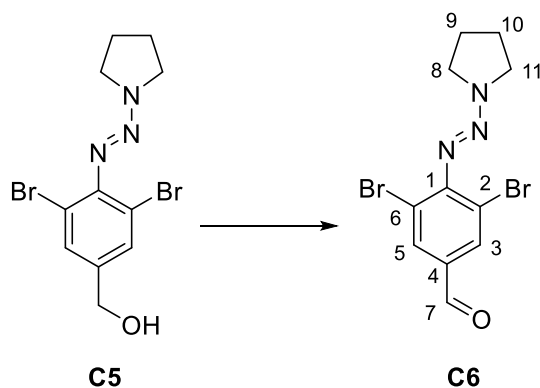
Scheme 2. 16: Atom numbering of the aldehyde **C6**.

The aldehyde product **C6** formation was confirmed using ^{1}H NMR spectroscopy (Scheme 2.18 for atom numbering). The aldehyde proton of C-7 produced a singlet at 9.84 ppm and the aromatic protons of C-3 and C-5 produced a singlet which was slightly deshielded compared with **C5** (from 7.52 ppm to 8.02 ppm). This is because of the conjugation effect of the carbonyl group, reducing electron-density around the protons. The chemical shifts of the pyrrolidine protons remain at similar ppm shifts to **C5** because of their distance from the newly formed aldehyde group.

2.2.6 Synthesis of styrene C7.
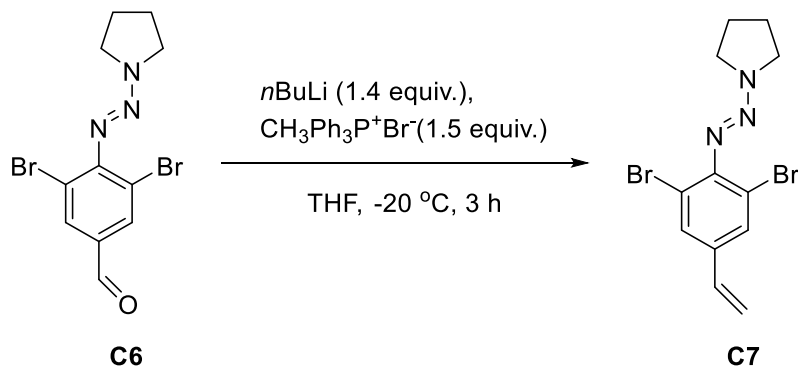
Scheme 2. 17: Synthesis of styrene compound **C7** using *n*-BuLi through a Wittig reaction.

The styrene **C7** was formed in 60% yield using a Wittig reaction. *n*-BuLi was added to methyltriphenylphosphonium bromide at -20 °C under anhydrous conditions. After 30 min, the aldehyde was added and furnished the alkene product after 3 h.

The Wittig reaction was first demonstrated in 1953 by Wittig and Geissler.[106] It is of high significance for use in the synthesis of alkenes from aldehydes and ketones,[107] and is characterised by the production of a C-C double bond via condensation of alkyl halides with carbonyl compounds by use of organophosphines.[108] The extent of the ylide stability plays a pivotal role in determination of the geometry of the

resulting olefin. Basically, non-stablised phosphonium ylides lead mainly to a *cis* alkene products (*Z* selectivity), whereas stabilised phosphonium ylides give rise to a *trans* alkene as a major product (*E* selectivity) (scheme 2.20).[109]
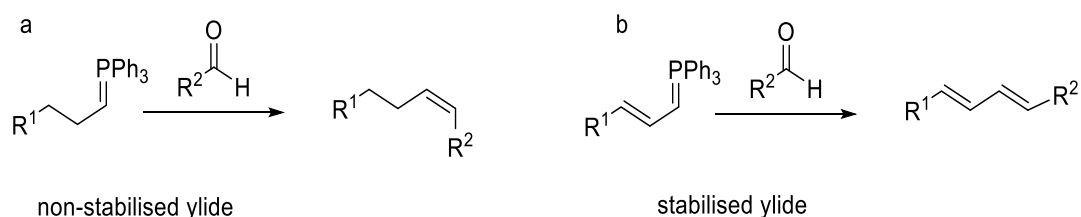
Scheme 2. 18: Illustration of non-stabilised (a) and stabilised (b) ylide forms.[107]

The ylide required is formed in an S_N2 reaction. The lone pair of the polarised bond C-Li in *n*-BuLi attacks one of the three protons of the methyl group in methyltriphenyl phosphonium bromide leading to formation of the ylide. The latter would be in a resonance state between its polarized and double-bonded variants. Upon presence of the aldehyde compound the ylide would be added in 2+2 cycloaddition reaction forming an oxaphosphetane intermediate, which is a four-membered cyclic compound. This intermediate rapidly collapses to furnish the very stable triphenyl phosphine oxide and the styrene product (Scheme 2.21). An alternative proposal is that the reaction proceeds in a nucleophilic addition rather than 2+2 cycloaddition forming a betaine intermediate before transforming to the four-membered ring intermediate (Scheme 2.22).[110]
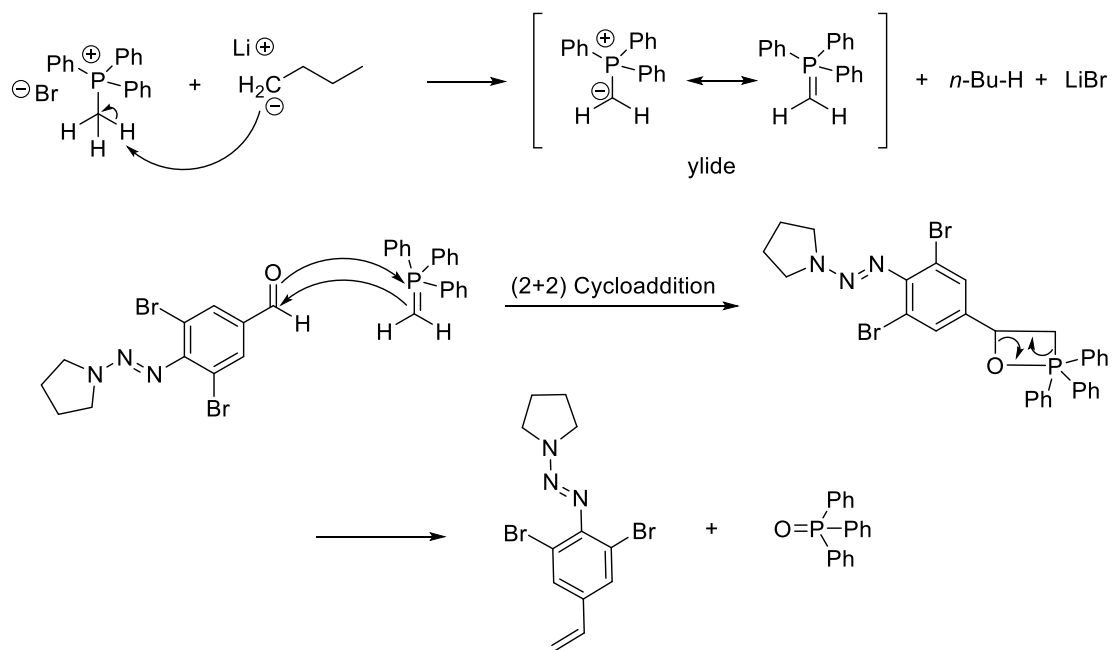
Scheme 2. 19: Illustartion of 2+2 cycloaddition mechanism of formation of styrene compound **C7** through Wittig reaction.
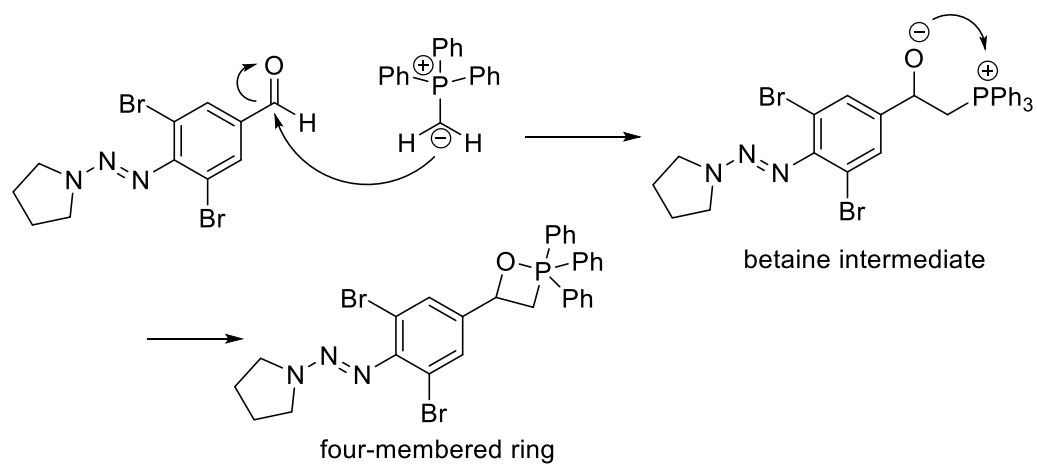
Scheme 2. 20: Nucleophilic addition proposal for styrene formation.
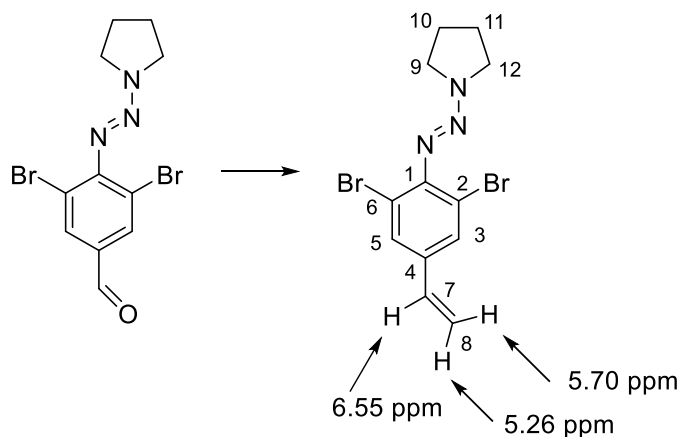
Scheme 2. 21: Atom numbering of the alkene product.

The formation of the styrene product **C7** was confirmed using ^{1}H NMR spectroscopy (see scheme 2.23 for atom numbering). The two protons of the C-8 alkene furnished a doublet each. The first at 5.70 ppm, with coupling constant of 17.5 Hz characteristic of coupling to neighbouring *trans*-H of C-7, and the second at 5.26 ppm with constant coupling of 10.9 Hz, characteristic of coupling to the neighbouring *cis*-H on C-7. The proton of the alkene C-7 gave rise to doublet of doublets, at 6.55, with coupling constants of 17.5 Hz and 10.8 Hz. Disappearance of the aldehyde proton at 9.84 ppm and movement of the singlet peak of the aromatic protons (C-3 and C-5) to a lower chemical shift (from 8.04 to 7.57 ppm) gives further evidence of the formation of styrene group and disappearance of the carbonyl group. Again, the peaks of the pyrrolidine protons had similar shifts to **C6** due to their distance away from the reaction site.

2.2.7 Synthesis of the diol compound C8 using Sharpless AD.
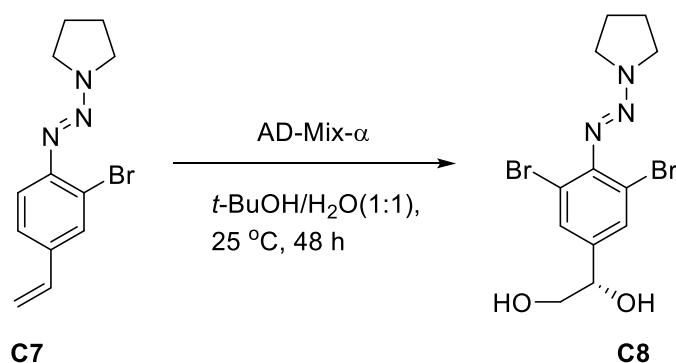
Scheme 2. 22: Synthesis of the diol compound **C8** using AD-Mix-α through Sharpless AD reaction.

Treatment of styrene **C7** with AD-mix-α furnished the diol **C8**. The styrene was stirred in t-BuOH/H$_2$O for 8 h with AD-Mix-α. At the end of this time, **C7** was still present, so the reaction was stirred for 24 h. After work-up, the diol **C8** was obtained in 99% yield. This is an example of the Sharpless asymmetric dihydroxylation reaction (SAD). SAD involves the application of commercially available pre-mixed reagents, AD-Mix-α and AD-Mix-β, to generate diols in a stereoselective fashion. These premixes contain almost the same reagents except that they differ in the chiral ligand, AD-Mix-α contains a phthalazine adduct with dihydroquinine ((DHQ)$_2$PHAL) and AD-Mix-β contains a phthalazine adduct with dihydroquinidine ((DHQD)$_2$PHAL) (Figure 2.5). AD-Mix-β and AD-Mix-α are named so as they attack the olefin either at top face (β face) or at bottom face (α face) respectively (Scheme 2.25).[111] The other common reagents are: potassium osmate K$_2$OsO$_2$(OH)$_4$ which acts as non-volatile source of the oxidant osmium tetraoxide, potassium ferricyanide K$_3$Fe(CN)$_6$, which is the reoxidant in the catalytic cycle, and potassium carbonate. These premixes are used for limited forms of olefins, which are terminal 1,1-disubstituted, 1,2-trans-substituted and tri-substituted olefins.[111]

AD-mix-α   AD-mix-β
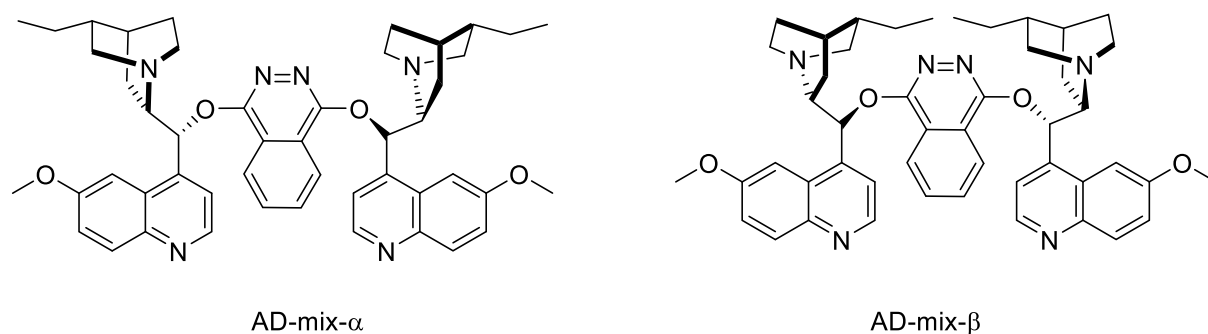
Figure 2. 4: Chemical structure of the chiral ligands of AD-mix-α, (DHQ)2PHAL, and of AD-mix-β, (DHQD)2PHAL.
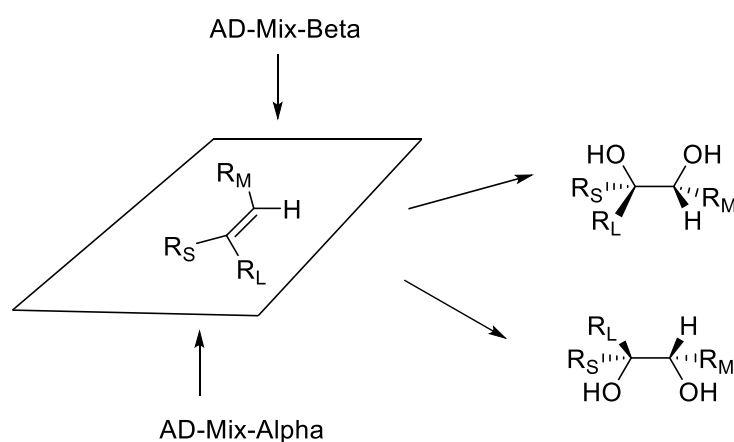
Scheme 2. 23: Illustrating how β- and α-diol results based on the attack orientation of AD-Mix-β and AD-Mix-α.

The importance of SAD is represented by its ability to produce pure cis-diol with great stereoselectivity.[112] Mechanistically, the reaction works by an asymmetric induction mechanism, via which a chiral ligand (catalyst) is used to convert optically inactive compounds to optically active (chiral) products.[113] There are two suggested mechanisms for SAD: a stepwise [2+2]-addition followed by rearrangement (Scheme 2.26a), and a concerted cycloaddition [3+2] (Scheme 2.26b). The latter mechanism has a strong evidence base.[114] In the concept of a 3+2 mechanism, the presence of the ligand accelerates, to a significant extent, the catalytic reaction of AD due to its ability to transform OsO_4 to 1,3-dipole over reaction with olefins.[115],[114] Therefore, depending on whether the double bond substituents of reacting olefin are electron-donating or withdrawing, the 1,3 dipole renders the electron movement from olefin to the dipole and from the dipole to the olefin so slow that the stereoselectivity becomes much higher (see chapter 4 for full discussion of the mechanism).
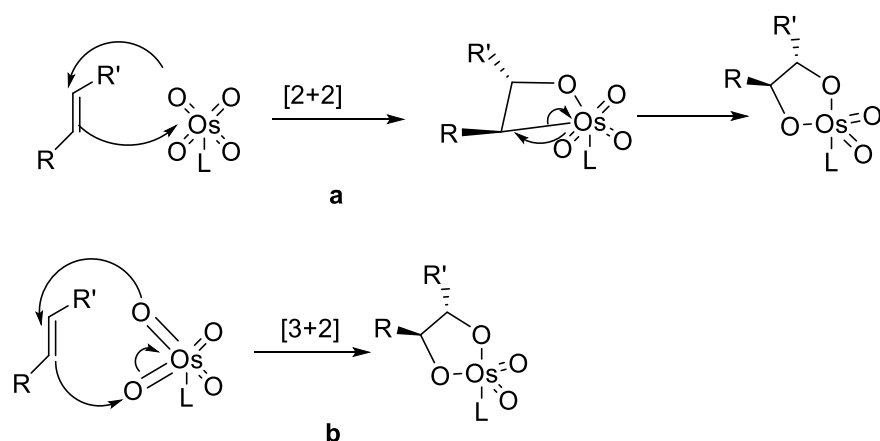
Scheme 2. 24: Two different proposals for the Sharpless AD reaction mechanism: a) stepwise [2+2]-addition; b) concerted cycloaddition [3+2].
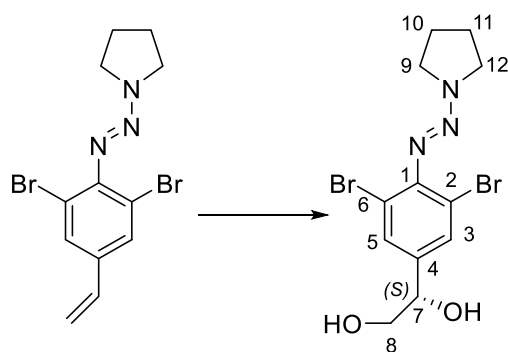
Scheme 2. 25: Atom numbering of the beta diol compound **C8**.

The success of the reaction was confirmed using ^{1}H NMR spectroscopy (Scheme 2.27 for atom numbering). The proton of C-7 gave a doublet of doublets at 4.73 ppm with coupling constants of 8.04, 3.53 Hz, characteristic of coupling to neighbouring protons of C-8. Another two doublets of doublets peaks came out at 3.68 and 3.57 ppm. Both corresponding to two protons of C-8 with coupling constants 11.1, 3.5 Hz and 11.1, 8.04 Hz respectively. These coupling constants are characteristic of coupling to each other and to the proton of C-7. There is a dramatic difference in chemical shift between the doublet corresponding to the proton on C-7 and the other two doublets for the protons on C-8. This is because of the presence of the secondary hydroxyl group attached to the same C-7 (two bonds away) in which the electronegativity pulls electron density away from the C-7 proton rendering it more deshielded. In addition, the presence of the C-7 proton close to the aromatic ring boosts the de-shielding effect. Polarimetric rotation was calculated at 22 °C: [α]= +82.05 (c=0.078 g/mL, CHCl$_3$). The literature value at 22 °C is [α]=+79.4 (c=1.21, CHCl$_3$).[99] It can be concluded that the compound **C8** produced in this work is purer than the literature counterpart, i.e. has less the opposite enantiomere.

2.2.8. Synthesis of TBS-protected diol C9.
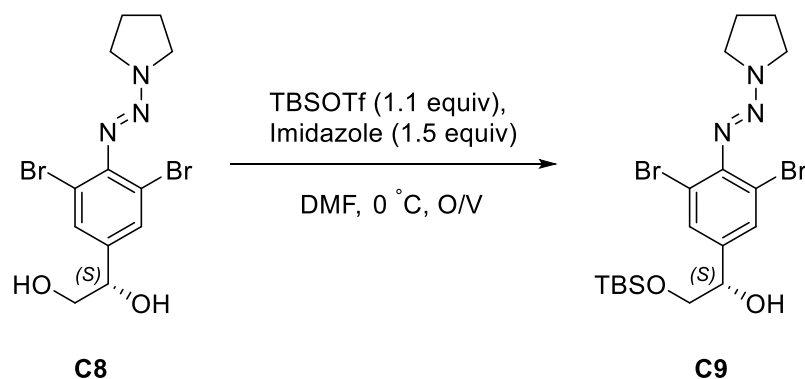
Scheme 2. 26: TBS protection of the primary alcohol using TBSOTf.

Compound **C9** was obtained using TBSOTf with imidazole in DMF at 0 °C. Although, the reaction was successful, a low yield of 22% of product was obtained (Scheme 2.28). The TBS group was introduced as it is more stable than other types of silyl ether protecting groups, for example, it is up to 10^4 times more stable to hydrolysis than a TMS group.[116],[117],[118] In addition, TBS is widely applied for primary and secondary alcohol protection due to its facile removal and compatibility with many chemical reactions.[119] TBS reacts very slowly with alcohols, so addition of imidazole or DMAP in DMF as a solvent increases its reactivity significantly.[117],[116] An initial trial followed the literature approach for alcohol protection. When TBSCI was used alongside imidazole as a base catalyst, the reaction gave no product (Scheme 2.29).
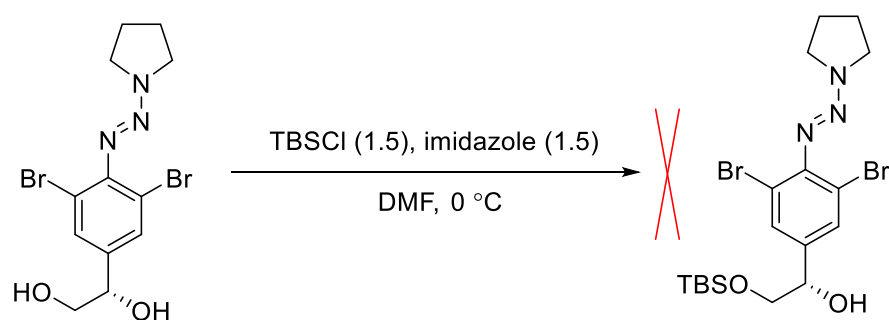
Scheme 2. 27: The unsuccessful reaction of TBS protection of alcohol using TBS-CI and imidazole.

Using highly reactive TBSOTf led to di-protected by-product in a yield of 32%. On TLC basis, the product and the TBS-diprotected by-product were recognised as two dense spots near the top of the plate. TBSOTf is characterized by its high reactivity even with more sterically hindered hydroxyl groups.[116] The TBS-diol was purified with flash column chromatography to be used later to regenerate the diol compound. This reaction was carried out using TBAF in THF as a reaction solvent giving to the product in 80% yield (Scheme 2.30).
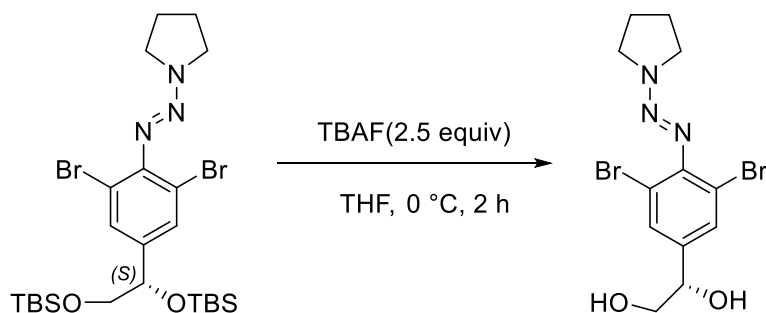
Scheme 2. 28: The TBS-deprotection of alcohol using TBAF reagent.

Another trial was attempted using a different base catalyst, DMAP (0.1 equiv.) and anhydrous Et_3N (1.5 equiv) (Scheme 2.31), alongside TBS-Cl in anhydrous DCM solvent. This was an attempt to avoid the di-protected by-product generated by TBSOTf. Interestingly, the reaction worked within 2 h and gave a 63% yield of the desired mono-protected compound. This approach was used for the scale-up of the reaction. Thus, a solution of diol and DMAP in dry DCM was cooled to 0 °C under N_2. Dry Et_3N and TBS-Cl were added sequentially and the mixture stirred for 2 h at room temperature. After purification with flash chromatography, the mono-protected diol was afforded as a yellow powder in a yield of 67%.
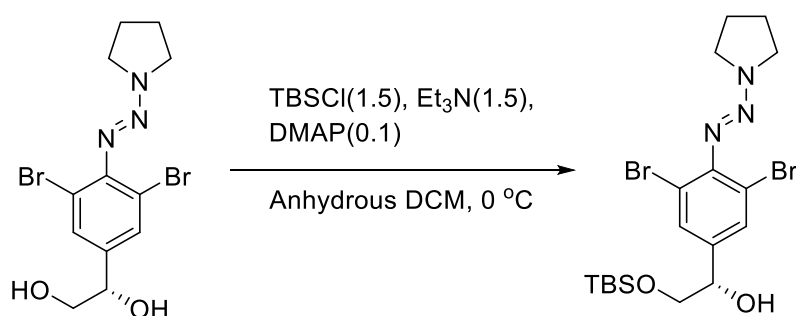
Scheme 2. 29: The TBS-protection reaction of alcohol using TBS-Cl, Et_3N and DMAP reagents.

Herein, the mechanism of the reaction using TBSOTf is demonstrated as prototype of the other TBS-protection of alcohol reactions (Scheme 2.32). TBS protection of

alcohol **C8** is a nucleophilic reaction. The lone pair on N-3 in imidazole attacks the polarised silicon atom in TBSOTf, displacing triflate ion as a leaving group. Since the intermediate is more activated, the terminal alcohol of the diol attacks the silicon atom expelling imidazole as a leaving group. The triflate ion deprotonates the oxonium ion furnishing the TBS-protected product.
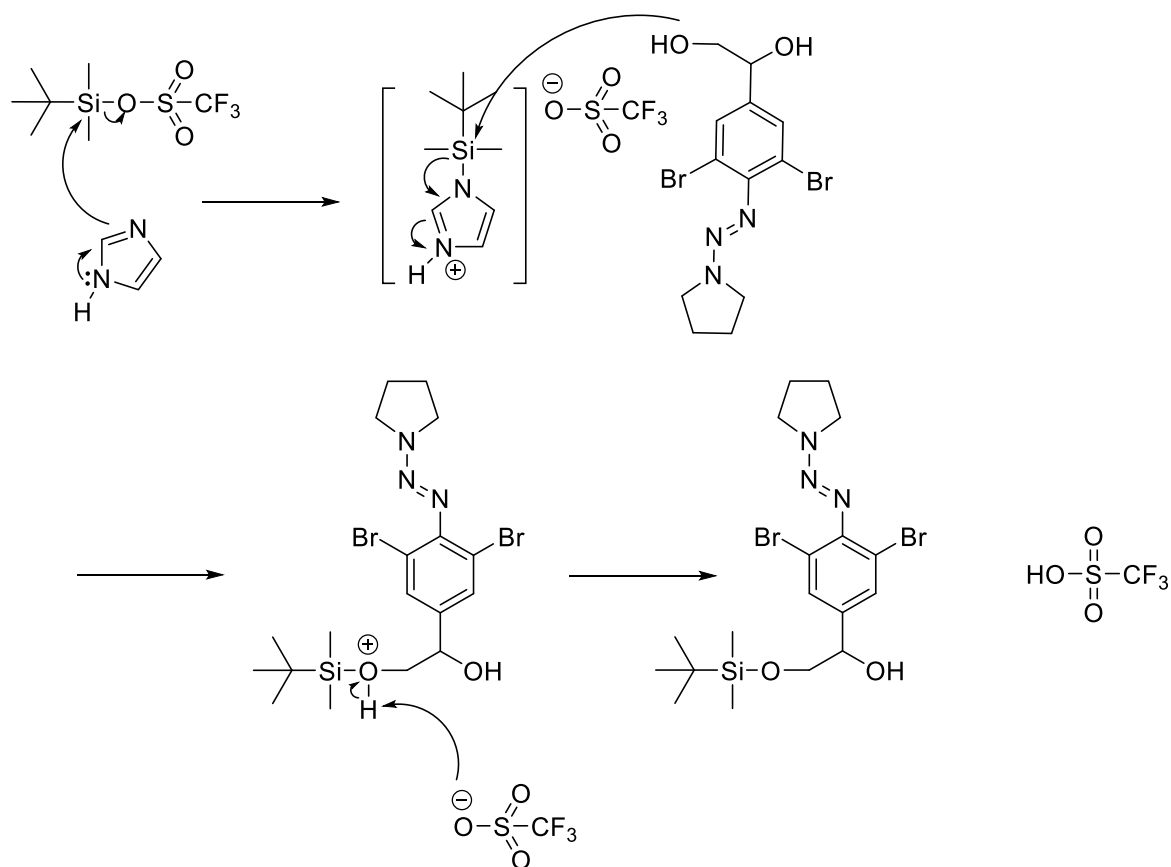
Scheme 2. 30: Mechanism of TBS-protection of primary alcohol.
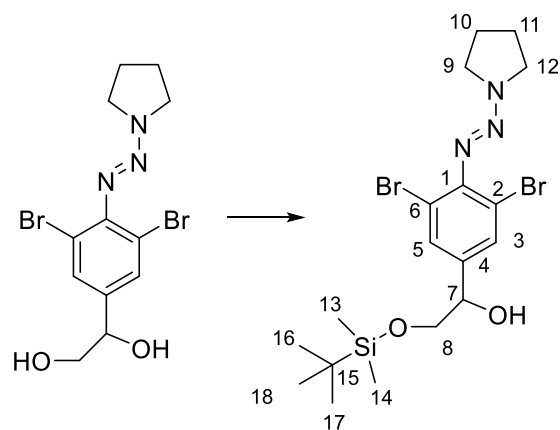
Scheme 2. 31: Atom numbering of the TBS-protected alcohol compound **C9**.

The TBS-protected structure was confirmed using ^{1}H NMR spectroscopy (see scheme 2.33 for atom numbering). The most characteristic change is the emergence of two large single peaks at 0.94 and 0.07 ppm, which correspond to the nine protons of C-16, C-17, and C-18 and six protons of C-13 and C-14 respectively. The integration of the former was nine and for the later was six which indicated the tertiary butyl and dimethyl groups respectively. The polarimetric rotation value was observed at 22 °C: [α]=+18 (0.026 g/mL, CHCl$_3$). The literature value was +22.8. (c=1.43, CHCl$_3$).[99] Therefore, it can be inferred that the purity of compound **C9** is slightly less than that of the literature compound, i.e. has more the ooposite enantimere.

2.2.9. Synthesis of azide compound C10.
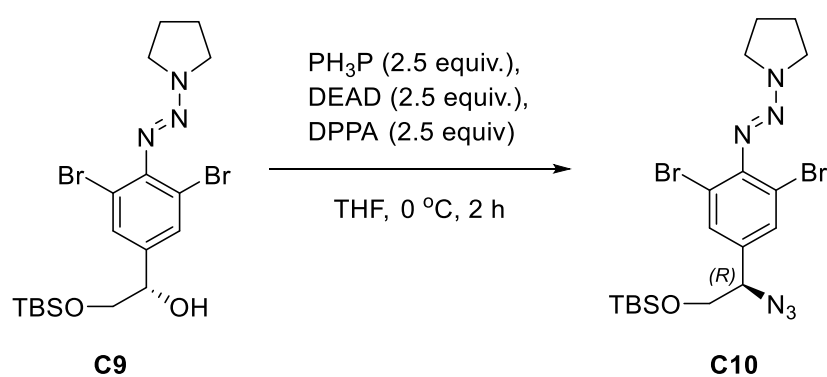
Scheme 2. 32: Mitsunobu reaction for azide formation using Ph$_3$P, DEAD, and DPPA reagents.

The azide **C10** was obtained using Ph$_3$P, DPPA and DIAD (Scheme 2.34). Because of toxicity concerns DIAD reagent was used instead of DEAD.[120] The Mitsunobu reaction is one of the most useful reactions in organic synthesis for producing various acid derivatives such esters, imides, ethers, azides, and so on.[121] This reaction proceeds via dehydrative coupling of an alcohol with a suitable nucleophile. The most important characteristic feature of this reaction is the stereochemical inversion of the alcohol substrate.[122],[120] Three proposals have been made for the mechanism via which the first step of Mitsunobu reaction proceeds and leads to formation of the betaine intermediate (Scheme 2.35):

1) Michael-type nucleophilic attack,

2) Single electron transfer (SET), and

3) [4+2] cycloaddition reaction followed by ring opening.

Michael type reaction is the more accepted mechanism for the first step.[123]

1)
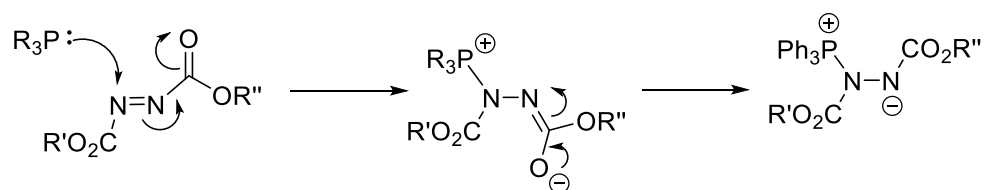
2)
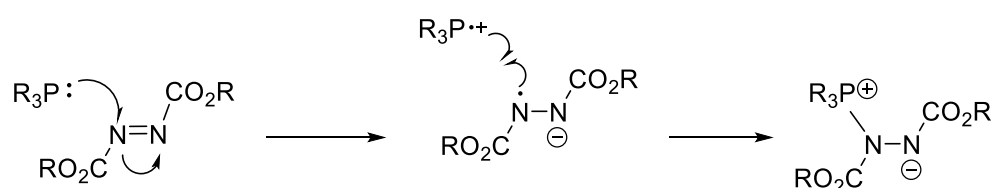
3)
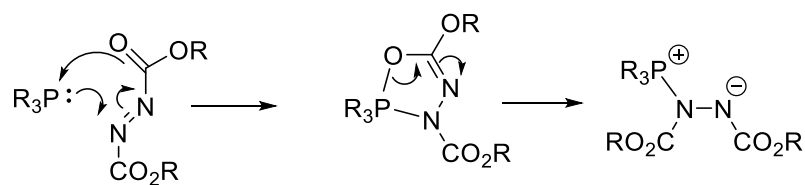
Scheme 2. 33: The three proposals of the mechanism of the first step in Mitsunobu reaction for azide formation; 1) Michael addition, 2) Radical reaction, 3) Cycloaddition reaction.

In general, the mechanism of Mitsunobu reaction involves three steps: 1) Adduct formation, in which a dialkylazodicarboxylate and Ph₃P react with each other in a nucleophilic reaction to form a betaine intermediate.

2) Alcohol activation, in which the alcohol is deprotonated to form oxyphosphonium ion. Formation of the oxyphsphonium ion relies mostly on basicity of the conjugate base of the adduct and reduced polarity of the solvent.

3) Reaction of the nucleophile with the oxyphosphonium intermediate via S_N2 reaction, which is accompanied by complete inversion in stereochemistry.[124]

Triphenyl phosphine (Ph₃P) attacks diisopropylazodicarboxylate (DIAD) in a nucleophilic reaction (Michael-addition reaction) leading to formation of a betaine intermediate (Scheme 2.36). The latter deprotonates the alcohol substrate to form an ion pair of phosphonium and alkoxide ions, which carries out a nucleophilic attack on the phosphonium ion forming compounds **4** and **5**. The compound **5** then attacks diisophenyl phosphorylazide releasing the azide anion. Then, the azide ion attacks **4**

in S$_N$2 nucleophilic reaction affording the azide compound **C10** and triphenyl phosphine oxide. This addition of the azide is characterized by a complete inversion in stereochemistry of the original hydroxyl group.
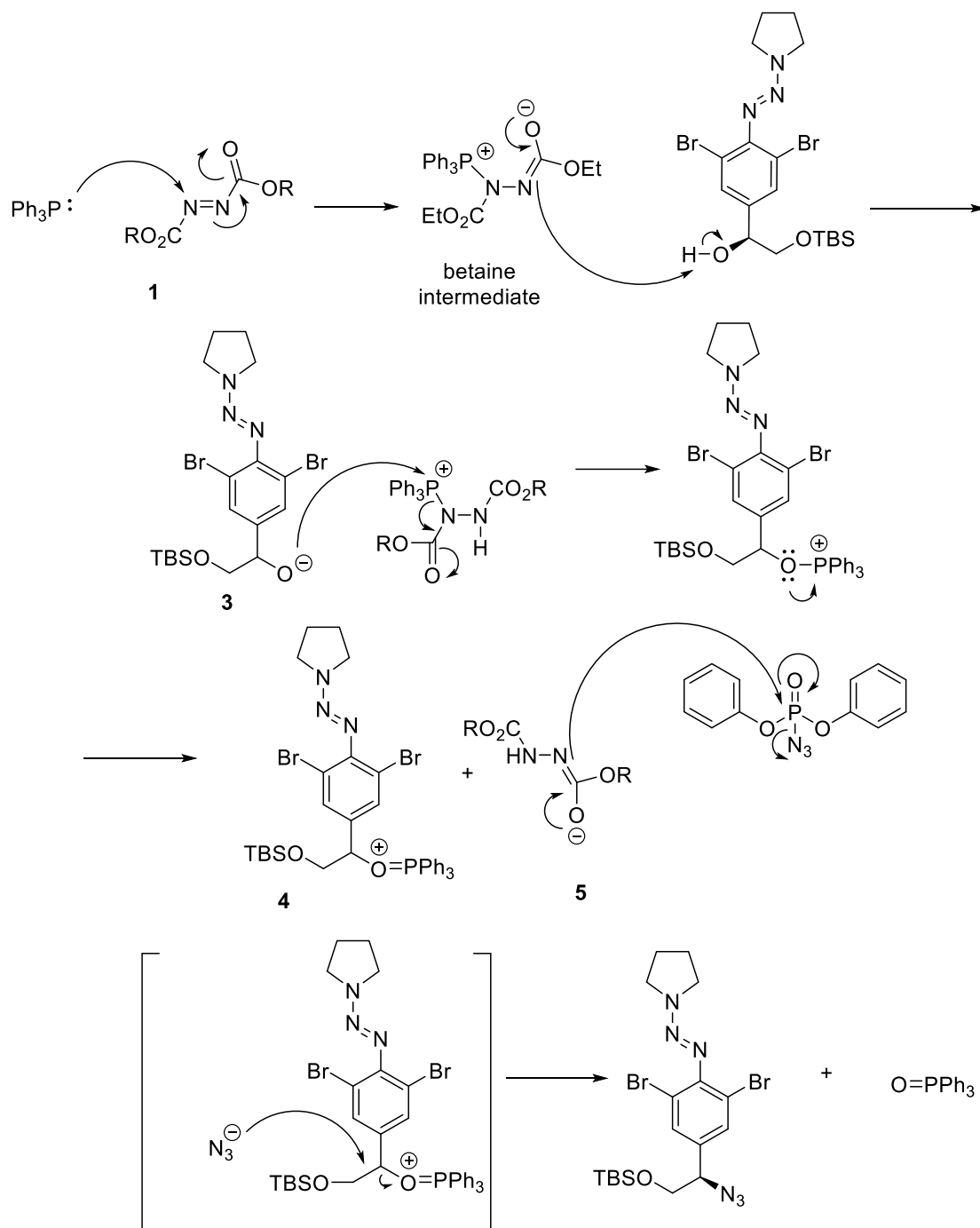
Scheme 2. 34: Mechanism of Mitsunobu reaction for azide product **C10** formation.
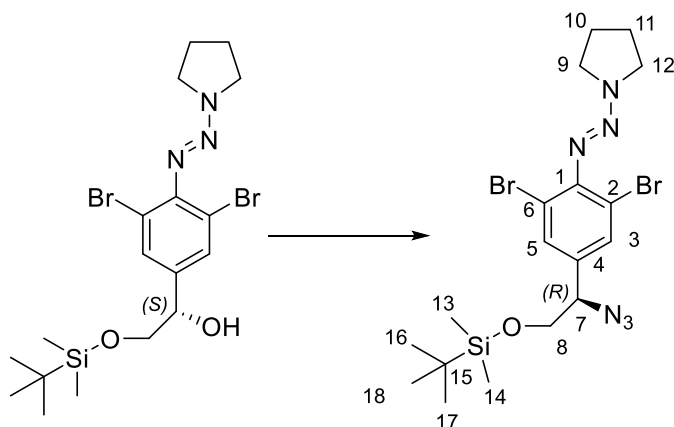
Scheme 2. 35: Atom numbering of the azide product **C10**.

In this case, ^{1}H NMR gave little information about the formation of the azide compound. Therefore, the presence of azide group was confirmed with FT-IR as a peak was present at 2100 cm^{-1}. On the NMR spectroscopy (see scheme 2.37 for the atom numbering) two peaks were present, a multiplet and doublet, at 5.5 and 1.6 ppm respectively. These peaks correspond to isopropanol, which was formed as a by-product through the use of DIAD. The doublet of doublet peak corresponding to the proton of C-7 slightly shifted upfield (from 4.66-4.49 ppm), which is explained as the azide group is less electronegative than hydroxyl group, which makes the proton of C-7 less deshielded. The two doublets of doublets at 3.78 and 3.71 ppm which correspond to the two protons of C-8 are superimposed over the broad singlet that corresponds to the protons of either C-9 or C-12 of pyrrolidine.

Although this reaction was successful on small scale synthesis (up to 0.5 g, 1.00 mmol), on scale up to just twice this amount, the exact product was not identified (although starting material was consumed). As this was the case, the SM was divided into thirteen 0.5 g batches and the reactions were carried out in parallel on this scale. The presence of the side product isopropanol proved difficult to remove, making a yield difficult to quantify and so this material was used as crude form in the next reaction. The polarimetric rotation value was observed at 22 °C: [α]= - 102 (0.076 g/mL, CHCl$_3$). The literature value: - 43 (c=1.30, CHCl$_3$).[99] Obviously, the rotation value of **C10** is much more than that of the literature value, which indicates that the purity of **C10** is much higher than the literature compound.

2.2.10. Synthesis of amine compound C11.
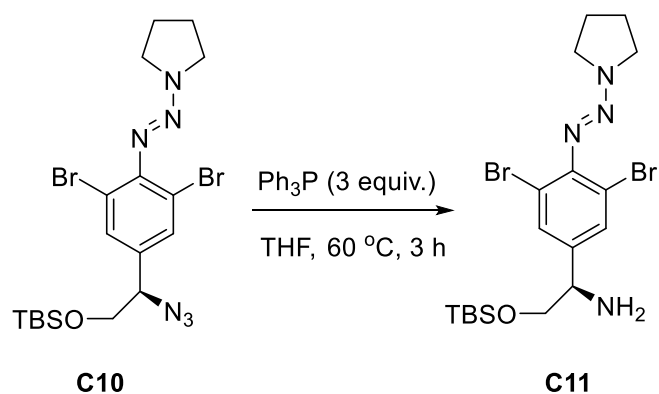
Scheme 2. 36: Reaction of azide reduction to an amine product using Ph₃P reagent.

Reduction of azide to amine was carried out on crude **C10** using Ph₃P (Scheme 2.38). This reaction, a Staudinger reaction, mechanistically involves nucleophilic addition of Ph₃P to the terminal nitrogen atom of azide forming a phosphazide intermediate, which rapidly loses a nitrogen molecule giving the iminophosphorane compound (Scheme 2.39). Upon addition of water, iminophosphorane is hydrolysed affording the amine **C11** compound and the phosphine oxide by-product.
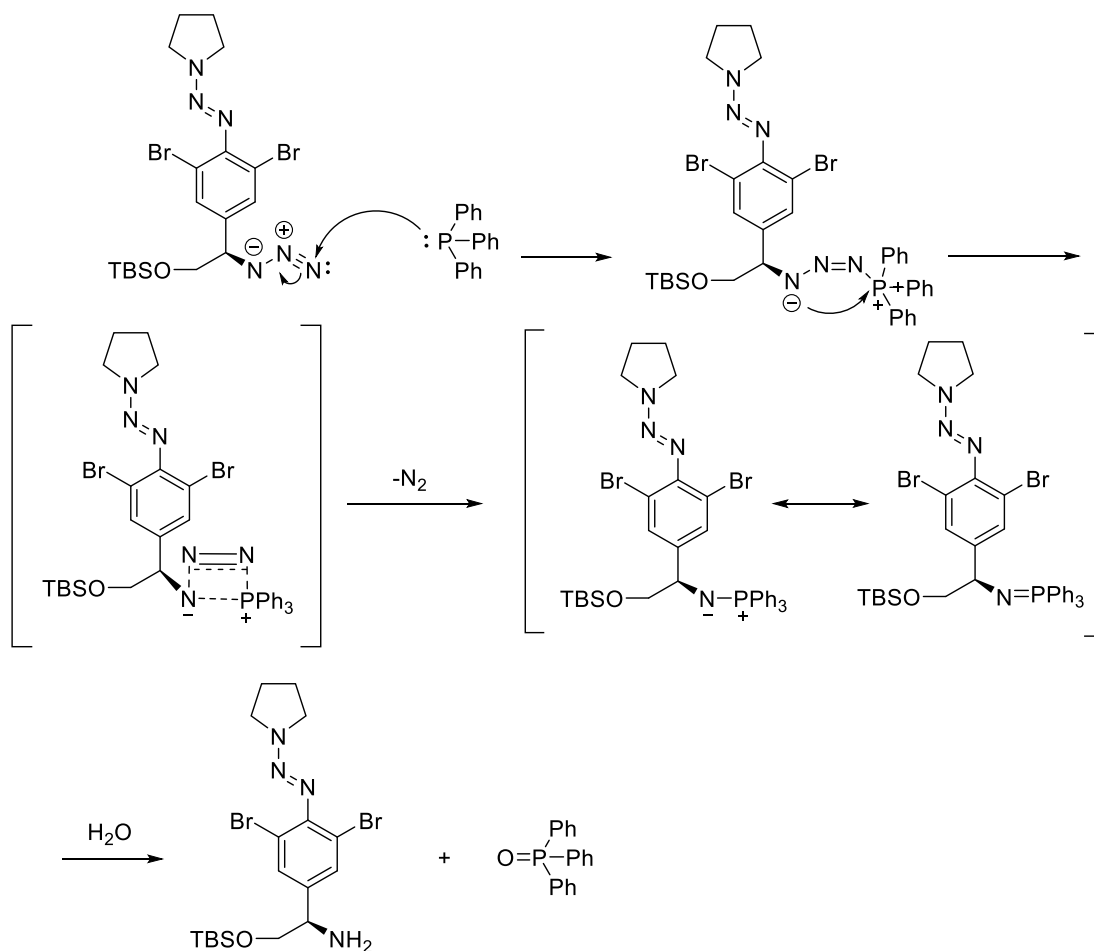
Scheme 2. 37: Mechanism of azide reduction to the amine **C11** using Ph₃P.
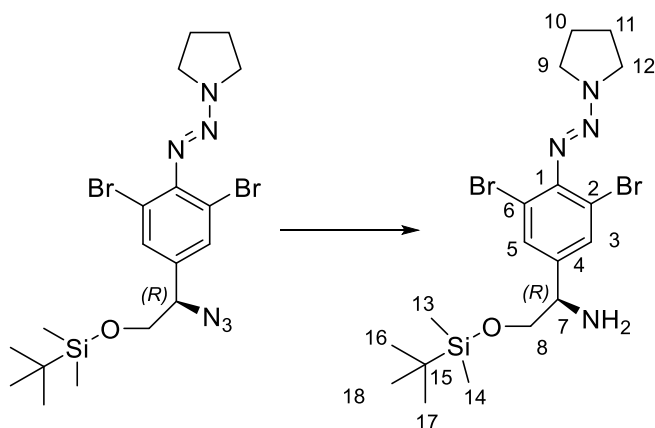
Scheme 2. 38: Atom numbering of the amine compound **C11**.

The amine product was confirmed using ¹H NMR spectroscopy (see scheme 2.40 for atom numbering). A significant change in chemical shift was noticed for the doublet of doublets peak corresponding to the proton of C-7, where it was shifted upfield from 4.5 to 3.93 ppm. That is explained as the azide reduced to amine which is less

electron-withdrawing so the proton of C-7 would become more shielded with electron density. Moreover, a broad singlet peak has emerged at 6.45 ppm, corresponding to the amine protons. In spite of repeated purification, the isopropanol peaks were still seen in the spectrum of the amine's product. Again, the crude material was submitted to the next step. Reaching this point, formation of the amine, was a crucial step as it was the entrance to the Fmoc-protection, which is the cornerstone in the project plan. Also, it was only few steps from the final desired compound. The polarimetric rotation value was observed at 22 °C: [α]= - 10.7 (0.11 g/mL, CHCl$_3$), and the literature's value: -22.0 (c=1.53, CHCl$_3$).[99] The big difference between the two values reflects the difference in the purity, i.e. **C11** is less pure than the literature compound.

2.2.11. Synthesis of Fmoc-protected compound C12.
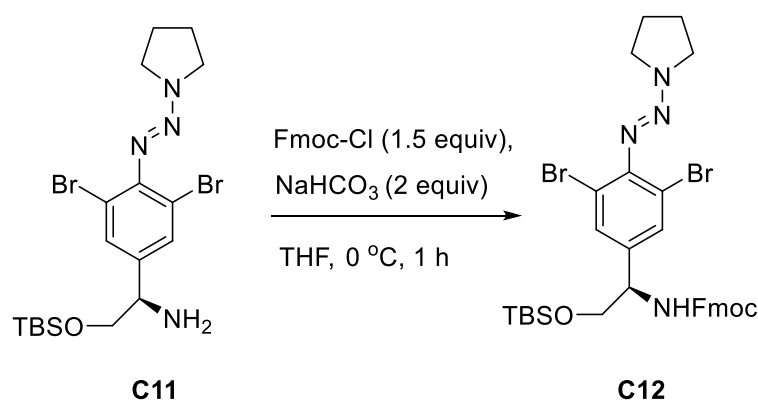
Scheme 2.39: Fmoc-protection reaction of the amine compound using Fmoc-Cl.

Given the project objective is the synthesis of vancomycin using solid phase synthesis methods, Fmoc-protection of the amine was required. Therefore, treating the amine product with Fmoc-Cl afforded the Fmoc-protected as crude product due to the presence of isopropanol. This reaction was affected by dissolving the amine **C11** in THF at 0 °C and adding aqueous NaHCO$_3$ and Fmoc-Cl sequentially affording the Fmoc-protected compound **C12** in 50% yield over the last three steps (Scheme 2.41). The mechanism of this reaction starts with the nucleophilic attack of the primary amine on the carbonyl atom and formation of a tetrahedral intermediate (Scheme 2.42). The carbonyl group is reformed and chloride ion removed as a leaving group. Loss of a proton furnishes the Fmoc-protected amine and HCl.
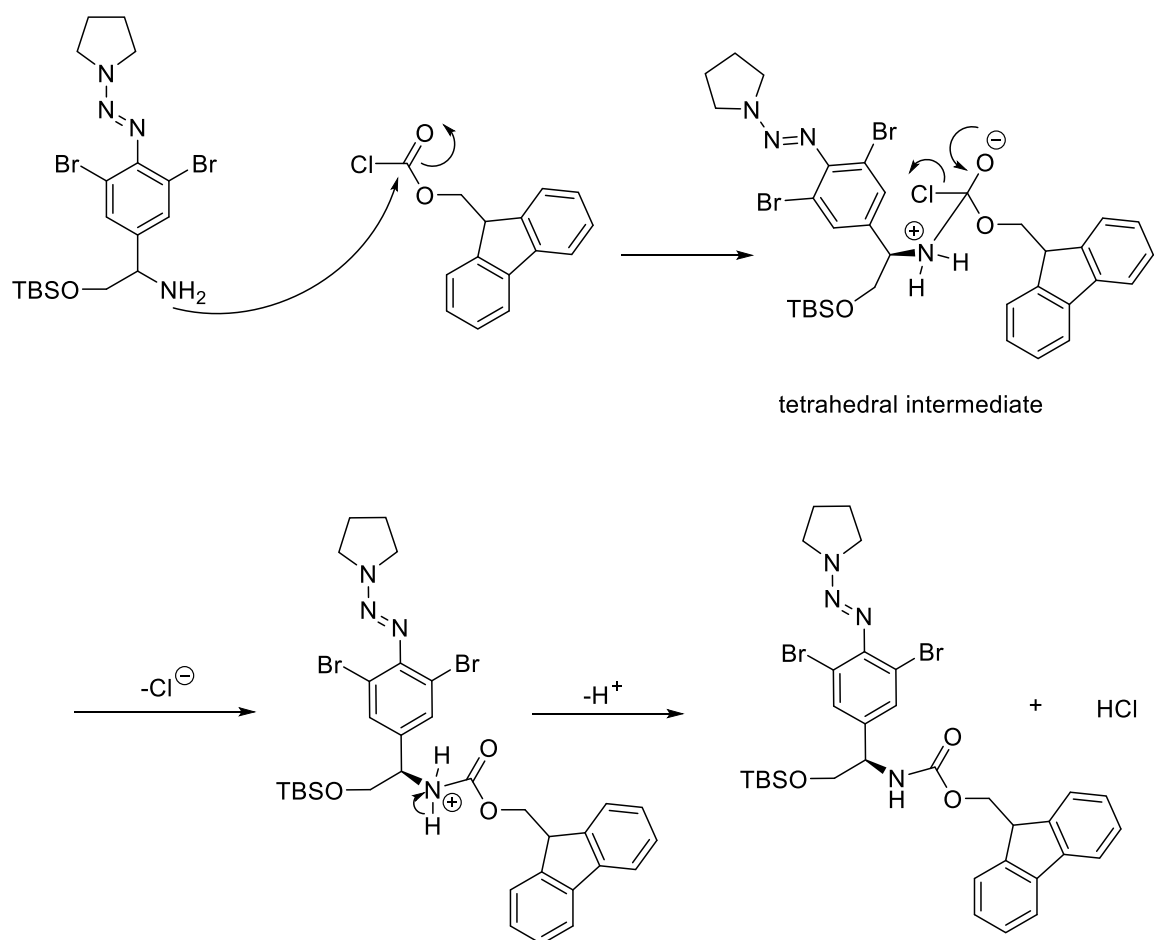
Scheme 2. 40: Mechanism of Fmoc-protected amine compound **C12**.
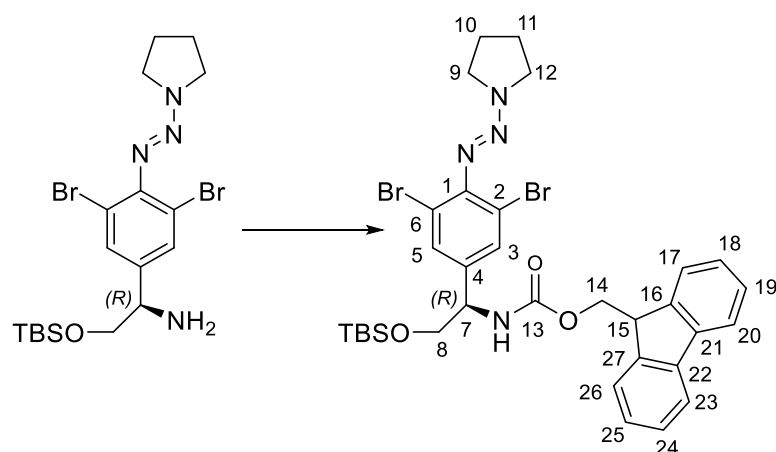
Scheme 2. 41: Atom numbering of the Fmoc-protected amine compound **C12**.

The attachment of Fmoc group was confirmed using ^{1}H NMR spectroscopy (Scheme 2.43 for atom numbering). The spectrum peaks appeared broadened when chloroform solvent was used but in DMSO they were sharp enough for assignment. The Fmoc group emerged as six chemical shifts, four in the aromatic region at 7.92,

7.72, 7.44, and 7.35 ppm each of which integrates for two protons. The first two peaks at 7.92 and 7.72 ppm shifts are doublet and multiplet corresponding to protons of carbons (C-17, C-26) and (C-20, C-23) respectively. The protons of C-17, C-26 experienced more de-shielding than the protons of carbon C-20, C-23 due to the closer position to the amide bond which is electron-withdrawing. In conclusion, the protons of carbons (C-20, C-23) are farther from the amide bond so their representative doublet (7.72 ppm) is slightly lower in the NMR spectrum.

The peaks at 7.44 and 7.35 are multiplets corresponding to protons of carbons (C-18, C-25) and (C-19, C-24) respectively. The other two of the six Fmoc group peaks are the doublet at 4.26 ppm and the triplet at 4.18 ppm, corresponding to the two protons of methylene C-14 and the proton of the tertiary C-15. Obviously, the latter two groups of protons are quite de-shielded because of the direct influence of the withdrawing effect of the amide bond. In addition, one of the quite prominent changes in the NMR spectrum for Fmoc-protected compound is the shift in the peak of the proton of C-7 to a higher chemical shift, 4.64 ppm, that is explained by its close position to the newly formed amide bond (two bonds distance). Moreover, it is noticeable that the multiplet for two methylene protons of C-8 has moved to a higher chemical shift, 3.72 ppm, also because of the influence of the amide bond. The polarimetric rotation value was observed at 22 °C: [α]= - 42.9 (0.067 g/mL, CHCl$_3$).

2.2.12. Deprotection of TBS group producing alcohol compound C13.
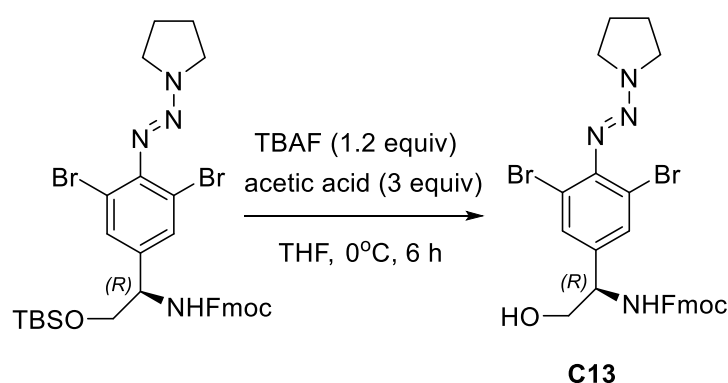
Scheme 2. 42: Deprotection of TBS protection group forming the alcohol compound **C13**.

As has been mentioned earlier in this chapter, use of TBS protecting groups has been of importance due to its facile installation and removal, stability, and suitability for many of reactions.[119],[125] Herein, a TBS-deprotection was carried out with tetrabutylammonium fluoride (TBAF) (Scheme 2.44). The mechanism involves a

nucleophilic attack of the fluoride ion of TBAF onto the silicon atom forming a very strong Si-F bond (Scheme 2.45). This strong bond would be the driving force of the cleavage. Thus, after forming a pentavalent intermediate, the alkoxy group acts as a leaving group so the bond between oxygen and silicon breaks forming an alkoxide ion which abstracts a proton from water affording the alcohol product **C13**. Since the presence of water in TBAF solution would generate a basic solution which strongly affects the protection of amine, the addition of acetic acid is very productive approach to neutralize that basic condition leading to a significant increase in the product yield (95%).[126] Therefore, addition of 3 equivalents of acetic acid was helpful and increased the amount of the product 2-fold. However, it also slowed the reaction rate down, so the reaction time increased from 2 h to 6 h.
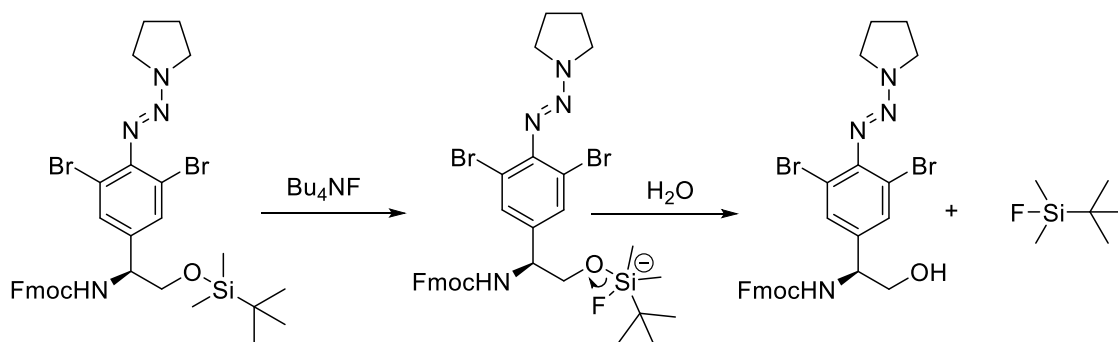
Scheme 2. 43: Mechanism of TBS-deprotection using Bu₄NF.
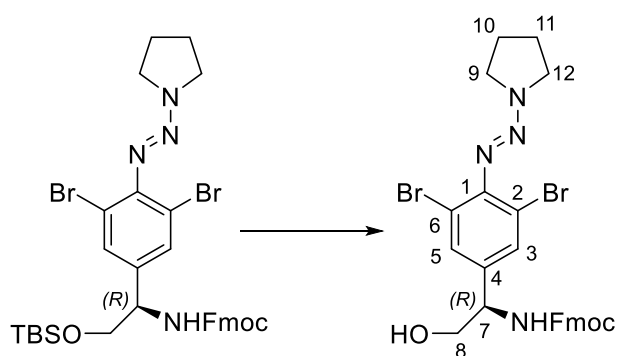
Scheme 2. 44: Atom numbering of the alcohol compound (TBS-deprotected) **C13**.

TBS-deprotection was confirmed with ^{1}H NMR (see scheme 4.46 form atom numbering). Obviously, the three peaks of TBS group at 0.85 ppm, 0.01 and at -0.02 ppm in C-12 compound were no longer present in the NMR spectrum of the **C13** compound. In addition, a new triplet peak at 4.97 ppm which integrates to one proton, corresponds to the primary hydroxyl group, restored after TBS-deprotection. The multiplet peak at 3.63-3.52 ppm corresponded to the four protons of the C-8

(methylene) and C-12. Noticeably, the peak corresponding to the protons of C-8 moved slightly to a lower position, comparing to the C-8 in the compound **C12**, to be overlapped with the signal of C-12 in the pyrrolidine moiety. That is because of a reduction in the electron-withdrawing influence of alcohol in comparison to the TBS protecting group. As has been mentioned earlier above, acetic acid was added to neutralise the basic by-product of TBAF reagent. Although addition of acetic acid increased the productivity significantly, the reaction lasted longer to completion (6 h rather than 2 h). A pinkish fluffy powder of alcohol was obtained from TBS deprotection step. The polarimetric rotation value was observed at 22 °C: [α]= - 32.4 (0.056 g/mL, CHCl$_3$).

2.2.13. Oxidation of alcohol to carboxylic acid using TEMPO C14.

TEMPO(1 equiv),NaOCl(3 equiv), KBr(0.1 equiv)

5% NaHCO$_3$: Acetone (1:1), 0 °C
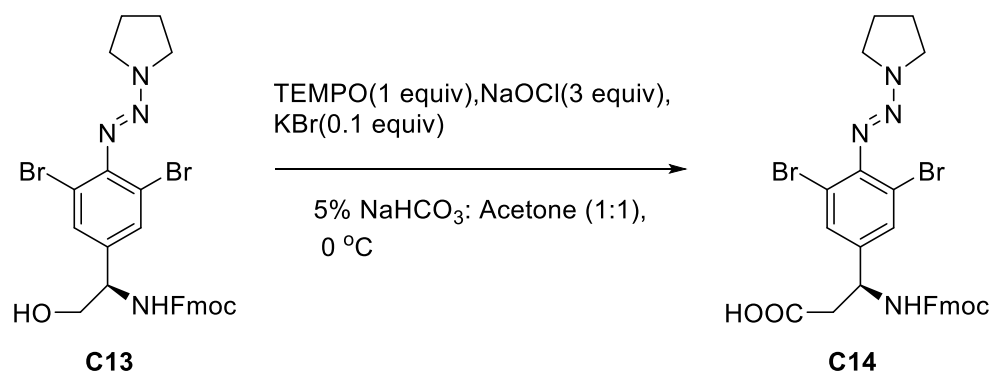
Scheme 2. 45: Reaction of formation of the carboxylic compound **C14** using TEMPO reagent.

The alcohol was oxidised to a carboxylic acid by using the above reagents (scheme 2.47). The product was afforded in 65% yield and the right molecular weight was confirmed with high resolution MS. The selective oxidation of alcohol to aldehyde or carboxylic acid that was described by Anelli et al, posed a breakthrough for an easy, fast and cheap type of oxidation.[127] The mechanism of this reaction proceeds on two oxidation stages: 1) conversion of alcohol to an aldehyde, 2) conversion of aldehyde to a carboxylic acid.

After formation of oxoammonium salt from oxidization of TEMPO radical with potassium bromide, it is attacked by the deprotonated alcohol substrate with the basic reagent, NaHCO$_3$, forming an intermediate adduct (Scheme 2.48). This adduct undergoes either intramolecular or intermolecular proton abstraction leading to formation of hydroxylamine and aldehyde product.[127] In order for the oxidation process to further proceed to afford the required carboxylic acid, the oxoammonium

salt has to be regenerated. Therefore, sodium hypochlorite is added as a co-oxidant to accomplish this task by oxidizing bromide to hypobromite which functions as a secondary oxidant to regenerate the primary oxidant, oxoammonium salt (scheme 2.49).[128] Thus, with the presence of water, aldehyde would be in equilibrium with its hydrated form which in turn undergoes the same fate of oxidation in presence of oxoammonium salt to end up with carboxylic acid (Scheme 2.50).
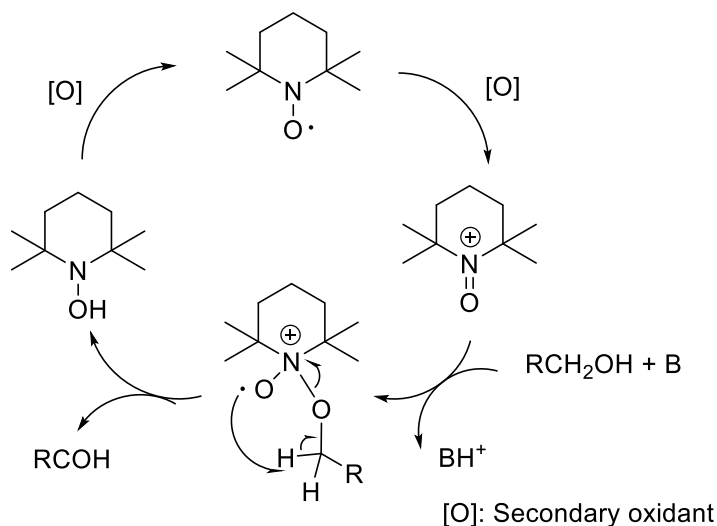
Scheme 2. 46: Illustartion of formation of oxoammonium ion and its role in formation of the aldehyde intermediate.
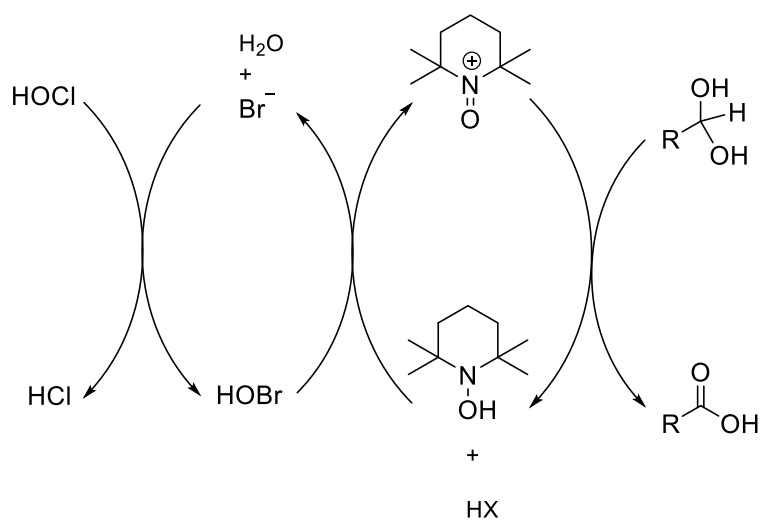
Scheme 2. 47: Illustrates the role of KBr in oxidation of alcohols into corresponding carboxylic acid using TEMPO oxidizing reagent.[128]

102
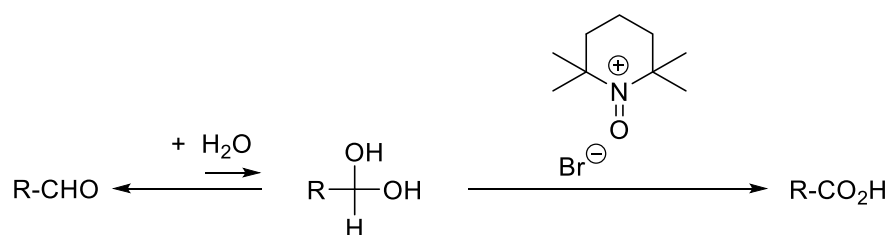
Scheme 2. 48: The oxidation stage of aldehyde to the corresponding carboxylic acid with oxoammonium salt.

It is important to illustrate some tips about TEMPO oxidation reaction in terms of conditions and reagents being used:

1) It is more selective for primary alcohols than for secondary, as steric hindrance plays a role in this sense.

2) To take the oxidation process further to the carboxylic acid formation, it is important to keep the reaction temperature as low as 0 °C in presence of water. The oxoammonium salt decomposes in aqueous medium at room temperature.

3) The oxidation is accelerated at slightly basic pH, 8.6, which is provided by addition of $NaHCO_3$. Whereas at very high pH the concentration of HOBr would be too low to oxidize hydroxylamine to oxoammonium slat which in turn oxidizes aldehyde to carboxylic acid.

4) Biphasic solvent is of high importance if the alcohol oxidation is required to proceed to the carboxylic acid stage. Otherwise, the oxidation is more likely to stop at the aldehyde stage.[129]
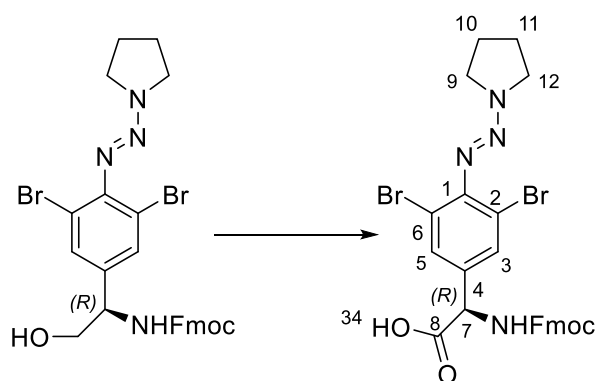
Scheme 2.49: Atom numbering of the carboxylic acid compound.

The assignment for this amino acid **C14** was confirmed using ^{1}H NMR spectroscopy (see scheme 2.51 for atom numbering). The first sign that oxidation was affected successfully, the disappearance of the peak of protons of C-8 from the spectrum.

Secondly, the transfer of the doublet peak of the C-7 proton to a singlet peak and its movement to a higher ppm shift was another effective evidence that the oxidation was complete and the characteristic coupling to the neighbouring protons was lost. The polarimetric rotation value was calculated at 22 °C: [α]= - 28.4 (0.062 g/mL, MeOH).

2.3. Summary.

This chapter discusses the first successful synthesis of the central amino acid of vancomycin protected for Fmoc-synthesis and set up for the application of, for example, Ullman type coupling reactions to form cyclic ethers with neighbouring tyrosine analogues. Interestingly, the compound could also be incorporated into other peptides and used to introduce other functionality though, for example, cross coupling reactions. The synthesis is highly efficient, with several steps having high yields that are consistent in moving to scale-up reactions to produce the amounts required for solid phase synthesis. Only the Mitsunobu reaction proved intractable to scale-up and required multiple small-scale reactions. The reasons for this are not clear but it may be that for example, mixing was less efficient on a large scale and that is crucial for the reaction. In the next chapter, efforts to apply the compound to the solid phase will be described.

Chapter 3.

Investigation of eligibility of the synthesised central amino acid to the solid phase synthesis.

3.1. Solid phase synthesis.

Proteins and peptides have a significant position in all biological processes across all kinds of living organisms. Peptides in particular, have entered the therapeutic field and medicinal research as a starting structure for many pharmaceutical and therapeutic agents due to their small size.[130] Recently, the tendency towards the use of peptides in pharmaceutical industry has increased tremendously as there are more than 100 peptides in therapeutic use and more than 400 in clinical trials.[131] Solution phase synthesis and SPPS represent the main methods of chemical synthesis of peptides.[132] SPPS, in particular, has had a crucial role in the thriving peptide industry due to its efficiency, feasibility, and facile purification procedures.[131] It was first described by Merrifield in 1963 as a possible means for linking four amino acids to each other via an amide linkage making a tetrapeptide.[133] Although many bids to improve the implementation of SPPS or to discover more efficient methods have being trialled, SPPS remains as the method of choice for peptide synthesis over a broad spectrum of scales from milligrams to multi-kilograms.[134]

The basic principle of the SPPS strategy largely relies on four fundamentals (Scheme 3.1): i) using a solid support, to which the first amino acid is attached; ii) convenient protecting groups for N of amino acid and the side-chain functions; iii) coupling reagents for carboxylic acid activation; and iv) a suitable system for deprotection of the side chain-protecting group and final release of the peptide.[135],[136] The synthesis of peptides on solid phase progresses from the C-terminus rather than N-terminus. This is to minimize the racemisation problem that accompanies the formation of oxazolones. The latter is formed via activation of the C-terminus and leads to a large amount of racemisation under basic conditions.[137] Two common methods are used in SPPS;

1) The Boc/Bz strategy, which uses acid labile *tert*-butyloxy carbonyl[80] for temporary amine protection and benzyl for side chain permanent protection.

2) The Fmoc method, which adopts base labile 9-fluorenylmethoxy carbonyl (Fmoc) for the α-amine protection.

The Boc method is less preferred nowadays than the Fmoc strategy due, mainly, to the requirements for a highly toxic and corrosive HF cleavage step to remove the peptide from the resin.[138] The base-lability of the Fmoc group has offered an orthogonal nature to other acid-labile side chain-protecting groups such as tert-butyl ester, ethers and carbamates. This has offered it more applicability in various

chemical syntheses.[139] In addition, its simplicity and efficiency have made it a most efficient method for obtaining active therapeutic peptides.[140] A TFA-based cleavage system is used in Fmoc chemistry for side chain deprotection and for the release of the peptide at the end of the synthesis.[136]

In general, SPPS has several limitations: 1) aggregation of relatively long peptides at a certain point, which leads to difficult accessibility of reagents to the reactive sites; 2) the use of excess solvents and reacting reagents, which can lead to increases in toxicity exposure and in the procedure cost, 3) the presence of secondary amines or bulky side-chain protecting groups could cause a decrease in reaction rate as a result of steric hindrance, and 4) long reaction times and repetitive steps.[141]
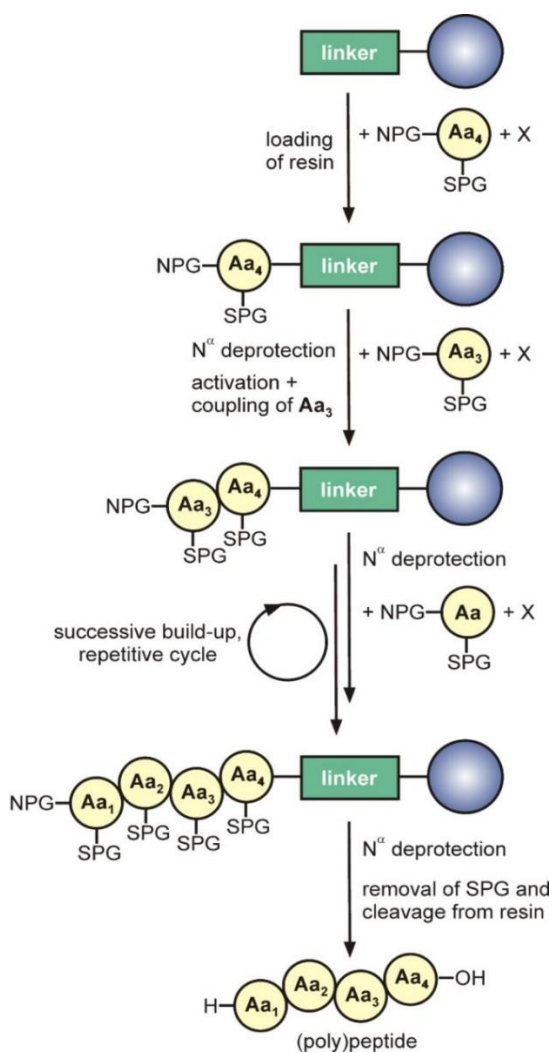
Scheme 3.1: The steps of solid phase synthesis process; 1) resin loading, 2) *N*-deprotection, 3) coupling process, 4) cleavage process. NPG: N-protecting group, X: activator, SPG: side-chain protecting group, Aa: amino acid. (Taken from reference [138]).

The most common side chain protecting groups, solid supports, linkers and coupling reagents are outlined below.

3.1.1. Side chain protecting groups.

The main function of the side chain protecting group is the prevention of side reactions of the amino acids and the formation of branched peptides.[142] The nature of the side chain function of the amino acid determines the choice of the protecting group.[142] For example, 4-methoxy-2,3,6-trimethylbenzene sulphonyl (Mtr) is commonly used for protection of the guanidine group in Arg, and 2-chlorobenzyloxy carbonyl is used for side chain protection of Lys. Tert-butyl ethers are used for protection of the hydroxyl functionality of Ser, Thr and Tyr, as ethers confer more stability than other protecting groups for hydroxyl side chain.[139, 143] Tert-butyl esters are utilised for side

chain protection in Asp and Glu.[139] The combination of Fmoc/^{t}Bu is the most commonly used strategy in solid phase peptide synthesis.[144] The concentration of the acid used for the removal of the side chain protecting group is based on the lability of the protecting group itself. For example, *t*-butyl (^{t}Bu), is removed with high concentrations of TFA (90% TFA in DCM), while, 2-chlorotrityl (2-Cl-Trt) can be cleaved with only 1% TFA in DCM.[142]

Allyloxy carbonyl (Alloc) protecting group strategies can be used as an alternative or alongside the Boc or Fmoc strategy, due to its removal orthogonality.[145] The possibility of deprotection of Alloc function under neutral conditions, catalysed by Pd(PPh$_3$)$_4$ and phenylsilane as scavenger, in DMF confers a high selectivity for deprotection in the presence of other protecting groups.[146, 147] The main use of the Alloc group is for the synthesis of cyclic and branched peptides in three-dimensional orthogonal protocols alongside Fmoc and ^{t}Bu.[148] The amino-side chain function is more basic than α-amino group and hence their protecting groups are more difficult to remove.[142] Therefore, a more electron rich group (e.g. Mtt) is chosen for protection of an amino side chain (e.g. ω-amino group).[142] Table 3.1 illustrates the commonly used protecting groups in SPPS, their uses, and removal conditions.
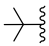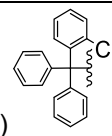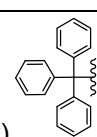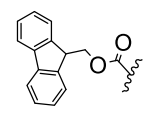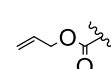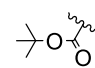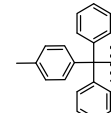
Protecting group	Main Use	Removal condition
t-Butyl (tBu)	α-carboxylic acid protection	90% TFA-DCM (solid and solution phase)
2-Chlorotrityl (2-Cl-Trt)	α-Carboxylic acid protection	1% TFA-DCM
Trityl(Trt)	α-Amino-group protection	1% TFA-DCM
9-Fluorenylmethoxycarbonyl (Fmoc)	α-Amino-group protection	20% Piperidne-DMF
Allyloxycarbonyl (Alloc)	α-Amino-group protection	Pd(PPh$_3$)$_4$ cat., PhSiH$_3$ scavenger
t-butyloxycarbonyl (80)	α-Amino-group protection	25-50% TFA-DCM
4-Methyltrityl (Mtt)	ω-amino group protection	1% TFA-DCM

Table 3.1: The commonly used protecting groups in SPPS, their uses, and their removal conditions.

3.1.2. Solid support resin.

The solid support is the essential element in SPPS, which its success, to a large extent, depends on. It should have several features to be competent for use in SPPS, which can be listed as follows:

1) Resistance to the various conditions used in SPPS, from basic to highly acidic.

2) Good swelling properties in different solvents.

3) Good accessibility for the different reagents used in the process.

4) Mechanically stable.[80, 149]

Accordingly, different solid supports have been developed (Figure 3.1). Polystyrene (PS) based resins are commonly used due to their mechanical and chemical stability, good swelling in organic solvents and they are cheap and easy to functionalise.[150] PS crossed-linked resins have more mechanical resistance and improved swelling properties, for example Merrifield resin (MR) is PS resin crossed linked to 2% with divinylbenzene (DVB).[149, 151] Other important types of resin used in SPPS are polyethylene glycol (PEG) resins, which have good swelling properties in both organic and aqueous solvents. However, their high hydrophilicity and ability to act as a Lewis acid sometimes limits their use.[149] PS cross-linked to PEG offers more swelling features in comparison to DVB-PS.[152] In 2000 Jandajel resin, a PS resin cross linked to tetrahydrofuran, was introduced as a resin that swells twice as well as MR.[153] To improve their compatibility with polar solvents, solid supports were incorporated with polar matrices like polyester, polyamide, and polysaccharides. However, these matrices contain a high chemically active species interfering with many reactions on solid phase that restrict their utility.[152] In conclusion, although it emerged back in the first evolution of SPPS, MR is still the support of choice for most syntheses on solid phase, mainly due to its compatibility with a lot of chemical reactions.[153]

PEG-PS

Polytetrahydrofuran

Merrifield resin

JandaJel resin
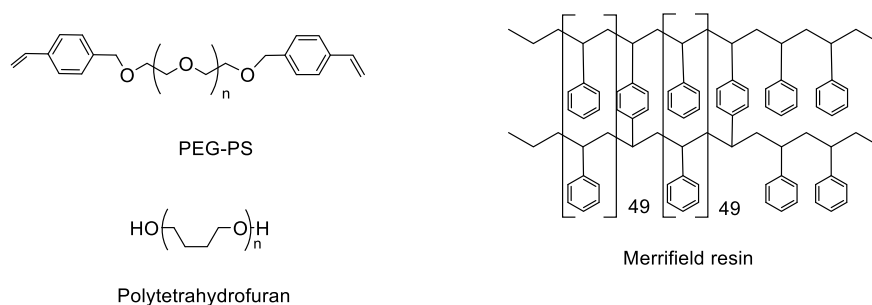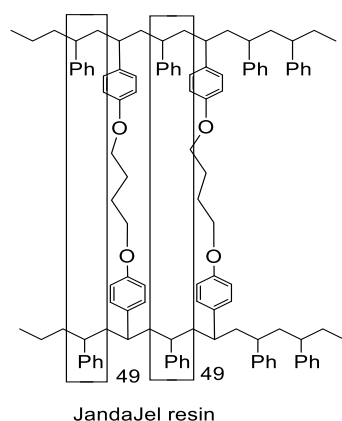
Figure 3.1: The common used solid supports in SPPS.

3.1.3. Linkers used in SPPS.

The linker is a molecule that has two functionalised ends, the first end is attached to the solid support in a permanent way, while the second end is linked to the developing peptide chain in a temporary manner. Connection of the peptide to the solid support via a linker has the following advantages:

1) It provides more flexibility for the use of a wider range of previously functionalised solid support.

2) It reduces undesirable reactions, including racemisation, to the minimum.

3) It facilitates the monitoring of yields of growing peptide at any step.

4) The loading level can be determined and controlled easily with the use of linkers.

5) It can be adjusted to provide optimal yields in the attachment and cleavage steps.[154]

In addition, the most important properties of the linker are that it should be inert during coupling and deprotection steps, attach efficiently to the first building unit, and the conditions used for peptide release should not influence the final products.[155]

Acid labile linkers are most widely used in SPPS Fmoc/^{t}Bu strategy. The stability of the carbocation formed after treatment with acid, mostly TFA, specifies the acid lability of the linker. Thus, the more stable carbocation, the more acid labile the linker. For example, the carbocation of trityl compounds is more stable than other types of linker like benzhydryl and benzylic structures. In general, there are three chemical categories of linkers: 1) benzyl-based linkers like Sheppard and HAL linkers, 2) benzhydryl-based linkers, such as Rink acid and Rink chloride analogue, and 3) trityl-based linkers, such as 2-chlorotrityl chloride linker (2-Cl-TC).(154, 155) The latter is

more commonly used due to the following: 1) It can be reused for another cycle of synthesis, 2) its use results in minimum formation of diketopiperazine side product due to steric hindrance effect of the trityl group, 3) the first amino acid attachment is accompanied by relatively low epimerization, and 4) it allows for peptides to be released under low acidic conditions.[154] The commonly used linkers are depicted in figure 3.2.

HMPB linker   Sheppard linker   HAL linker

Rink acid resin   Benzhydryl chloride linker

2-CTC resin
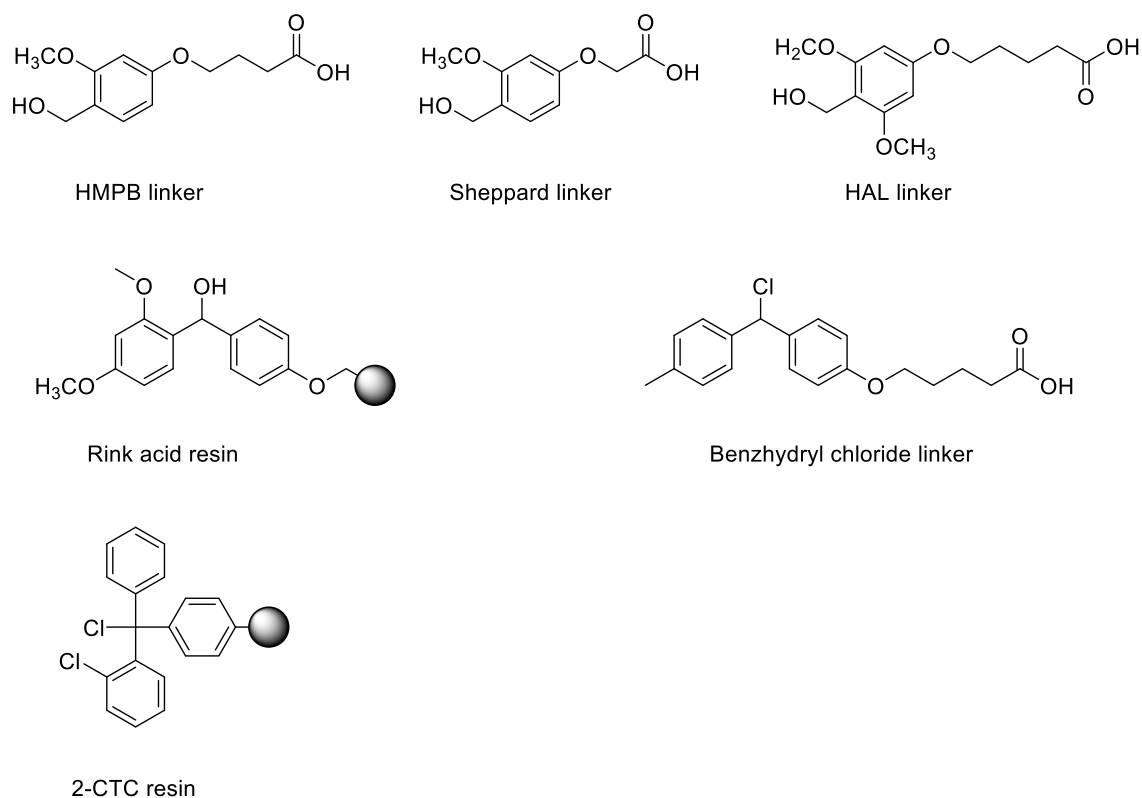
Figure 3. 2: Commonly used linkers in SPPS.

3.1.4. Coupling reagents.

Formation of the amide linkage is not spontaneous and can occur directly only under high temperatures.[156] Therefore, the presence of coupling reagent for conversion of OH in the carboxylic acid into a good leaving group is necessary for the integrity of the reactants.[156] Coupling reagents can be defined as reagents used to link two amino acids by activation of the carbonyl group in the C-terminal part of the first amino acid to be attacked by the nucleophilic amine group from the other amino acid, forming the peptide bond (Scheme 3.2).[157] A typical procedure for peptide bond formation is by dehydrative coupling between a carboxylic acid and an amino group.[158] The ideal coupling reagent should have the following properties: 1) increase the coupling reaction rate, 2) keep side reaction production to a minimum,

and 3) effectively work through difficult steps, for example, when the peptide is aggregated where the access of the reagents become difficult to the active sites.[159] There are many coupling reagents that have been developed for activation of the carboxylic acid group. The main chemical categories of these reagents are carbodiimides such as DCC and DIC, phosphonium reagents such as BOP and PyBOP, aminium/uronium salts as HBTU and HATU.[157, 158]
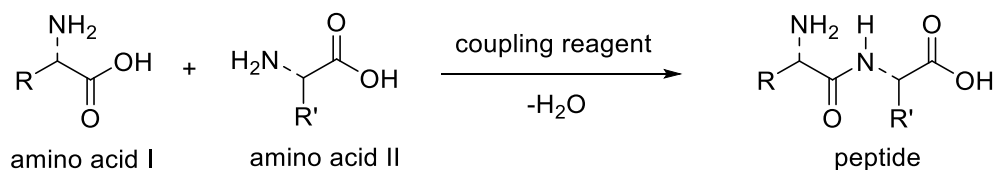
Scheme 3. 2: Coupling step mechanism of formation of peptide bond.

 Mainly, there are three undesirable reactions intrinsically associated with coupling procedure (Scheme 3.3). Namely, N-carboxy-anhydride formation associated with carbamate-protected α-amine (Scheme 3.3a), formation of diketopiperazine which usually occurs after formation of a dipeptide (Scheme 3.3b), and formation of a guanidine by-product when aminium/uronium coupling reagents are used (scheme 3.3 c). Guanidination occurs either by attack of the amino group on the coupling reagent and/or when the carboxylic acid is slowly activated by the reagent due to steric hindrance.[157, 160] In addition, racemisation of the amino acid is one of the challenging issues in SPPS that is associated mostly with activation of carboxylic acid terminus with carbodiimide forming an oxazolone (Scheme 3.4).[161] Therefore, addition of additives, for example HOBt, has been considered as one of the solutions to suppress or minimize this problem.[161]

a

oxazolonium ion

N-carboxyanhydride
side product

b

diketopiperazine side product

c

HAMDU

guanidine side product
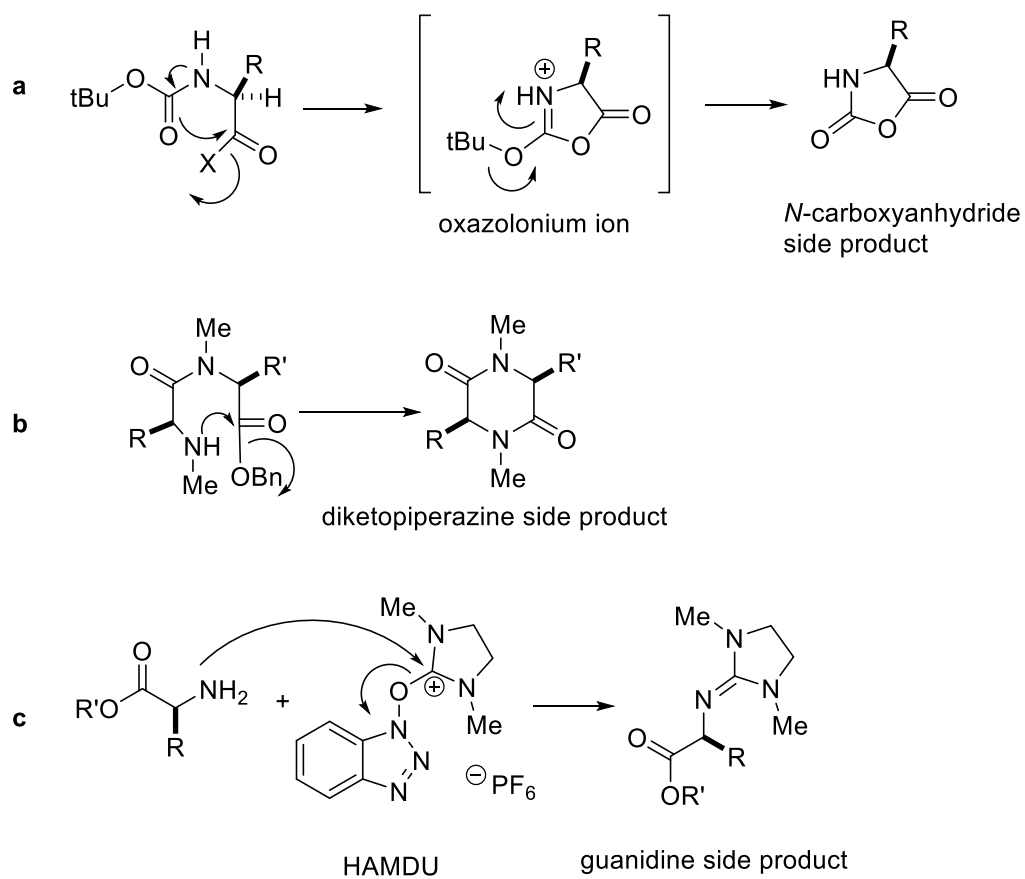
Scheme 3. 3: Side reactions in the coupling step; a) formation of *N*-carboxyanhydride, b) formation of diketopiperazine, c) formation of guanidinated side product.
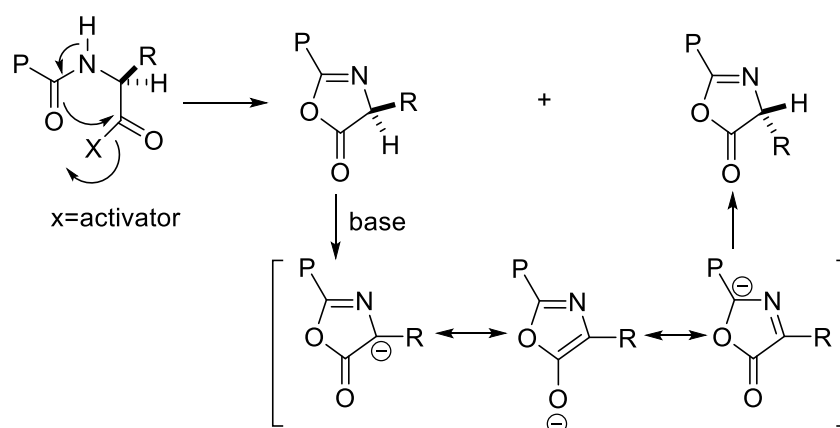
Scheme 3. 4: Racemisation side reaction in SPPS during coupling step using carbodiimides.

3.1.4.1. Carbodiimides.

As has been mentioned earlier in this chapter, the typical examples of carbodiimides are DCC and DIC. Their efficiency and low cost are behind their extensive use in peptide synthesis. Due to its insoluble by-product, which can be separated easily, the use of DCC is encouraged in solution phase.[160] This property has been problematic in SPPS especially in the synthesis of long peptides. Therefore, use of DIC has been suggested as an alternative due to relative solubility of its by-product in DCM.[160] Use of carbodiimides leads to formation of a highly reactive intermediate called an *O*-acylisourea (Scheme 3.5), which can undergo a rearrangement forming less active species.[161] Use of additives, has improved the activity of carbodiimides in terms of increasing the reaction rate and minimising the racemisation via conversion of *O*-acylisourea to active esters.(161) The latter are characterised by less activity and more stability than *O*-acylisourea.[161] Therefore, these additives can prevent the conversion of the *O*-acylisourea intermediate to inactive *N*-acylurea or oxazolone, which can lead to racemization (Scheme 3.5).[162] HOBt is one of hydroxylamine additives which have been used in this regard. EDC/HOBt was applied by Boger in the synthesis of vancomycin for the closure of the AB ring system.[163]

oxazolone

O-acylisourea

N-acylurea

Scheme 3. 5: Conversion of o-acylisourea into inactive species, N-acylures or O-acylisourea.

3.1.4.2. Phosphonium reagents.

These reagents do not contain a guanidinium moiety and hence do not generate guanidinated by-products.[156] The most common phosphonium salts are those of HOBt or HOAt based reagents.[156] BOP (Benzotriazol-1-yloxy) tris(dimethylamino) phosphonium hexafluorophosphate) is the typical example of phosphonium reagents associated with good yields and few and easily separable side-products.[164] It is an HOBt derivative, contains a dimethylamine moiety which was replaced with pyrrolidine in more recent reagents as PyBOP.[165] Pyrrolidine reacts with a carboxylic acid forming a pyrrolidide derivative.[165] PyBOP is also an HOBt analogue phosphonium salt (Figure 3.3) and was one of set of reagents introduced to avoid the formation of the carcinogenic hexamethyl phosphoramide (HMPA)-side product that is generated with BOP reagent.[166] It is mainly useful in cyclisation steps, due its efficiency in activation of hindered amino acids, and as alternative to the uronium reagents when guanidination is a problem.[165]

Figure 3. 3: Chemical structure of phosphonium reagents, a) BOP, b) PyBOP.

3.1.4.3. Aminium/uronium reagents.

In general, these reagents are much more stable than corresponding phosphonium reagents and confer more efficient and rapid coupling process.[167, 168] Their use is associated with formation of toxic by-product, tetramethylurea.[168] HBTU is considered as the precursor of all other uronium reagents.[164] Structurally, it contains guanidine group and hexafluoro phosphate as a counter ion.[157] HATU is an HBTU analogue, which displays more stability and coupling efficiency.(164) Due to the reaction of the guanidine group with the free amine, these reagents can form guanidinated peptide side-product which results in blockage of peptide elongation.[167] Uronium reagents have a similar coupling mechanism to phosphonium reagents. So, the mechanism is based on formation of activated alkyl ester for carboxylic acid activation. In case of HATU, it reacts with the carboxylate forming HOAt ester and releasing tetramethylurea as side-product. The HOAt ester then reacts with available amine to afford the corresponding peptide, via formation of amide bond, and releasing HOAt as by-product (Scheme 3.6).[168]
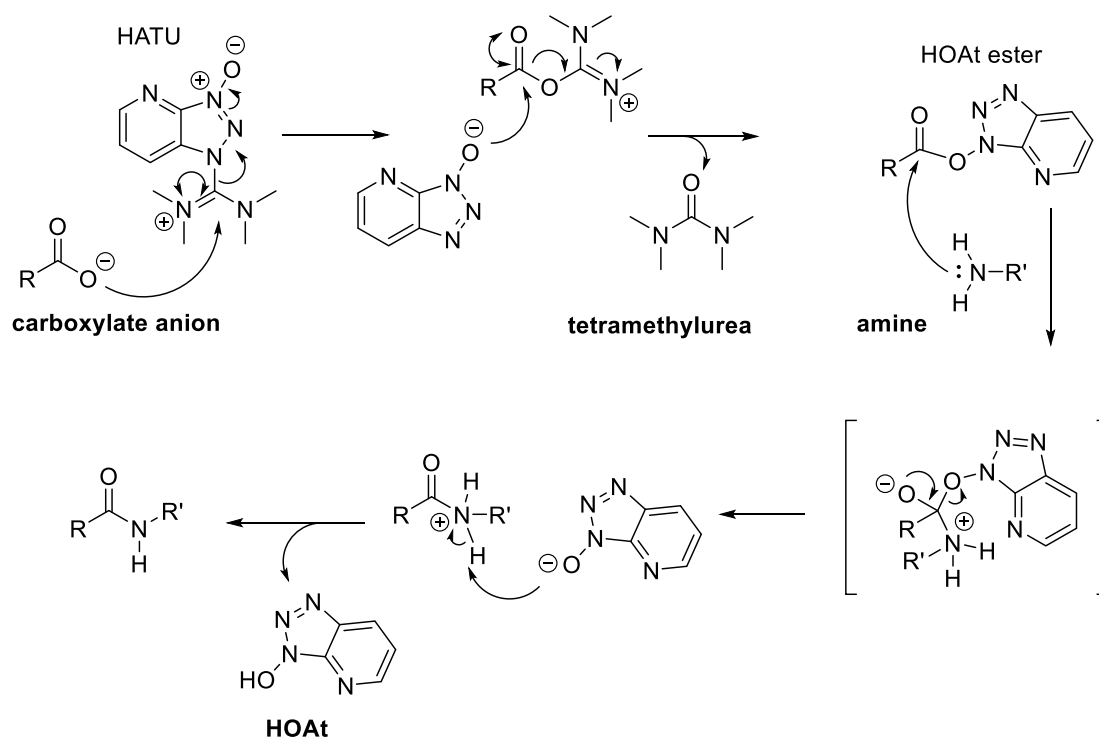
Scheme 3. 6: Mechanism of activation of carboxylic acid of amino acid by HATU coupling reagent.

In terms of solvents, DMF is the most convenient solvent for all coupling reagents in terms of stability and activity.[166] In addition, it has been found that the carboxylate anion is necessary for an efficient activation therefore presence of base, DIPEA, is crucial in this regard.[166, 169]

3.2. The practical aspect of solid phase synthesis.

With the analogue of the central residue **C14** in hand, it was the time to demonstrate the eligibility of this residue to the solid phase. Therefore, this chapter discloses multiple trials of coupling of this amino acid to other amino acid analogues of vancomycin on the solid phase. Two issues had to be taken into the consideration, 1) the conditions used for the peptide cleavage should not be as highly acidic as it may deprotect the triazene moiety, the cleaving condition of triazene group is 50% TFA/DCM. So, the choice of the solid support (resin) had to be cleavable with low acidic condition. Therefore, the 2-chorotrityl chloride was the resin of choice for this task. Peptide loaded on the chlorotrityl resin can be released with 1% TFA in DCM. 2) The amino acid analogues to be coupled to the central residue should be structurally convenient for the potential macrocyclisation. In other words, the coupled analogue, alongside the triazene residue, should be a suitable substrate for the reaction condition that will be used for the potential macrocyclisation step.

3.2.1. Attempted syntheses of a tetrapeptide containing the triazene-protected compound.

For the first experiment, to be consistent with our initial proposal of using sensitive acid labile linker, the commercially available preloaded tyrosine 2-chlorotrityl resin (H-Tyr(tBu)-2-ClTrt resin) was chosen (Figure 3.4). The amino acid is attached to the linker via an ester bond with a substitution level of 1.6 mmol/g. The latter is defined as an estimation of the amount of the first amino acid loaded on the resin.[170]
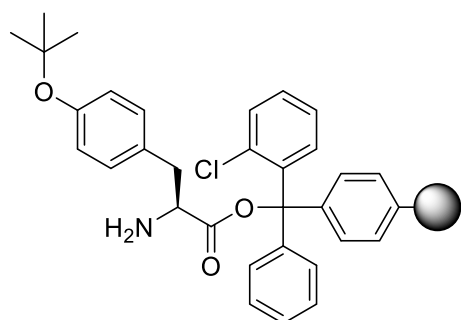
Figure 3.4: Chemical structure of preloaded tyrosine 2-chlorotrityl resin.

As discussed, peptides can be released from the 2-ClTrt linker with 1-5% TFA/DCM. Additives such as HOBt were not used in the coupling reaction as the acidic nature of the compound could lead to triazene deprotection.[171] A standard procedure in SPPS is resin swelling. This step is performed to facilitate access of the reagents to the active sites of the substrates attached to the resin by expanding the resin beads.[172] Thus, 3 ml of DMF was added to the resin in the peptide vessel reactor and allowed to shake for 10 min. This procedure was repeated three times, draining the solvent after each time period. The coupling step was performed using equimolar quantities (4 equiv.) of both the amino acid and the coupling reagent, HATU. As has been mentioned previously, reaction of HATU with a free amino group could result in a blocked-peptide, therefore, both the amino acid of free carboxylic group, and HATU were mixed separately in a minimum amount of DMF. DIPEA was added to the mixture in an excess (10 equiv.) to generate the carboxylate ion, which is necessary for the coupling reaction. The coupling mixture then was added immediately to the resin-bound N-deprotected amino acid and agitated for 30 min. HATU is used due to high yields and high efficiency, even for more sterically hindered coupling reactions. Although, its structure is similar to HBTU structure, it causes less epimerization.[173] After completion of the reaction, the solution was filtered and the resin washed five times with 5 ml of DMF. For the next step, the Fmoc-protected N-terminus of the resin-

bound peptide was subject to deprotection. This step was carried out with 40% piperidine added to the peptide vessel, which was shaken for 10 min. Then, the solution was filtered followed by addition of 5% piperidine and shaken for 5 min. The last step was repeated twice. The solution was filtered and the resin washed with DMF. Monitoring of the coupling and deprotection steps used the Kaiser test. This test was first introduced in 1970 by E. Kaiser and co-workers for rapid detection of coupling reactions in SPPS.[174] It is a colour test based on formation of a chromophore compound called Ruhemann's purple from reaction of ninhydrin with the amine group. [175] The Kaiser test is composed of three solutions, i) 0.5 g of ninhydrin/10 mL alcohol, ii) 0.8 g of phenol/20 mL alcohol, iii) 2 mL of KCN solution (0.001 M) diluted up to 100 mL of pyridine. In general, with the addition of 2-3 drops of each solution to an aliquot of the resin there are two colours that can be detected.[174] With a free amino group (deprotected), the beads and solution turn to a dark blue colour (positive result) after heating to 120 °C for at least 2 min. The beads would remain white and the solution turn either yellow or brown, after heating for 3-5 min, if most of the amino group has reacted (coupled forming amide bond) giving a negative result.[174]

The Kaiser test is useful mainly for detection of primary amines due to presence of the alpha proton, which is necessary for Schiff base formation.[176] The mechanism of the Kaiser test starts with nucleophilic displacement of the hydroxyl group of the ninhydrin, which exists in an equilibrium with indan-1,2,3-trione in the presence of water, by the amine moiety (Scheme 3.7).[176, 177] An imine (Schiff base 1) is formed after losing a second water molecule. A second form of imine (Schiff base 2) is formed as a result of deprotonation of the alpha proton. In the presence of water, the second imine is hydrolysed releasing the aldehyde and amine compounds. The latter reacts with another molecule of ninhydrin affording the Ruhemann' purple.[176]
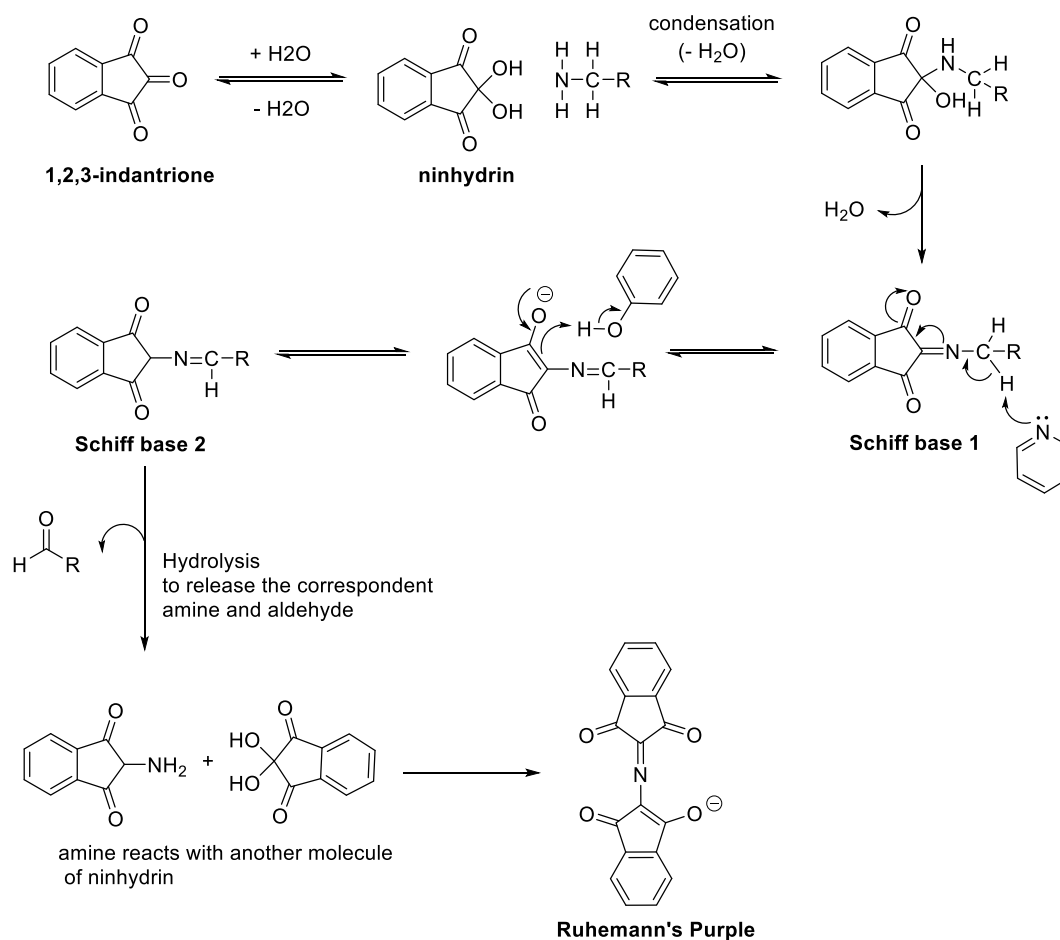
Scheme 3. 7: Kaiser test mechanism and formation of Ruhemann's Purple.

In this experiment, it was proposed to synthesise a tetrapeptide consisting of the following amino acids: Fmoc-Tyr(tBu)-OH, Fmoc-Tyr(OH)-OH, Fmoc-Ala-OH and the Fmoc-Tyr (triazene)-OH (Figure 3.5).
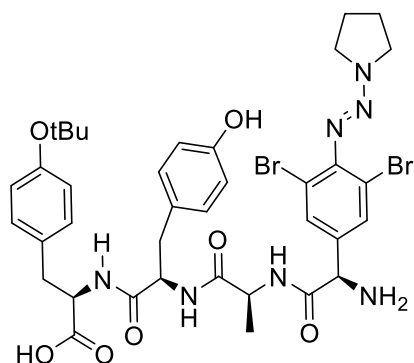
Figure 3.5: The chemical structure of the tetrapeptide: Tyr-Tyr-Ala-Gly.

The first amino acid was commercially available, preloaded on the ClTrt resin. As discussed, the deprotection of the butyl group needs a high acid concentration that was avoided to keep the triazene group on. The 2nd aa was chosen to act as a suitable substrate for the potential cyclisation (discussed earlier). The amino acids and the coupling reagent, HATU, were used in equimolar quantities (4 equivalents for each). The coupling of the last amino acid was left overnight as the Kaiser test displayed a negative result on the next day. Although the Fmoc-deprotection for the last aa was trialled three times, the Kaiser test was still giving negative result (brown beads colour). In spite of this, cleavage was performed with 1% TFA, and 10% TIPS in DCM. Following cleavage, the analytical HPLC showed two major peaks for the crude before purification with preparative HPLC (Figure 3.6).
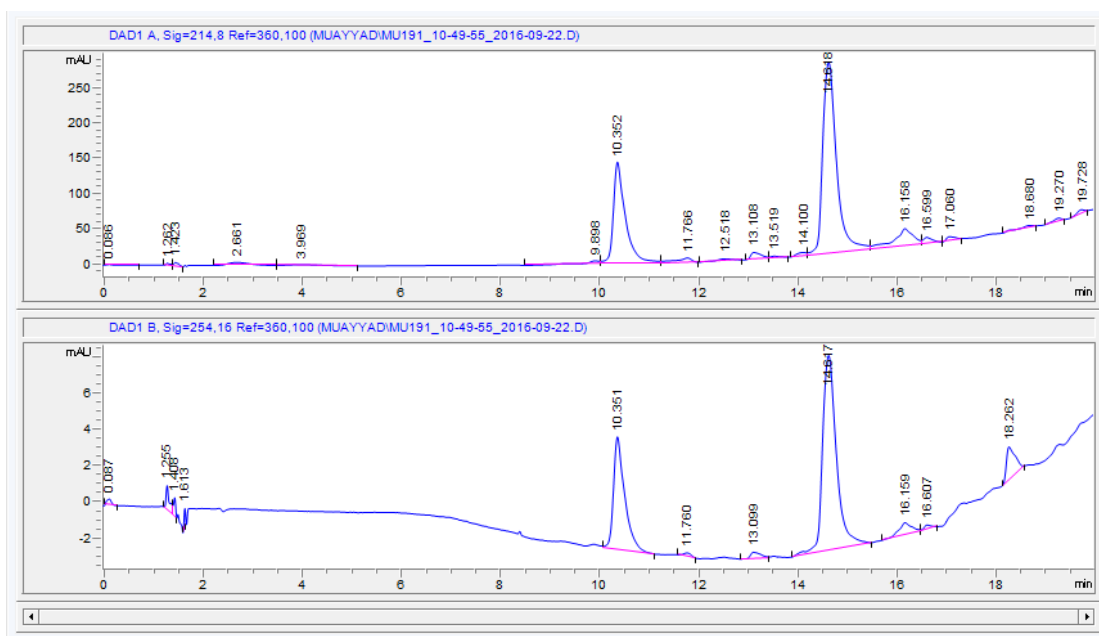
Figure 3. 6: HPLC analysis of the crude, before purification.

After purification with prep. HPLC (Figures 3.7 and 3.8), both purified samples showed masses of m/z: 571 and 553 with MALDI analysis (Figures 3.9, and 3.10).

Noticeably, neither of these masses was relevant to the mass of the required tetrapeptide, m/z=859.
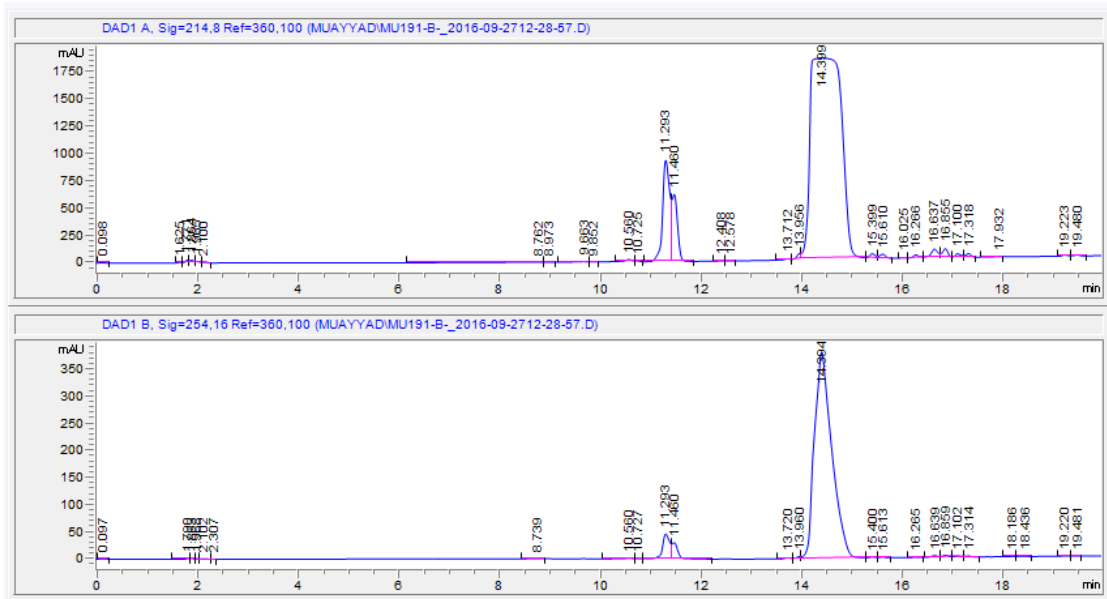
Figure 3. 7: HPLC analysis of the first separated sample with prep. HPLC.
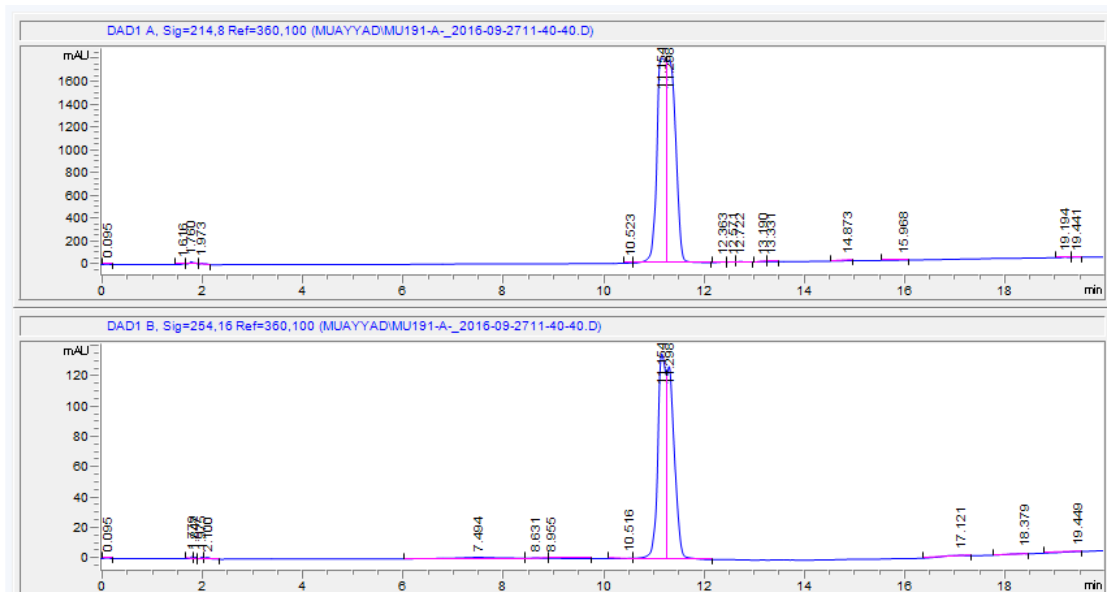
Figure 3. 8: HPLC analysis of the second purified sample with prep. HPLC.
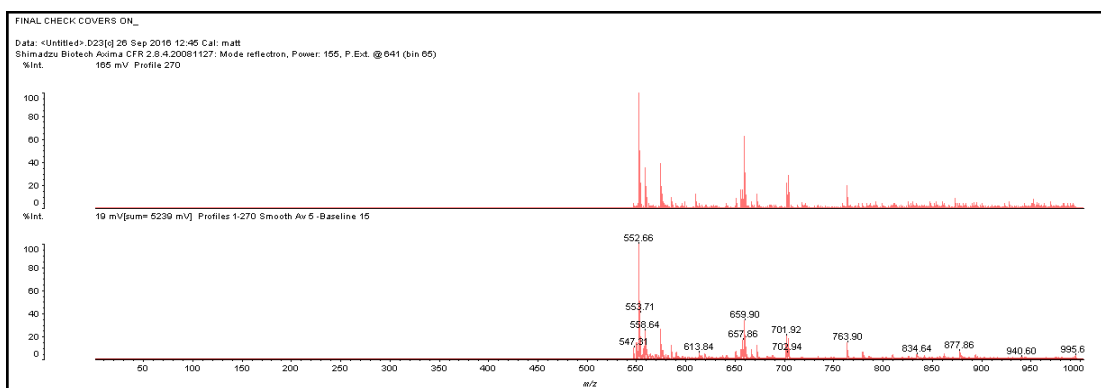
Figure 3. 9: MALDI results of the first sample showed mass m/z: 552.66
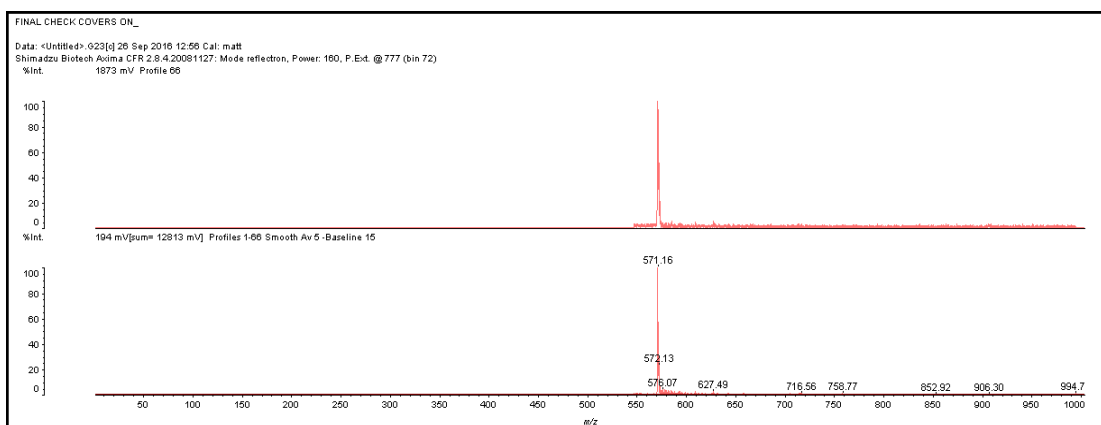
Figure 3. 10: MALDI results of the second sample is showing mass m/z: 571.16.

3.2.2. A model reaction to synthesise H₂N-Ala-Tyr-Tyr(OᵗBu)-COOH using HATU.

To exclude any issues which might be caused by the synthesised triazene-protected central unit, it was decided to synthesise the tripeptide of Tyr-Tyr-Ala (Figure 3.11). As has been mentioned above, the three amino acids of this trimer were commercially provided. Therefore, the same experiment with the same conditions and reagents was repeated but without coupling the central unit (Figure 3.11).

Exact Mass: 471.24
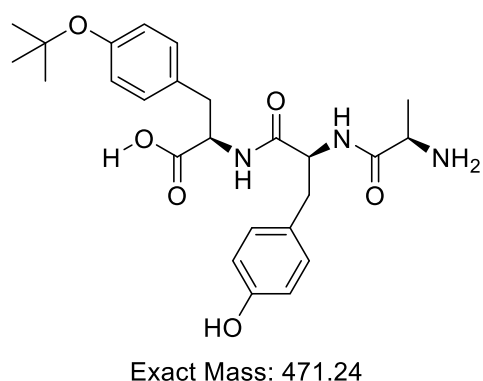
Figure 3. 11: Chemical structure of the tripeptide; Tyr-Tyr-Ala.

MALDI showed two major peaks m/z= (570, 499) (Figure 3.12). Noticeably, neither of these masses was the right mass of the required tripeptide, m/z=471.24. As mentioned earlier, the coupling reagent used, HATU, could have caused capping of resin-bound amino groups through formation of N-terminally guanidinated peptides. Based on the masses that were obtained with MALDI, 499 and 570, it was likely that they were a guanidinated dipeptide and tripeptide respectively (Figure 3.13).
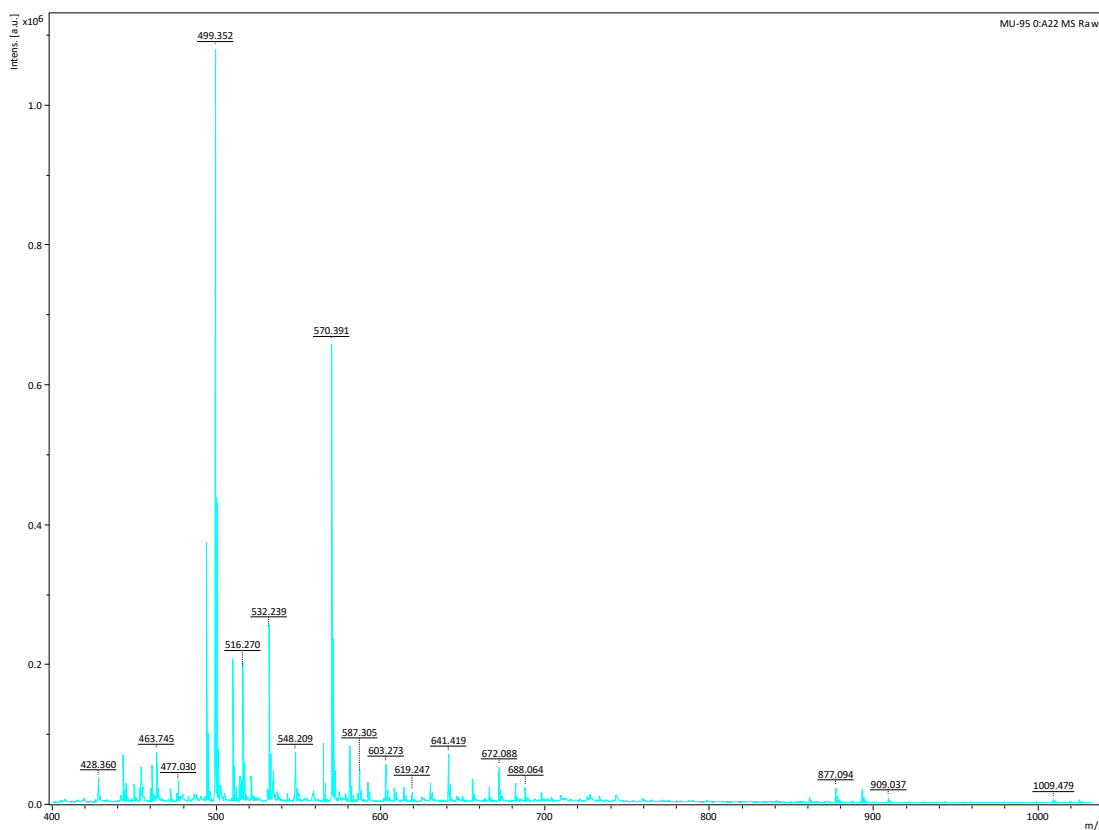
Figure 3. 12: The MALDI results showing the masses of the guanidinated dipeptide and tripeptide.

The tripeptide was suspected to be guanidinated at the hydroxyl group rather than on the amine moiety of Ala. That is because the deprotection of the Fmoc group of the terminal aa (Ala) occurred after the coupling reagents had been removed by filtration. Hydroxyl guanidination, could also have happened with the dipeptide.
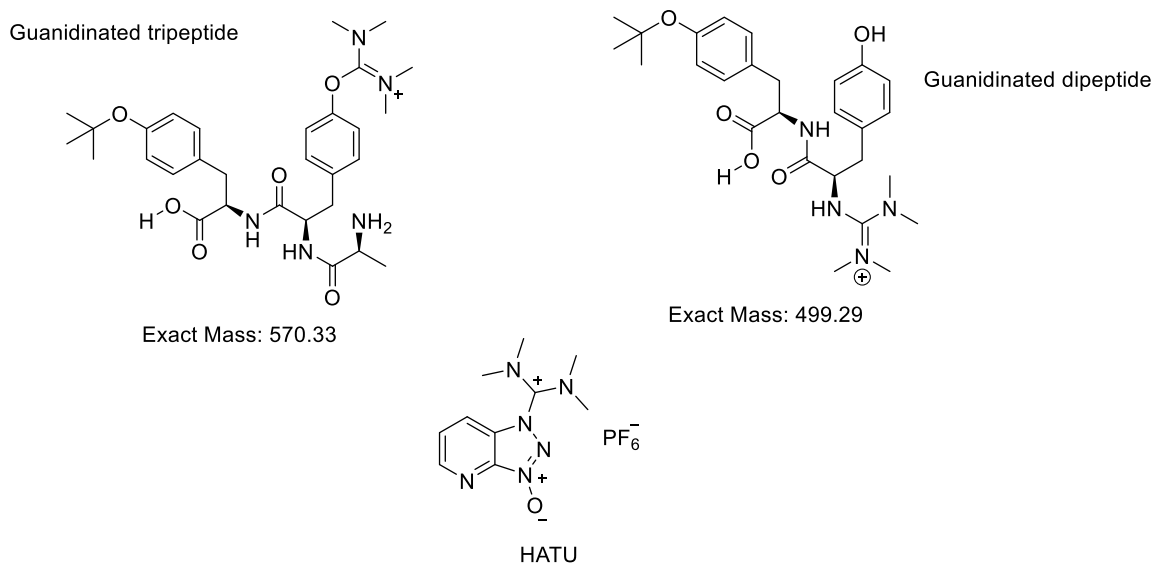
Figure 3.13: Chemical structures of the guanidinated side products.

3.2.3. A model reaction to synthesise H$_2$N-Ala-Tyr-Tyr(O^{t}Bu)-COOH using PyBOP.

To confirm that the issue was caused with HATU, the use of a coupling reagent without guanidine, and hence not prone to cause the guanidination side reaction, was the advisable next step. The phosphonium derivative, PyBOP, was trialled for the synthesis of the same tripeptide sequence. Thus, the tripeptide was synthesized on 100 mg of the 2-chlorotrityl resin. In this instance, analysis of the crude cleavage mixture with MALDI showed two masses of m/z 494 and 510 (Figure 3.14), which correspond to the [M+Na]$^+$ and [M+K]$^+$ peaks for the correct mass. This is very suggestive that it was, indeed, the use of excess HATU that led to guanidination, probably on the unprotected Tyr-OH. This suggested two further approaches-use of PyBOP to generate the target compound tetrapeptide or the use of a low excess of HATU for the same reaction.
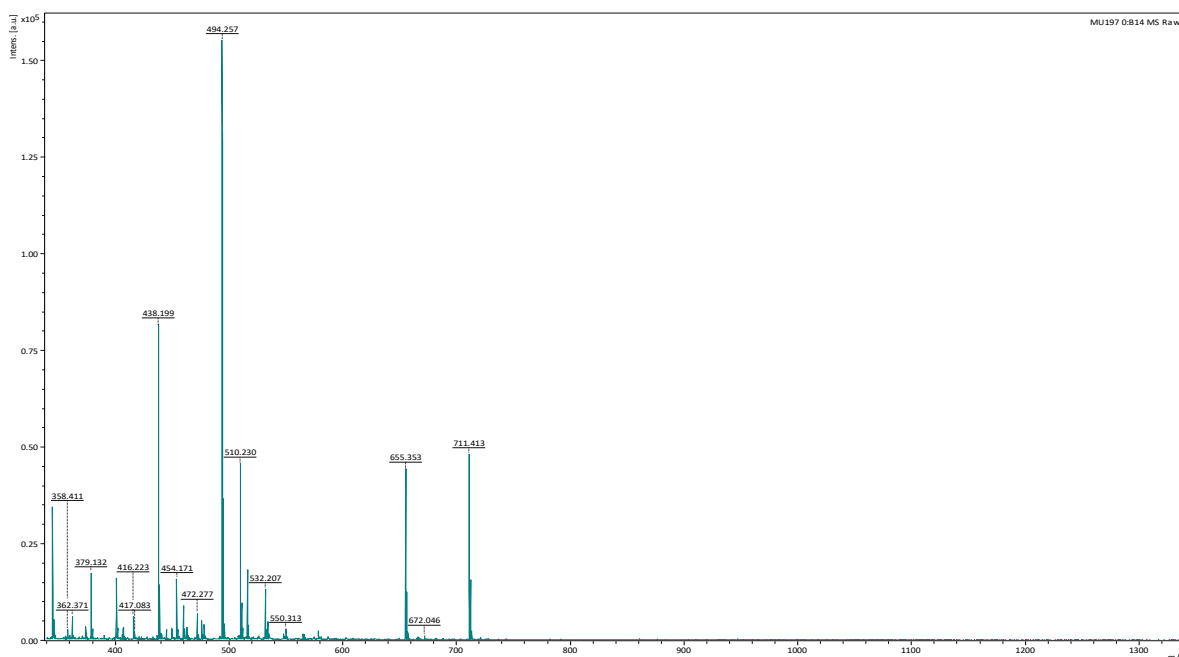
Figure 3. 14: MALDI result of the tripeptide model: Tyr-Tyr-Ala.

3.2.4. Synthesis of a tetrapeptide compound using PyBOP.

In the next experiment, the synthesis of the same sequence of the tetrapeptide in the 1st experiment was explored using PyBOP. The tyrosine preloaded resin was used on 100 mg scale and PyBOP was used for the coupling reaction. Also, the last coupling was left overnight and the Kaiser test showed a negative result on the next day. The resin was divided into two halves. The first half was Fmoc-deprotected and cleaved from the resin. Upon deprotection of the terminal amine, which was repeated

three times, again the blue colour of the resin beads was not seen (remained negative with Kaiser test). Although the HPLC showed one major peak, MALDI did not display the expected mass, m/z= 859, and showed a mass of m/z= 714 instead (Figure 3.15). The second half of the peptide was cleaved with the Fmoc group of the last residue on. The required mass was not obtained with MALDI as well (Figure 3.16).
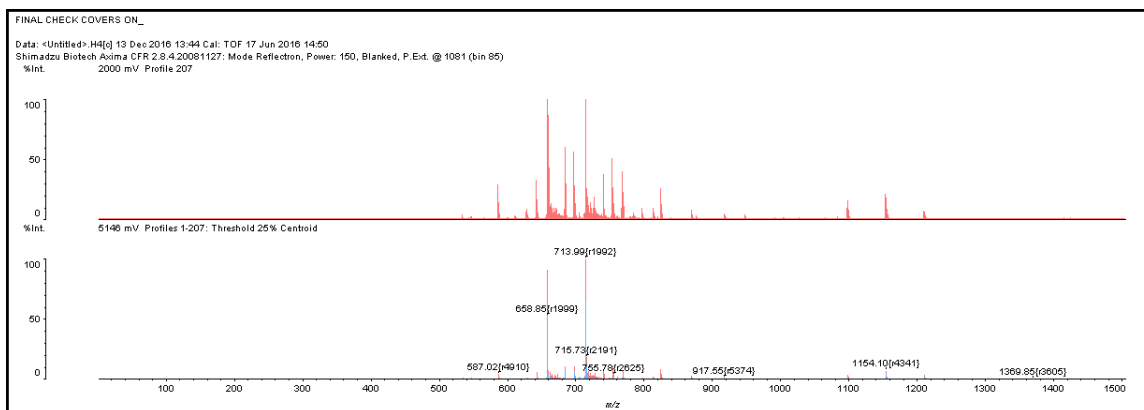
Figure 3.15: MALDI result of the first part of the Fmoc-deprotected tripeptide.

Figure 3.16: MALDI result of the Fmoc-protected tripeptide part.

3.2.5. Synthesis of tripeptide of Tyr, Gly and triazene-protected compound using HATU for coupling and Wang resin as supporting solid.

This synthesis was trialled using HATU as a coupling reagent but with only two equivalents rather than four. As discussed, that even the gentle acidic cleavage condition from the ClTrt resin can cleave the triazene group, it was decided to perform this reaction through use of Wang resin and apply an aggressive condition for cleavage (90% TFA). In this experiment, as the plan was to demonstrate the eligibility of the triazene-protected compound to the solid phase, so the synthesis of tripeptide was trialled rather than tetrapeptide.

This experiment was carried out on 100 mg of preloaded Fmoc-Tyr (tBu)-OH Wang resin. Attempting to avoid the guanidination issue of HATU, an excess of the amino acids was used compared to HATU. Thus, three equivalences of each amino acid were added. Upon dissolving the triazene in DMF the solution turned dark brown colour which may reflect the typical colour of azo dye. The coupling of the last unit, triazene derivative, was checked with Kaiser test three times after 45 min, 1.5 h, and 2.5 h but the result was positive for each. Then, the coupling was repeated with fresh reagents and left overnight. On the next day, the Kaiser test showed a negative result, brown beads and solution. After Fmoc-deprotection of the last unit, the resin was cleaved with 95% TFA over 2 h. Mass spectrometry was performed with MALDI using freshly prepared cinnamic acid matrix. The mass of desired trimer could be recognized, m/z= 627 [M+H] (Figure 3.17). Another more prominent mass of 530 [M+H]$^+$ was recognized. The latter could be a fragmented trimer at the bond between the triazene and the aromatic ring (Figure 3.18).
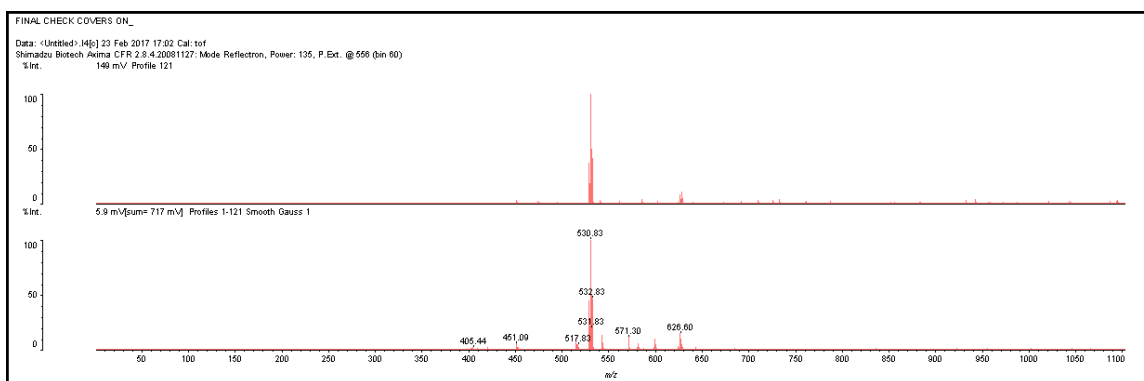
Figure 3.17: MALDI result of the tripeptide: Tyr-Gly-PhGly.

a	b
Molecular Weight: 626.31	Molecular Weight: 529.19
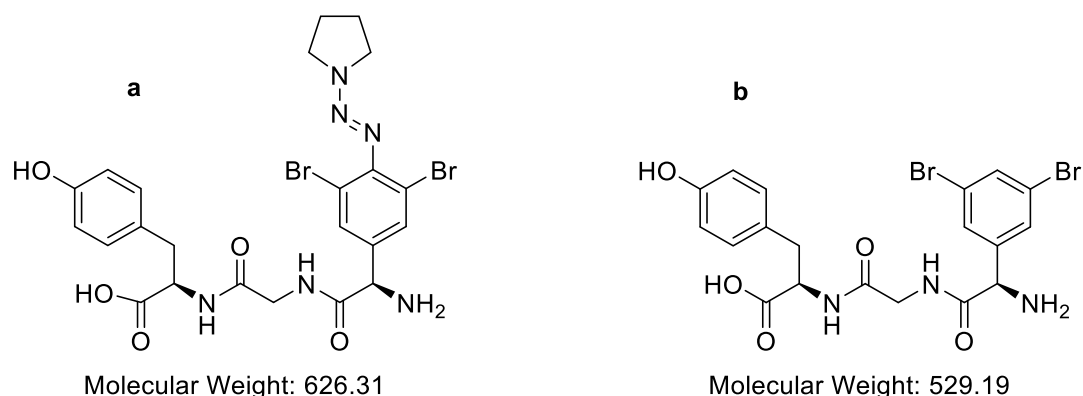
Figure 3. 18: The chemical sturcture of the tripeptide (a) and its supposed fragment (b).

The experiment was scaled up to 200 mg of the pre-loaded Wang resin and the same masses could be recognized as well with MALDI. After purification with prep. HPLC

three fractions were obtained, but none contained the expected masses. This suggests that the products of the reaction are unstable and are decomposed on purification. To test this, it was decided to try an alternative solution phase synthesis.

3.3. Solution phase synthesis;

3.3.1. The synthesis of Fmoc-protected dipeptide D1 using EDC/HOBt in DMF.

These results suggested that the analogue of the central amino acid either cannot be coupled successfully and/or could not be characterised properly when it is reacted on the solid phase. Accordingly, it was important to try a solution phase method to prove that the right compound can be synthesised or to confirm it is not eligible for the solid phase. The first trial in this regard was to synthesise a tripeptide consisting of tyrosine, glycine, and the central amino acid. The tyrosine aa is protected at the carboxylic acid with methyl ester and with free amino moiety. The methyl ester of tyrosine and Fmoc-protected glycine were reacted in DMF using HOBt/EDC as coupling system (Scheme 3.8). EDC is a typical example of carbodiimides, which, mechanistically, reacts with the carboxylic acid in stoichiometric reaction giving *O*-acylisourea intermediate (Scheme 3.9).[178] As previously discussed, using HOBt, is essential to reduce racemisation, which is common with carbodiimides. It reacts in a catalytic reaction with the o-acylisourea forming an activated ester and releasing urea as side product. The activated ester, the HOBt ester, acts as the source of acylation of the amine compound to afford a peptide or amide bond and releasing HOBt. Thus, 100 mg of Fmoc-Gly-OH was dissolved in 1 mL DMF and 1 equivalent of each of HOBt, EDC, and Et_3N was added sequentially. The reaction was monitored with TLC and after 1 h of stirring some of SM was still present. A further 0.5 equiv of EDC was added and the reaction left overnight. On work up, the reaction had not worked.
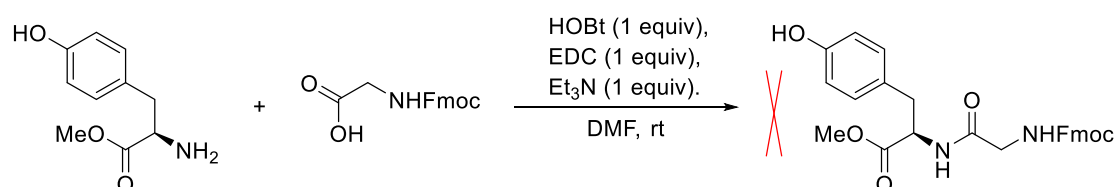
Scheme 3. 8: Reaction of dipeptide formation, Tyr-Gly, using EDC coupling reagent in DMF solvent.
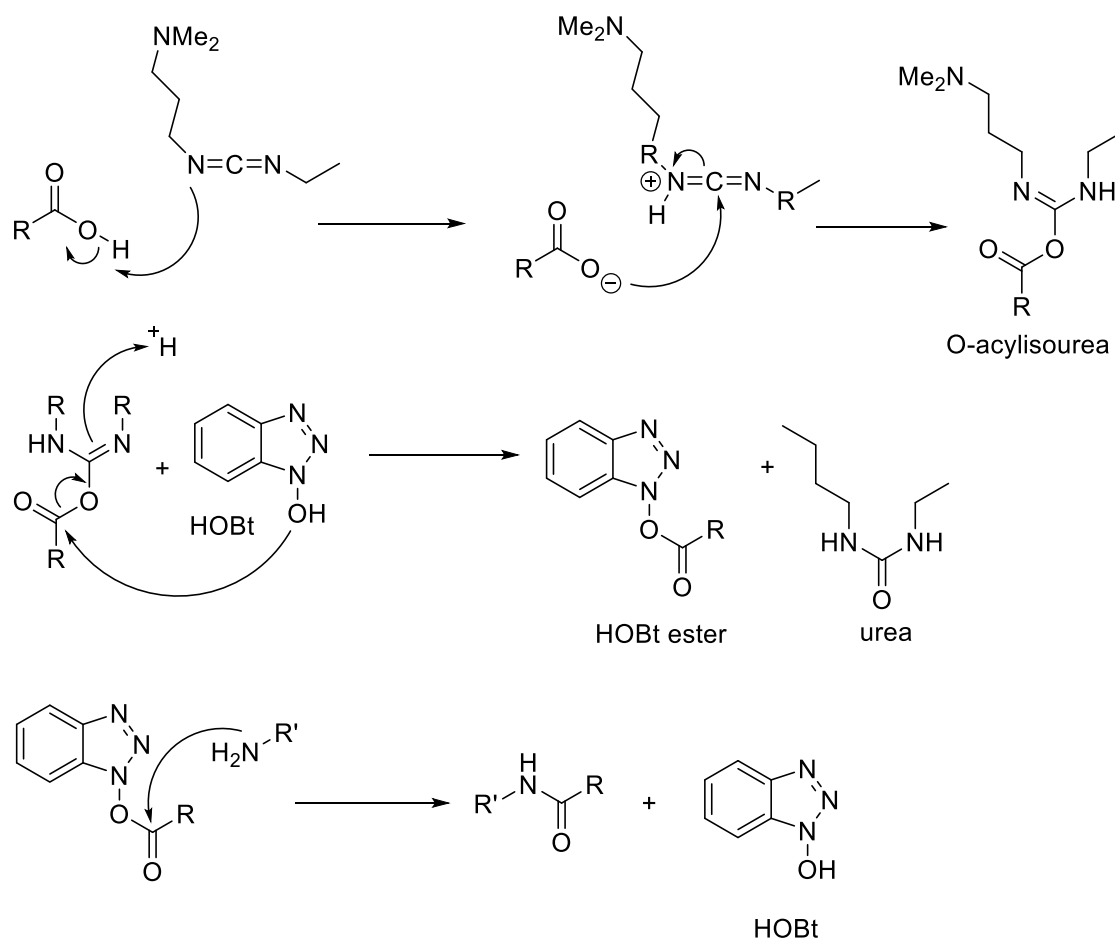
Scheme 3. 9: Mechanism of peptide bond formation using EDC as a coupling reagent and HOBt as a racemisation suppressent.

3.3.2. The synthesis of Fmoc-protected dipeptide D1 using EDC/HOBt in acetone.

For the next experiment, the solvent was changed to acetone and the Tyr was dissolved first (Scheme 3.10).[179] The HOBt, Gly, and EDC were added sequentially with stirring. After 2 h the dipeptide precipitated as a colourless solid. The solvent was evaporated and the residue washed with diethyl ether then purified with flash chromatography.
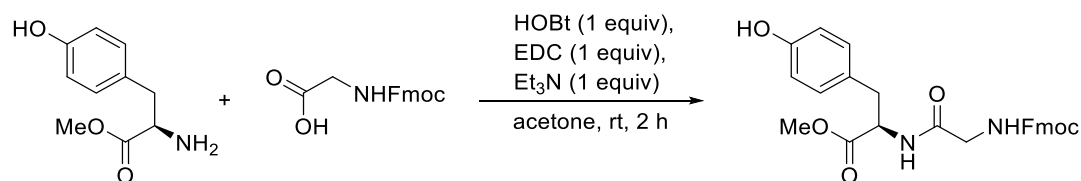
Scheme 3. 10: Reaction of dipeptide formation, Tyr-Gly, using EDC coupling reagent in acetone solvent.
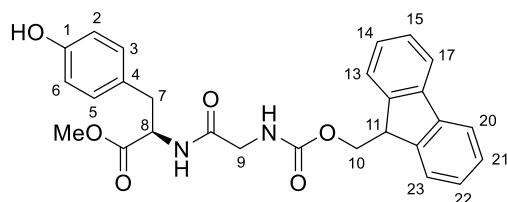
Figure 3. 19: Atom numbering of the dipeptide.

The product was confirmed using ^{1}H NMR spectroscopy (see figure 3.19 for atom numbering). The presence of the signals of the Fmoc group is a prominent confirmation of the success of the reaction. As has been mentioned earlier there are five signals of the Fmoc group. Four of them are in the aromatic region, two doublets and two triplets. The two doublets are at chemical shifts 7.78 and 7.65 ppm with coupling value of 7.5 and 7.1 Hz respectively. The triplets are at chemical shifts 7.38 and 7.30 ppm with coupling value 7.5 Hz for each. The doublet at 6.99 ppm corresponds to the aromatic protons of C-3 and C-5 and has coupling value of 8.4 Hz. While, the protons of the C-2 and C-6 are represented by the doublet at 6.71 ppm. The reason that the latter doublet is at lower chemical shift than the former one is because of the electron-donating effect of the hydroxyl functionality (Scheme 3.11). This effect is concentrating the electron density at ortho and para positions of the aromatic ring so their shielding from the magnetic field would increase pushing the signals to a lower chemical shift upfield.
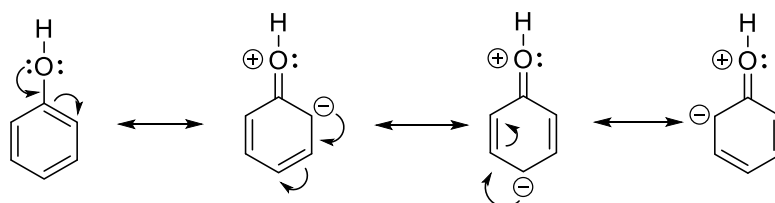
Scheme 3. 11: Illustration of the resonance of the aromatic hydroxyl group.

The multiplet at 4.65 ppm corresponds to the proton C-8. Another two signals belong to the Fmoc group at 4.34 and 4.20 ppm. The former is a doublet with *J* value of 6.5

133

Hz and latter is triplet of the same *J* value. The doublet at 3.78 ppm corresponds to the methylene protons of C-7. The methyl group is matched by the singlet at 3.37 ppm. The multiplet at 3.05-2.87 ppm corresponds to two methylene protons of C-9.

3.3.3. Deprotection of the Fmoc group; synthesis of the dipeptide D2.

The next step was the deprotection of the Fmoc group. (20%) piperidine was used to accomplish this reaction and the solution was stirred for 20 min. The product was precipitated with hexane.

^{1}H NMR spectroscopy showed no methyl group. This suggests that under basic condition of the Fmoc deprotection, the free amine has undergone a cyclization reaction as shown in scheme 3.12.
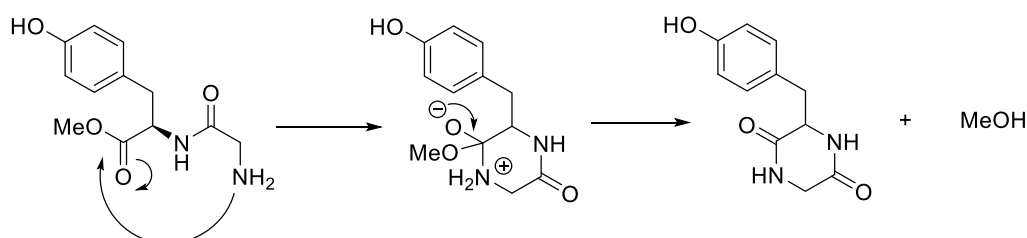
Scheme 3.12: Proposal of the cyclization of the free amine.

3.3.4. Synthesis of dipeptide D3 using Boc-protected Gly.

The next approach was to use Boc-protected glycine. That is because the deprotection of Boc group can be carried out under acidic conditions which in turn acidify the free amino group leading to lowering its reactivity (the protonated amino group is less nucleophilic). The coupling reaction was carried out at room temperature and left overnight (Scheme 3.13). After purification with flash chromatography, the product was characterized using ^{1}H NMR spectroscopy which showed the right dipeptide terminally protected at the amine group.
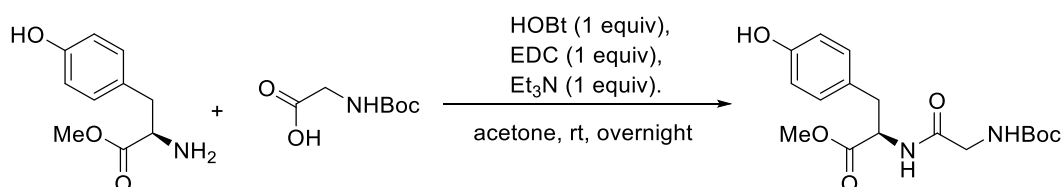
Scheme 3.13: Reaction formation of dipeptide using Boc-protected glycine at amine functionality.
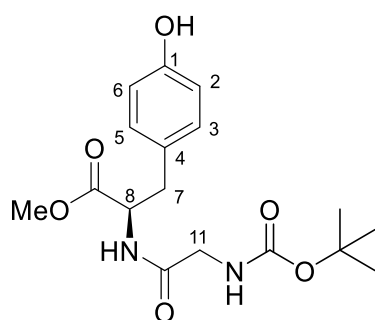
Figure 3. 20: Atom numbering of the Boc-protected dipeptide

This product was confirmed using ^{1}H NMR spectroscopy (see figure 3.20 for atom numbering). Noticeably, the singlet 1.45 ppm signal corresponds to the nine protons of the Boc moiety and so is considered as an evident confirmation of the coupling. The two doublets at 7.00 and 6.72 ppm correspond to the aromatic protons. For the same reason mentioned earlier (see scheme 3.11) the protons of the C-6 and C-2 are represented by the doublet of the higher chemical shift, 7.00 ppm. The triplet at 4.65 ppm corresponds to the proton of carbon C-8. The multiplet 3.72-3.69 ppm matches the five protons of C-7 and the methyl group. While, the two protons of C-11 are represented by the multiplet of 3.07-2.91. They are not identical although attached to the same carbon atom because of the enantiotopic effect.

3.3.5. Deprotection of Boc group; synthesis of D4.

The Boc deprotection reaction was carried out with 50% TFA/DCM. The product was purified with flash column chromatography.
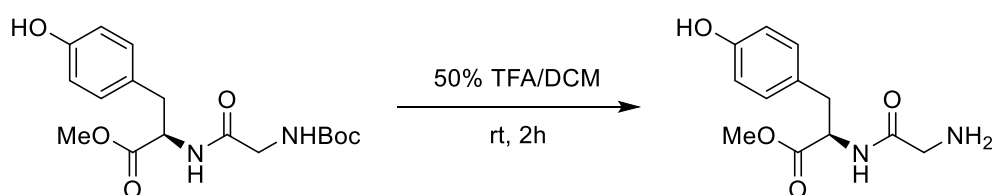
Scheme 3. 14: Reaction of Boc-deprotection with acidic conditions.
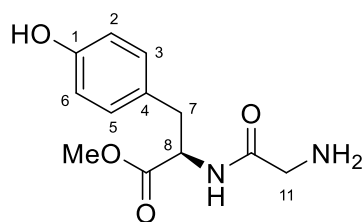
Figure 3. 21: Atom numbering of the Boc-deprotected dipeptide.

The product structure of the Boc deprotection reaction was confirmed using ^{1}H NMR spectroscopy (see figure 3.21 for atom numbering). It is recognizable that the singlet corresponding to the Boc group is no longer present. Each of the two protons of C-11 can be recognized as a doublet of doublets at 3.01 and 2.85 ppm. The singlet at 3.31 ppm corresponds the two protons of the amine group.

3.3.6. Synthesis of the tripeptide D5; attachment of the central unit to the dipeptide.
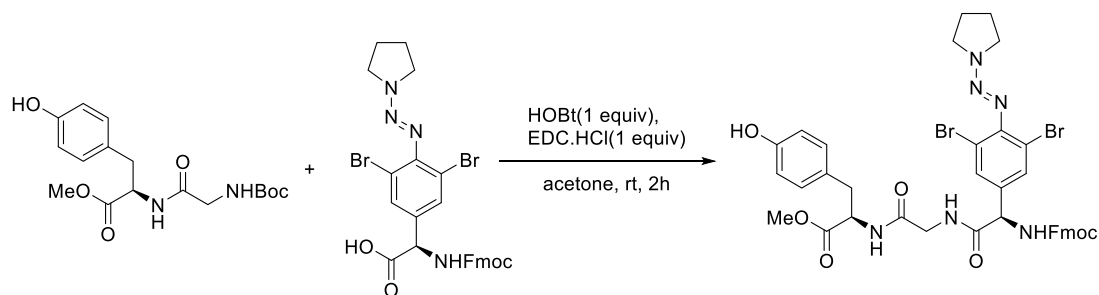
Scheme 3. 15: Reaction of attachement of the synthesised triazene-protected unit to the dipeptide via a peptide bond.

The last step in the solution synthesis involved coupling the central unit analogue to the dipeptide that was made earlier (Scheme 3.15). This experiment posed a critical step whether the analogue is eligible for the coupling with other amino acids in its Fmoc-protected form. The coupling reaction, the triazene derivative with the dipeptide, was carried out using the HOBt/EDC coupling system. After 2 h the product was purified with flash chromatography. The ^{1}H NMR spectroscopy was carried out for it and showed the right tripeptide. In addition, LC-MS was used to confirm the right mass, which was (m/z=863), (Figure 3.22).
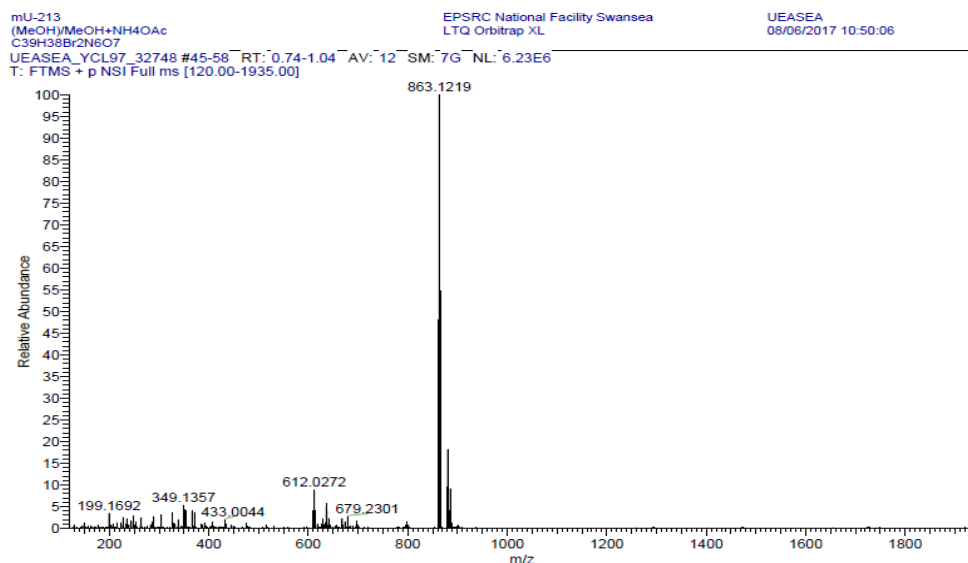
Figure 3. 22: The Mass spec. of the tripeptide showing the desired mass.
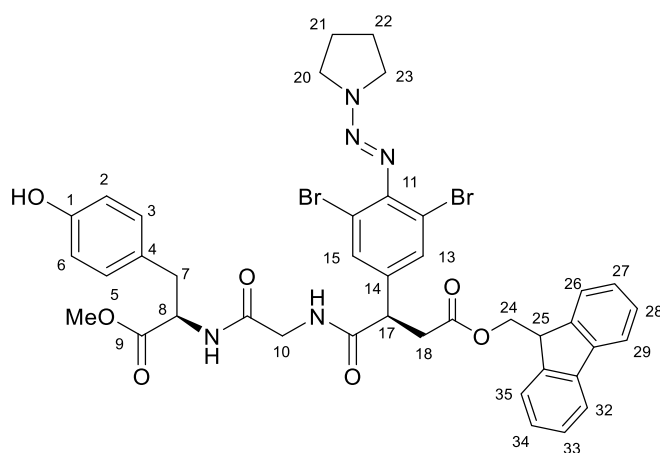
Figure 3. 23: Atom numbering of the tripeptide.

The tripeptide product was confirmed using ^{1}H NMR spectroscopy (see figure 3.23 for atom numbering). As always with the presence of the Fmoc moiety, six signals matching the protons of the Fmoc are recognisable. The four in the aromatic region are the doublet at 7.69 ppm, the broad singlet at 7.54 ppm, the triplet at 7.33 ppm, and the triplet 7.23 ppm. Each of them integrates to two protons and all of them belong to the aromatic part of the Fmoc group. The broad singlet at 7.63 ppm corresponds to the two aromatic protons of C-13 and C-15. The doublet of doublets at 6.84 ppm corresponds to the two aromatic protons at C-3 and C-5, while the triplet at 6.61 ppm corresponds to the two aromatic protons of C-4 and C-6. The multiplet at 4.77 ppm integrates to one proton and corresponds to the proton of C-8. The other two signals of the Fmoc protons are the broad singlet at 4.41 ppm which corresponds to the two protons of C-24 and the broad singlet at 4.19 which corresponds to the proton of C-

25. There is another broad singlet at 3.93 ppm which corresponds to the two protons of C-23. The multiplet at 3.80-3.64 is a collection of different corresponding protons which involves the methyl protons, the methylene protons (C-7), and the two protons of C-20. The broad singlet at 2.08 ppm matches the four protons of C-21 and C-22.

3.4. Conclusion

This chapter displays the successful coupling of the synthesised Fmoc-protected central residue of vancomycin using solution phase synthesis methodology. However, the synthesis on the solid phase was not successful. The characterisation and purification operations that are followed in the solid phase may have a detrimental impact on the triazene-protected moiety. In the solid phase technique, the use of HATU in a reduced amount as a coupling reagent and Wang resin as a supporting solid were shown to generate a promising result, but it is evident that more work is required to successfully use solid phase methodology with this reagent. It may be that other central units, containing a different residue in place of the triazene protection would be more amenable to solid phase methods.

In order to initiate studies of the other suitable units for peptide synthesis for vancomycin, the final chapter describes the synthesis of the amino acids 2 and 6 of the overall structure.

Chapter 4.

Synthesis of the Fmoc-protected ester analogues of the amino acids 2 and 6 of vancomycin

4.1. The design of the tyrosine derivatives.

This chapter focuses on the synthesis of the tyrosine units in the vancomycin structure amino acid 2 and amino acid 6 of the heptapeptide backbone. As with the design of the central residue, the aim of synthesis of each amino acid constituting the structure of vancomycin is to be Fmoc-protected at the amine functionality and have its carboxylic acid group unprotected, to comply with the criteria required for Fmoc chemistry.
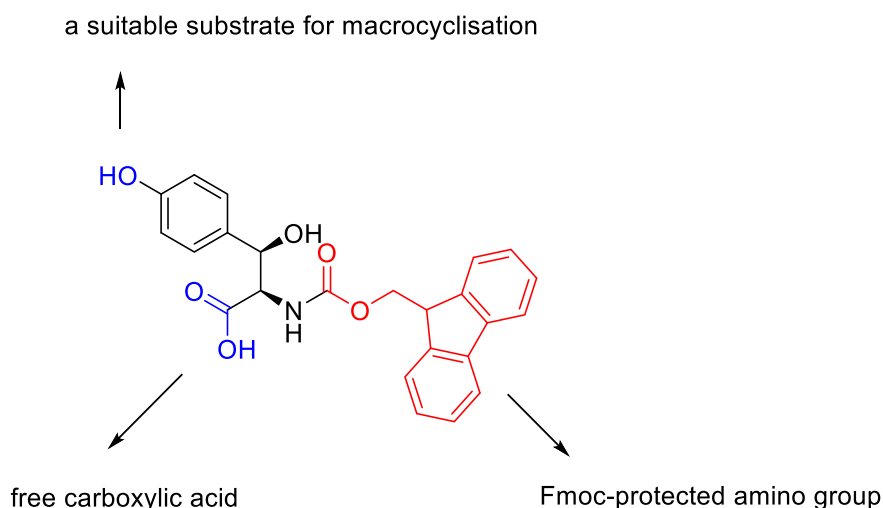
Figure 4. 1: Chemical structure design of the tyrosine derivative aa in vancomycin backbone.

Moreover, finding a feasible way for having a phenol group to be a convenient substrate in the potential macrocyclization was another synthetic approach in the synthesis. Regarding chirality, this residue contains two chiral centres, therefore work on finding a way to introduce the chiral centres selectively and to maintain them through the steps of the synthesis was an important endeavour. As will be shown later in this chapter, Nicolaou's approach has been followed to achieve the exact chirality using Sharpless AD. Using this approach, it was possible to complete the syntheses of the tyrosine analogues in Fmoc protected form of ethyl ester derivatives.

4.2. Synthesis of the ethyl ester of the Fmoc-protected amino acid-2 (Tyrosine derivative).

As mentioned above, the plan was to synthesise these units in their free carboxylic acid forms (Fmoc-protected amino acids) but for reasons discussed later in this chapter, the ethyl ester variants were successfully generated. Below, the full scheme of the synthesis of ethyl ester form of amino acid 2 is shown in scheme 4.1.
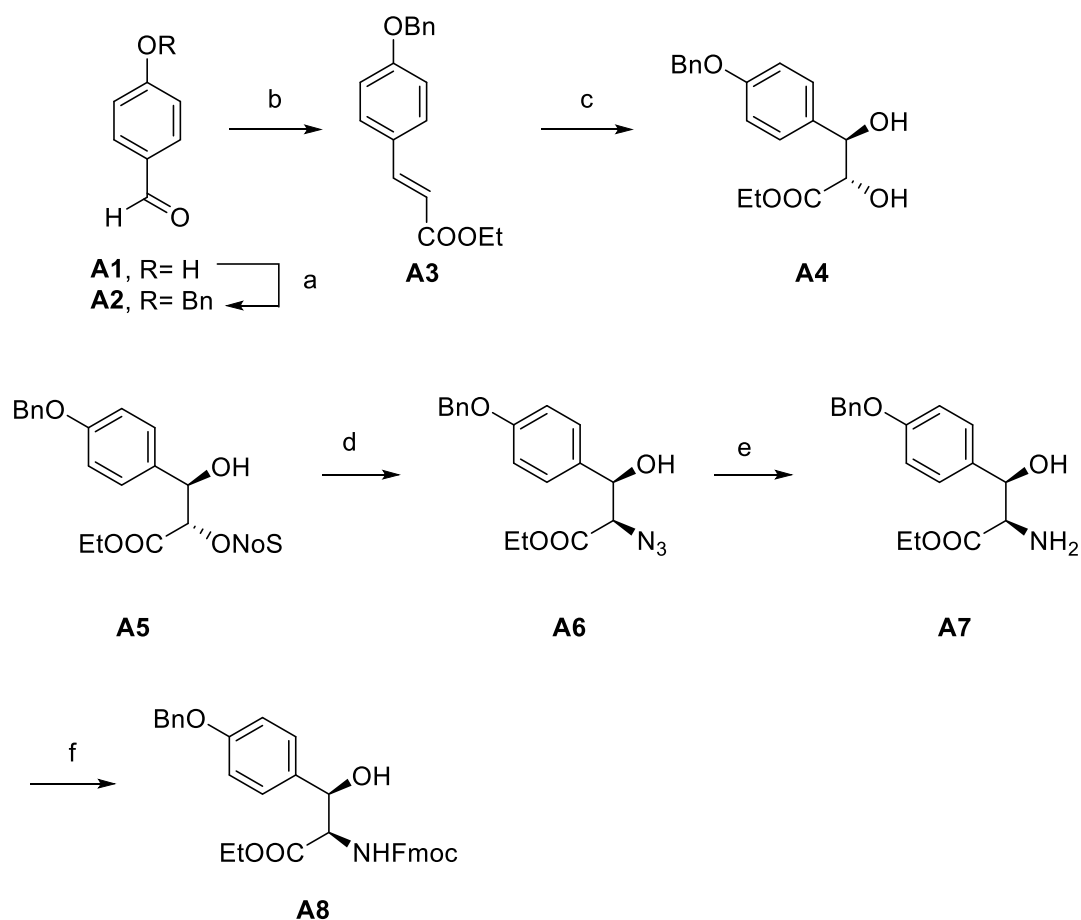
Scheme 4. 1: Synthetic route of the third aa in vancomycin peptidic backbone; Reagents and conditions: a) K_2CO_3 (1.5 equiv), BnBr (1.0 equiv), KI (0.1 equiv), DMF, 25 °C, 3 h, 86%; b) $(EtO)_2(O)PCH_2$-COOEt (1.1 equiv), KOH (1.5 equiv), THF, 25 °C, 3 h, 87%; c) AD-β, (1.4 gmmol^{-1}), $MeSO_2NH_2$ (1.0 equiv), t-BuOH/H$_2$O (1:1), 25 °C, 12 h, 48% (92% ee); d) NosCl (1.0 equiv), Et$_3$N (2.0 equiv), DMF, 0 °C, 24 h, 70%; e) NaN$_3$ (1.5 equiv), DMF, 55 °C, 8 h, 90%; f) SnCl$_2$. H$_2$O (2.0 equiv), MeOH, 25 °C, 3 h, 78%.

4.2.1. Synthesis of the benzyl-protected phenol A2.
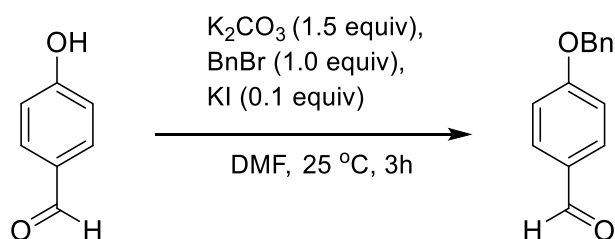
Scheme 4. 2: Chemical reaction of the synthesis of the **A2** using BnBr reagent.

p-Hydroxyl benzaldehyde **A1** was used as the SM to begin this synthesis. It is important to protect the phenol with a suitable group to withstand the different conditions of the subsequent steps of the reactions. Therefore, Nicolaou's approach

using a benzyl protecting group was followed. Thus, *p*-hydroxybenzaldehyde was dissolved in DMF and K_2CO_3, KI, and BnBr added sequentially. Then, the mixture was stirred at room temperature for 3 h to furnish the product **A2** in 86% yield following purification (Scheme 4.2).

The mechanism of reaction proceeds according to Williamson ether synthesis which includes reaction of alkoxide with organohalide in an SN2 reaction furnishing the corresponding ether (Scheme 4.3). The presence of the base catalyst is important to deprotonate the alcohol to produce the alkoxide. The alkoxide intermediate approaches the polarised methylene carbon in benzyl bromide from the opposite site to the carbon bromide bond. As the bond between the oxygen and carbon starts to form, the carbon bromide bond starts to weaken. Whilst the bond strength between oxygen and carbon increases, the bond between carbon and bromide increasingly weakens until complete removal of bromide ion as leaving group occurs. It is known that a SN2 reaction is accompanied with complete inversion in the chirality of carbon group, although it is not applicable in this reaction as the carbon involved is achiral. A primary halide is more reactive than other types, secondary and tertiary. Furthermore, the solvent (DMF) has a clear influence in promoting the SN2 mechanism for the reaction over other kind of mechanisms, i.e S_N1, because it is a polar aprotic solvent which tends more to dissolve K^+ cation, counterion of the intermediate, than the alkoxide ion (Figure 4.2).[180] Therefore, the alkoxide ion would have more electron density making it more reactive to attack the electrophilic carbon.
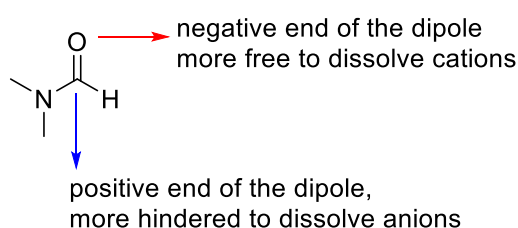
Figure 4. 2: Illustrating the role of DMF in preferentially dissolving cations.[180]
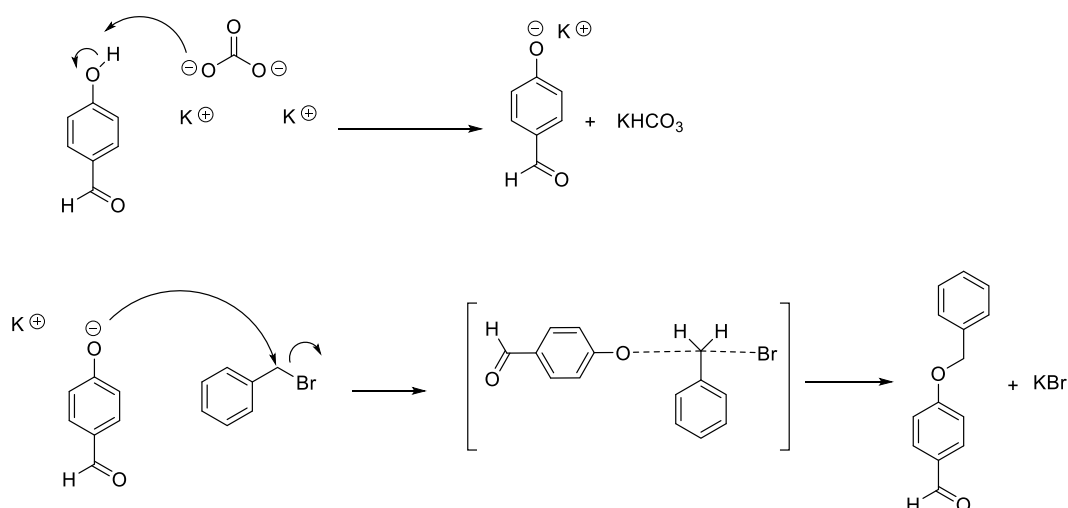
Scheme 4.3: Mechanism of the synthesis of the **A2**.

Accordingly, it is very unlikely the reaction proceeds via an SN1 mechanism due to following reasons:

-Using primary halide, which is more reactive than secondary and tertiary counterparts.

-Polar aprotic solvent.

-Use of strong nucleophile, alkoxide.
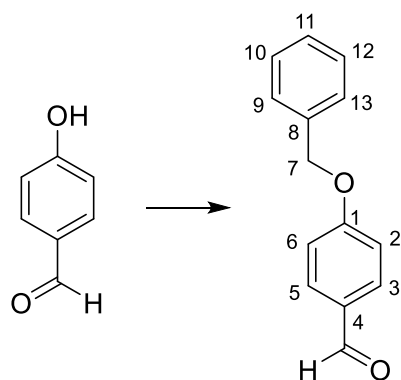
Scheme 4. 4: Atom numbering of the **A2** compound.

This product was confirmed using ^{1}H NMR spectroscopty (see scheme 4.4 for atom numbering). It is noticeable that the singlet peak at 9.89 ppm corresponds to the aldehyde proton. The doublet peak, with coupling value 8.8 Hz, at 7.84 ppm corresponds to the two aromatic protons of C-5 and C-3. The position of the latter peak is downfield due to the electron-withdrawing effect of the aldehyde group which pulls the electrons away, reducing the electron density around the C-5 and C-3. The multiplet peak of the range of the chemical shift between 7.45 and 7.32 is due to the five aromatic protons of C-9, C-10, C-11, C-12, and C-13. Confirming the success of

143

the reaction is the singlet signal at 5.15 ppm matching the methylene protons (C-7). The doublet at 7.08 ppm corresponding is to the two aromatic protons of C-6 and C-2. The mass was confirmed with high resolution-mass spectrometry; m/z: 213.0910.

4.2.2. Synthesis of the cinnamate A3.
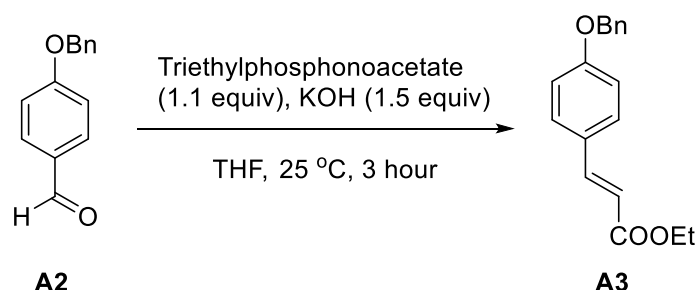
Scheme 4.5: Chemical reaction of the synthesis of the **A3** compound via Horner-Wadsworth Emmons reaction.

This reaction was carried out under N_2. The aldehyde was dissolved in THF then KOH and Horner-Wadsworth Emmons reagent were added sequentially. The mixture was stirred for 3 h to furnish the cinnamate product **A3** in 87% yield after purification (Scheme 4.5). This reaction proceeds via the mechanism of the Horner-Wadswoth-Emmons [181] reaction (Scheme 4.6). It is a modification of the Wittig reaction using phosphonate-stabilised carbanions for the generation of α, β unsaturated esters.[182] One of the acidic methylene protons in the phosphonate reagent is deprotonated with strong base producing the phosphonate anion. The resulting enol then attacks the carbonyl carbon leading to formation of two oxyanions as erythro and threo diastereomers. In both oxyanions, the lone pair on oxygen would attack the polarised phosphorus so the π bond between the latter and oxygen opens forming a four-membered ring intermediate, oxaphosphetane. This intermediate would decompose to furnish olefins of two isomers, cis and trans. The HWE reaction preferentially gives rise to *E*-olefins (*trans*-isomer) as the pro(*E*)-oxyanion (threo adduct) is more thermodynamically stable than erythro adduct.[182-184] Unlike the Wittig reaction, the phosphate by-product is readily separable by washing only with water.[182]
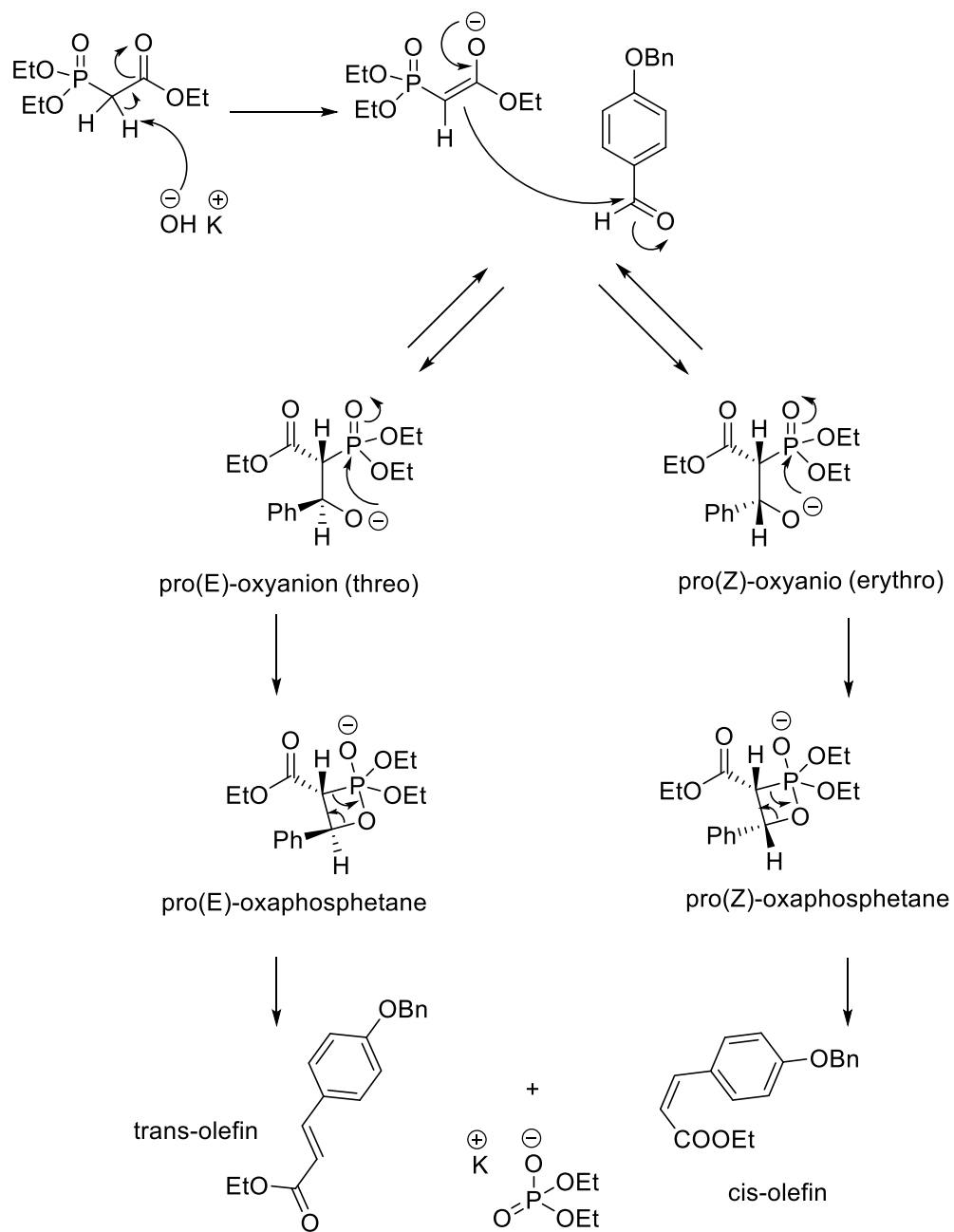
Scheme 4. 5: Mechanism of the synthesis of the **A3** compound.
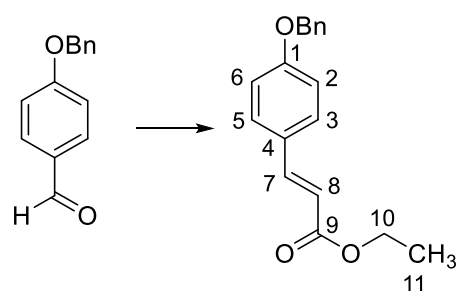
Scheme 4. 6: Atom numbering of the styrene compound.

The product was confirmed using ^{1}H NMR spectroscopy (see scheme 4.7 for atom numbering). The apparent confirmation that the reaction has proceeded properly is the presence of the two doublets corresponding to the protons of the olefin carbons, C-7 and C-8. Hence, the two doublets at 7.63 and 6.30 ppm each with coupling value of 15.9 Hz correspond to the protons on C-7 and C-8 respectively. The large value of the coupling constant (15.9 Hz) indicates the two protons are in trans position. Due to the e-donating property of the benzyl oxygen, the aryl group would have a positive inductive effect that leads to increasing the electron density around the C-8 proton through the resonance effect, (Scheme 4.8). Although, the ethyl ester has an electron-withdrawing effect, its impact of deshielding the C-8 proton is overwhelmed by the e-donating effect of the substituted aryl ring. Therefore, the C-8 proton has emerged at a lower position than the C-7 proton. Further evidence of the success of the reaction is the appearance of the quartet and triplet peaks that belong to the ethyl group. The quartet peak at 4.25 ppm with coupling value 7.1 Hz, corresponds to the two protons of C-10. While the triplet at 1.33 ppm with coupling value 7.1 Hz belongs to the three protons of C-11. The absence of the aldehyde group has the impact of shifting the doublet corresponding to the aromatic protons at C-5 and C-3 to a lower position up-field at 7.47 ppm.
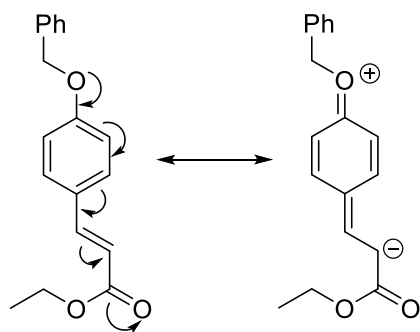
Scheme 4.7: Illustration of the inductive effect of the benzyl oxygen atom and its role in increasing the electron density around the C-8 through the resonance influence.

4.2.3. Hydrolysis of the ethyl ester; synthesis of carboxylic acid A9.

Before proceeding with the Sharpless AD, it was envisioned that hydrolysis of the ester in the final step in this synthesis might impact the potential Fmoc-protecting group. The hydrolysis of ethyl esters is often carried out using basic conditions, which, in turn, could deprotect the Fmoc group. Therefore, the suggestion was to replace the

ethyl ester with an acid labile ester to be consistent with standard conditions used in SPPS. *t*-Butyl ester was the choice of protecting group to accomplish this task. Therefore, the plan was to hydrolyse the ethyl ester using LiOH and incorporate the *t*-butyl group using *t*-BuOH. Initially, two equivalents of LiOH were used to perform hydrolysis in a biphasic solvent, THF/H$_2$O (1:1), (Scheme 4.8). The reaction was set up at 0 °C for 1 h and then allowed to warm to rt.
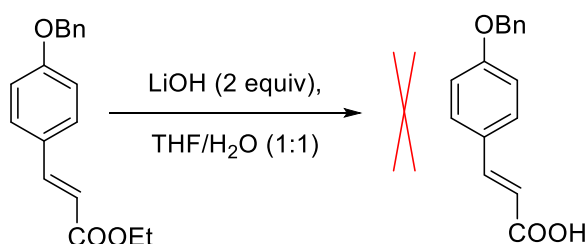
Scheme 4. 8: Unsuccessful reaction of the hydrolysis of the ethyle ester.

The reaction was not successful. An alternative approach using three equivalents of LiOH and a solvent system consisting of three solvents, THF, MeOH, and water in ratio 3:1:1 respectively (Scheme 4.10), and the resulting mixture was left overnight until thereaction was shown to be complete by tlc. After work up, the product **A9** was afforded in 85% yield without purification.
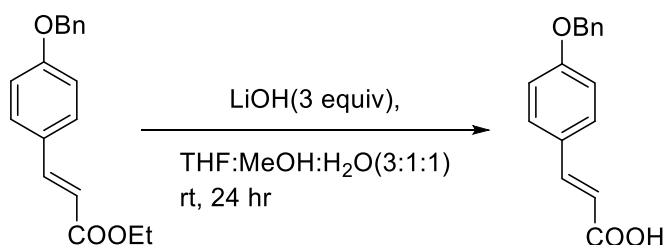
Scheme 4. 9: Hydrolysis reaction of the ethyl moiety using LiOH in THF:MeOH:H$_2$O solvent system.
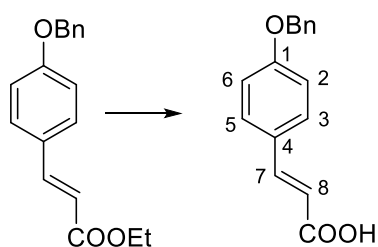
Scheme 4. 10: Atom numbering of the carboxylic compound.

The success of the hydrolysis reaction of the ethyl ester was confirmed using ^{1}H NMR (see scheme 4.11 for atom numbering). The doublet that corresponds to the proton of C-7 has shifted from 7.63 ppm in the ethyl ester to 7.73 ppm in the carboxylic acid. It can be concluded, that the proton of the C-7 is in *cis* position to the carboxylic acid (Figure 4.3). This conclusion is based on the fact that the mutual coupling value between C-7 and C-8 protons is 16 Hz, which indicates they are in a *trans* position. As the carboxylic acid is geminal to the C-8 proton therefore it should be in a *cis* position to the C-7 proton. It is known that the cis proton is more influenced by the e-withdrawing effect of the carboxylic acid than other type of protons, geminal and trans. This is an additional factor to the positive inductive effect of the substituted aryl ring, causing a more deshielding effect on the C-7 proton.[185] It is noticeable that both signals, quartet and triplet, corresponding to the ethyl group are not present in NMR spectrum of the carboxylic acid compound. This provides a confirmation of the success of the reaction.
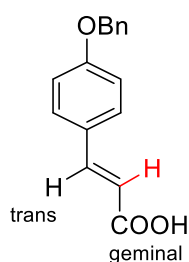
Figure 4. 3: Illustration of the cis position of the carboxylic acid to the proton across the alkene bond.

4.2.4. Synthesis of the butyl ester A10.

Initial attempts to form the *t*-Bu ester utilized a standard carbodiimide coupling approach (EDCl, *t*-BuOH, DMAP, anhydrous CH_2Cl_2) that was unsuccessful, (Scheme 4.12a). Treatment of the acid with oxalyl chloride at RT with catalytic DMF, to generate the more reactive acid chloride, was also unsuccessful, (Scheme 4.12b).
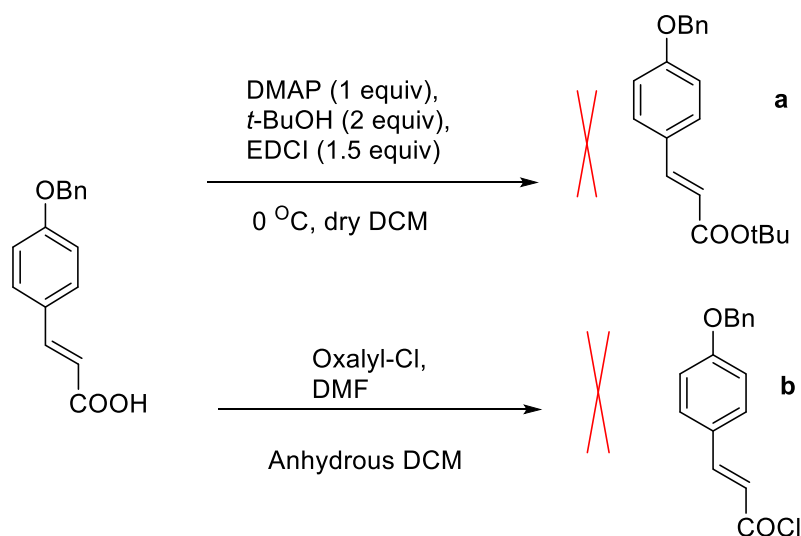
Scheme 4. 11: a) Unsuccessful reaction of the butyl ester formation using *t*-BuOH, DMAP and EDCI; b) unsuccessful reaction of production of acyl chloride using oxalyi-Cl.

Fortunately, heating the acid to reflux with thionyl chloride using *t*-BuOH as solvent furnished the product **A10** in 85% yield, (Scheme 4.13).
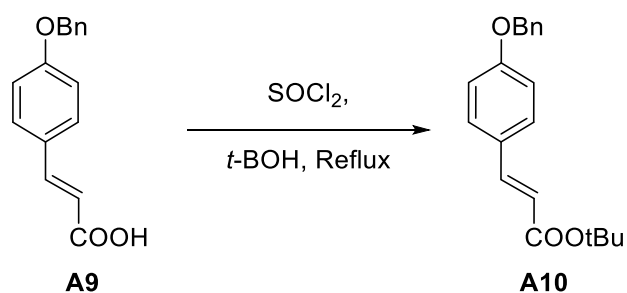
Scheme 4. 12: Formation of the butyl ester **A10** using $SOCl_2$.
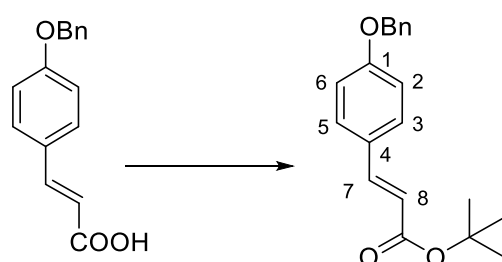
Scheme 4. 13: Atom numbering of the butyl ester compound **A10**.

The structure of the product was confirmed using ^{1}H NMR spectroscopy (see scheme 4.14 for atom numbering). The most prominent confirmation of the reaction is the emergence of the singlet signal corresponding to the nine butyl protons at 1.53 ppm. The doublet signal corresponding to the C-7 proton shifted from 7.73 ppm in the

carboxylic acid compound to 7.53 ppm in the butyl ester compound is due to the moderate electron-donating effect of the butyl ester. This in turn has increased the shielding impact to the protons leaving them less exposed to the magnetic field. For the same reason, the doublet corresponding to the C-8 proton has appeared at a lower chemical shift, 6.24 ppm, than its counterpart in the carboxylic acid compound, 6.32 ppm.

4.2.5. Synthesis of the diol A4.

After the butyl ester was obtained, all attempts to oxidize the alkene failed (Scheme 4.15). The Sharpless AD reaction was trialed in order to form the diol compound. The SM was suspended in t-BuOH/H_2O solvent system, then AD-Mix-β and MeSO$_2$NH$_2$ added sequentially. The mixture was stirred at room temperature and left overnight. TLC analysis showed only the SM. Another batch of the same reaction was set up with addition of NaHCO$_3$ as it has been argued that is the buffer solution could prevent ester hydrolysis.(186) A solution of AD-Mix-β and MeSO$_2$NH$_2$ in a solvent system of t-BuOH/H_2O containing NaHCO$_3$ was made. The solution cooled to 0 °C and the SM added and the mixture stirred at that temperature. Then, the solution was allowed to warm up to rt. Again, this reaction did not work. Methods using less selective conditions, such as treatment with potassium permanganate or N-methylmorpholine-N-oxide(151) and osmium tetra-oxide also returned starting material and were unsuccessful. The lack of success of formation of the diol was surprising. It is possible that the conjugated alkene was unreactive to these conditions, but results with the ethyl ester (see below) demonstrated that this was not the case. It would seem that the introduction of the more sterically demanding t-Bu in place of the ethyl ester was responsible for the lack of activity.
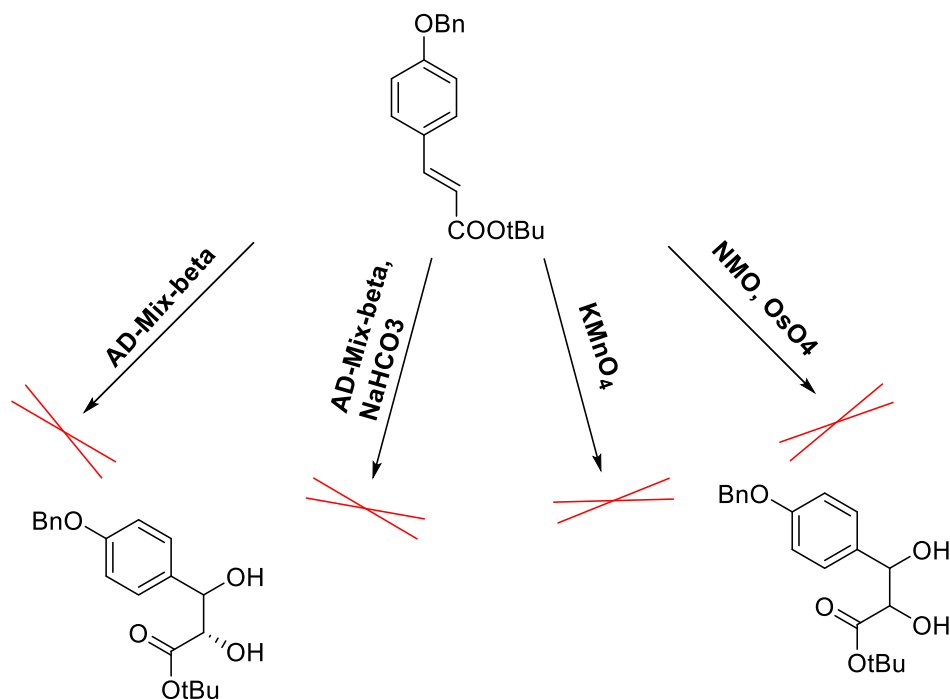
Scheme 4.14: Unsuccessful trials for oxidisation of the olefinic bond.

Following these disappointments, it was decided to proceed with Nicolaou's approach using the ethyl ester as the SM to carry out the Sharpless AD with AD-Mix-β. AD-Mix-β was added to a stirred solution of the ethyl ester and methanesulfonamide tBuOH/H$_2$O. After 48 h stirring at rt, the diol **A4** was furnished as a yellow powder in 82% yield after purification (Scheme 4.16).
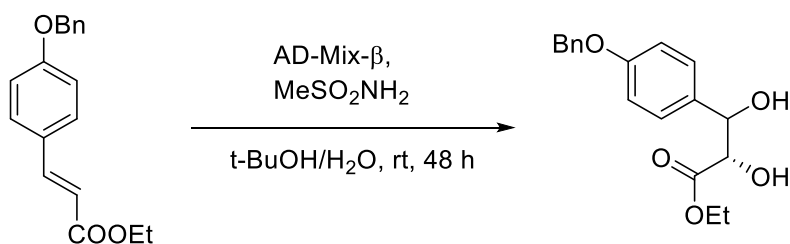
Scheme 4. 15: The synthesis reaction of the diol compoiund **A4** from **A3** using AD-Mix-β.

The expense and high toxicity of osmium tetra-oxide had urged researchers to develop a way to reduce the amount that is used in diol formation. Therefore, addition of potassium ferricyanide was a significant advance as it acts as a reoxidant, regenerating osmium tetra-oxide in the reaction and hence the latter reagent can be used in catalytic amounts. The first step in the reaction mechanism is the complexation of osmium tetra-oxide with the ligand via N-Os bond (Figure 4.4). This complexation is considered as the determining step for the stereochemisty of the diol

product. So, the olefin substrate is held in an extremely constrained-position within the U-shaped binding pocket of the osmium-ligand complex. This minimal-motion lets the liganded OsO_4 approach the alkene in a way that would allow concerted cycloaddition via a [3+2] mechanism to occur forming the pentacoordinated-osmate ester in the desired stereochemistry.[187] In the presence of water, the osmate ester is hydrolysed, giving rise to the diol, which escapes, alongside the ligand, into the organic phase and $OsO_2(OH)_4^{-2}$ which goes into aqueous phase (Scheme 4.17).[188] The latter is re-oxidised with stoichiometric reagent potassium ferricyanide back to OsO_4 to be involved in another catalytic cycle of AD reaction. The presence of methanesulfonamide is very important as a cosolvant agent, it acts on solvation of the biphasic solvent system leading to acceleration of the hydrolysis process of the osmate ester that is derived from nonterminal alkenes. This is because the osmate ester has a limited access to the aqueous phase due to its relative hydrophobicity. Noteworthy, methanesulfonamide has a reverse impact in the AD of terminal olefins where it leads to slowing down the reaction rate.

The explanation of this is the osmate ester of terminal olefin is highly hydrophilic and therefore resides in the aqueous pahse. The presence of methanesulfonamide can reduce the number of hydroxide ions, due to its solvation effect, needed for the hydrolysis step in aqueous phase leading to sluggishness in the hydrolysis. *t*-BuOH is a protic solvent and therefore can trap hydroxide ions via hydrogen bonding and hence accelerate the hydrolysis step for nonterminal olefins in particular. Looking at the structure of the olefin, it has two functionally opposite substituents, an electron-donating aromatic group and an electron-withdrawing ethyl ester group. While the aromatic moiety can decrease the electrophilicity of the osmate ester and hence slow down the reaction rate, the ethyl ester would increase its electrophilicty making it more reactive towards nucleophilic hydroxide ions.
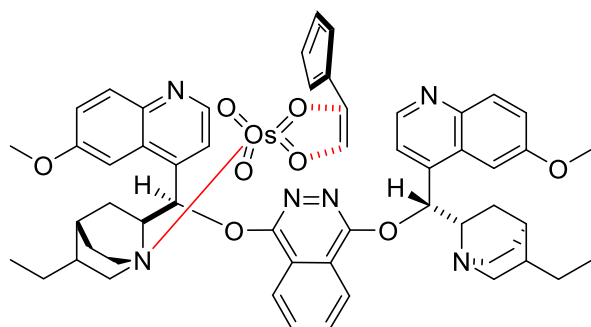
Figure 4. 4: Complexation of the osmium tetra-oxide within the chiral ligand via N-Os bond.
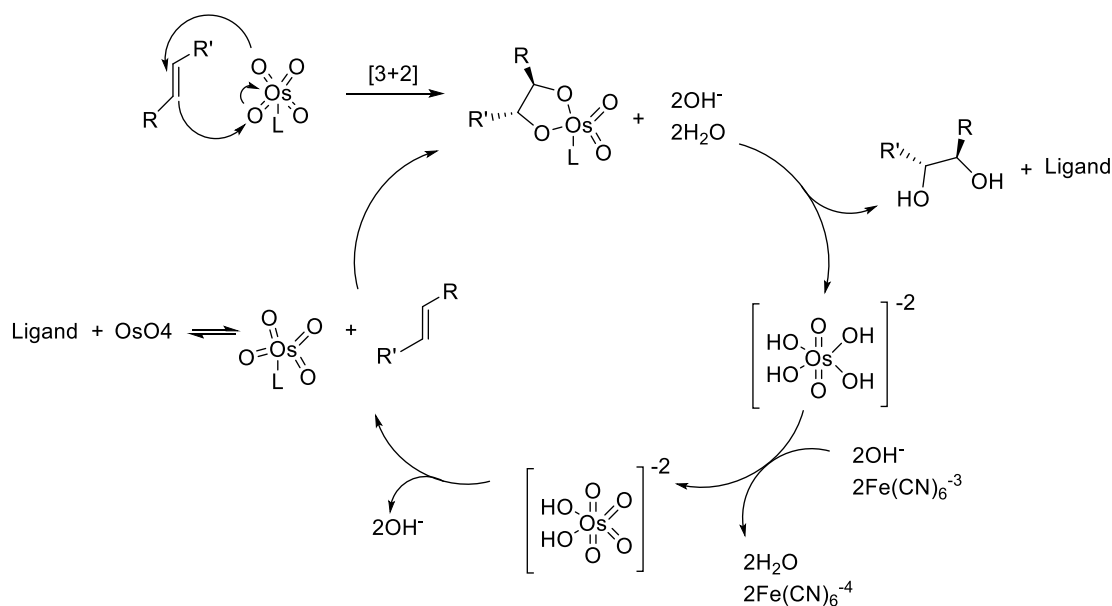
Scheme 4. 16: Mechanism of the diol formation via Sharpless AD reaction.
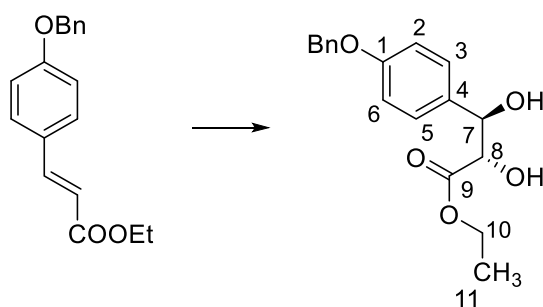
Scheme 4.17: Atom numbering of the diol compound **A4**.

^{1}H NMR spectroscopy was used for assignment of the product of the SAD reaction (see scheme 4.18 for atom numbering). The appearance of the two doublets signals at 3.07 and 2.61 ppm corresponding to the both hydroxyl groups on C-8 and C-7 respectively, is a noticeable confirmation of the success of the reaction. The former doublet has a coupling value of 5.9 Hz and the latter has a coupling value of 6.9 Hz. The two doublets of doublets at 4.93 and 4.31 pmm, which each integrate to 1 proton, correspond to the protons of C-7 and C-8 respectively. Both of them have a mutual J value of 3.1 Hz which confirms the reciprocal coupling. Another J value of the doublet of doublets at 4.93 is 6.9 Hz, which indicates the mutual coupling effect with the hydroxyl, of the same carbon C-7, that has the same J value. On the other hand, the additional J value for the doublet of doublets at 4.31 ppm is 5.9 Hz, which also indicates a spin-spin coupling with the other hydroxyl of the C-8. Noteworthy, the signals of the two protons and two hydroxyls of the carbon atoms C-7 and C-8 are recorded in the Nicoalou's literature as broad singlets. The disappearence of the

153

alkene group has caused the doublet of the aromatic protons of C-5 and C-3 to move a slightly lower position upfield to be overlapped with the multiplet peak of five protons of the benzylic group. The polarimetric rotation value was calculated at 22 °C: [α]= -11.0 (c=0.062 g/mL, MeOH). The literature value is -31.3 (c=1.15, CHCl$_3$).[99] Noticebly, the solvent used in calculation of the polarimetric rotation value for compound A4, MeOH, is differnet to that used for the literature value, CHCl$_3$, resulting in different values. In addition, **A4** might have less purity than the literature value.

4.2.6. Synthesis of the nosylated-diol A5.

The nosylated diol was obtained via the reaction of 4-nitrobenzenesulfonyl chloride (1 equiv) and Et$_3$N (2 equiv) with the diol in DMF at 0 °C (Scheme 4.19). The mixture, was stirred for 24 h to furnish nosyl-protected compound **A5** in 70% yield. Formation of the nosylated-compound is a preparation step for the subsequent reaction involving azide substitution. Hydroxide is a strong base and hence acts as a poor leaving group in the substitution reactions.
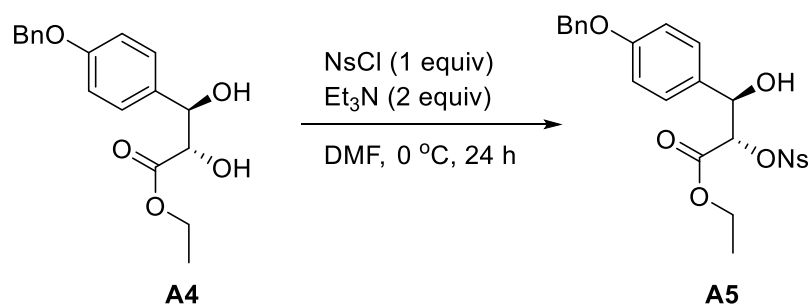
Scheme 4. 18: Reaction of the formation of the nosyl-protected diol using nosyl chloride.

The introduction of the nosyl group makes the substitution reaction easier and faster as the leaving nosylate ion is a weak nucleophile and would not react with nucleophiles. The reaction proceeds in SN2 mechanism where the alcohol attacks the electrophilic sulfur forming the pentavalent intermediate that loses chloride ion as leaving group (Scheme 4.20). The latter in turn deprotonates the positively charged alcohol producing HCl, which reacts with the Et$_3$N and the nosylated compound. There are two factors reducing the opportunity of the other alcohol group, next to aromatic ring from being nosylated: 1) the aromatic moiety is more electron-withdrawing than the ethyl ester group so the aromatic hydroxyl would be less nucleophilic than the ester hydroxyl, 2) the position of the bulky aromatic ring close to it would pose a kind of steric hindrance, which in turn can prevent the introduction of the bulky nosyl group, 3) using nosyl chloride in a stoichiometric amount would prefer its reaction with the relative more reactive alcohol.
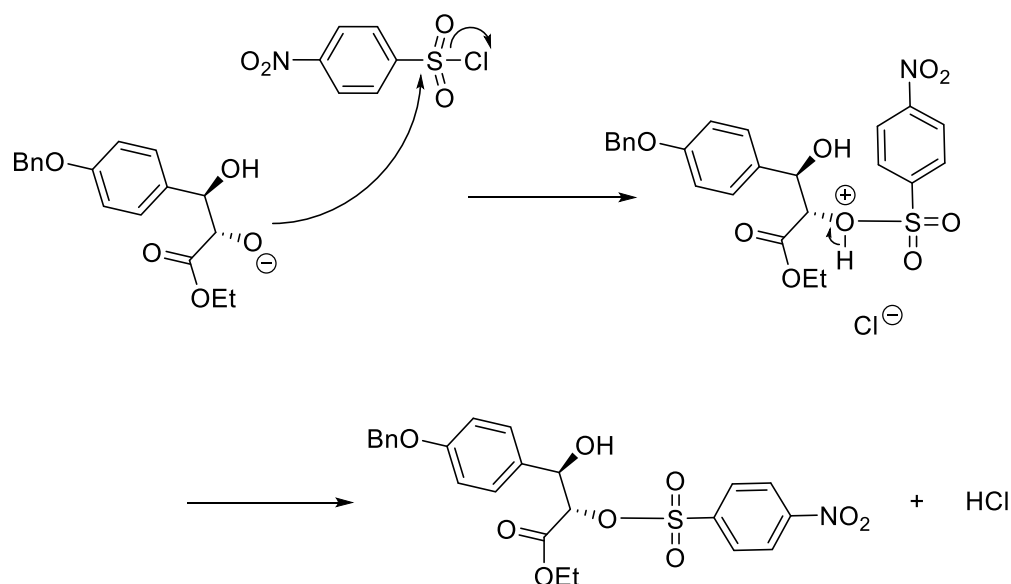
Scheme 4. 19: Mechanism of the nosyl-protected diol **A6** using nosylchloride.
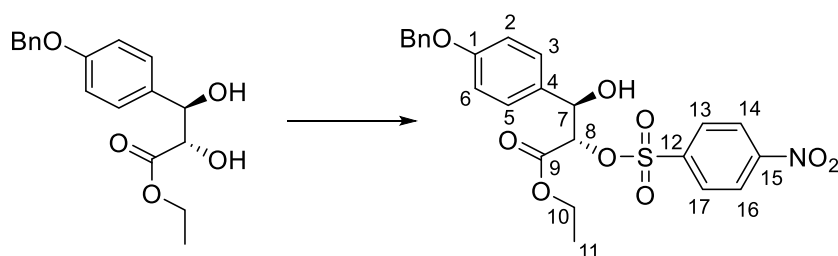
Scheme 4. 20: Atom numbering of the nosylated compound **A5**.

The nosylation reaction product was confirmed using 1H NMR spectroscopy (see scheme 4.21 for atom numbering). A clear confirmation, that the reaction was successflu is the two doublets at 8.24 and 7.87 ppm, which have coupling value 9.0 Hz and correspondent to the four aromatic protons of the nosyl group. The former doublet corresponds to the two protons of C-13 and C-17 and the latter represents the two protons on C-14 and C-16. Both the nitro and sulfonate are strong electron withdrawing groups. A significant change in the chemical shift of the proton of the carbon C-8 is due to the direct attachment to the nosyl group. While it was a doublet of doublets at 4.31 ppm of the diol compound, it has emerged at higher chemical shift downfield at 5.15 ppm as a triplet in the nosylated compound, the shift being due to the electron-withdrawing sulfonate group. A doublet corresponding to the proton of C-7 has moved to a higher downfield position from 3.07 ppm in diol compound to the 4.98 ppm in the nosylated compound due to the negative inductive effect of the nosyl group as well. Another noticeable change in the chemical shift is the movement of the doublet corresponding to the aromatic protons of C-3 and C-5 to a lower position at 7.16 ppm. The polarimetric rotation value was calculated at 22 °C: [α]= - 46.2 (c=0.058

g/mL, CHCl$_3$). The literature's value is + 43.0.[99] Obviously, the nagative rotation value of **A5**, is opposite to the lietarture value, positive. In an RSC advances paper,[189] the optical rotation for the same compound (**A5**, 18 in the paper) is –40 (nagative sign). Therefore, it confirms that the measured rotation of **A5** in thesis is right and indicates that the older paper is wrong.

4.2.7. Synthesis of the azide compound A6.
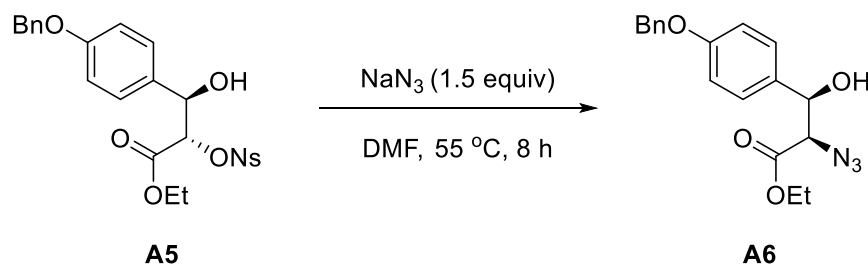
Scheme 4.21: Synthesis of the azide compound **A6** using NaN$_3$.

The azide compound **A6** was furnished in 90% yield by reaction of the nosylated compound, with NaN$_3$ in DMF at 55 °C for 8 h (Scheme 4.22). This reaction is a substitution reaction in which the azide replaces the nosylate group via an SN2 mechanism (Scheme 4.23). The nucleophilic terminal nitrogen in NaN$_3$ attacks the polarised carbon that is bonded to the nosylate. The latter is removed as a leaving group furnishing the azide compound.
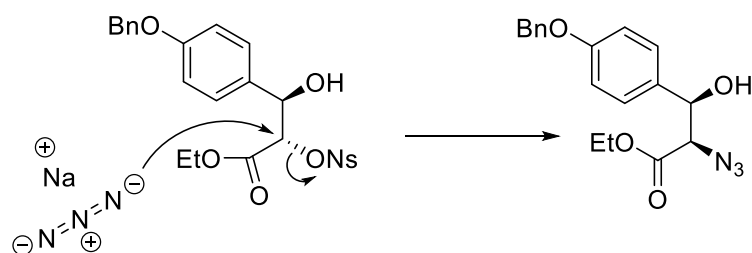
**Scheme 4. 22:** Mechanism of the azide compound **A6** formation using NaN$_3$.
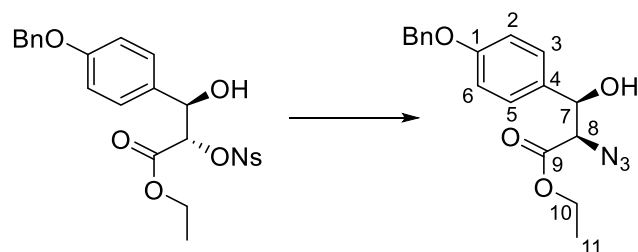
Scheme 4. 23: Atom numbering of the azide product **A6**.

This structure of the product was confirmed usign ^{1}H NMR spectroscopy (see scheme 4.24 for atom numbering). A clear indication that the reaction was successful is that

the two doublets corresponding to the aromatic protons of the nosyl group are no longer present in the NMR spectrum of the azide compound. Since the electron-withdrawing effect of the nosyl group was removed, the doublet peak of the proton of C-8 emerged at 4.08 ppm with a coupling value 7.1 Hz. In contrast to the nosylated compound, where the proton of the C-8 appeared as a triplet at a higher downfield position at 5.15 ppm. The two doublets of the aromatic four protons of C-3 and C-5 and C-6 and C-2 have moved a slightly to a higher position where the doublet that is corresponding to C-3 and C-5 has been overlaped with multiplet corresponding to the benzyl protons. IR was performed for the azide compound and the transmitance peak of the azide group was sharp and clear at 2113 cm^{-1} %T.

The polarimetric rotation value was calculated at 22 °C: $[\alpha]$= -1.3 (c=0.062 g/mL, $CHCl_3$). The literature's value is +3.09 (c=1.26, $CHCl_3$).[99] In the same RSC paper,[189] the rotation value of the azide compound is positive, +63.8 (c=6.0, $CHCl_3$), but much higher than that of the thesis's and the Nicolauo's values. This may suggest some racemisation has occurred in the synthesis. Also, the big difference in the magnitude between the RSC paper value and the Nicolaua's literature value might be enough to suggest that there is some disagreement about the true value of the optical rotation.

4.2.8. Synthesis of the amine A7.
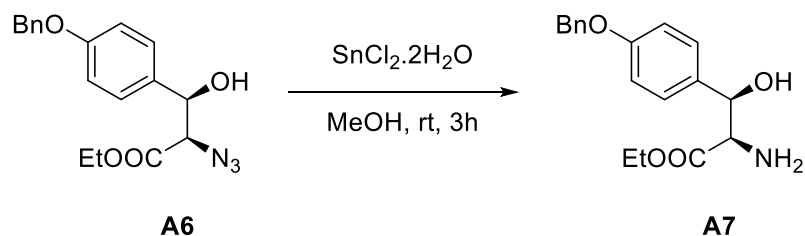
Scheme 4. 24: The synthesis reaction of the amine compound **A7** via reduction of the azide **A6** using hydrous tin chloride.

The amine was obtained via reaction of azide with tin (II) chloride dihydrate in methanol at room temperature for 3 h. It was furnished in 78% yield after purification (Scheme 4.25).
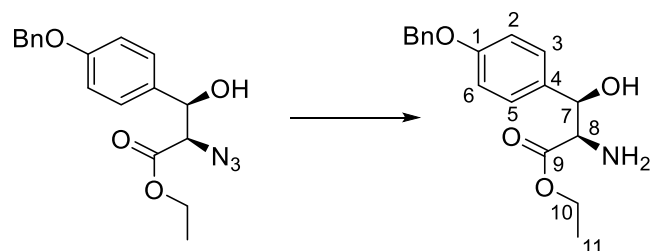
Scheme 4. 25: Atom numbering of the amine compound **A7**.

The reduction of the azide to the amine was confirmed using ^{1}H NMR (see scheme 4.26 for atom numbering). In general, no significant changes in chemical shifts of the proton signals influenced by the reduction step have been noticed. All the relavant peaks have shifted slightly to a lower position upfield as a result of introduction of the amine. Consequently, these protons become more shielded in the amine product compared to the azide compound. For example, the doublet corresponding to the proton of the C-8, has changed from a 4.08 ppm in the azide compound to a 3.77 ppm, with a coupling value 5.9 Hz, in the. A well recognised doublet corresponding to the two aromatic protons of C-3 and C-5 appears at 7.22 ppm with a coupling value 8.8 Hz.

4.2.9. Synthesis of the Fmoc-protected amine A8.

As it has been mentioned earlier in this chapter it was expected that basic hydrolysis to the ethyl ester would be likely to deprotect the Fmoc-protecting group. Therefore, as a bid to avoid that potential, it was decided to protect the amine functionality with a suitable protecting group that can withstand basic conditions. The Boc protecting group was the choice to protect the amine functionality temporarly so after hydrolysis of the ethyl ester, the Fmoc group can be attached following Boc deprotection.
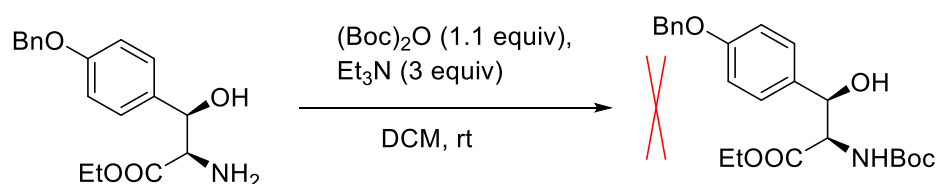
Scheme 4. 26: Unsuccessful reaction to protect the amine with Boc protecting group.

The above reaction (Scheme 4.27) was trialled to attach Boc group on the amine but did not work. The reaction was repeated with DMAP used instead of Et$_3$N. Also, nothing obtained relevant to the product. In view of this, it was decided to proceed to produce the Fmoc protected compound and to investigate approaches to ester hydrolysis that would not deprotect the amine.
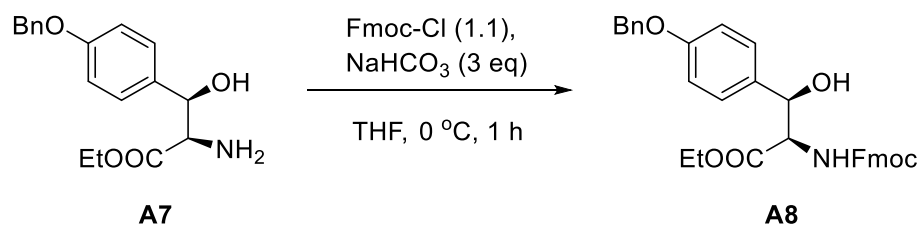
Scheme 4. 27: Fmoc-protection reaction of the amine compound using Fmoc-Cl.

The Fmoc-protected **A8** compound was obtained by reaction of the SM with Fmoc-Cl and $NaHCO_3$ in THF at 0 °C (Scheme 4.28). The mixture was stirred for 1 h to afford the compound **A8** in 95% yield after purification.
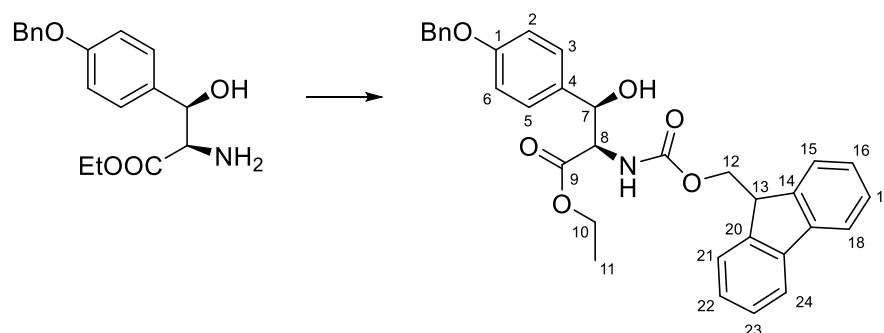
Scheme 4. 28: Atom numbering of the Fmoc-protected compound **A8**.

The assignment of the Fmoc protected amine using ^{1}H NMR is discussed here (see scheme 4.29 for atom numbering). The first confirmation of success of the reaction is the presence of all the peaks related to the protons of the attached Fmoc group. Two peaks, doublet and triplet, both with coupling value 7.4 Hz are present at 7.77 and 7.57 ppm repectively. The doublet peak is due to the protons of C-15 and C-21, which are chemically equivalent. Meanwhile, the triplet peak is relevent to the protons on the C-16 and C-22 carbons. Another two peaks matching the protons of the Fmoc group on C-17, C-18, C-23 and C-24 overlap with the multiplet of the five protons of the benzyl group over the chemical shitf range 7.44-7.29 ppm. As a result, this range integrates to nine protons, matching the benzylic five protons added to the four protons of the Fmoc relevant carbons. Additional peaks related to the Fmoc group are the two doublets of doublets at 4.51 and 4.37 which correspond to the two protons of the methylene carbon (C-12). Although the two protons of the C-12 are attached to the same carbon atom, they are not chemically equivalent. This is attributed to their enantiotopic properties. The last noticeable peak of Fmoc protons is the one corresponding to the proton of C-13 which overlaps with the signal corresponding to

the two protons of C-10 carbon of the ethyl group. This overlap results in a multiplet signal which integrates for three protons and extends over the chemical shift range 4.24-4.10 ppm. An interesting change in the peaks matching the protons of C-7 and C-8 carbons was noticed on the NMR spectrum of Fmoc-protected amine compound compared to the spectrum of the amine compound. Both peaks have moved significantly to a higher chemical shift downfield. The doublet corresponding to the proton of C-7 has shifted from 4.90 ppm in the amine to 5.52 ppm, with coupling value 8 Hz, in the Fmoc-protected amine. Meanwhile, the doublet of doublets, with coupling values 4 and 8 Hz, and matching the proton of the C-8 carbon has shifted from 3.77 ppm in the amine, to 4.74 ppm in the product.

Another doublet with coupling value 4 Hz at 5.17 ppm, matches the carbamate amide proton. To exclude any confusion that might have been seen over the latter three peaks for C-8, C-7 and carbamate proton, a ^{1}H Cosy NMR was used (Figure 4.5). It is noticed that the amide proton has a spin-spin coupling with J value 4 Hz with the proton of C-8 carbon. In addition, a spin-spin coupling with J value 8 Hz is recognised between the protons of C-7 and C-8. There is no coupling effect between the carbamate proton and the C-7 proton. Noteworthy, it has been recognised that the chemical shift of the of C-8 proton in last three compounds, azide, amine and Fmoc-protected is lower than that of the C-7, whereas, it is higher than the C-7 proton in the nosylated compound. That can be explained by the fact that the sulfonate group in the nosylated compound is a strong electron-withdrawing group. So, it pulls the electron density away from the proton of the carbon C-7, leaving it unshielded and ultimately the corresponding peak would present at a higher chemical shift. In contrast, the azide, amine, and the carbamate are positively activating groups, donating electrons, so the proton of C-8 would be shielded from the magnetic field. Therefore, the chemical shift of the C-8 proton would be at a lower position than that of C-7 proton.
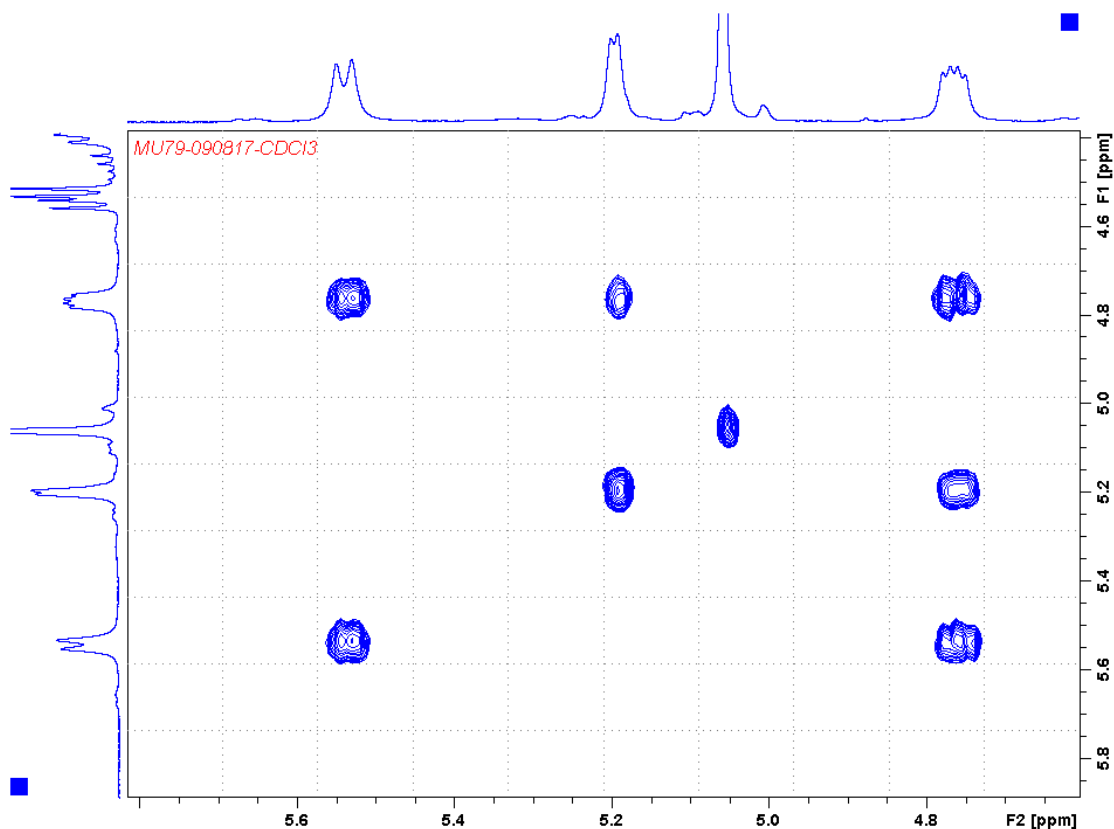
Figure 4. 5: ^{1}H Cosy NMR of the Fmoc-protected compound **A8**.

The polarimetric rotation value was calculated at 22 °C: [α]= - 29.8 (c=0.063 g/mL, CHCl$_3$).

4.2.10. Hydrolysis of the ethyl ester.
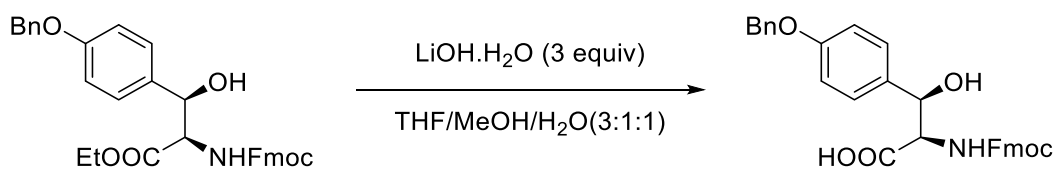
Scheme 4. 29: The chemical reaction of hydrolysis of ethyl ester using LiOH.

This step was considered to be last step in the synthesis of the 2nd building unit and crucial in the course of the work. The above reaction (Scheme 4.30) was trialled using LiOH to hydrolyse the ethyl ester. TLC analysis showed no SM was left, NMR showed neither ethyl nor Fmoc groups however.
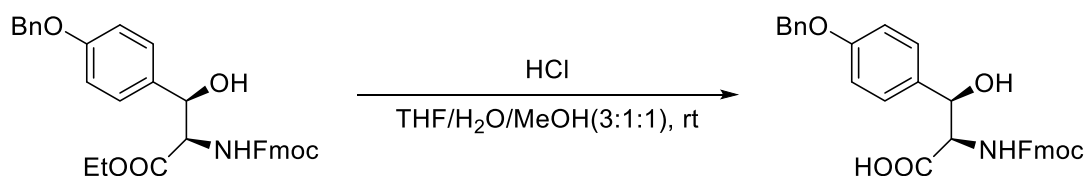
Scheme 4.30: The chemical reaction of acid hydrolysis of the ethyl ester.

Alternatively, acid hydrolysis was trialled to avoid removal of the Fmoc group (Scheme 4.31). Upon tlc, a highly polar product was formed that was proved to be intractable to isolation and identification. A protonation of the side-chain hydroxyl under acidic condition might have occurred, and can potentially lead to elimination, in addition to the ester hydrolysis (Scheme 4.32).
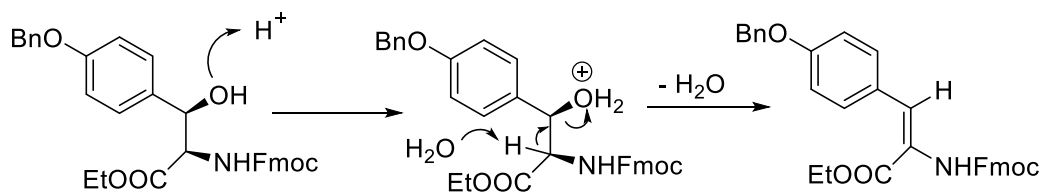
Scheme 4. 31: Illustration of the elimination of H_2O molecule because of protonation of hydroxyl group.

4.3. Synthesis of the Fmoc-protected ethyl ester, B5, analogue of the amino acid-6 (α-enantiomer).

In parallel to the successful synthesis of ethyl ester **A8**, the opposite enantiomer was also generated using a similar approach. This is detailed briefly in the following section (Scheme 4.33).
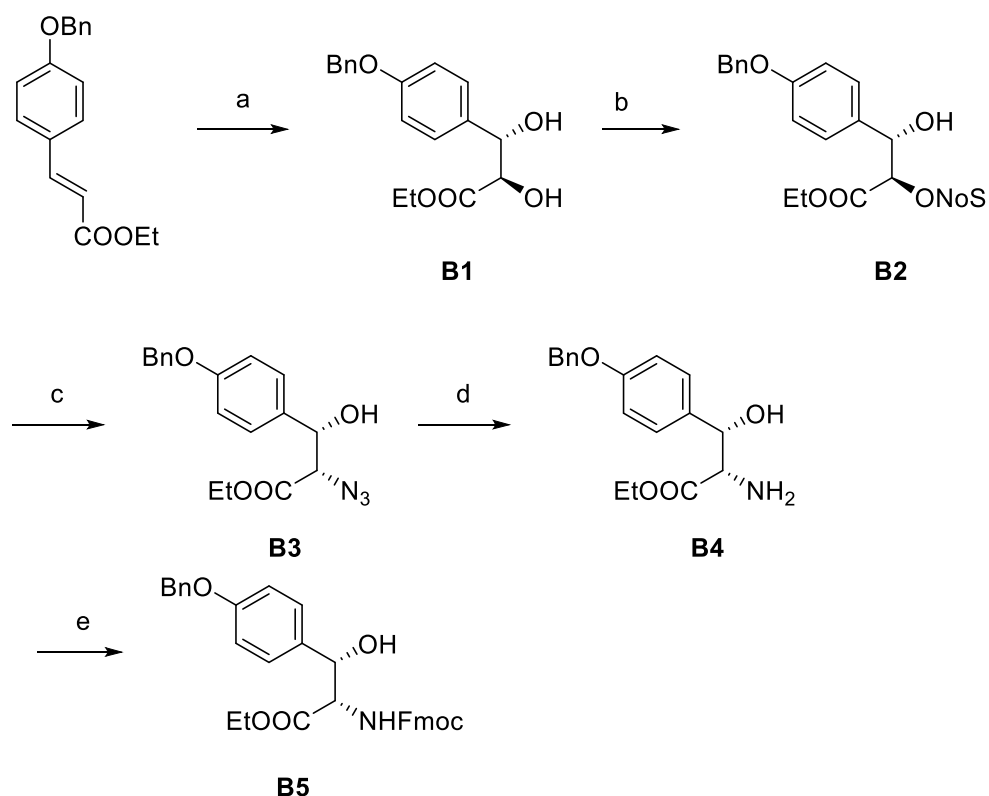
Scheme 4. 32: The synthetic route of the ethyl ester compound **B5**. Reagents and conditions: a) AD-α, (1.4 gmmol⁻¹), MeSO₂NH₂ (1.0 equiv), t-BuOH/H₂O (1:1), 25 °C, 12 h; b) NsCl (1.0 equiv), Et₃N (2.0 equiv), DMF, 0 °C, 5 h, 44%; c) NaN₃ (1.5 equiv), DMF, 55 °C, 12 h; d) SnCl₂. H₂O (2.0 equiv), MeOH, 25 °C, 2 h; e) Fmoc-Cl (1.1 equiv), NaHCO₃ (2 equiv), THF, H₂O, 0 °C ,3 h.

4.3.1. Synthesis of the diol B1 (α-enantiomer).

The synthesis process was started with the cinnamate intermediate **A3**. The latter was subjected to SAD reaction using AD-Mix-α and methanesulfonamide to furnish the diol **B1** in 70% yield as a white amorphous solid (Scheme 4.34).
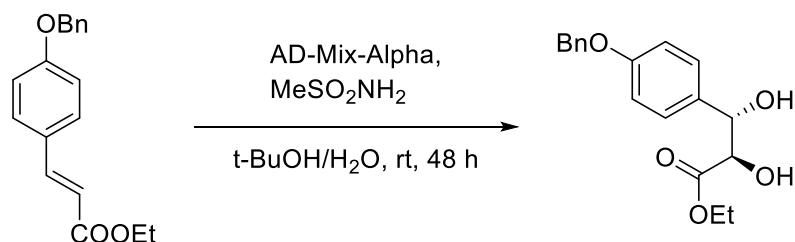
Scheme 4. 33: The reaction of production of the diol compound **B1** through SAD using AD-Mix-α.

The polarimetric rotation value was calculated at 22 °C: [α]= +16.16 (c= 0.049, EtOAc).

4.3.2. Synthesis of the nosylated diol B2.

As it was shown with the β-diol, the hydroxyl group was needed to be more reactive to act as a leaving group in a preparation step for the subsequent azide reaction. The reaction proceeded for 5 hours to give the product **B2** in 44% after purification with flash chromatography (Scheme 4.35).
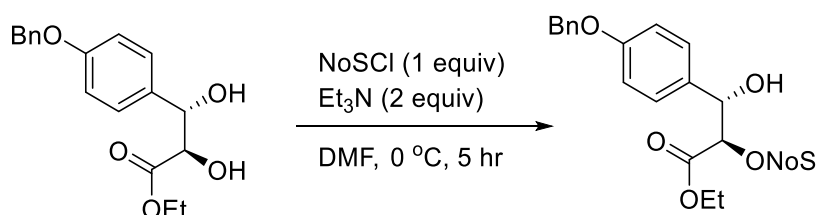
Scheme 4. 34: Synthetic reaction of the nosylated compound **B2**.

The polarimetric rotation value was calculated at 22 °C: [α]= +65.2 (c= 0.0065, EtOAc).

4.3.3. Synthesis of the azide compound B3.

This reaction was left overnight to furnish the product **B3** in 68% after purification with flash chromatography (Scheme 4.36).
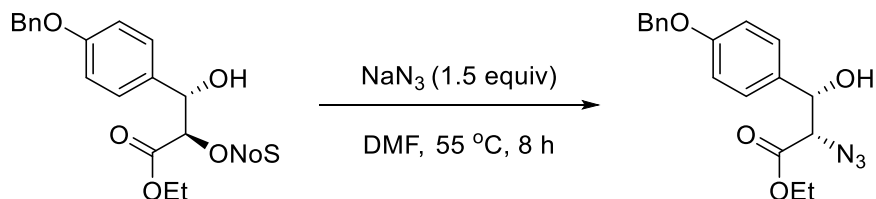
Scheme 4.35: The chemical reaction of production of the azide compound **B3**.

The polarimetric rotation value was calculated at 22 °C: [α]= -2.2 (c= 0.054, CHCl$_3$).

4.3.4. Synthesis of the amine compound B4.

The reduction was carried out using SnCl$_2$ in MeOH at room temperature. After 2 hour of stirring the product **B4** was furnished in 84% (Scheme 4.37).
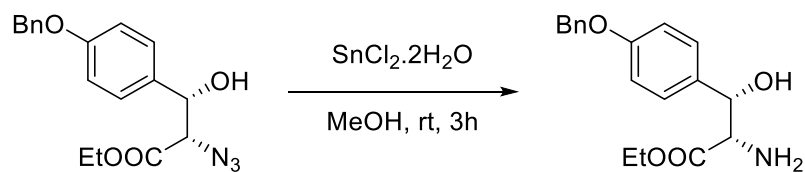
Scheme 4.36: The reduction reaction of the azide compound to produce the amine compound **B4**.

4.3.5. Synthesis of the Fmoc-protected amine B5.

The reaction of the Fmoc protection was proceeded for 1 h (Scheme 4.38). The Fmoc-protected compound **B5** was given in 80% after purification with flash chromatography.
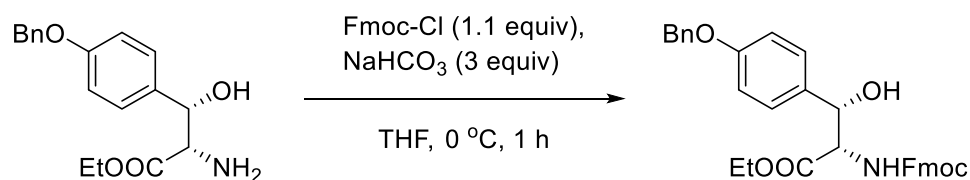
Scheme 4.37: The reaction of formation of the Fmoc-protected compound **B5** using Fmoc-Cl.

The polarimetric rotation value was calculated at 22 °C: [α]= +30.0 (c= 0.058, CHCl$_3$).

4.4. Synthesis of the TBS-protected compound B6.
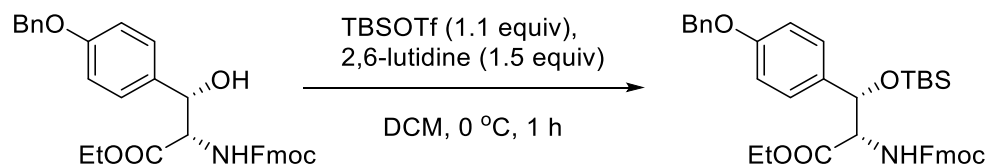
Scheme 4. 38: Reaction of production of the TBS-protected hydroxyl compound **B6**.

In order to investigate the effects of the β-OH group on the hydrolysis reaction, and also as a potential protecting group for solid phase synthesis, we briefly investigated introducing a TBS group. TBSOTf was used as a source of TBS group and 2,6-lutidine as a catalyst base (Scheme 4.39). The SM was dissolved in DCM and the TBSOTf and 2,6-lutidine were added sequencially. The mixture was stirred for 1 h. After purification, the product **B6** was furnished in 89% as a transparent oil.
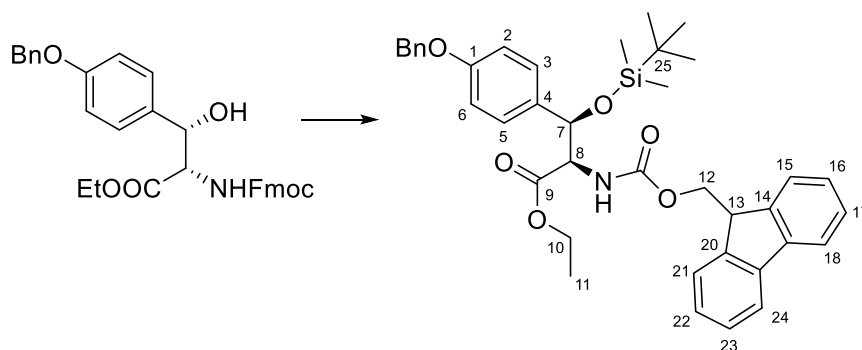
Scheme 4. 39: Atom numbering of the TBS-protected compound **B6**.

The TBS-protection product was confirmed using ^{1}H NMR spectroscopy (see scheme 4.40 for atom numbering). As the SM was fully assigned previously, the main change in the NMR spectrum for the product is the emergence of three signals related to the TBS group. The singlet at 0.92 ppm corresponds to the nine protons of the three methyl group attached to the C-25 carbon. The other two singlet signals at 0.07 ppm and -0.01 ppm correspond to the protons of both methyl groups attached to the silicon atom. Each of these singlets integrates to three protons. The doublet signal that corresponds to the amine proton has shifted slightly to a lower chemical shift at 5.07 ppm. Unlike the Fmoc-protected amine, the signal that corresponds to the acidic proton of the Fmoc group (C-13) is appeared as a prominent triplet at 4.22 ppm.

4.4.1. Hydrolysis of the ethyl ester compound B6.

Hydrolysis of the TBS protected ethyl ester was attempted under neutral conditions, using methyltrichlorosilane and sodium iodide, however this led to preferential removal of the TBS group (Scheme 4.41). After two hour of stirring, the reaction mixture was worked up and purified with flash chromatography. NMR showed no TBS group while the ethyl group was still attached. Due to time constrains, further attempts to hydrolyse the ester function were not made.
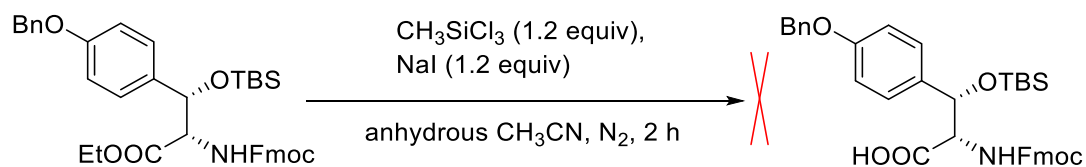
Scheme 4. 40: Unsuccessful reaction for hydrolysis of the ethyl ester.

4.5. Summary

In summary, this chapter discusses the synthesis of two Fmoc-protected stereoisomers, which following the identification of appropriate methods of the removal of the ethyl ester group, are suitable for solid phase synthesis. The synthetic route, based on the the Nicolauo's approach, involved the successful use of the Sharpless AD reaction to set the stereochemistry of the two compounds. The failure of the *t*-Bu protected compound to undergo sharpless AD or dihydroxylation under harsh conditions was surprising and led to complications later in the synthesis due to the presence of the ethyl ester groups. Both basic and acidic conditions for the hydrolysis of the ethyl ester were unsuccessful, at least in initial trials. A hydrolysis method using neutral conditions, methyltrichlorosilane and sodium iodide, was also briefly investigated but without a productive result.

The recommendation to resolve this problem is hydrolysis of the ethyl ester before attachment of Fmoc group and the resulting zwitterionic compound can be isolated using preparative-HPLC. Another approach is via the use of a buffer system to precisely adjusting the pH of the zwitterion solution until neutral pH is reached and hence the amino acid would be precipitated and isolated.

Chapter 5. Summary

5.1. The Synthesis of the central unit C14 of vancomycin.

Due to the demanding nature of the solution phase synthesis of a complex natural product like vancomycin, which requires multiple protection and deprotection steps and purification at every stage, a solid phase synthesis approach was an attractive aim. The feasibility of SPPS, which requires less purification steps and could potentially generate analogues in a rapid timeframe, was not clear for this complex molecule, therefore, the synthesis of the amino acid components of vancomycin in Fmoc-protected forms was the central idea in the project plan.

The synthesis of the central unit of vancomycin was successfully carried out following a variation of the approach developed by Nicoloau and co-workers but which required some modification in order to generate the correctly substituted Fmoc protected amino acid suitable for SPPS. The synthesis started with *p*-amino benzoic acid **C1**, which was esterified to the methyl ester **C2** using methanol. The **C1** was converted to the more reactive intermediate, acyl chloride, via the use of thionyl chloride. Dibromination was carried out to the **C2** producing **C3** by using liquid bromine and alcohol as solvent. The methyl ester moiety of **C3**, was reduced to the primary alcohol using $LiAlH_4$ in THF at 0 °C, furnishing **C4,** which was protected at the aniline function by triazene group using nitrous oxide and pyrrolidine in $AcOH/H_2O$ solvent system at 0 °C affording **C5**. The latter, was subjected to an oxidation reaction using PCC in DCM at room temperature giving the aldehyde **C6.** A Wittig reaction was implemented to convert the **C6** to the cinnamate **C7**, which was converted to the diol **C8** via Sharpless AD reaction using AD-mix-α in *t*-BuOH/H_2O solvent system. The primary hydroxyl group of **C8** was protected by TBS group using TBSOTf in DMF at 0 °C giving **C9**. Then, through a Mitsunobu reaction, the secondary hydroxyl group was displaced by azide function via a nucleophilic reaction using Ph_3P, DPPA and DIAD to furnish azide compound **C10.** The latter was reduced to the amine compound **C11** using Ph_3P. The Fmoc protection reaction was carried out to the amine **C11**, using Fmoc-Cl in THF at 0 °C, affording Fmoc-protected **C12.** The TBS-deprotection reaction was performed using TBAF in THF at 0 °C converting the **C12** to the alcohol **C13**. Finally, via an oxidation reaction using TEMPO the desired amino acid **C14** with free carboxylic acid and Fmoc-protected amine was afforded. This multi-step synthesis demonstrates that, while the target compound was relatively simple, the oxygenated structure and the requirement for suitable substitution on the aromatic ring to aid eventual ring forming reactions, leads to a complex route to synthesis. In retrospect, the incorporation of the triazene group to both direct ring closing reactions

and to act as a protecting group may have been ambitious in the context of SPPS and led to complications with cleavage from the resin and identification of the final product.

5.2. Solid phase synthesis incorporating C14.

The central unit **C14** was taken through several trials of solid phase synthesis. In the first trial, a model of tetrapeptide was proposed consisting of the following amino acids: Fmoc-Tyr(tBu)-OH, Fmoc-Tyr(OH)-OH, Fmoc-Ala-OH and the Fmoc-Tyr(tirazene)-OH. Using the ClTrt resin as a supporting solid and HATU as a coupling reagent, this trial ended unsuccessful. In the 2nd trial, the central unit was removed from the above model to exclude any potential issue might be caused by the triazene group. Using the same reagents and conditions, we also failed to obtain the required tripeptide, which was shown to be guanidinated due to the use of the HATU reagent. This is promising in that the peptide was present but undergoing a side reaction due to the use of excess HATU that was not predicted. In the 3rd trial, PyBOP was used as a coupling reagent instead of HATU and the result was successful in the synthesis of the tripeptide model. Including the central residue **C14**, the earlier model of tetrapeptide was trialled using PyBOP as a coupling reagent but the target tetrapeptide was not obtained. This suggests that the Fmoc protected amino acid, as the triazene derivative, may well be unsuitable as a reagent in the synthesis of vancomycin analogues on the solid phase. It may be that the triazene unit is not stable enough to be applied to these conditions. In the last trial, the supporting solid was changed to Wang resin and a model of tripeptide of Tyr, Gly, and the triazene derivative **C14** was trialled but also no positive result was reached.

5.3. Solution phase synthesis using C14.

After the unsuccessful trials of the solid phase synthesis of the central residue **C14**, it was taken through a solution phase synthesis model to explore its compatibility to this type of chemistry (i.e. peptide coupling). A model of tripeptide of methyl ester of tyrosine, Fmoc-protected glycine and the central unit **C14** was proposed. The methyl ester of tyrosine and the Fmoc-protected glycine were reacted in acetone using HOBt/EDC as a coupling system producing the Fmoc-protected dipeptide **D1**. The latter, was then deprotected by 20% piperidine furnishing the Fmoc-deprotected dipeptide **D2**. As ^{1}H NMR result showed no methyl group was present, this suggested that under basic condition of the Fmoc deprotection, the free amine has undergone a cyclization reaction. Therefore, the Fmoc-protected glycine was replaced by Boc-protected glycine and the coupling proceeded using the same reagents and

conditions, affording the Boc-protected dipeptide **D3**. Then, the Boc deprotection reaction of the latter was carried out with 50% TFA/DCM to give the Boc-deprotected dipeptide **D4**. The final step in the solution phase synthesis, involved the attachment of the triazene derivative to the **D4** in acetone and that culminated successfully in production of the desired tripeptide **D5** including the compound **C14**. This demonstrates that, under peptide coupling conditions, it is possible to generate the desired peptides, at least under solution phase conditions. Further work needs to be carried out to optimise the conditions to be able to use **C14** as a reagent for solid phase synthesis.

5.4. The Synthesis of A8.

To continue towards the aim of the project, for the synthesis of all the amino acid components of the vancomycin structure in their Fmoc-protected forms, the synthesis of tyrosine derivatives, amino acids 2 and 6, was trialled. The ethyl esters of the latter amino acids protected by Fmoc group at the α-amine, compounds **A8** and **B5** respectively, were obtained.

The synthesis of **A8** started with the benzylation of *p*-hydroxybenzaldehyde **A1** using BnBr in DMF producing the **A2** compound. The latter, was then taken through a Horner-Wadworth-Emmons reaction to afford the styrene **A3**. Using AD-Mix-β, the styrene **A3** was oxidised to the diol **A4** via a Sharpless AD reaction. The diol then was protected using NoSCl in DMF giving the nosylated compound **A5**. The latter, was subjected to a SN2 reaction by NaN$_3$ in DMF affording the aizde derivative **A6**. The amine **A7** was produced by reacting SnCl$_2$ with **A6** in MeOH. Finally, the Fmoc-protected ethyl ester **A8** was furnished via the reaction of **A7** with Fmoc-Cl in THF.

5.5. The synthesis of B5.

The opposite enantiomer of the **A8** compound, compound **B5**, was obtained successfully using the same approach, which started with the **A3** intermediate. The latter was subjected to the Sharpless AD reaction using AD-Mix-α and methanesulfonamide to furnish the diol **B1**. The nosylated compound **B2** was afforded via the reaction of the **B1** with NoSCl in DMF. The **B2** was reacted with NaN$_3$ in DMF to give the azide **B3.** The latter was subjected to SnCl$_2$ in MeOH affording the amine **B4**. The Fmoc-protected compound **B5** was obtained by the reaction of the **B4** with Fmoc-Cl in THF.

Several procedures were trialed to hydrolyse the ethyl ester of both **A8** and **B5** but without successful results. The hydrolysis with LiOH led, predictably, to deprotection

of the Fmoc group, while the hydrolysis under acidic conditions using HCl and under neutral conditions using CH_3SiCl_3 did not generate the products. There are potential alternative approaches to generate the free acid, Fmoc protected derivatives. Notably, deprotection of the ester through hydrolysis prior to Fmoc protection could be carried out. Time constraints meant that this approach was pursued.

5.6. Conclusions.

The first goal of this project was partially accomplished in that, the synthesis of the Fmoc-protected forms of the amino acid components of vancomycin was successfully carried out, albeit with two of the compounds still in Me ester protected form. The synthesis of **C14** was efficient, with several steps having high yields that are consistent in moving to scale-up reactions to produce the amounts required for solid phase synthesis. The successful routes to the synthesis of the Fmoc-protected forms of the ethyl esters of the tyrosine derivatives, **A8** and **B5** were also disclosed, although the hydrolysis of the ethyl ester was not successfully demonstrated.

The successful coupling of the synthesised Fmoc-protected central residue **C14** of vancomycin using solution phase synthesis methodology was disclosed. However, to date, the application of the synthesis to the solid phase has not been successful. The synthesis utilising the triazene moiety is likely to be having a detrimental effect on the solid phase route and, in future work, it would probably be reasonable to replace this moiety with other groups.

Chapter 6. Experimental

6.1. General experimental

Sigma Aldrich was the main source of purchasing most of the chemicals as reganet grade. Also, some of chemicals were purchased from Novabiochem, Fluorochem, or Fisher Scientific. All solvents were bought as anhydrous and supposed to comply the manofactureeres' standards. Distilled water was used for all specified experiments. Peptide grade DMF was used for the solid phase peptide synthesis. All solvents for HPLC mobile phases solvents were purchased as HPLC grade.

^{1}H and ^{13}C-NMR spectrometry with Fourier Transform mode on a Bruker B-ACS 60 Ultrashield 400 plus spectrometer, operating at a nominal ^{1}H NMR frequency of 400 MHz, was used for the chemical structure assignments of the reaction products. All specified spolvents for NMR were used as deuterated. Topspin 3.0 software was used for spectra processing. The peaks of both ^{1}H and ^{13}C-spectra were reported as chemical shifts in ppm and the chemical shift of the specified residual solvent peak was assigned as a reference. The peaks of NMR spectra are described as multipulities as follows: s = singlet, d = doublet, dd = doublet of doublets, t = triplet, q = quartet, m = multiplet and br = broad. The coupling constants, J, are recorded in Hz. EPSRC National Mass Spectrometry Service Centre, Swansea, was used for accurate recorded-mass spectra. A Perkin-Elmer Spectrum BX FT-IR was used for recording Infrared spectra, which were manipulated using Spectrum v5.3 Software.

Thin layer chromatography (TLC) was carried out using Merck aluminium plates, coated with 0.2 mm silica gel-60 F_{254}, as a stationary phase, which after elution were visualised under UV light.

Both normal and automated flash chromatography were used for crude compound purification as specified. The normal flash chromatography was carried out using glass columns filled with silica gel (particle size 60 μm) for column chromatography and the application of positive pressure was performed using hand bellows. The automated flash chromatography was performed on a Biotage Isolera 4, using as specified a pre-packed Biotage SNAP column.

RP-HPLC was carried out as specified on an Agilent 1200 using an Agilent eclipse XDB-C18 column, 4.6 x 150mm, 5 μm and a flow rate of 1 mL/min. Solvent A = H_2O + 0.05% TFA and Solvent B = MeOH + 0.05% TFA. Gradient 5% B → 95% B over 15 minutes 95% B → 5 % B over 5 mins. Detection wavelength 254 nm.

Preparative RP-HPLC was performed as spacified on an Agilent 1260 infinity using an Agilent eclipse XDB-C18 column, 21.2 x 150 mm, 5 μm and a flow rate of 20

mL/min. Solvent A = 95% H_2O + 5% MeOH + 0.05% TFA and Solvent B = 95 % MeOH + 5 % H_2O + 0.05% TFA. Gradient 0 % B $\rightarrow$ 100 % B over 15 minutes, 100 % B $\rightarrow$ 0 % B over 5 mins. Detection wavelength 254 nm.

6.2. Organic synthesis.

6.2.1. Synthesis of C14.
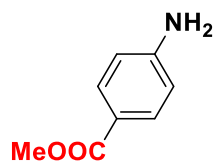
C2[99]: thionyl chloride (10.6 mL, 146 mmol) was added slowly to a solution of **C1** (20 g, 146 mmol) in MeOH (200 mL). The resulting solution was heated at reflux for 15 h until the reaction was shown to be complete by tlc. The solvent was removed under reduced pressure and the residue was dissolved in saturated aqueous $NaHCO_3$ solution (150 mL) and extracted with EtOAc (3 x 120 mL). The combined extracts were washed with H_2O (150 mL), brine (150 mL), dried (Na_2SO_4), filtered and the solvent was removed under reduced pressure to give C2 as a light yellow amorphous solid in a 97% yield without purification. mp 114-122 °C; ^{1}H NMR (400 MHz, CDCl$_3$): ppm=7.85 (d, J=8.8 Hz, 2H, ArH), 6.64, (d, J=8.8, 2H, ArH), 3.85 (s, 3H, CH$_3$); ^{13}C NMR (400 MHz, CDCl$_3$): ppm=167.17, 150.82, 131.61, 119.75, 113.80, 51.61; IR: 3463, 3368, 1678, 1593, 1567, 1520, 1434, 1313, 1286, 1180, 1167, 1121 cm^{-1}; HRMS calculated for $C_8H_{10}NO_2$ 152.0706 [M+H]$^+$ observed 152.0703.
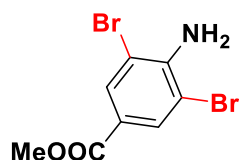
C3[99]: bromine (2.7 mL, 52.8 mmol) was added slowly to a solution of **C2** (4 g, 26.4 mmol) in ethanol (50 mL). The resulting mixture was stirred for 30 min at rt until until the reaction was shown to be complete by tlc. The solvent was removed under reduced pressure, and the residue triturated with 10% aqueous of solution sodium thiosulfate (20 mL) and extracted with EtOAc (3 x 20 mL). 1M NaOH (25 mL) was

added to remove the sulfur precipitate that formed during the extraction process. The organic layers were washed with H_2O (20 mL), brine (20 mL), dried (Na_2SO_4), filtered and concentrated under reduced pressure. The crude was purified by flash chromatography to give 71% yield of the product as a white amorphous solid. On the large scale (21.5 g, 142 mmol), the precipitated product after 30 min of stirring was only filtered under reduced pressure and triturated with ethanol to give the dibrominated product **C3** in 82% yield without purification. mp 133-137 °C; ^{1}H NMR (400 MHz, CDCl$_3$): ppm=8.07(s, 2H, ArH), 4.99 (br. s, 2H, NH$_2$), 3.87(s, 3H, CH$_3$); ^{13}C NMR (400 MHz, CDCl$_3$): ppm=164.99, 145.76, 133.40, 120.93, 107.40, 52.15; IR: 3423, 3320, 1720, 1606, 1547, 1430, 1300, 1255 cm^{-1}; HRMS calculated for $C_8H_7Br_2NO_2$ 309.8902 [M+H]$^+$ observed 309.8901.
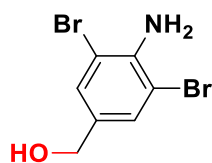
C4[99]: a solution of **C3** (2.83 g, 9.2 mmol) in 30 mL anhydrous THF was added dropwise, to a cooled suspension at 0 °C of LiAlH$_4$ (0.7 g, 18.4 mmol) in 15 mL anhydrous THF. The resulting mixture was stirred at this temperature for 3 h until the reaction was shown to be complete by tlc. The mixture then quenched with slow addition of NH$_4$Cl (15 mL), filtered and extracted with EtOAc (20 mL x 3). The combined organic extracts were washed with H_2O (20 mL), brine (20 mL), dried (Na_2SO_4) and the solvent was removed under reduced pressure. Purification was carried out with column flash chromatography giving the product, as a dark yellow amorphous solid, in 87% yield. The largescale reaction (20.1 g, 65.00 mmol) reached to completion after 1 h of stirring, furnishing the product in 86% yield without purification. mp 127-130 °C; ^{1}H NMR (400 MHz, CDCl$_3$): ppm=7.40(s, 2H, ArH), 4.54 (s, 2H, CH$_2$), 4.54 (br. s, 2H, NH$_2$); ^{13}C NMR (400 MHz, CDCl$_3$): ppm=141.44, 132.29, 130.75, 108.68, 63.95. IR: 3419, 3308, 2916, 2865, 1612, 1580, 1544, 1509, 1476, 1405, 1350, 1282, 1199, 1024 cm^{-1}; HRMS calculated for $C_7H_6Br_2NO$ 279.8801 [M-H]- observed 279.8802.
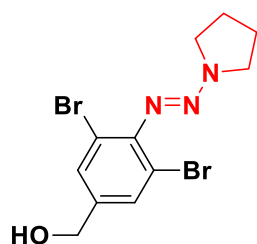
C5[(99)]: 6 M HCl (7.5 mL) and NaNO$_2$ (736 mg, 10.7 mmol) were added sequentially to a suspention of **C4** (2.5 g, 8.9 mmol) in acetic acid/H$_2$O (30 mL, 1:1) at 0 °C and the resulting mixture was stirred at this temperature for 45 min. The resulting solution was transferred slowly to another flask containing KOH (15 g, 267 mmol) and pyrrolidine (1.1 mL, 13.35 mmol) in an 80 mL of water. Upon the addition, a brown sticky solid was precipitated. The mixture was extracted with EtOAc (100 mL × 3) and washed with H$_2$O (100 mL) and brine (100 mL). Without purification, the product was afforded as a brown amorphous solid in 85% yield. The SM's spot turned to yellow while the product's spot turned to grey. This reaction was scaled up on two stages, first **C4** was used in 8 g (28.5 mmol) to give 9.56 g (93% yield). In the 2nd stage, 24.5 g of **C4** (87.1 mmol) was used and gave to 15.5 g of a brown amorphous solid (50% yield) after purification with column flash chromatography. EtoAc/*n*-hexane was used as a mobile phase in a gradient elution, 15-30%. On the large-scale reactions, the crude product was filtered under vacuum rather than extracted. mp 106-115 °C; ^{1}H NMR (400 MHz, CDCl$_3$): ppm=7.52 (s, 2H, ArH),4.61(s, 2H *CH$_2$*OH), 3.95 (br s, 2H, NC*H$_2$*), 3.73(br s, 2H, NC*H$_2$*), 2.08 (br. s, 4H, NCH$_2$*CH$_2$*, NCH$_2$*CH$_2$*); ^{13}C NMR(400 MHz, CDCl$_3$): ppm=145.96, 140.86, 130.03, 117.78, 62.99, 51.46, 46.81, 23.92, 23.72; IR: 3324, 2947, 2874, 1539, 1405, 1339, 1309, 1260, 1191, 1048 cm^{-1}; HRMS calculated for C$_{11}$H$_{13}$Br$_2$ N$_3$OH 363.9478 [M+H]$^+$ observed 363.9480.
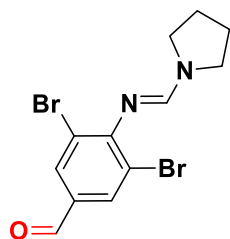
C6[(99)]: PCC (2.3 g, 12.45 mmol) was mixed with 2 g silica and added to a stirring solution of **C5** (3 g, 8.3 mmol) in DCM (40 mL). The resulting mixture was stirred for 5 h until the reaction was shown to be complete by tlc. The mixture was filtered through Florisil® (60-100) (in the literature, celite was reported[(99)]) and washed with H_2O (15 mL), brine (15 mL), dried (Na_2SO_4) and the solvent was removed under reduced pressure to give the aldehyde **C6** in 90% yield as a dark brown solid (2.7 g) without purification. This reaction was scaled up to 15.5 g (4.2 mmol) of **C5** and the product was filtered through silica under reduced pressure instead of Florisil® to give the aldehyde in 91% yield (13.82 g). mp 105-112 °C; ^{1}H NMR (400 MHz, CDCl$_3$): ppm= 9.84 (s, 1H, C*H*O), 8.04(s, 2H, Ar*H*), 3.99(s, 2H, NC*H$_2$*), 3.75(s, 2H, NC*H$_2$*), 2.11 (br. s, 4H, NCH$_2$C*H$_2$*C*H$_2$*); ^{13}C NMR(400 MHz, CDCl$_3$): ppm=188.88, 152.80, 134.11, 133.63, 118.51, 51.44, 46.94, 24.01, 23.54; IR: 3359, 3048, 2971, 2871, 2834, 1688(C=O, aldehyde), 1579, 1536, 1407, 1337, 1307, 1260, 1222, 1191, 1103, 1026 cm^{-1}; HRMS calculated for C$_{12}$H$_{12}$Br$_2$N$_2$OH 360.9369 [M+H]$^+$ observed 361.9325.
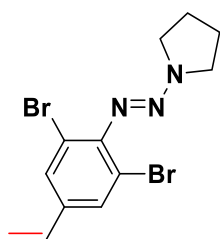
C7[(99)]: *n*-BuLi (12.12 ml) was handled under inert conditions (N$_2$) and added dropewise to a suspension of methyltriphenylphosphonium bromide (7.43 g) in 40 mL anhydrous THF, at -20 °C. The resulting mixture was stirred under N$_2$ for 0.5 h. A solution of **C6** (5 g, 13.85 mmol) in 30 mL anhydrous THF was added to the resulting suspension at that temperature and the resulting mixture was left overnight for stirring under N$_2$ untile the reaction was shown to be complete by tlc. The resulting mixture was quenched with H$_2$O (50 mL), extracted with EtOAc (50 mL × 4), washed with of

H$_2$O (2 x 50 mL), brine (50 mL), and dried (Na$_2$SO$_4$). The crude was purified by flash chromatography using ether/*n*-Hexane system as a mobile phase, which was run in a linear gradient 4-8%. The product was furnished in a 58% yield as a yellow/brown oil. This reaction was scaled up to 13.5 g of **C6** and the same above procedure was followed to give the product in 55% yield (7.5 g). ^{1}H NMR (400 MHz, CDCl$_3$): ppm=7.57 (s, 2H, ArH), 6.55 (dd, *J*=17.5, 10.9 Hz, 1H, ArCH), 5.70 (d, *J*=17.5 Hz, 1H, ArCH=C*H*H), 5.26 (d, *J*=10.9 Hz, 1H, ArCH=CH*H*), 3.96 (br. s, 2H,NC*H*2), 3.73(br. s, 2H, NC $_2$), 2.08 (br. s, 4H, NCH$_2$C*H$_2$*C*H$_2$*); ^{13}C NMR(400 MHz, CDCl$_3$): ppm=147.34, 136.49, 134.22, 130.17, 118.01, 115.39, 51.31, 46.73, 24.12, 23.77; IR: 2976, 2946, 2873, 1520, 1446, 1402, 1380, 1353, 1337, 1305, 1256, 1223, 1194 cm^{-1}; HRMS calculated for C$_{12}$H$_{13}$Br$_2$N$_3$ 359.9529 [M + H]+ observed 359.9529.
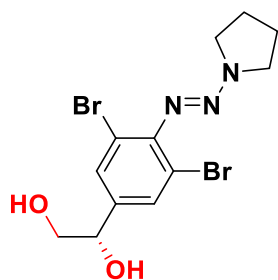
C8[(99)]: AD-Mix-α (30.22 g) powder was added to a stirring suspension of **C7** (7.75 g, 216 mmol) in 200 mL *t*-BuOH/H$_2$O (1:1) at rt, and the resulting mixture was stirred for 48 h until the reaction was shown to be complete by tlc. Then, Sodium sulfite (32.4 g) was added to the suspension and the resulting mixture was stirred for 1 h and extracted with EtOAc (100 mL × 3) and the combined extracts were washed with H$_2$O (100 mL) and brine (100 mL). Without purification, the product was furnished in 97% yield (8.28 g) as a yellow amorphous solid. mp= 120-130 °C; ^{1}H NMR (400 MHz, CDCl$_3$): ppm=7.50 (s, 2H, ArH), 4.73 (dd, J=8.04, 3.53 Hz, 1H, ArC*H*), 3.95 (br. s, 2H, NC*H$_2$*), 3.71(br. s, 2H, NC*H$_2$*), 3.68 (dd, J=11.1, 3.5 Hz, 1H, C*H*HOH), 3.57 (dd, J=11.1, 8.04 Hz, 1H, CH*H*OH), 2.09 (br s, 4H, NCH2C*H$_2$*C*H$_2$*); ^{13}C NMR(400 MHz, CDCl$_3$): ppm=146.35, 140.75, 129.86, 117.98, 72.94, 67.71, 51.57, 46.86, 23.90, 23.74; IR: 3548, 3274, 2960, 2874, 1540, 1405, 1309, 1262, 1209, 1083, 1029 cm^{-1}; HRMS calculated for C$_{12}$H$_{14}$Br$_2$N$_3$O$_2$ 393.9583 [M+H]$^+$ observed 393.9583; polarimetric rotation was calculated at 22 °C: [α] =+82.05 (c=0.078 g/mL, CHCl$_3$).
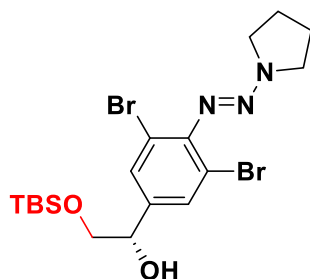
C9[99]: anhydrous Et₃N (1.37 mL) and TBS-Cl (1.5 g, 9.81 mmol) were added sequentially to a solution of **C8** (2.57 mg, 6.54 mmol) and DMAP (79.8 mg) in DCM (50 mL) at 0 °C and under inert atmosphere (N_2), The resulting mixture was stirred at that temperature for 2 h before quenching with saturated aqueous solution of NH_4Cl (20 mL). The organic layer was separated, and the aqueous layer was extracted with DCM (30 mL × 3). The combined organic extracts were washed with H_2O (30 mL) brine (30 mL), dried with sodium sulfate and concentrated under reduced pressure. Purification was carried out with an automated flash chromatography system. The crude was dry loaded on 100 g SNAP Ultra preloaded column, and a mobile phase system of EtOAc/*n*-Hexan was run in a linear gradient 10-30%. The TBS-protected diol **C9** was furnished in a 63% yield as a yellow oil. This reaction was scaled up to 8.9 g of **C8** using the same conditions and reagents, and the product was purified with the automated flash chromatography in a similar way to that of the small scale to give the TBS-protected diol **C9** in 67% yield. ¹H NMR (400 MHz, CDCl₃): ppm=7.54 (s, 2H, ArH), 4.66 (dd, *J*=8.2, 3.6, 1H, ArC*H*), 3.85 (br. s, 4H, NC*H₂*), 3.73 (dd, *J*=10.1, 3.6, 1H, C*H*HOSi), 3.49 (dd, *J*=10.1, 8.2 Hz, 1H, CH*H*OSi), 2.08 (br. s, 4H, NCH₂CH₂C*H₂*), 0.91 (s, 9H, ᵗBuSi), 0.07 (s, 3H, CH₃Si), 0.06(s, 3H, CH₃Si); ¹³C NMR(400 MHz, CDCl₃): δ=146.84, 140.25, 130.08, 117.61,72.83, 68.45, 51.29, 46.69, 25.89, 23.97, 23.69, 18.29, -5.36. IR: 3361, 3300, 2926, 2856, 1541, 1417, 1360, 1328, 1314, 1253, 1225, 1111 cm⁻¹; HRMS calculated for C18H29Br2N3O2Si 508.0449 [M+H]⁺ observed 508.0441; polarimetric rotation value was observed at 22 °C: [α]=+18 (0.026 g/mL, CHCl₃).
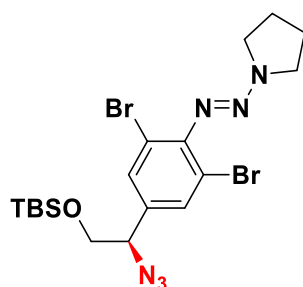
C10[99]: Triphenylphosphine (780 mg, 3 mmol), diisopropylazo dicarboxylate (DIAD) (590.4 µl, 3 mmol) and diphenylphosphoryl azide (DPPA) (640 µl, 3 mmol) were added sequentially to a solution **C9** (600 mg, 1.2 mmol) in an anhydrous THF (3 mL) at 0 °C under inert atmosphere (N$_2$). The resulting mixture was stirred at this temperature for 2 h until the reaction was shown to be complete by tlc. The solvent was removed under reduced pressure and the residue was purified with the automated flash chromatography as a mobile phase of ether/*n*-hexane was run in a linear gradient 5-10%. 450 mg of the crude (still contained isopropanol) was obtained as a yellow oil. As mentioned in chapter 2, all attempts to scale up this reaction more than 700 mg of the SM failed to give the right azide compound. However, the amount of the crude azide product was obtained from the reaction of alcohol **C9** (9.00 g, 17.75 mmol), was 6.8 g. ^{1}H NMR (400 MHz, CDCl$_3$): δ=7.49 (s, 2H, ArH), 4.49 (dd, *J*=7.7, 4.4 Hz, 1H, ArCH), 3.92 (br. s, 2H, NCH$_2$), 3.76 (br. s, 2H, NCH$_2$) 3.78 (dd, *J*=10.6, 4.4 Hz, 1H,C*H*HOSi), 3.71(dd, *J*=10.6, 7.7 Hz, 1H, CH*H*OSi), 2.08 (br. s, 4H, NCH$_2$CH$_2$), 0.90 (s, 9H, tBuSi), 0.07 (s, 3H, CH$_3$Si), 0.06 (s, 3H, CH$_3$Si); ^{13}C NMR (400 MHz, CDCl$_3$): ppm=148.05, 135.81, 131.10, 117.95, 67.92, 65.67, 51.33, 46.72, 25.89, 24.12, 23.75, 18.35, -5.39, -5.44; IR: 2983, 2929, 2857, 2100, 1773, 1416, 1315, 1239 cm^{-1}; HRMS calculated for C$_{18}$H$_{28}$Br$_2$N$_6$OSi 533.0514 [M+H]$^+$ observed 533.0506; polarimetric rotation value was observed at 22 °C: [α]= - 102 (0.076 g/mL, CHCl$_3$).
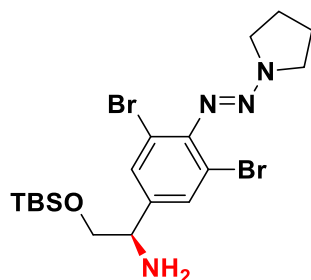
C11[(99)]: Triphenyl phosphane (400 mg, 1.52 mmol) and H_2O (93 µl, 5 mmol) were added sequentially to a solution of **C10** (270 mg, 0.507 mmol) in an anhydrous THF (5 mL). The the resulting mixture was heated to 60 °C and stirred for 2 h untile the reaction was showen to be complete by tlc. The resulting solution was cooled down to rt, the solvent was removed under reduced pressure and the residue was purified using the automated flash chromatography. The crude was dry loaded on 25g SNAP Ultra preloaded column and a mobile phase system of EtOAc/*n*-hexane was run in a linear gradient 10-30%. The crude was furnished in a 200-mg weight as a light-yellow oil. On the large-scale reaction, 4.64 g of **C10** was used, furnishing 4 g of the crude after purification with normal column flash chromatography as a mobile phase system of EtOAc/*n*-Hexane was used in a 30-40% gradient. ^{1}H NMR (400 MHz, $CDCl_3$): ppm=7.55 (s, 2H, ArH), 3.98 (dd, *J*=7.5, 4.0 Hz, 1H, ArCH), 3.93 (br. s, 2H, NCH_2), 3.70 (br. s, 2H, NCH_2), 3.67 (dd, *J*=9.7, 4.0 Hz, 1H, CH*H*OSi), 3.47 (dd, *J*=9.7, 7.5 Hz, 1H, CH*H*OSi), 2.06 (br. s, 4H, NCH_2C*H*$_2$, NCH_2C*H*$_2$), 0.89 (s, 9H, tBu-Si), 0.02 (s, 6H, $(CH_3)_2$-Si); ^{13}C NMR (400 MHz, $CDCl_3$): ppm=147.06, 141.85, 130.90, 117.58, 68.94,56.34, 51.17, 46.58, 25.90, 23.90, 23.70, 18.27, -5.40, -5.42; IR: 3208, 2927, 2855, 1711,1534, 1590,1467, 1414, 1313, 1251, 1223, 1179, 1112 cm^{-1}; HRMS calculated for $C_{18}H_{30}Br_2N_4OSi$ 507.0609 [M + H]$^{+}$ observed 507.0602; the polarimetric rotation value was observed at 22 °C: [α]= - 10.7 (0.11 g/mL, $CHCl_3$).
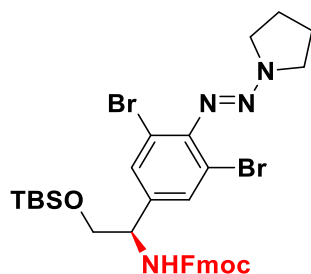
C12: An aqueous solution of $NaHCO_3$ (66.6 mg, 0.8 mmol, 1 mL H_2O) was added to a solution of **C11** (200 mg, 0.4 mmol) in THF (3 mL) at 0 °C, and the resulting mixture was stirred. Then, a cooled solution at 0 °C, of Fmoc-Cl (153.3 mg, 0.6 mmol) in THF

(2 mL) was added dropwise to the stirring mixture and the resulting mixture was stirred for 3 h untile the reaction was showen to be complete by tlc. The THF solvent was removed under reduced pressure and the emaining aqueous residue was extracted with EtOAc (2 mL × 3). The combined organic extracts were washed with H_2O (3 mL), brine (3 mL), dried with sodium sulfate and concentrated under reduced pressure. The purification was performed with the automated flash chromatography as the crude was dry loaded on 25 g SNAP Ultra preloaded column and EtOAc/*n*-Hexane mobile phase was run in a linear gradient, 5-20%. A 240mg weight of the pure product was obtained as a yellow fluffy solid. On the scale up steps, the average yield over the last four reactions, bigning with **C9** (9.00 g, 17.75 mmol) and ending up with **C12** (6.5 g, 9.00 mmol), was 50% and the the Fmoc-protected product **C12** was purified with normal column flash chromatography (gradient elution, 10-20% EtOAc/n-Hexane). mp 70-85 °C; ^1H NMR (400 MHz, $CDCl_3$): ppm=7.92(d, *J*=7.4 Hz, 2H, Ar-Fmoc), 7.72(m, 2H, Ar-Fmoc), 7.67(s, 2H, ArH), 7.44(m, 2H, Ar-Fmoc), 7.35 (m, 2H, Ar-Fmoc), 4.64(m, 2H, CHNH), 4.34(d, *J*=7 Hz, 2H, CH_2-Fmoc), 4.26(t, *J*=7 Hz, 1H, Ar-Fmoc), 3.91(br. s, 2H, NCH_2), 3.72(br. s, 2H, CH_2OH), 3.60(br. s, 2H, NCH_2), 2.03(m, 4H, NCH_2CH_2), 0.85(s, 9H, $(CH_3)3$-TBS), 0.01(s, 3H, CH_3, TBS), -0.02(s, 3H, CH_3, TBS); ^{13}C NMR (400 MHz, $CDCl_3$): ppm=155.86, 147.39, 143.92, 141.39, 139.35, 130.99, 127.79, 127.19, 125.13, 120.05, 117.78, 67.08, 66.01, 55.21, 51.30, 47.27, 46.65, 25.91, 24.04, 23.81, 18.33, -5.52; IR: 2950, 1706, 1501, 1414, 1315, 1253, 1104 cm^{-1}; HRMS calculated for $C_{33}H_{40}Br_2N_4O_3Si$ 729.1292 $[M + H]^+$ observed 729.1290; the polarimetric rotation value was observed at 22 °C: [α]= - 42.9 (0.067 g/mL, $CHCl_3$).
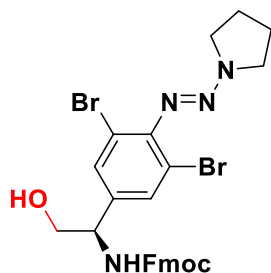
C13: AcOH (44 µl, 0.9 mmol) and TBAF (0.35 ml, 0.36 mmol) were added sequentially to a solution of **C12** (220 mg, 0.3 mmol) in THF (3 mL) at 0 °C. The resulting solution was stirred at that temp for 6 h untile the reaction was showen to be complete by tlc. The rsulting solution was quenched with saturated aqueous solution of NH_4Cl (2 mL) and extracted with EtOAc (3 mL × 3). The combined organic extracts were washed with H_2O (4 mL), brine (4 mL) and concentrated under reduced pressure. The residue

was purified using automated flash chromatography, so it dry loaded on 25 g SNAP Ultar preloaded column. A mobile phase system of EtOAc/*n*-Hexane was run in a linear gradient, 20-50%, affording the alcohol **C13** in 92% yield as an orange amorphous solid. This reaction was scaled up using 6.0 g of **C12** and purified with normal column flash chromatography to afford the product in 98% yield (5.00 g). A mobile phase system of EtoAc/*n*-Hexane was run in a gradient elution 30-60%. mp 85-125 °C; ^{1}H NMR (400 MHz, DMSO-D$_6$): ppm=7.92 (d, *J*=7.4 Hz, 2H, Ar-Fmoc), 7.74(d *J*=7.4 hz, 2H, Ar-Fmoc), 7.62 (s, 2H, ArH), 7.44(m, 2H, Ar-Fmoc), 7.36 (m, 2H, Ar-Fmoc), 4.97(t, *J*=5.5, 1H, OH), 4.58 (m, 1H, CHNH), 4.37-4.23(m, 3H, CH$_2$ArH-Fmoc), 3.91(br. s, 2H, NCH$_2$), 3.63-3.52 (m, 4H, NCH$_2$, CH$_2$OH), 2.11-1.95(m, 4H, NCH$_2$CH$_2$CH$_2$); ^{13}C NMR (400 MHz, CDCl$_3$): ppm=156.28, 147.61, 143.84, 141.39, 138.52, 130.52, 127.82, 127.22, 125.11, 120.05, 118.22, 67.03, 65.77, 55.74, 51.34, 47.27, 46.73, 24.07, 23.77; IR: 3400, 3309, 2947, 2873, 1696, 1535, 1448, 1411, 1333, 1313, 1257, 1222, 1052 cm^{-1}; HRMS calculated for C$_{27}$H$_{26}$Br$_2$N$_4$O$_3$ 615.0426 [M+H]$^+$ observed 615.0417; the polarimetric rotation value was observed at 22 °C: [α]= - 32.4 (0.056 g/mL, CHCl$_3$).
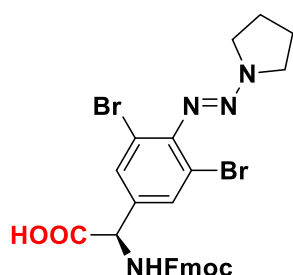
C14: The small scale was performed on 50 mg (0.1 mmol) of **C13,** which was dissolved in 1 mL acetone at 0 °C. 5% aqueous solution of NaHCO$_3$ (1 mL) was added to the solution of **C13** and the resulting mixture was stirred vigorously at that temperature. KBr (0.244 mg) and TEMPO (15.85 mg) were added sequentially to the stirring mixture before addition of NaOCl (0.4 mL) dropwise. The resulting mixture was stirred at 0 °C for 1 h until the reaction was showen to be complete by tlc. H$_2$O (5 mL) and EtOAc (5 mL) were added sequentionally the resulting solution. The organic layer was separated and the aqueous layer was extracted with EtOAc (3 mL × 3). The combined organic extracts were washed with H$_2$O (7 mL), brine (7 mL), dried with sodium sulfate and concentrated under reduced pressure. The residue was purified with automated flash chromatography using preloaded 10 g SNAP Ultra column and a mobile phase system of MeOH/DCM was run in a linear gradient, 5-20%. The acid **C14** was obtained in a 47% yield as a yellow/brown amorphous solid.

The reaction was scaled up to 4.5 g of **C13** and purified with automated flash chromatography device as the crude was dry loaded on 50 g SNAP Ultra pre-loaded column and a mobile phase of MeOH/DCM was run in a linear gradient, 5-10% to give the acid product **C14** in 61% yield (2.82 g). mp 105-135 °C[1]H; NMR (400 MHz, DMSO): ppm=7.93(d, J=7.4 Hz, 2H, Ar-Fmoc), 7.76(d J=7.4 Hz, 2H, Ar-Fmoc), 7.70 (s, 2H, ArH),7.48-7.41(m, 2H, Ar-Fmoc), 7.40-7.32 (m, 2H, Ar-Fmoc), 5.05 (br. s, 1H, CHNH), 4.34-4.23 (m, CH_2ArH-Fmoc), 3.91(br. s, 2H, NCH_2), 3.61(m, 2H, NCH_2), 2.12-1.96(m, 4H, $NCH_2CH_2CH_2$); ^{13}C NMR (400 MHz, $CDCl_3$): ppm=155.55, 147.86, 143.90, 141.34, 137.10, 131.32, 127.78, 127.23, 125.21, 120.01, 118.07, 67.23, 56.42, 51.26, 47.21, 45.31, 24.07, 23.77; IR: 3383, 2957, 1693, 1608, 1448, 1409, 1312, 1260, 1223, 1048 cm^{-1}; HRMS calculated for $C_{27}H_{23}Br_2N_4O_4$ 627.0073 [M-H]$^-$ observed 627.0071; the polarimetric rotation value was calculated at 22 °C: [α]= -28.4 (0.062 g/mL, MeOH).

6.2.2. Synthesis of A8.
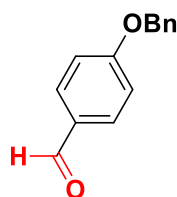
A2[99]: K_2CO_3 (8.49 g, 61.5 mmol) and KI (0.7 g, 4.1 mmol) were added sequentially to a solution of 4-hydroxybenzaldehyde (5 g, 41 mmol) in DMF (50 mL). The resulting mixture was stirred at rt, then BnBr (7.00 g, 41 mmol) was added dropwise. The resulting mixture was stirred for 2 h until the reaction was shown to be complete by tlc. The solution was extracted with EtOAc (40 mL × 5), washed with H_2O (50 mL) and brine (50 mL), dried with $MgSO_4$ and concentrated under reduced pressure. The 4-benzylbenzaldehyde was obtained as an orange powder in 70% yield, without purification. mp 69-72 °C; ^{1}H NMR(400 MHz, $CDCl_3$): ppm= 9.89(s, 1H, CHO), 7.84 (d, J=8.8, 2H, ArH), 7.45-7.32 (m, 5H, ArH), 7.08 (d, J=8.8, 2H, ArH), 5.15(s, 2H, OCH_2Ph); ^{13}C NMR (400 MHz, $CDCl_3$): ppm= 190.81, 163.76, 135.99, 32.03, 130.15, 128.76, 128.36, 127.53, 115.1, 70.28; IR: 2828, 2744, 1685, 1598, 1573, 1508, 1453, 1424, 1393, 1300, 1255, 1162, 1017. 1685, 1598, 1573, 1508, 1453, 1424, 1393, 1300, 1255, 1162, 1017 cm^{-1}; HRMS calculated for $C_{14}H_{12}O_2$ 213.0910 [M+H]$^+$ observed 213.0910.
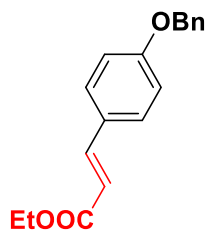
A3[99]: KOH (1.00 g, 17.7 mmol) and $(EtO)_2(O)PCH_2COOEt$ (2.6 mL,13.00 mmol) were added sequentially to a solution of **A2** (2.5 g, 11.8 mmol) in an anhydrous THF (30 mL) at rt. The resulting mixture was stirred at rt for 3 h until the reaction was shown to be complete by tlc. The solvent was removed under reduced pressure and the solvent was removed under reduced pressure, and the residue dissolved in DCM (30mL) and washed with H_2O (10 mL ×3) and brine (15 mL). The cinnamate compound **A3** was obtained in 87% yield as a white amorphous solid without purification. mp= 75-81 °C; ^{1}H NMR (400 MHz, $CDCl_3$): ppm=7.63 (d, J=15.9Hz, 1H, CH=CHCO_2Et), 7.47(d, J=8.8Hz, 2H, ArH), 7.44-7.30 (m, 5H, ArH), 6.97 (d, J=8.8 Hz, 2H, ArH),6.30 (d, J=15.9 Hz, 1H, CH=CHCO_2Et),5.10 (s, 2H, OCH_2Ph), 4.25 (q, J=7.1 Hz, 2H, CH_2CH_3), 1.33 (t, J=7.1 Hz, 3H, CH_2CH_3); ^{13}C NMR (400MHz, $CDCl_3$): ppm= 167.32, 160.53, 144.20, 136.51, 129.73, 128.69, 128.17, 127.48, 127.46, 115.93, 115.22, 70.08, 60.35, 14.40; IR: 2988, 2941, 2859, 1709, 1631, 1601, 1572, 1508, 1460, 1420, 1378, 1300, 1283, 1247, 1204, 1160, 1010, 982 cm^{-1}; HRMS calculated for $C_{18}H_{18}O_3$ 283.1329 [M+H]+ observed 283.1328.
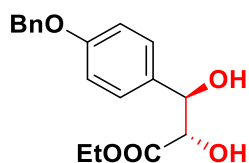
A4[99]: methanesulfonamide (0.7 g, 7.4 mmol) and AD-Mix-β (10.36 g, 1.4 gmol[-1]) were added sequentially to a stirring suspension of **A3** (2.00 g, 7.4 mmol) in *t*-BuOH/H_2O (40 mL, 1:1) at rt. The mixture was stirred for 48 h until the reaction completion was confirmed by tlc. The solution was extracted with EtOAc (25 mL × 3) and washed with H_2O (30 mL) and brine (30 mL). Purification was performed using column flash chromatography in a 10-40% gradient elution of mobile phase of EtoAc/*n*-Hexane. The diol product **A4** was obtained in 82% yield as a white amorphous powder. mp 100-106 °C; ^{1}H NMR (400 MHz, $CDCl_3$): ppm=7.44-7.31(m, 7H, ArH), 6.97(d, J= 8.8 Hz, 2H, ArH), 5.07(s, 2H, OCH_2Ph), 4.93 (dd, J=3.1, 6.9 Hz, 1H, ArCHOH*),*4.31(dd, J=3.2, 5.9 Hz, 1H, CHCOOEt), 4.26 (q, J=7.1 Hz,

2H=CH_2CH$_3$), 3.07 (d, J=5.9 Hz, 1H, OH), 2.61(d, *J*=6.9 Hz, 1H, O*H*), 1.26 (t, J=7.1 Hz, 3H, CH$_2$C*H*$_3$); ^{13}C NMR (400 MHz, CDCl$_3$): ppm= 172.86, 158.67, 137.01, 132.49, 128.67, 120.06, 127.76, 127.52, 114.84, 74.91, 74.34, 70.09, 62.15, 14.17. IR: 3452, 2907, 1720, 1700, 1611, 1585, 1512, 1454, 1385, 1300, 1238, 1175, 1095, 1054, 1018 cm^{-1}; HRMS calculated for C$_{18}$H$_{20}$O$_5$ 334.1649 [M+NH$_4$]$^+$ observed 334.1651; polarimetric rotation value was calculated at 22 °C: [α]= - 11.0 (c=0.062 g/mL, MeOH).
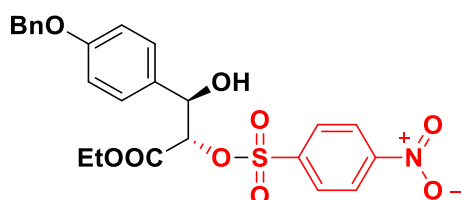
A5[99]: NsCl (2.73 g, 12.33 mmol) and Et$_3$N (o.9 mL, 6.32 mmol) were added sequentially to a solution of diol **A4** (3.9 g, 12.33 mmol) in DCM (60 mL) at 0 °C. The resulting mixture was stirred at this temperature for 4 h before quenching with aqueous saturated NH$_4$Cl (20 mL). The organic layer was separated and washed with 1 $_N$ HCl (20 mL), H$_2$O (20 mL), and brine (20 mL), and concentrated under reduced pressure. The purification was carried out using column flash chromatography with a gradient elution (10-40%) using EtOAc/*n*-Hexane as a mobile phase. The nosylated compound **A5** was obtained as a dark brown powder in 60% yield. mp 114-124 °C; ^{1}H NMR (400 MHz, CDCl$_3$): 8.24 (d, J=9.0 Hz, 2H=ArH), 7.87 (d, J=9.0 Hz, 2H, ArH), 7.45-7.31 (m, 5H, ArH), 7.16 (d, J=8.6 Hz, 2H, ArH), 6.83 (d, *J*=8.7 Hz, 2H, ArH), 5.15 (t, *J*=4.3 1H, CHCOOEt), 5.01 (s, 2H, CH$_2$Ph), 4.98 (d, *J*=4.2 Hz, 1H, CHOH), 4.16 (q, *J*=7.2 Hz, 2H, OCH$_2$CH$_3$), 2.42 (d, *J*=5.1 Hz, 1H, OH), 1.18 (t, *J*=7.1 Hz, 3H, OCH$_2$CH$_3$); ^{13}C NMR (400 MHz, CDCl$_3$): ppm=166.57,158.96, 150.52, 141.45, 136.50, 129.74, 129.15, 128.64, 128.15, 127.59, 127.50, 124.10, 114.74, 82.60, 73.06, 70.00, 62.51, 13.89; IR: 3517, 3106, 2978, 2876, 1763, 1714, 1607, 1584, 1530, 1510, 1457, 1389, 1348, 1308, 1244, 1204, 1178, 1091, 1024 cm^{-1}; HRMS calculated for C$_{24}$H$_{23}$NO$_9$S [M+NH$_4$]$^+$ observed 520.1439; polarimetric rotation value was calculated at 22 °C: [α]= - 46.2 (c=0.058 g/mL, MeOH).
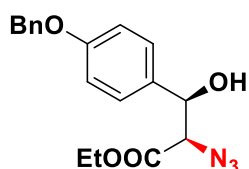
A6[(99)]: NaN$_3$ (585 mg, 9 mmol) was added to a solution of **A5** (3 g, 6 mmol) in DMF (30 mL) at rt. The resulting mixture was heated to 55 °C, and left overnight for stirring until the completion was confirmed by tlc. The resulting solution was diluted with H$_2$O (60 mL), extracted with EtOAc (50 mL × 4), washed with H$_2$O (60 mL) and brine (60 mL), dried with MgSO$_4$ and concentrated under reduced pressure. The purification was carried out with the automated flash chromatography system using a pre-loaded 10 g SNAP Ultra column. A mobile phase system of EtOAc/*n*-Hexane was run in a linear gradient 10-40%. The azide product **A6** was obtained in an 81% yield as a yellow oily solid. mp 83-93 °C; ^{1}H NMR (400 MHz, CDCl$_3$): ppm=7.45-7.30 (m, 7H, ArH), 6.98 (d, *J*=8.8 Hz, 2H, ArH), 5.07 (s, 2H, CH$_2$Ph), 4.97 (dd, *J*=4.5 Hz, 7.1 Hz, 1H, CHOH), 4.25 (q, *J*=7.1 Hz, 2H, OCH$_2$CH$_3$), 4.08 (d, *J*=7.1 Hz, 1H, CHCOOEt), 2.80 (d, *J*=4.5, 1H, OH), 1.27(t, *J*=7.1 Hz, 3H, OCH$_2$CH$_3$); ^{13}C NMR (400 MHz, CDCl$_3$): ppm=169.08, 159.17, 136.88, 131.47, 128.70, 128.12, 128.08, 127.56, 115.04, 73.79, 70.12, 66.95, 62.24, 14.18; IR: 3436, 2981, 2911, 2126, 2114, 1725, 1608, 1513, 1463, 1454, 1368, 1245, 1208. HRMS calculated for C$_{18}$H$_{19}$N$_3$O$_4$ [M +NH$_4$][+] 359.1714 found 359.1715; polarimetric rotation value was calculated at 22 °C: [α]= -1.3 (c=0.062 g/mL, CHCl$_3$).
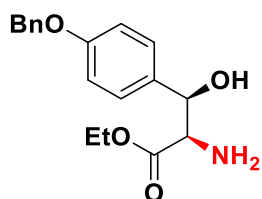
A7[(99)]: A hydrous tin chloride (SnCl$_2$) (2 g, 9 mmol) was added to a solution of **A6** (1.5 g, 4.5 mmol) in MeOH (30 mL). The resulting mixture was stirred at rt for 2 h until the reaction was confirmed to be complet by tlc. The solvent was removed under reduced pressure and the residue was dissolved in EtOAc (30 mL) and washed with 3 N NaOH (15 mL ×3), H$_2$O (15 mL) and brine (15 mL). The solvent was removed under reduced pressure to give the amine **A7** as a yellow oil in a 78% yield. ^{1}H NMR (500 MHz, CDCl$_3$): ppm=7.45 -7.30 (m, 5H, ArH), 7.22 (d, *J*=8.8 Hz, 2H, ArH), 6.94 (d, *J*=8.8 Hz, 2H, ArH), 5.05 (s, 2H, CH$_2$Ph), 4.90 (d, *J*=5.8 Hz, 1H, CHOH), 4.18-4.10 (m, 2H, OCH$_2$CH$_3$), 3.77 (d, *J*=5.9 Hz, 1H, CHCOOEt), 3.48(s, 1H, OH), 1.24 (t, *J*=7.1Hz, 3H,

OCH$_2$CH_3); ^{13}C NMR (400 MHz, CDCl$_3$): ppm=172.27, 158.56, 136.90, 131.93, 128.58, 127.98, 127.58, 127.47,114.64, 73.58, 69.98, 61.32, 59.93, 14.04; IR: 3034, 2977, 2922, 2109, 1716, 1645, 1604, 1510, 1454, 1380, 1300, 1238, 1218, 1171, 1111, 1037, 1023; HRMS calculated for C$_{18}$H$_{21}$NO$_4$ 316.1543 [M + H]$^+$ observed 316.1544.
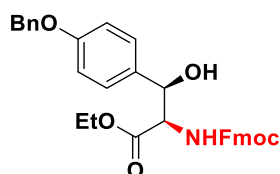
A8: An aqueous solution of NaHCO$_3$ (600 mg) was added to a solution of **A7** (750 mg, 2.38 mmol) in 10 mL THF (10 mL) at 0 °C. A cooled solution of Fmoc-Cl (677.5 mg) to 0 °C was added dropwise to the resuling solution. The resulting mixture was stirred at this temperature for 1 h until the reaction was shown to be complete by tlc. The solvent was removed under reduced pressure and the residue was purified using column chromatography with a linear gradient (10-30%, EtOAc/*n*-Hexane) to give an 80% yield of the Fmoc-protected product **A8** as a yellow powder. mp 135-143 °C; ^{1}H NMR (500 MHz, CDCl$_3$): ppm=7.77 (d, *J*=7.5 Hz 2H, ArH-Fmoc), 7.57 (t, *J*=7.5 Hz, 2H, ArH-Fmoc), 7.44-7.29 (m, 9H, ArH), 7.18 (d, *J*=8.4 Hz, 2H, ArH), 6.93 (d, *J*=8.58 Hz, 2H, ArH), 5.52 (d, *J*=8 Hz, 1H,C*H*OH), 5.17 (d, *J*=4 Hz, 1H, NH), 5.04(s, 2H, PhCH$_2$), 4.74 (dd, *J*=4, 8 Hz, 1H, CHN), 4.51 (dd, *J*=6.9 Hz, 10.5 Hz, 1H, CHH-Fmoc), 4.37 (dd, *J*=6.9, 10.5 Hz, 1H, CHH-Fmoc), 4.24-4.10 (m, 3H, CH-Fmoc+C*H*$_2$CH$_3$), 2.95 (br. s, 1H, OH), 1.21 (t, *J*=7.1 Hz, 3H, CH$_2$C*H*$_3$); ^{13}C NMR (400 MHz, CDCl$_3$): ppm=169.81, 158.77, 156.79, 143.75, 141.42, 136.94, 131.34, 128.68, 127.86, 127.55, 127.44, 127.19, 125.24, 125.12, 120.12, 114.79, 74.59, 70.08, 67.36, 61.92, 60.00, 47.22, 14.12; IR: 3402, 3038, 2972, 1727, 1609, 1511, 1447, 1370, 1347, 1228, 1196, 1010 cm^{-1}, HRMS calculated for C$_{33}$H$_{31}$NO$_6$ 555.2490 [M +NH$_4$]$^+$ observed 555.2482; polarimetric rotation value was calculated at 22 °C: [α]= - 29.8 (c=0.063 g/mL, CHCl$_3$).

6.2.3. Synthesis of A9.
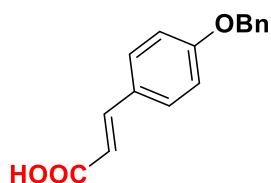
A9: LiOH.H$_2$O (9.00 mg, 21.3 mmol) was added to a solution of **A3** (2.00 g, 7.1 mmol) in a solvent system of THF, MeOH, and H$_2$O (70 mL, 3:1:1) at rt. The resulting mixture was stirred for overnight until the reaction was shown to be complete by tlc. The resulting solution was quenched with 1 M HCl (20 mL) and extracted was with EtOAc (40 mL × 3), washed with H$_2$O (20 mL), and brine (20 mL), dried with Na$_2$SO$_4$ and concentrated under reduced pressure. The acid product **A9** was obtained as a white amorphous solid in an 85% without purification. mp 193-200 °C; ^{1}H NMR (400 MHz, CDCl$_3$): ppm=7.73 (d, *J*=16, 1H, CHCHCOOH), 7.5 (d, *J*=8.8 Hz, 2H, ArH), 7.45-7.31(m, 5H, ArH), 6.99(d, J=8.8, 2H, ArH), 6.32(d, *J*=16, 1H, C*H*COOH), 5.11 (s, 1H, PhCH$_2$); ^{13}C NMR (400 MHz, CDCl$_3$): ppm=168.64,160.36, 143.80, 137.187, 130.28, 128.92, 128.38, 128.18, 127.59, 117.51, 115.64, 69.78; IR: 3328, 2576, 1660, 1622, 1599, 1572, 1510, 1452, 1429, 1385, 1308, 1284, 1245, 1171, 1078, 1017, 980 cm^{-1}; HRMS calculated for C$_{16}$H$_{14}$O$_3$ 255.1016 [M+H]$^+$ observed 255.1017.

6.2.4. Synthesis of A10.
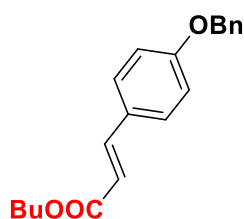
A10: A mixture of 20 mL SOCl$_2$ and **A9** (2.00 g, 7.87 mmol) were shacked thoroughly**,** heated at reflux and stirred for 1 h until the reaction completion was confirmed by tlc. The mixture was cooled down to rt, SOCl$_2$ was removed under reduced pressure and the residue was washed with DCM (15 mL × 2) and concentrated under reduced pressure (to co-evaporate SOCl$_2$ with DCM). Excess *t*-BuOH (25 mL) was added to the residue and the resulting mixture was stirred for 30 min at rt before addition of aqueous saturated NaHCO$_3$ (20 mL) (to remove any remaining residue of the **A9**). The butyl ester product **A10** was obtained as a white amorphous solid in 78% yield

after purification with normal column chromatography using EtoAc/*n*-Hexane system as a mobile phase in a gradient elution 1-5%. mp 90-95 °C; ^{1}H NMR (400 MHz, CDCl$_3$): ppm=7.53 (d, *J*=16, 1H, CHCHOOtBu), 7.47-7.33 (m, 7H, ArH), 6.96 (d, *J*=8.8, 2H, ArH), 6.24(d, *J*=16, 1H, C*H*COOtBu), 5.09 (s, 2H, PhCH$_2$), 1.53(s, 9H, COOtBu); ^{13}C NMR (400 MHz, CDCl$_3$): ppm=166.68, 160.33, 143.18, 136.56, 129.60, 128.68, 128.15, 127.66, 127.50, 117.89, 115.17, 80.25, 70.07, 28.28; IR: 2971, 1708, 1692, 1631, 1600, 1509, 1453, 1422, 1366, 1326, 1252, 1141 cm^{-1}; HRMS calculated for C$_{20}$H$_{22}$O$_3$ 311.1642 [M+H]$^+$ observed 311.1644.

6.2.5. Synthesis of B6.
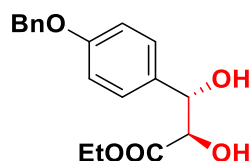
B1: Methanesulfonamide (1.35, 14.2 mmol) and AD-Mix-α (19.9 g, 1.4 g mmol^{-1}) were added sequentially to a stirring suspension of **A3** (4.00 g, 14.2 mmol) in *t*-BuOH/H$_2$O (150 mL, 1:1) at rt. The resulting mixture was stirred for 48 h, before addition a 21.3 g of sodium sulphite (1.5 g mmol^{-1}) and stirred for further 1 h. The mixture was extracted with EtOAc (100 mL × 3) and washed with H$_2$O (100 mL) and brine (100 mL) and the solvent was removed under reduced pressure to give the diol product **B1** in an 89% yield as a yellow amorphous solid without purification. mp 81-93°C; ^{1}H NMR (400 MHz, CDCl$_3$): ppm=7.45-7.31(m, 7H= ArH), 6.97(d, *J*= 8.8 Hz, 2H=ArH), 5.07(s, 2H, OC*H*$_2$Ph), 4.93 (dd, *J*=3.1, 6.9 Hz, 1H, ArC*H*OH*), 4.31(dd, *J*=3.2, 5.9 Hz, 1H, C*H*COOEt), 4.26(q, *J*=7.1 Hz, 2H, C*H*$_2$CH$_3$), 3.07 (d, *J*=5.9 Hz, 1H, OH), 2.61(d, *J*=6.9 Hz, 1H, O*H*), 1.26(t, *J*=7.1 Hz, 3H, CH$_2$C*H*$_3$); ^{13}C NMR (400MHz, CDCl$_3$): ppm= 172.79, 158.63, 136.91, 132.37, 128.60, 127.99, 127.66, 127.44, 114.80, 74.73, 74.23, 70.0281, 62.1532, 14.1008; IR: 3327, 3252, 2923, 1713, 1610, 1581, 1512, 1467, 1380, 1300, 1246, 1162, 1097, 1012, 986; HRMS calculated for C$_{18}$H$_{20}$O$_5$NH$_4$ 334.1649 [M+NH$_4$]$^+$ observed 334.1652; polarimetric rotation value was calculated at 22 °C: [α]= +16.16 (c= 0.049, EtOAc).
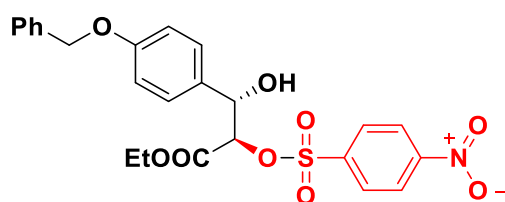
B2: NoSCl (3.1g, 12.6 mmol) and Et₃N (3.5 ml, 23.2 mmol) were added sequentially to a solution of diol **B1** (4 g, 12.6 mmol) in DCM (50 mL) at 0 °C, The resulting mixture was stirred at this temperature for 5 h before quenching with aqueous saturated NH₄Cl (20 ml). The organic layer was separated and washed with 1 N HCl (15 mL), H₂O (15 mL), brine (15 mL) and concentrated under reduced pressure. The purification was carried out using the automated flash chromatography. The crude was dry loaded on a 340 g SNAP Ultra preloaded column and a mobile phase system of EtOAc/*n*-Hexane was run in a linear gradient 20-50%. The nosylated product **B2** was furnished in a 44% yield as a black/brown amorphous solid. mp-109-115 °C; ¹H NMR (400 MHz, CDCl₃): ppm= 8.24 (d, *J*=9.0 Hz, 2H, ArH), 7.87 (d, *J*=9.0 Hz, 2H, ArH), 7.45-7.31 (m, 5H, ArH), 7.16 (d, *J*=8.6 Hz, 2H, ArH), 6.83 (d, J=8.7 Hz, 2H, ArH), 5.15 (t, *J*=4.3 1H, C*H*COOEt), 5.01 (s, 2H, C*H₂*Ph), 4.98 (d, *J*=4.2 Hz, 1H, C*H*OH), 4.16 (q, *J*=7.2 Hz, 2H, OC*H₂*CH₃), 2.39 (d, *J*=5.1 Hz, 1H, OH), 1.18 (t, *J*=7.1 Hz, 3H, OCH₂C*H₃*); ¹³C NMR (400 MHz, CDCl₃): ppm=166.42, 159.08, 150.57, 141.55, 136.47, 129.53, 129.17, 128.66, 128.16, 127.56, 127.48, 124.09,114.83, 82.39, 73.19, 70.03, 62.51, 13.90; IR: 3518, 3106, 1763, 1607, 1530, 1511, 1454, 1348, 1243, 1177, 1091, 1025; HRMS calculated for C₂₄H₂₃NO₉S 519.1432 [M+NH₄]⁺ observed 519.1420; polarimetric rotation value was calculated at 22 °C: [α]= +65.2 (c= 0.0065, EtoAc).
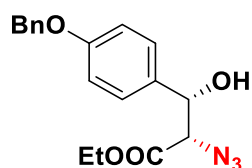
B3: NaN₃ (780 mg, 12 mmol) was added to a solution of **B2** (4 g, 8 mmol) in DMF (50 mL) at rt. The resulting mixture was heated to 55 °C, and stirred for 15 h until the reaction was confirmed to be complete by tlc. The mixture was diluted with H₂O (100 mL), extracted with diethylether (100 mL × 4), washed with H₂O (100 mL), brine (100 mL), dried with MgSO₄ and concentrated under reduced pressure. The purification was performed using automated flash chromatography as the crude was dry loaded on a 50 g SNAP Ultra preloaded column and a mobile phase of EtOAc/*n*-hexane was

run in a linear gradient 5-20%. The azide product was obtained in a 72% yield as yellow oily solid. mp 85-94 °C; ^{1}H NMR (400 MHz, CDCl$_3$): ppm= 7.45-7.30 (m, 7H, ArH), 6.98 (d, J=8.8 Hz, 2H, ArH), 5.07 (s, 2H, CH_2Ph), 4.97 (dd, J=4.5 Hz, 7.1 Hz, 1H, CHOH), 4.25 (q, J=7.1 Hz, 2H, OCH_2CH$_3$), 4.08 (d, J=7.1 Hz, 1H, CHCOOEt), 2.74 (d, J=4.5, 1H, OH), 1.27 (t, J=7.1 Hz, 3H,OCH$_2$CH_3); ^{13}C NMR (400 MHz, CDCl$_3$): ppm=168.99, 159.10, 136.80, 131.38, 128.62, 128.04, 127.99, 127.48, 114.96, 73.71, 70.04, 66.85, 62.16, 14.10; IR: 3434, 2981, 2902, 2113, 1725, 1610, 1588, 1512, 1454, 1384, 1305, 1245, 1206, 1168, 1072, 1009 cm^{-1}; HRMS calculated for C$_{18}$H$_{19}$N$_3$O$_4$ 359.1719 [M+NH$_4$]$^+$ observed 359.1710; polarimetric rotation value was calculated at 22 °C: [α]= -2.2 (c= 0.054, CHCl$_3$).
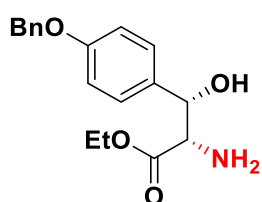
B4: SnCl$_2$.H$_2$O (675 mg, 2.29 mmol) was added to a solution of **B3** (500 mg, 1.46 mmol) in MeOH (10 mL). The mixture was stirred at rt for 2 h until the reaction was shown to be complete by tlc. The solvent was removed under reduced pressure and the residue dissolved in EtOAc (10 mL) and the resulting solution was washed with 3 N NaOH (5 mL ×3), H$_2$O (5 mL) and brine (5 mL). The solvent was removed under reduced pressure to give the amine product **B4** as a yellow oil in an 87% yield without purification. ^{1}H NMR (400 MHz, CDCl$_3$): ppm= 7.45 -7.30 (m, 5H, ArH), 7.22 (d, J=8.8 Hz, 2H, ArH), 6.94 (d, J=8.8 Hz, 2H, ArH), 5.05 (s, 2H, CH_2Ph), 4.90 (d, J=5.8 Hz, 1H, CHOH), 4.18-4.10 (m, 2H, OCH_2CH$_3$), 3.77 (d, J=5.9 Hz, 1H, CHCOOEt), 3.48 (s, 1H, OH), 1.24 (t, J=7.1Hz, 3H, OCH$_2$CH_3); IR: 2983, 2932, 2871, 1737, 1646, 1604, 1510, 1454, 1422, 1378, 1300, 1251, 1225, 1190, 1160, 1066, 1007 cm^{-1}; HRMS calculated for C$_{18}$H$_{21}$NO$_4$ 338.1363 [M+Na]$^+$ observed 338.1363.
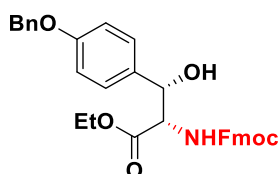
B5: an aqueous solution of NaHCO$_3$ (400 mg, 4.74 mmol) was added to a solution of **B4** (500 mg, 1.58 mmol) in THF (10 mL) at 0 °C. Then, a cooled solution of Fmoc-Cl (450 mg) at 0 °C was added dropwise to the resulting solution. The resulting mixture

was stirred at this temperature for 1 h until the reaction completion was confirmed by tlc. The solvent was removed under reduced pressure and the residue was purified by automated flash chromatography using a 25 g SNAP Ultra preloaded column and a mobile phase of EtOAc/n-Hexane in a linear gradient, 10-50%. The Fmoc-protected **B5** was obtained in an 80% yield as a white amorphous solid. mp 130-14 °C; ^{1}H NMR (400 MHz, CDCl$_3$): ppm=7.77 (d, J=7.5 Hz 2H, ArH-Fmoc), 7.57 (t, J=7.5 Hz, 2H, ArH-Fmoc), 7.44-7.29 (m, 9H, ArH), 7.17 (d, J=8.4 Hz, 2H, ArH), 6.92 (d, J=8.58 Hz, 2H, ArH), 5.48 (d, J=8 Hz, 1H, CHOH), 5.17 (s, 1H, NH), 5.04 (s, 2H, PhC$H2$), 4.74 (dd, J=4, 8 Hz, 1H, CHN), 4.51 (dd, J=6.9 Hz, 10.5 Hz, 1H, CHH-Fmoc), 4.37 (dd, J=6.9, 10.5 Hz, Hz, 1H, CHH-Fmoc), 4.24-4.10 (m, 3H, CH-Fmoc+CH_2CH$_3$), 3.37(d, J=5.4 Hz, 1H, OH), 1.21 (t, J=7.1 Hz, 3H, CH$_2$CH_3); ^{13}C NMR (400 MHz, CDCl$_3$): ppm=169.66, 158.71, 156.72, 143.70, 141.34, 136.86, 131.21, 128.60, 128.01, 127.78, 127.47, 127.34, 127.11, 125.15, 120.04, 114.72, 74.58, 70.01, 67.27, 61.87, 59.90, 47.15, 14.05; IR: 3396, 2902, 1723, 1706, 1610, 1511, 1449, 1380, 1226, 1196, 1174, 1016 cm^{-1}; HRMS calculated for C$_{33}$H$_{31}$NO$_6$ 560.2044 [M+Na]$^+$ observed 560.2033; polarimetric rotation value was calculated at 22 °C: [α]= +30.0 (c= 0.058, CHCl$_3$).
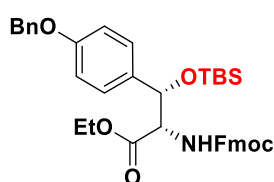
B6: 2,6-Lutidine (162.5 µl, 1.4 mmol) and TBSoTf (225 µl, 1.023 mmol) were added sequentially to a solution of **B5** (500 g, 0.93 mmol) in DCM (7 mL) at 0 °C. The resulting mixture was stirred at this temperature for 30 min before quenching with aqueous saturated solution of NaHCO$_3$ (4 mL). The organic layer was separated and extracted with DCM (3 mL × 3). The combined organic extracts were washed with NaHCO$_3$ (5 mL), H$_2$O (5 mL), and brine (5 mL), dried with Na$_2$SO$_4$ and concentrated under reduced pressure. The TBS-protected **B6** was obtained in an 89% yield as a transparent oil after purification with the automated flash chromatography as the crude was dry loaded on a 50 g SNAP Ultar pre-loaded column and a mobile phase of EtoAc/n-Hexane was run in a linear gradient 15-30%. ^{1}H NMR (500 MHz, CDCl$_3$): ppm=7.78 (d, J=7.5 Hz 2H, ArH-Fmoc), 7.59 (t, J=8.3 Hz, 2H, ArH-Fmoc), 7.44-7.28 (m, 11H, ArH, benzyl-H, Fmoc-4H), 6.95 (d, J=8.5 Hz, 2H, ArH), 5.48 (d, J=8.8 Hz, 1H, ArCH), 5.07 (d, J=4.2 Hz, 1H,NH), 5.04 (s, 2H, PhCH$_2$), 4.60 (dd, J=4.2, 8.6 Hz,1H, CHN), 4.42-4.30 (m, 2H, CH$_2$-Fmoc), 4.22 (t, J=7.3 1H, CH-Fmoc), 4.12 (q, J=7.4, 2H, CH_2CH$_3$), 1.18(t, J=7.3 Hz, 3H, CH$_2$CH_3), 0.92 (s, 9H, TBS), 0.07(s, 3H,

TBS), -0.01(s, 3H, TBS); ^{13}C NMR (400 MHz, CDCl$_3$): ppm=169.91,158.57, 155.66,143.97, 141.40,137.04, 132.70,128.67, 128.08,127.80, 127.65, 127.61, 127.15, 125.26, 120.09, 114.50, 75.30, 70.11, 67.23, 61.38, 61.23,47.21, 25.81,18.24,14.14, -4.67, -5.16; IR: 3342, 2929, 2855, 1718, 1610, 1508, 1450, 1371, 1344, 1242, 1090, 1029 cm^{-1}; HRMS calculated for C$_{39}$H$_{45}$NO$_6$SiNH$_4$ 669.3354 [M + NH$_4$]+ observed 669.3348.

6.2.6. Synthesis of D4.
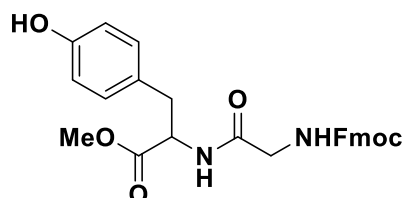
D1: HOBt (157 mg, 1.02 mmol), Fmoc-Gly-OH (333.58 mg, 1.12 mmol) and EDC.HCl (215 mg, 1.12 mmol) were added sequentially to a solution of MeOH-Tyr-NH$_2$ (200 mg, 1.02 mmol) in 4 mL acetone. The equivalences in this reaction were calculated based on the equivalence of the amino acid with free terminal amine, tyrosine. The resulting mixture was stirred at rt for 2 h until the reaction was confirmed to be complete by tlc. The solvent was removed under reduced pressure and the residue was purified with automated flash chromatography using 25 g SNAP Ultra preloaded column and EtOAc/n-Hexane system as a mobile phase system in a linear gradient, 30-70%, giving the the dipeptide **D1** as a white amorphous solid in 60% yield. ^{1}H NMR (400 MHz, CDCl$_3$): ppm= 7.78 (d, J=7.5 Hz, 2H, Fmoc), 7.65 (d, J=7.1 Hz, 2H, Fmoc), 7.38 (t, J=7.5 Hz, 2H, Fmoc), 7.30 (t, J=7.5 Hz, 2H, Fmoc), 6.99 (d, J=8.4 Hz, 2H, ArH), 6.71 (d, J=8.4 Hz, 2H, ArH), 4.65 (m, 1H, CHNH$_2$), 4.34 (d, J=6.7 Hz, 2H, Fmoc), 4.20 (t, J=6.7 Hz, 1H, Fmoc), 3.78 (d, J=5.4 Hz, 2H, ArCH$_2$),3.67 (s, 3H, COOCH_3), 3.37 (s, 1H, NHFmoc), 3.05-2.87 (m, 2H, CH_2NHFmoc); ^{13}C NMR (400 MHz, CDCl$_3$): ppm= 171.60, 168.712, 156.17, 144.11, 141.13, 130.22, 127.58, 127.17, 127.01, 125.23, 119.84, 115.05, 66.43, 54.49, 53.59, 51.31, 47.02, 43.64, 41.86, 36.57; IR: 3318, 2926, 2481, 1693, 1661, 1613, 1514, 1445, 1358, 1247, 1201; HRMS calculated for C$_{27}$H$_{26}$N2O$_6$ 475.1864 [M+H]$^+$ observed 475.1861.
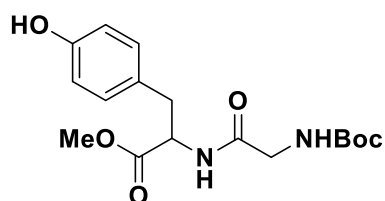
D2: HOBt (234.24 mg, 1.53 mmol), Fmoc-Gly-OH (333.58 mg, 1.68 mmol) and EDC.HCl (300 µl, 1.68 mmol) were added sequentially to a solution of MeOH-Tyr-NH$_2$ (300 mg, 1.53 mmol) in 10 mL acetone. The equivalences in this reaction were calculated based on the equivalence of the amino acid with free terminal amine, tyrosine. The resulting mixture was stirred at rt and left overnight until the reaction was confirmed to be complete by tlc. The solvent was removed under reduced pressure and the crude residue was purified by automated flash chromatography. The crude was dry loaded on 100 g snap Ultra preloaded column using a mobile phase of EtoAc/*n*-Hexane in a linear gradient, 30-60%, to give the Boc-protected dipeptide **D2** as a colourless oil in 61% yield. ^{1}H NMR (400 MHz, MeOH-D$_4$): ppm=7.00 (d, *J*=8.5 Hz, 2H, ArH), 6.72 (d, *J*=8.5 Hz, 2H, ArH), 4.65 (t, *J*=6.5 Hz, 1H, C*H*NH$_2$), 3.72-3.69 (m, 5H, Ar-CH$_2$, -CH$_3$), 3.07-2.91 (m, 2H, C*H*$_2$NH), 1.45 (s, 9H, Boc); ^{13}C NMR (400 MHz, MeOH-D$_4$): ppm=173.34, 172.20, 158.32, 157.61, 131.25, 128.24, 116.37, 80.74, 55.25, 52.66, 44.39, 37.68, 28.68; IR: 3319, 2977, 1738, 1662, 1613, 1595, 1514, 1444, 1365, 1391, 1246, 1216, 1161; MRMS calculated for C$_{17}$H$_{24}$N$_2$O$_6$ 353.1707 [M+H]$^+$ observed 353.1710.
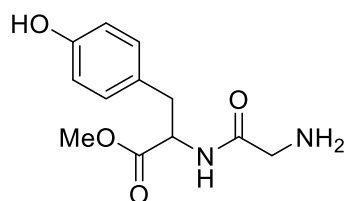
D3: A 50% TFA in DCM (5 mL) was added to a 200 mg of **D2** and the resulting mixture was stirred for 2 h until the reaction was shown to be complete by tlc. The solvent was removed under reduced pressure and the residue was purified by automated flash chromatography as the crude was wet loaded on a 50-g preloaded column, and a mobile phase of MeOH/DCM was used in a linear gradient 10-30% to give the deprotected-dipeptide **D3** as a white/yellow oil in a 90% yield. ^{1}H NMR (400 MHz, MeOH-D$_4$): ppm=6.97 (d, *J*=8.5 Hz, 2H, ArH), 6.68 (d, *J*=8.5 Hz, 2H, ArH), 4.64 (m, 1H, C*H*NH$_2$), 3.72-3.60 (m, 5H, Ar-CH$_2$, CH$_3$), 3.31 (s, 2H,, NH$_2$), 3.01(dd, *J*=5.6, 14

Hz, 1H, CHHNH$_2$), 2.85 (dd, J=8.4, 14 Hz, 1H, CHHNH$_2$); ^{13}C NMR (400 MHz, MeOH-D$_4$): ppm= 173.25, 167.20, 157.54, 131.20, 128.40, 116.32, 55.67, 52.77, 41.33, 37.70; IR: 3027, 1731, 1665, 1614, 1554, 1515, 437, 1355, 1181, 1123 cm^{-1}; HRMS calculated for C$_{12}$H$_{16}$N$_2$O$_4$ 253.1183 [M + H]+ observed 253.1185.
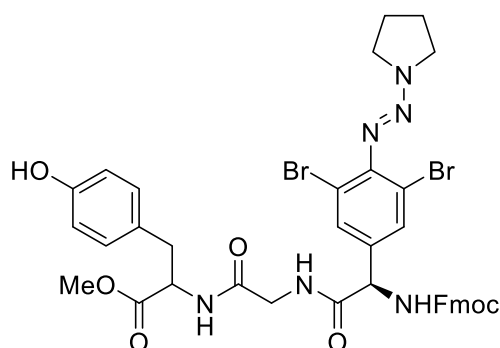
D4: HOBt (78.1 mg, 0.51 mmol), **C14** (320 mg, 1.68 mmol) and EDC.HCl (100 µl) were added sequentially to a solution of **D3** (130 mg, 0.51 mmol) in acetone (5 mL). The equivalences in this reaction were calculated based on the equivalence of the amino acid with free terminal amine, tyrosine. The resulting mixture was stirred at rt and left overnight until the reaction was shown to be complete by tlc. The solvent was removed under reduced pressure and the residue was purified by automated flash chromatography as the crude was dry loaded on a 50-g preloaded column and a mobile phase system of EtoAc/*n*-Hexane was used in a linear gradient, 15-60%, giving the tripeptide **D3** as a yellow amorphous solid. ^{1}H NMR(400 MHz, CDCl$_3$): δ=7.69 (d, *J*=7.5 Hz, 2H, Fmoc), 7.63 (br. s, 2H, ArH), 7.54 (br. s, 2H, Fmoc), 7.33 (t, *J*=7.5 Hz, 2H, Fmoc), 7.23 (t, *J*=7.5 Hz, 2H, Fmoc), 5.29 (s, 1H, C*H*NHFmoc), 6.84 (dd, *J*=8.3, 11.5 Hz, 2H, ArH), 6.61(t, *J*=7.5 Hz, 2H, ArH), 4.77(m, 1H, C*H*NHCO), 4.41(br. s, 2H, Fmoc), 4.19(br. s, 1H, Fmoc), 3.93 (br. s, 2H, NCH$_2$), 3.8-3.64 (m, 7H, CH$_3$, ArCH$_2$, NCH$_2$), 2.08 (br. s, 4H, NCH$_2$C*H$_2$*C*H$_2$*); ^{13}C NMR (400 MHz, CDCl$_3$): ppm=171.95, 168.52, 155.93, 155.44, 148.12, 143.58, 141.22, 136.34, 131.19, 130.32, 127.72, 127.11, 125.13, 119.92, 118.38, 115.61, 67.46, 57.26, 53.77, 52.51, 50.72, 47.01, 46.73, 43.28, 37.10, 23.61; IR: 3280, 2951, 1638, 1514, 1445,

1413, 1356, 1311, 1223, 1104, 1042, 907 cm^{-1}; HRMS calculated for C$_{39}$H$_{38}$Br$_2$N$_6$O$_7$ 863.1225 [M+H]$^+$ observed 863.1204.

6.2.7. Synthesis of D5.
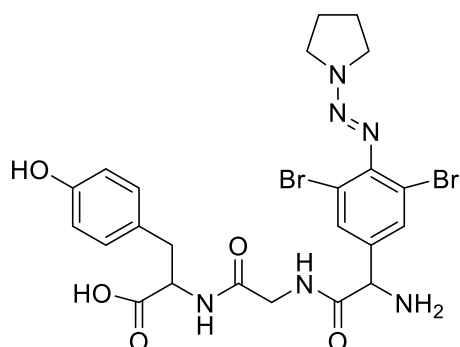
D5: a 100 mg of Fmoc-Tyr-Wang Resin was swelled in DMF (5 mL) for a 30 min of shaking. The Fmoc-protecting group was removed using a 40% piperidine (5 mL) for 10 min shaking, then 20% piperidine (5 mL × 2) for 5 min shaking. The deprotection was confirmed by a Kaiser test. A solution of Fmoc-Gly-OH (76.1 mg), HATU (48.6 mg), and DIPEA (111.2 μl) in a least dissolving amount of DMF, was added to the resin and was shacked for 1 h until the reaction was shown to be complete by with a Kaiser test (negative result). The solution was filtered and the resin was washed with DMF (5 mL × 5). Then, a solution of triazene protected residue (80 mg), HATU (48.6 mg) and DIPEA (111.2 μl) was added to the resin, and left for shaking. A Kaiser test was carried out and indicated a positive result (still blue) after 45 min and 2.5 h of the shaking. The solution was filtered, and the resin washed with DMF (5 mL × 5), then the coupling process was repeated with fresh reagents. The resin was left overnight for shaking, until a Kaiser test indicated a negative result (brown beads). The solution was filtered and the resin was washed with DMF (5 mL × 5). The Fmoc deprotection was performed using of 40% piperidine (5 mL) for 10 min shaking, 20% piperidine (5 mL × 2) for 5 min shaking and monitored with a Kaiser test. The solution was drained

and the resin was washed with DMF (5 mL × 5). Cleavage step was carried out with 5 mL TFA/TIPS/H_2O (95:2.5:2.5) by shaking for 2 h and the TFA was removed under reduced pressure, and the peptide was precipitated with a cold diethylether. Mass spectrometry was carried out for the peptide which showed the desired MW, [M+H]$^+$= 626.6.

Chapter 7. References

1.   Aminov R. History of antimicrobial drug discovery: Major classes and health impact. Biochemical Pharmacology. 2017;133:4-19.

2.   Yılmaz Ç, Özcengiz G. Antibiotics: Pharmacokinetics, toxicity, resistance and multidrug efflux pumps. Biochemical Pharmacology. 2017;133:43-62.

3.   Vardanyan R, Hruby V. Chapter 30 - Antibiotics. Synthesis of Best-Seller Drugs. Boston: Academic Press; 2016. p. 573-643.

4.   Kohanski MA, Dwyer DJ, Hayete B, Lawrence CA, Collins JJ. A Common Mechanism of Cellular Death Induced by Bactericidal Antibiotics. Cell. 2007;130(5):797-810.

5.   Kohanski MA, Dwyer DJ, Collins JJ. How antibiotics kill bacteria: from targets to networks. Nat Rev Micro. 2010;8(6):423-35.

6.   Park M, Rafii F. Exposure to β-lactams results in the alteration of penicillin-binding proteins in Clostridium perfringens. Anaerobe. 2017;45:78-85.

7.   Romantsov T, Guan Z, Wood JM. Cardiolipin and the osmotic stress responses of bacteria. Biochimica et Biophysica Acta (BBA) - Biomembranes. 2009;1788(10):2092-100.

8.   Oliphant CM, Eroschenko K. Antibiotic Resistance, Part 1: Gram-positive Pathogens. The Journal for Nurse Practitioners. 2015;11(1):70-8.

9.   Walsh C. Molecular mechanisms that confer antibacterial drug resistance. Nature. 2000;406(6797):775-81.

10.   Levy SB, Marshall B. Antibacterial resistance worldwide: causes, challenges and responses. Nature Medicine. 2004;10:S122.

11.   Aziz A-M. The role of healthcare strategies in controlling antibiotic resistance. British Journal of Nursing. 2013;22(18):1066-74.

12.   Davies J. Inactivation of Antibiotics and the Dissemination of Resistance Genes. Science. 1994;264(5157):375-82.

13.   Chigor VN, Umoh VJ, Smith SI, Igbinosa EO, Okoh AI. Multidrug Resistance and Plasmid Patterns of *Escherichia coli* O157 and Other *Escherichia coli* Isolated from Diarrhoeal Stools and Surface Waters from Some Selected Sources in Zaria, Nigeria. International Journal of Environmental Research and Public Health. 2010;7(10):3831-41.

14.   Martinez JL, Coque TM, Baquero F. What is a resistance gene? Ranking risk in resistomes. Nat Rev Micro. 2015;13(2):116-23.

15.   Bryan J, Leonard N, Fanning S, Katz L, Duggan V. Antimicrobial resistance in commensal faecal *Escherichia coli* of hospitalised horses. Irish Veterinary Journal. 2010;63(6):373.

16.   Anago E, Ayi-Fanou L, Akpovi C, Hounkpe W, Agassounon-Djikpo Tchibozo M, Bankole H, et al. Antibiotic resistance and genotype of beta-lactamase producing *Escherichia coli* in nosocomial infections in Cotonou, Benin. Annals of clinical microbiology and antimicrobials. 2015;14(1):5.

17.   Haug JB, Berild D, Walberg M, Reikvam Å. Hospital- and patient-related factors associated with differences in hospital antibiotic use: analysis of national surveillance results. Antimicrobial Resistance and Infection Control. 2014;3(1):40.

18.   Lee M-L, Cho C-Y, Hsu C-L, Chen C-J, Chang L-Y, Lee Y-S, et al. Recent trends in antibiotic prescriptions for acute respiratory tract infections in pediatric ambulatory care in Taiwan, 2000-2009: A nationwide population-based study. J Microbiol Immunol Infect. 2016;49(4):554-60.

19.   Lee H-S, Loh Y-X, Lee J-J, Liu C-S, Chu C. Antimicrobial consumption and resistance in five Gram-negative bacterial species in a hospital from 2003 to 2011. Journal of Microbiology, Immunology and Infection. 2015;48(6):647-54.

20.   Tan C-K, Tang H-J, Lai C-C, Chen Y-Y, Chang P-C, Liu W-L. Correlation between antibiotic consumption and carbapenem-resistant Acinetobacter baumannii causing health care-associated infections at a hospital from 2005 to 2010. Journal of Microbiology, Immunology and Infection. 2015;48(5):540-4.

21.   Andreassen AES, Jacobsen CM, de Blasio B, White R, Kristiansen IS, Elstrøm P. The impact of methicillin-resistant S. aureus on length of stay, readmissions and costs: a register based case-control study of patients hospitalized in Norway. Antimicrobial Resistance & Infection Control. 2017;6(1):74.

22.   B.T.Thomas HIE, A.Davies and A. Oluwadun. Prevalence of Antibiotic-Resistant Bacteria in Dried Cassava Powder (Garri) Circulating in Ogun State, Nigeria. Academia Arena. 2012;4(1):9-13.

23.   Olawale AK, Akintobi, Akinbiyi Olubiyi and Famurewa, Oladiran. Prevalence of Antibiotic Resistant Enterococci in Fast food Outlets in Osun State Nigeria. New York Science Journal. 2010;3(1):70-5.

24.   Maltezou HC, Theodoridou M, Daikos GL. Antimicrobial resistance and the current refugee crisis. Journal of Global Antimicrobial Resistance. 2017;10:75-9.

25.   Kaeseberg T, Blumensaat F, Zhang J, Krebs P. Assessing antibiotic resistance of microorganisms in sanitary sewage. Water Science And Technology: A Journal Of The International Association On Water Pollution Research. 2015;71(2):168-73.

26.   Diwan V, Tamhankar AJ, Khandal RK, Sen S, Aggarwal M, Marothi Y, et al. Antibiotics and antibiotic-resistant bacteria in waters associated with a hospital in Ujjain, India. BMC Public Health. 2010;10(1):414.

27.   Ström G, Halje M, Karlsson D, Jiwakanon J, Pringle M, Fernström L-L, et al. Antimicrobial use and antimicrobial susceptibility in *Escherichia coli* on small- and medium-scale pig farms in north-eastern Thailand. Antimicrobial Resistance & Infection Control. 2017;6(1):75.

28.   Adebowale Idris Adebiyi AFF, Nurudeen Afolabi Fasasi , Oladokun Amos Folawiyo. Antibiotic Resistance in Enteric Bacterial Isolates from Marketed Fish in Ibadan Metropolis, Southwest Nigeria. New York Science Journal. 2014;7(8):46-50.

29.   Stewart PS, William Costerton J. Antibiotic resistance of bacteria in biofilms. The Lancet. 2001;358(9276):135-8.

30.   Mah T-FC, O'Toole GA. Mechanisms of biofilm resistance to antimicrobial agents. Trends in Microbiology. 2001;9(1):34-9.

31.   Stephens C. Microbiology: Breaking Down Biofilms. Current Biology. 2002;12(4):R132-R4.

32.   Høiby N, Bjarnsholt T, Givskov M, Molin S, Ciofu O. Antibiotic resistance of bacterial biofilms. International Journal of Antimicrobial Agents. 2010;35(4):322-32.

33.   Bilal M, Rasheed T, Iqbal HMN, Hu H, Wang W, Zhang X. Macromolecular agents with antimicrobial potentialities: A drive to combat antimicrobial resistance. International Journal of Biological Macromolecules. 2017;103:554-74.

34.   Wong Weng R, Oliver Allen G, Linington Roger G. Development of Antibiotic Activity Profile Screening for the Classification and Discovery of Natural Product Antibiotics. Chemistry & Biology. 2012;19(11):1483-95.

35.   Oliphant CM. New Antimicrobial Agents. The Journal for Nurse Practitioners. 2016;12(3):e91-e100.

36.   Fernandes P, Martens E. Antibiotics in late clinical development. Biochemical Pharmacology. 2017;133:152-63.

37.   Lipinski CA, Lombardo F, Dominy BW, Feeney PJ. Experimental and computational approaches to estimate solubility and permeability in drug discovery and development settings. Advanced Drug Delivery Reviews. 1997;23(1):3-25.

38.   Petit J, Meurice N, Kaiser C, Maggiora G. Softening the Rule of Five--where to draw the line? Bioorganic & medicinal chemistry. 2012;20(18):5343-51.

39.   Bullough L, White E. New approaches to combating antibiotic resistance. Wounds UK. 2014;10(4):50-3.

40.   Frick L, Craft E. Antimicrobial Stewardship. The Journal for Nurse Practitioners. 2012;8(2):152-3.

41.   Greco A, De Marco R, Tani S, Giacomini D, Galletti P, Tolomelli A, et al. Convenient Synthesis of the Antibiotic Linezolid via an Oxazolidine-2,4-dione Intermediate Derived from the Chiral Building Block Isoserine. European Journal of Organic Chemistry. 2014;2014(34):7614-20.

42.   Oliphant CM, Eroschenko K. Antibiotic Resistance, Part 2: Gram-negative Pathogens. The Journal for Nurse Practitioners. 2015;11(1):79-86.

43.   Livermore DM. beta-Lactamases in laboratory and clinical resistance. Clinical microbiology reviews. 1995;8(4):557-84.

44.   Hawkey PM. The origins and molecular basis of antibiotic resistance. BMJ (Clinical Research Ed). 1998;317(7159):657-60.

45.   Salton MRJ. Studies of the bacterial cell wall: IV. The composition of the cell walls of some gram-positive and gram-negative bacteria. Biochimica et Biophysica Acta. 1953;10:512-23.

46.   BUCKS JD. Nonstaining (KOH) Method for Determination ofGram Reactions of Marine Bacteriat. 1982.

47.   Chitsaz M, Brown MH. The role played by drug efflux pumps in bacterial multidrug resistance. Essays In Biochemistry. 2017;61(1):127-39.

48.   Chopra I, Hawkey PM, Hinton M. Tetracyclines, molecular and clinical aspects. The Journal of antimicrobial chemotherapy. 1992;29(3):245-77.

49.   Tomasz A, Munoz R. Beta-Lactam antibiotic resistance in gram-positive bacterial pathogens of the upper respiratory tract: a brief overview of mechanisms. Microbial drug resistance (Larchmont, NY). 1995;1(2):103-9.

50.   Hawkey PM. The origins and molecular basis of antibiotic resistance1998 1998-09-05 07:00:00. 657-60 p.

51.   Garcia-Bustos J, Tomasz A. A biological price of antibiotic resistance: major changes in the peptidoglycan structure of penicillin-resistant pneumococci.

Proceedings of the National Academy of Sciences of the United States of America. 1990;87(14):5415-9.

52.   Woodford N, Palepou MF, Johnson AP, Chadwick PR, Bates J. Methicillin-resistant Staphylococcus aureus and vancomycin-resistant enterococci. The Lancet. 1997;350(9079):738.

53.   Paradis-Bleau C, Lloyd A, Sanschagrin F, Clarke T, Blewett A, Bugg TD, et al. Phage display-derived inhibitor of the essential cell wall biosynthesis enzyme MurF. BMC Biochemistry. 2008;9(1):33.

54.   Chapot-Chartier M-P, Kulakauskas S. Cell wall structure and function in lactic acid bacteria. Microbial Cell Factories. 2014;13(1):S9.

55.   Cho H, Wivagg CN, Kapoor M, Barry Z, Rohs PDA, Suh H, et al. Bacterial cell wall biogenesis is mediated by SEDS and PBP polymerase families functioning semi-autonomously. 2016;1:16172.

56.   Gampe CM, Tsukamoto H, Wang T-SA, Walker S, Kahne D. Modular synthesis of diphospholipid oligosaccharide fragments of the bacterial cell wall and their use to study the mechanism of moenomycin and other antibiotics. Tetrahedron. 2011;67(51):9771-8.

57.   Mesleh MF, Rajaratnam P, Conrad M, Chandrasekaran V, Liu CM, Pandya BA, et al. Targeting Bacterial Cell Wall Peptidoglycan Synthesis by Inhibition of Glycosyltransferase Activity. Chemical Biology & Drug Design. 2016;87(2):190-9.

58.   Narayan RS, VanNieuwenhze MS. Synthesis of Substrates and Biochemical Probes for Study of the Peptidoglycan Biosynthetic Pathway. European Journal of Organic Chemistry. 2007;2007(9):1399-414.

59.   Egan AJF, Cleverley RM, Peters K, Lewis RJ, Vollmer W. Regulation of bacterial cell wall growth. The FEBS Journal. 2017;284(6):851-67.

60.   Leclercq R, Courvalin P. Resistance to glycopeptides in enterococci. Clinical infectious diseases : an official publication of the Infectious Diseases Society of America. 1997;24(4):545-54; quiz 55-6.

61.   Arthur M, Reynolds P, Courvalin P. Glycopeptide resistance in enterococci. Trends in microbiology. 1996;4(10):401-7.

62.   Courvalin P. Vancomycin Resistance in Gram-Positive Cocci. Clinical Infectious Diseases. 2006;42(Supplement 1):S25-S34.

63.   Spencelayh MJ, Cheng Y, Bushby RJ, Bugg TDH, Li J-j, Henderson PJF, et al. Antibiotic Action and Peptidoglycan Formation on Tethered Lipid Bilayer Membranes. Angewandte Chemie. 2006;118(13):2165-70.

64.   Wright GD, Walsh CT. D-Alanyl-D-alanine ligases and the molecular mechanism of vancomycin resistance. Accounts of Chemical Research. 1992;25(10):468-73.

65.   Chiosis G, Boneca IG. Selective cleavage of D-Ala-D-Lac by small molecules: Re-sensitizing resistant bacteria to vancomycin. Science. 2001;293(5534):1484-7.

66.   Cattoir V, Leclercq R. Twenty-five years of shared life with vancomycin-resistant enterococci: is it time to divorce? Journal of Antimicrobial Chemotherapy. 2013;68(4):731-42.

67.   Ranotkar S, Kumar P, Zutshi S, Prashanth KS, Bezbaruah B, Anand J, et al. Vancomycin-resistant enterococci: Troublemaker of the 21st century. Journal of Global Antimicrobial Resistance. 2014;2(4):205-12.

68.   Williams DH. Synthetic chemistry: Sugaring vancomycin. Nature. 1999;397(6720):567-8.

69.   Boger DL, Borzilleri RM, Nukui S. Synthesis of (R)-(4-Methoxy-3,5-dihydroxyphenyl)glycine Derivatives: The Central Amino Acid of Vancomycin and Related Agents. The Journal of Organic Chemistry. 1996;61(10):3561-5.

70.   Nicolaou KC, Li H, Boddy CNC, Ramanjulu JM, Yue T-Y, Natarajan S, et al. Total Synthesis of Vancomycin—Part 1: Design and Development of Methodology. Chemistry – A European Journal. 1999;5(9):2584-601.

71.   Nicolaou KC, Cho SY, Hughes R, Winssinger N, Smethurst C, Labischinski H, et al. Solid- and Solution-Phase Synthesis of Vancomycin and Vancomycin Analogues with Activity against Vancomycin-Resistant Bacteria. Chemistry – A European Journal. 2001;7(17):3798-823.

72.   Hunt AH, Dorman DE, Debono M, Molloy RM. Structure of antibiotic A41030A. The Journal of Organic Chemistry. 1985;50(12):2031-5.

73.   Boger DL, Borzilleri RM, Nukui S, Beresis RT. Synthesis of the Vancomycin CD and DE Ring Systems. The Journal of Organic Chemistry. 1997;62(14):4721-36.

74.   Evans DA, Wood MR, Trotter BW, Richardson TI, Barrow JC, Katz JL. Total Syntheses of Vancomycin and Eremomycin Aglycons. Angewandte Chemie International Edition. 1998;37(19):2700-4.

75.   Nicolaou KC, Natarajan S, Li H, Jain NF, Hughes R, Solomon ME, et al. Total Synthesis of Vancomycin Aglycon—Part 1: Synthesis of Amino Acids 4–7 and Construction of the AB-COD Ring Skeleton. Angewandte Chemie International Edition. 1998;37(19):2708-14.

76.   Nicolaou KC, Jain NF, Natarajan S, Hughes R, Solomon ME, Li H, et al. Total Synthesis of Vancomycin Aglycon—Part 2: Synthesis of Amino Acids 1–3 and Construction of the AB-COD-DOE Ring Skeleton. Angewandte Chemie International Edition. 1998;37(19):2714-6.

77.   Evans DA, Evrad DA, Rychnovsky SD, Früh T, Whittingham WG, deVries KM. A general approach to the asymmetric synthesis of vancomycin-related arylglycines by enolate azidation. Tetrahedron Letters. 1992;33(9):1189-92.

78.   Walter J, Loach DM, Alqumber M, Rockel C, Hermann C, Pfitzenmaier M, et al. D-alanyl ester depletion of teichoic acids in Lactobacillus reuteri 100-23 results in impaired colonization of the mouse gastrointestinal tract. Environ Microbiol. 2007;9.

79.   Evans DA, Watson PS. Synthesis of the orienticin C M(2–4) macrocycle utilizing a nucleophilic aromatic substitution strategy. Tetrahedron Letters. 1996;37(19):3251-4.

80.   Kessler M, Glatthar R, Giese B, Bochet CG. Sequentially Photocleavable Protecting Groups in Solid-Phase Synthesis. Organic Letters. 2003;5(8):1179-81.

81.   Nicolaou KC, Koumbis AE, Takayanagi M, Natarajan S, Jain NF, Bando T, et al. Total Synthesis of Vancomycin—Part 3: Synthesis of the Aglycon. Chemistry – A European Journal. 1999;5(9):2622-47.

82.   Nicolaou KC, Boddy CNC, Li H, Koumbis AE, Hughes R, Natarajan S, et al. Total Synthesis of Vancomycin—Part 2: Retrosynthetic Analysis, Synthesis of Amino Acid Building Blocks and Strategy Evaluations. Chemistry – A European Journal. 1999;5(9):2602-21.

83.   Nicolaou KC, Mitchell HJ, Jain NF, Bando T, Hughes R, Winssinger N, et al. Total Synthesis of Vancomycin—Part 4: Attachment of the Sugar Moieties and Completion of the Synthesis. Chemistry – A European Journal. 1999;5(9):2648-67.

84.   Freund E, A. Robinson J. Solid-phase synthesis of a putative heptapeptide intermediate in vancomycin biosynthesis. Chemical Communications. 1999(24):2509-10.

85.   Freund E, Vitali F, Linden A, Robinson JA. Solid-Phase Synthesis Using (Allyloxy)carbonyl(Alloc) Chemistry of a Putative Heptapeptide Intermediate in Vancomycin Biosynthesis Containing m-Chloro-3-hydroxytyrosine. Helvetica Chimica Acta. 2000;83(9):2572-9.

86.   Hasan A, Stengele K-P, Giegrich H, Cornwell P, Isham KR, Sachleben RA, et al. Photolabile protecting groups for nucleosides: Synthesis and photodeprotection rates. Tetrahedron. 1997;53(12):4247-64.

87.   Nicolaou KC, Pastor J, Barluenga S, Winssinger N. Polymer-supported selenium reagents for organic synthesis. Chemical Communications. 1998(18):1947-8.

88.   Brieke C, Cryle MJ. A Facile Fmoc Solid Phase Synthesis Strategy To Access Epimerization-Prone Biosynthetic Intermediates of Glycopeptide Antibiotics. Organic Letters. 2014;16(9):2454-7.

89.   McComas CC, Crowley BM, Boger DL. Partitioning the loss in vancomycin binding affinity for D-Ala-D-Lac into lost H-bond and repulsive lone pair contributions. J Am Chem Soc. 2003;125(31):9314-5.

90.   Crowley BM, Boger DL. Total Synthesis and Evaluation of [Ψ[CH2NH]Tpg4]Vancomycin Aglycon: Reengineering Vancomycin for Dual D-Ala-D-Ala and D-Ala-D-Lac Binding. Journal of the American Chemical Society. 2006;128(9):2885-92.

91.   Crane CM, Boger DL. Synthesis and Evaluation of Vancomycin Aglycon Analogues That Bear Modifications in the N-Terminal D-Leucyl Amino Acid. Journal of Medicinal Chemistry. 2009;52(5):1471-6.

92.   Crane CM, Pierce JG, Leung SSF, Tirado-Rives J, Jorgensen WL, Boger DL. Synthesis and Evaluation of Selected Key Methyl Ether Derivatives of Vancomycin Aglycon. Journal of Medicinal Chemistry. 2010;53(19):7229-35.

93.   Xie J, Okano A, Pierce JG, James RC, Stamm S, Crane CM, et al. Total Synthesis of [Ψ[C(=S)NH]Tpg4]Vancomycin Aglycon, [Ψ[C(=NH)NH]Tpg4] Vancomycin Aglycon, and Related Key Compounds: Reengineering Vancomycin for Dual d-Ala-d-Ala and d-Ala-d-Lac Binding. Journal of the American Chemical Society. 2012;134(2):1284-97.

94.   Pathak TP, Miller SJ. Site-Selective Bromination of Vancomycin. Journal of the American Chemical Society. 2012;134(14):6120-3.

95.   Okano A, Nakayama A, Wu K, Lindsey EA, Schammel AW, Feng Y, et al. Total Syntheses and Initial Evaluation of [Ψ[C(=S)NH]Tpg4]vancomycin, [Ψ[C(=NH)NH]Tpg4]vancomycin, [Ψ[CH2NH]Tpg4]vancomycin, and Their (4-Chlorobiphenyl)methyl Derivatives: Synergistic Binding Pocket and Peripheral Modifications for the Glycopeptide Antibiotics. Journal of the American Chemical Society. 2015;137(10):3693-704.

96.   Ando S, Burrows J, Koide K. Synthesis of Violaceic Acid and Related Compounds through Aryl Triazene. Organic Letters. 2017;19(5):1116-9.

97.   Torres-García C, Pulido D, Albericio F, Royo M, Nicolás E. Triazene as a Powerful Tool for Solid-Phase Derivatization of Phenylalanine Containing Peptides: Zygosporamide Analogues as a Proof of Concept. The Journal of Organic Chemistry. 2014;79(23):11409-15.

98.   Liu C-Y, Knochel P. Preparation of Polyfunctional Arylmagnesium Reagents Bearing a Triazene Moiety. A New Carbazole Synthesis. Organic Letters. 2005;7(13):2543-6.

99.   Nicolauo KC, C. BCN, Hui L, E. KA, Robert H, Swaminathan N, et al. Total Synthesis of Vancomycin—Part 2: Retrosynthetic Analysis, Synthesis of Amino Acid Building Blocks and Strategy Evaluations. Chemistry – A European Journal. 1999;5(9):2602-21.

100.   Bandgar BP, Pandit SS. Synthesis of acyl azides from carboxylic acids using cyanuric chloride. Tetrahedron Letters. 2002;43(18):3413-4.

101.   Quesnel JS, Arndtsen BA. A Palladium-Catalyzed Carbonylation Approach to Acid Chloride Synthesis. Journal of the American Chemical Society. 2013;135(45):16841-4.

102.   Greenberg JA, Sammakia T. The Conversion of tert-Butyl Esters to Acid Chlorides Using Thionyl Chloride. The Journal of Organic Chemistry. 2017;82(6):3245-51.

103.   Dang Y, Chen Y. One-Pot Oxidation and Bromination of 3,4-Diaryl-2,5-dihydrothiophenes Using Br2: Synthesis and Application of 3,4-Diaryl-2,5-dibromothiophenes. The Journal of Organic Chemistry. 2007;72(18):6901-4.

104.   Kruszyk M, Jessing M, Kristensen JL, Jørgensen M. Computational Methods to Predict the Regioselectivity of Electrophilic Aromatic Substitution Reactions of Heteroaromatic Systems. The Journal of Organic Chemistry. 2016;81(12):5128-34.

105.   Ducry L, Roberge DM. Dibal-H Reduction of Methyl Butyrate into Butyraldehyde using Microreactors. Organic Process Research & Development. 2008;12(2):163-7.

106.   Tsai Y-L, Syu S-e, Yang S-M, Das U, Fan Y-S, Lee C-J, et al. Synthesis of multi-functional alkenes via Wittig reaction with a new-type of phosphorus ylides. Tetrahedron. 2014;70(34):5038-45.

107.   Nicolaou KC, Härter MW, Gunzner JL, Nadin A. The Wittig and Related Reactions in Natural Product Synthesis. Liebigs Annalen. 1997;1997(7):1283-301.

108.   Li L, Stimac JC, Geary LM. Synthesis of olefins via a Wittig reaction mediated by triphenylarsine. Tetrahedron letters. 2017;58(14):1379-81.

109.   Depré D, Vermeulen WAA, Lang Y, Dubois J, Vandevivere J, Vandermeersch J, et al. Origin of the E/Z Selectivity in the Synthesis of Tetrasubstituted Olefins by Wittig Reaction of α-Fluorophosphonium Ylides: An Explanation for the Low Stereoselectivity Observed in Reactions of α-Alkoxy Aldehydes. Organic Letters. 2017;19(6):1414-7.

110.   Byrne PA, Gilheany DG. The modern interpretation of the Wittig reaction mechanism. Chemical Society reviews. 2013;42(16):6670-96.

111.   Kolb HC, VanNieuwenhze MS, Sharpless KB. Catalytic Asymmetric Dihydroxylation. Chemical Reviews. 1994;94(8):2483-547.

112.   Gally C, Nestl BM, Hauer B. Engineering Rieske Non-Heme Iron Oxygenases for the Asymmetric Dihydroxylation of Alkenes. Angewandte Chemie International Edition. 2015;54(44):12952-6.

113.   Xing X, Zhao Y, Xu C, Zhao X, Wang DZ. Electronic helix theory-guided rational design of kinetic resolutions by means of the Sharpless asymmetric dihydroxylation reactions. Tetrahedron. 2012;68(36):7288-94.

114.   Periasamy M, Satish Kumar S, Sampath Kumar N. Catalytic asymmetric dihydroxylation of substituted trans-stilbene derivatives: implications of the variation

of enantioselectivities on the mechanism of OsO_4 addition to olefins. Tetrahedron letters. 2008;49(28):4416-9.

115.   Corey EJ, Jardine PD, Virgil S, Yuen PW, Connell RD. Enantioselective vicinal hydroxylation of terminal and E-1,2-disubstituted olefins by a chiral complex of osmium tetroxide. An effective controller system and a rational mechanistic model. Journal of the American Chemical Society. 1989;111(26):9243-4.

116.   Rúnarsson ÖV, Malainer C, Holappa J, Sigurdsson ST, Másson M. tert-Butyldimethylsilyl O-protected chitosan and chitooligosaccharides: useful precursors for N-modifications in common organic solvents. Carbohydrate Research. 2008;343(15):2576-82.

117.   Corey EJ, Venkateswarlu A. Protection of hydroxyl groups as tert-butyldimethylsilyl derivatives. Journal of the American Chemical Society. 1972;94(17):6190-1.

118.   Gopinath R, Patel BK. Tetrabutylammonium Tribromide (TBATB)−MeOH: An Efficient Chemoselective Reagent for the Cleavage of tert-Butyldimethylsilyl (TBDMS) Ethers. Organic Letters. 2000;2(26):4177-80.

119.   Das B, Reddy KR, Thirupathi P. A simple, efficient and highly selective deprotection of t-butyldimethylsilyl (TBDMS) ethers using silica supported sodium hydrogen sulfate as a heterogeneous catalyst. Tetrahedron letters. 2006;47(33):5855-7.

120.   Hirose D, Gazvoda M, Košmrlj J, Taniguchi T. The "Fully Catalytic System" in Mitsunobu Reaction Has Not Been Realized Yet. Organic Letters. 2016;18(16):4036-9.

121.   Wang G, Ella-Menye J-R, St. Martin M, Yang H, Williams K. Regioselective Esterification of Vicinal Diols on Monosaccharide Derivatives via Mitsunobu Reactions. Organic Letters. 2008;10(19):4203-6.

122.   But TYS, Toy PH. Organocatalytic Mitsunobu Reactions. Journal of the American Chemical Society. 2006;128(30):9636-7.

123. Camp D, von Itzstein M, Jenkins ID. The mechanism of the first step of the Mitsunobu reaction. Tetrahedron. 2015;71(30):4946-8.

124. Hughes DL, Reamer RA, Bergan JJ, Grabowski EJJ. A mechanistic study of the Mitsunobu esterification reaction. Journal of the American Chemical Society. 1988;110(19):6487-91.

125. Jadhav AH, Kim H. A mild, efficient, and selective deprotection of tert-butyldimethylsilyl (TBDMS) ethers using dicationic ionic liquid as a catalyst. Tetrahedron letters. 2012;53(39):5338-42.

126. DiLauro AM, Seo W, Phillips ST. Use of Catalytic Fluoride under Neutral Conditions for Cleaving Silicon–Oxygen Bonds. The Journal of Organic Chemistry. 2011;76(18):7352-8.

127. Lucio Anelli P, Biffi C, Montanari F, Quici S. Fast and selective oxidation of primary alcohols to aldehydes or to carboxylic acids and of secondary alcohols to ketones mediated by oxoammonium salts under two-phase conditions. The Journal of Organic Chemistry. 1987;52(12):2559-62.

128. Tebben L, Studer A. Nitroxides: Applications in Synthesis and in Polymer Chemistry. Angewandte Chemie International Edition. 2011;50(22):5034-68.

129. Angelin M, Hermansson M, Dong H, Ramström O. Direct, Mild, and Selective Synthesis of Unprotected Dialdo-Glycosides. European Journal of Organic Chemistry. 2006;2006(19):4323-6.

130. Kruijtzer JAW, Hofmeyer LJF, Heerma W, Versluis C, Liskamp RMJ. Solid-Phase Syntheses of Peptoids using Fmoc-Protected N-Substituted Glycines: The Synthesis of (Retro)Peptoids of Leu-Enkephalin and Substance P. Chemistry – A European Journal. 1998;4(8):1570-80.

131. Acosta GA, Royo M, de la Torre BG, Albericio F. Facile solid-phase synthesis of head-side chain cyclothiodepsipeptides through a cyclative cleavage from MeDbz-resin. Tetrahedron Letters. 2017;58(28):2788-91.

132.   Hojo K, Hara A, Kitai H, Onishi M, Ichikawa H, Fukumori Y, et al. Development of a method for environmentally friendly chemical peptide synthesis in water using water-dispersible amino acid nanoparticles. Chemistry Central Journal. 2011;5(1):49.

133.   Bodanszky M, Bednarek MA. Active esters in solid-phase peptide synthesis. Journal of Protein Chemistry. 1989;8(4):461-9.

134.   Albericio F. Developments in peptide and amide synthesis. Current opinion in chemical biology. 2004;8(3):211-21.

135.   Kumar A, Jad YE, El-Faham A, de la Torre BG, Albericio F. Green solid-phase peptide synthesis 4. γ-Valerolactone and N-formylmorpholine as green solvents for solid phase peptide synthesis. Tetrahedron Letters. 2017;58(30):2986-8.

136.   Alsina J, Jensen KJ, Albericio F, Barany G. Solid-Phase Synthesis with Tris(alkoxy)benzyl Backbone Amide Linkage (BAL)[≠]. Chemistry – A European Journal. 1999;5(10):2787-95.

137.   Montalbetti CAGN, Falque V. Amide bond formation and peptide coupling. Tetrahedron. 2005;61(46):10827-52.

138.   Mäde V, Els-Heindl S, Beck-Sickinger AG. Automated solid-phase peptide synthesis to obtain therapeutic peptides. Beilstein Journal of Organic Chemistry. 2014;10:1197-212.

139.   Wellings DA, Atherton E. Standard Fmoc protocols. Methods Enzymol. 1997;289:44-67.

140.   Liang C, Behnam MAM, Sundermann TR, Klein CD. Phenylglycine racemization in Fmoc-based solid-phase peptide synthesis: Stereochemical stability is achieved by choice of reaction conditions. Tetrahedron Letters. 2017;58(24):2325-9.

141.   Collins JM, Porter KA, Singh SK, Vanier GS. High-Efficiency Solid Phase Peptide Synthesis (HE-SPPS). Organic Letters. 2014;16(3):940-3.

142. Isidro-Llobet A, Álvarez M, Albericio F. Amino Acid-Protecting Groups. Chemical Reviews. 2009;109(6):2455-504.

143. Sharma A, Ramos-Tomillero I, El-Faham A, Rodríguez H, de la Torre BG, Albericio F. Tetrahydropyranyl: A Non-aromatic, Mild-Acid-Labile Group for Hydroxyl Protection in Solid-Phase Peptide Synthesis. ChemistryOpen. 2017;6(2):206-10.

144. Behrendt R, White P, Offer J. Advances in Fmoc solid-phase peptide synthesis. Journal of Peptide Science. 2016;22(1):4-27.

145. Thieriet N, Alsina J, Giralt E, Guibé F, Albericio F. Use of Alloc-amino acids in solid-phase peptide synthesis. Tandem deprotection-coupling reactions using neutral conditions. Tetrahedron Letters. 1997;38(41):7275-8.

146. Wilson KR, Sedberry S, Pescatore R, Vinton D, Love B, Ballard S, et al. Microwave-assisted cleavage of Alloc and Allyl Ester protecting groups in solid phase peptide synthesis. Journal of Peptide Science. 2016;22(10):622-7.

147. Fernández-Forner D, Casals G, Navarro Es, Ryder H, Albericio F. Solid-phase synthesis of 4-aminopiperidine analogues using the Alloc protecting group: an investigation of Alloc removal from secondary amines. Tetrahedron Letters. 2001;42(27):4471-4.

148. Albericio F. Orthogonal protecting groups for N(alpha)-amino and C-terminal carboxyl functions in solid-phase peptide synthesis. Biopolymers. 2000;55(2):123-39.

149. Weishaupt M, Eller S, Seeberger PH. Solid phase synthesis of oligosaccharides. Methods Enzymol. 2010;478:463-84.

150. Basudeb B, Susmita P. Solid-Phase Organic Synthesis and Catalysis: Some Recent Strategies Using Alumina, Silica, and Polyionic Resins. Journal of Catalysts. 2013;2013(1):1-1.

151. Patra T, Karmakar S, Upadhyayula S. Multifunctional ionic liquid-bound polystyrene resin with high loading capacity as support in solid-phase peptide synthesis. Tetrahedron Letters. 2017;58(15):1531-4.

152.	Toy PH, Reger TS, Garibay P, Garno JC, Malikayil JA, Liu G-y, et al. Polytetrahydrofuran Cross-Linked Polystyrene Resins for Solid-Phase Organic Synthesis. Journal of Combinatorial Chemistry. 2001;3(1):117-24.

153.	Vaino AR, Goodin DB, Janda KD. Investigating resins for solid phase organic synthesis: the relationship between swelling and microenvironment as probed by EPR and fluorescence spectroscopy. J Comb Chem. 2000;2(4):330-6.

154.	Góngora-Benítez M, Tulla-Puche J, Albericio F. Handles for Fmoc Solid-Phase Synthesis of Protected Peptides. ACS Combinatorial Science. 2013;15(5):217-28.

155.	Boas U, Christensen JB, Jensen KJ. Two Dialkoxynaphthalene Aldehydes as Backbone Amide Linkers for Solid-Phase Synthesis. Journal of Combinatorial Chemistry. 2004;6(4):497-503.

156.	Valeur E, Bradley M. Amide bond formation: beyond the myth of coupling reagents. Chemical Society reviews. 2009;38(2):606-31.

157.	El-Faham A, Albericio F. Peptide Coupling Reagents, More than a Letter Soup. Chemical Reviews. 2011;111(11):6557-602.

158.	Hu L, Xu S, Zhao Z, Yang Y, Peng Z, Yang M, et al. Ynamides as Racemization-Free Coupling Reagents for Amide and Peptide Synthesis. Journal of the American Chemical Society. 2016;138(40):13135-8.

159.	Alewood P, Alewood D, Miranda L, Love S, Meutermans W, Wilson D. Rapid in situ neutralization protocols for Boc and Fmoc solid-phase chemistries. Methods Enzymol. 1997;289:14-29.

160.	Han S-Y, Kim Y-A. Recent Development of Peptide Coupling Reagents in Organic Synthesis2004.

161.	Carpino LA, Xia J, Zhang C, El-Faham A. Organophosphorus and Nitro-Substituted Sulfonate Esters of 1-Hydroxy-7-azabenzotriazole as Highly Efficient Fast-Acting Peptide Coupling Reagents. The Journal of Organic Chemistry. 2004;69(1):62-71.

162.   Cherkupally P, Ramesh S, de la Torre BG, Govender T, Kruger HG, Albericio F. Immobilized Coupling Reagents: Synthesis of Amides/Peptides. ACS Combinatorial Science. 2014;16(11):579-601.

163.   Han S-Y, Kim Y-A. Recent development of peptide coupling reagents in organic synthesis. Tetrahedron. 2004;60(11):2447-67.

164.   Joullié MM, Lassen KM. Evolution of amide bond formation. Arkivoc: Online Journal of Organic Chemistry. 2010:189.

165.   Oleg M, Fernando A. Industrial Application of Coupling Reagents in Peptides. ChemInform. 2004;35(24):1.

166.   Albericio F, Bofill JM, El-Faham A, Kates SA. Use of Onium Salt-Based Coupling Reagents in Peptide Synthesis1. The Journal of Organic Chemistry. 1998;63(26):9678-83.

167.   Amblard M, Fehrentz J-A, Martinez J, Subra G. Methods and protocols of modern solid phase peptide synthesis. Molecular Biotechnology. 2006;33(3):239-54.

168.   Dunetz JR, Magano J, Weisenburger GA. Large-Scale Applications of Amide Coupling Reagents for the Synthesis of Pharmaceuticals. Organic Process Research & Development. 2016;20(2):140-77.

169.   El-Faham A, Albericio F. Novel Proton Acceptor Immonium-Type Coupling Reagents: Application in Solution and Solid-Phase Peptide Synthesis. Organic Letters. 2007;9(22):4475-7.

170.   Barlos K, Chatzi O, Gatos D, Stavropoulos G. 2-Chlorotrityl chloride resin. Studies on anchoring of Fmoc-amino acids and peptide cleavage. International journal of peptide and protein research. 1991;37(6):513-20.

171.   Subiros-Funosas R, El-Faham A, Albericio F. Use of Oxyma as pH modulatory agent to be used in the prevention of base-driven side reactions and its effect on 2-chlorotrityl chloride resin. Biopolymers. 2012;98(2):89-97.

172. Kao C-L, Huang AY-T, Chen H-T. Solid-Phase Synthesis of a Seventh-Generation Inverse Poly(amidoamine) Dendrimer: Importance of the Loading Ratio on the Resin. Macromolecular Rapid Communications. 2017;38(12):6.

173. R. Dunetz J, Magano J, A. Weisenburger G. Large-Scale Applications of Amide Coupling Reagents for the Synthesis of Pharmaceuticals2015.

174. Kaiser E, Colescott RL, Bossinger CD, Cook PI. Color test for detection of free terminal amino groups in the solid-phase synthesis of peptides. Analytical Biochemistry. 1970;34(2):595-8.

175. Fox JB, Fiddler RN. Ruhemann's purple from ninhydrin, ascorbate, and nitrite. Bioorganic Chemistry. 1984;12(3):235-41.

176. Friedman M. Applications of the ninhydrin reaction for analysis of amino acids, peptides, and proteins to agricultural and biomedical sciences. Journal of agricultural and food chemistry. 2004;52(3):385-406.

177. Bottom CB, Hanna SS, Siehr DJ. Mechanism of the ninhydrin reaction. Biochemical Education. 1978;6(1):4-5.

178. Chan LC, Cox BG. Kinetics of Amide Formation through Carbodiimide/N-Hydroxybenzotriazole (HOBt) Couplings. The Journal of Organic Chemistry. 2007;72(23):8863-9.

179. Tang X, Liu X, inventors; Achiever Biochem Co., Ltd., Peop. Rep. China . assignee. Method for synthesis of amino-protected glycine dipeptide derivative. patent CN101654473A. 2010.

180. Parker AJ. Protic-dipolar aprotic solvent effects on rates of bimolecular reactions. Chemical Reviews. 1969;69(1):1-32.

181. Austin PC, Rothwell DM, Tu JV. A comparison of statistical modeling strategies for analyzing length of stay after CABG surgery. Health Serv Outcomes Res Method. 2002;3.

182.   Ando K. A Mechanistic Study of the Horner−Wadsworth−Emmons Reaction: Computational Investigation on the Reaction Pass and the Stereochemistry in the Reaction of Lithium Enolate Derived from Trimethyl Phosphonoacetate with Acetaldehyde. The Journal of Organic Chemistry. 1999;64(18):6815-21.

183.   Ando K. Z-Selective Horner−Wadsworth−Emmons Reaction of α-Substituted Ethyl (Diarylphosphono)acetates with Aldehydes1. The Journal of Organic Chemistry. 1998;63(23):8411-6.

184.   Ando K, Narumiya K, Takada H, Teruya T. Z-Selective Intramolecular Horner−Wadsworth−Emmons Reaction for the Synthesis of Macrocyclic Lactones. Organic Letters. 2010;12(7):1460-3.

185.   https://www.chem.wisc.edu/areas/reich/nmr/h-data/hdata.htm.   [accessed Sep/2017].

186.   Casely-Hayford MA. Chemical synthesis and biological evaluation of potential Anti-Cancer Agents Based on the Azinomycin [PhD]: University of London; 2004.

187.   Corey EJ, Guzman-Perez A, Noe MC. The application of a mechanistic model leads to the extension of the Sharpless asymmetric dihydroxylation to allylic 4-methoxybenzoates and conformationally related amine and homoallylic alcohol derivatives. Journal of the American Chemical Society. 1995;117(44):10805-16.

188.   Ogino Y, Chen H, Kwong H-L, Sharpless KB. On the timing of hydrolysis / reoxidation in the osmium-catalyzed asymmetric dihydroxylation of olefins using potassium ferricyanide as the reoxidant. Tetrahedron Letters. 1991;32(32):3965-8.

189.   Dethe DH, Ranjan A. Enantioselective total syntheses and determination of absolute configuration of marine toxins, oxazinins. RSC Advances. 2013;3(45):23692-703.